# Nucleotide Excision Repair: Interplay between nuclear compartmentalization, histone modifications and signaling

Dissertation zur Erlangung des Grades

"Doktor der Naturwissenschaften"

am Fachbereich Biologie

der Johannes Gutenberg-Universität in Mainz

Shalaka Chitale

geb. am 20.06.1988 in Pune, India

Mainz, 2017

Tag der mündlichen Prüfung: 20.06.2017

# Table of Contents

# Summary

Maintaining the integrity of genetic information is one of the crucial functions of the cell. Depending on the type of DNA damage, there are several repair pathways dedicated to a quick and efficient repair of the damage. A major source of DNA damage is exposure to UV light, which causes formation of 6'-4'photoproducts and pyrimidine dimers. These are bulky DNA adducts that cause distortion of the helix structure. Such lesions are repaired by Nucleotide Excision Repair (NER). Nucleotide Excision Repair occurs by two sub-pathways, depending on the genomic location of the lesion. Transcription coupled NER (TC-NER) repairs lesions in actively transcribed genes, which global genomic NER (GG-NER) can repair all types of lesions. These two pathways differ in their recognition step. Lesion recognition is followed by verification of damage, excision of the damaged strand, and refilling of the gap by DNA synthesis. An important unanswered question in the field of NER is how the removal of lesions occurs in the context of chromatin structure. Recognition of lesions in heterochromatin requires a decondensation of chromatin to enable access by repair factors. Additionally, lesion recognition requires cascades of recruitment of the various proteins, in a tightly regulated and synchronized manner. We show that the recognition step during GG-NER consists of a ZRF1-DICER-MMSET axis linking lesion recognition via DDB2 to lesion verification via XPA followed by subsequent repair. ZRF1 recognizes the H2AK119 ub mark set by the UV-RING1B complex. This results in translocation of the lesion to the nucleolus, and remodeling of the complex to the UV-CUL4A complex. Formation of this complex enables the next phase of ubiquitylation that regulates NER repair proteins. ZRF1 in turn also contributed to chromatin decondensation through recruitment of DICER. DICER enables relaxation of chromatin structure in a PARP1 dependent manner. It also recruits MMSET, which sets the H4K20me2 mark. This histone mark serves as a tethering platform for recruitment of XPA, a core NER component which is essential for further repair to take place. Thus, we have discovered a novel and essential function for these proteins in NER.

# Zussamenfassung

**FACHBEREICH BIOLOGIE DER JOHANNES GUTENBERG-UNIVERSITÄT MAINZ**
Nr. / 20 **Zusammenfassung der Dissertation von** __Shalaka Chitale

Thema: Eine wesentliche Aufgabe der Zelle ist es die Integrität ihrer DNA zu schützen, um die darin enthaltene genetische Information zu erhalten. Abhängig von der Art der DNA-Schädigung werden in der Zelle unterschiedliche DNA-Reparaturmechanismen angeschaltet, die eine schnelle und effiziente Reparatur des Schadens gewährleisten. Eine der zahlreichen zellulären DNA Reparaturmechanismen ist die Nukleotidexzisionsreparatur (NER), welche unterschiedliche Schäden wie zum Beispiel Cyclobutanpyrimidin Dimere (CPD) und 6-4 Photoprodukte repariert, die nach der Bestrahlung mit UV Licht entstehen. In Säugerzellen werden in der NER Schäden durch zwei unterschiedliche Mechanismen repariert. Schäden in transkribierten genomischen Bereichen werden durch die sogenannte *transcription-coupled NER* (TC-NER) repariert, alle anderen genomische Bereiche werden durch *global genomic NER* (GG-NER) repariert. Diese beiden DNA Reparaturmechanismen unterscheiden sich lediglich in der Schadenserkennung. In deren Anschluss nutzen TC-NER und GG-NER einen gemeinsamen Mechanismus zur Verifizierung, zur Exzsion des Schadens und zur Auffüllung der entstandenen etwa 30 Nukleotide umfassenden Lücke durch DNA Synthese. Wie NER im Kontext der Chromatinstruktur verläuft ist eine bislang noch offene Frage. Die Schadenserkennung im Heterochromatin benötigt eine Dekondensierung bzw. Öffnung der Chromatinkonformation, um die Rekrutierung von DNA Reparaturfaktoren zu ermöglichen. Ausserdem werden während der Schadenserkennung unterschiedliche Proteinkomplexe in einer synchronisierten bzw. zeitlich festgelegten Folge zur DNA-Läsion rekrutiert. In der vorliegenden Arbeit wird gezeigt, dass während der GG-NER die Schadenserkennung durch das Zusammenspiel der Faktoren ZRF1, DICER und MMSET mit dem DNA Reparturerkennungsfaktor DDB2 geprägt ist, welches die Rekrutierung des DNA Reparaturfaktors XPA ermöglicht. Dabei bindet ZRF1 mono-ubiquitiniertes histone H2A (H2A-K119-Ub), welches durch den UV-RING1B Komplex katalysiert wird. Derart modifiziertes Chromatin wird zum Nukleolus transloziert, wo durch molekulares *Remodeling* der UV-RING1B Komplex in den UV-CUL4A Komplex umgebaut wird. Die Herstellung des UV-CUL4A Komplexes leitet dann die nächste Phase von Ubiquitinierungsreaktionen ein, welche wiederum nachfolgende Reparaturreaktionen regulieren. Weiterhin ist ZRF1 an der Chromatin-Dekondensierung beteiligt, da es über die Rekruiterung von DICER eine PARP1-abhängige Relaxation der Chromatin-Konformation hervorruft. DICER wiederum ist für die Rekruiterung des Methyltransferase MMSET essentiell, welche ein Methylierung am Histone H4 (H4K20me2) bedingt. Diese Histonmodifizierung dient als eine Art

Bindeplattform für den Reparaturfaktor XPA, eine der Hauptkomponenten der NER. Zusammengenommen konnte eine neue und essentielle Funktion der obengenannten Proteine bzw. deren Zusammenspiel während der NER entdeckt werden.

Genehmigt vom 1. Gutachter / von der 1. Gutachterin

_____ (Unterschrift)

# Introduction

## The need for efficient DNA repair:

One of the major biological discoveries in recent times, has been the central dogma that governs all biological systems. DNA uses a specific sequence of the four bases A,T,G,C to encode genetic information, this information is transmitted via RNA, and thus leads to formation of the specific proteins needed by an organism to survive. Considering the major role of DNA as a repository of the genetic information of an organism, maintaining the sequence integrity of DNA is one of the major functions of a cell. DNA is under threat from a variety of internal and external agents, that can directly or indirectly lead to changes in the DNA sequence. Persistent DNA damage can lead to mutations, cell cycle stalling and ultimately even cell death. Thus, the cell has devised a variety of pathways to ensure efficient repair of its DNA.

## Types of DNA damage:

DNA damage can occur due to a variety of endogenous and exogenous factors. Depending on the type of damage, the cell has evolved a corresponding variety of repair pathways that repair the damage. (Table 1) (reviewed in De Bont and van Larebeke, 2004; Helleday et.al. 2014) These pathways are shortly described below.

**Table 1**

**DNA damage sources and DNA repair pathways**

| Source | DNA modification | DNA repair pathway |
|---|---|---|
| <u>Endogenous</u> | | |
| Reactive oxygen species ($O_2^{-\bullet}$; $H_2O_2$; $OH^\bullet$; $^1O_2$) | Oxidation of bases (8-OH-dG)<br>DNA adducts (ethano-, propano-derived) | Base excision repair (BER)<br>Interstrand crosslink repair (ICL repair) |
| Endogenous alkylating agents (SAM) | Methylation of bases<br>$O^6$-methylguanine | BER<br>Direct reversal |
| Oestrogen metabolites | Oestrogen-DNA adducts | BER |

| | | |
|---|---|---|
| | Base modification (8-OH-dG)<br>Single strand breaks | Mismatch repair |
| Deamination | Base conversion (C→U; A →hypoxanthine) | Mismatch repair |
| Replication mismatches and error-prone repair | Base misincorporation | |
| Misincorporation of nucleotides | rNTP incorporation | RNAse H2 |
| <u>Exogenous</u> | | |
| Chemical adducts | Bulky chemical adducts (benzo[a]pyrene; aflatoxin; cisplatin) | Nucleotide excision repair (NER) |
| | Alkylation agents (N-methyl-nitrosoguanidine, sulfur mustard, nitrogen mustard) | BER, direct reversal |
| | DNA intercalators (proflavines) | ICL repair, NER |
| Irradiation | Ionizing Radiation:<br>double strand breaks | NHEJ, HR |
| | UV Radiation:<br>photoproducts | NER |

NHEJ – non-homologous end joining; HR – homologous recombination.

**Double strand break repair**

DNA Double strand breaks are one of the most dangerous types of DNA damage. They can lead to major chromosomal rearrangements and thus threated the integrity of the cell. The first step in double strand break repair is to sense and stabilize the DNA ends by binding of the MRN complex, consisting of MRE11, RAD50 and NBN (reviewed in Petrini and Stracker, 2003) The break is then repaired either via homologous recombination (HR) or non-homologous end joining (NHEJ), depending on the cell cycle state. (reviewed in Shiloh and Ziv, 2013 and Stracker and Petrini 2011).

Non homologous end joining (NHEJ) consists of directly joining the two broken ends of DNA (reviewed in Chapman et.al., 2012). It can take place during all phases of the cell cycle. Typically, NHEJ is mediated by the Ku70/80 dimer. Binding of 53BP1 blocks end-resection, and the DNA is ultimately repaired by the XRCC4/DNA ligase IV complex (reviewed in Zimmerman andde Lange 2014) (Figure 1).

Homologous recombination (HR) uses a sister chromatid or homologous chromosome as a template for error free filling of the DNA break. Since it requires a template, HR can only occur during the S or G2 phases of the cell cycle, when a template is readily available. The first step of HR is resection of the DNA ends leading to formation of a ssDNA region. This is mediated by the MRN complex, the BRCA1-BARD complex and endonucleases CtIP, Exo1. The resulting ssDNA is then protected by binding of RPA. This is followed by displacement of RPA by Rad51 and Rad54. Rad51 and Rad5 are recombinases and enable search for homologous sequences to complete DNA repair (reviewed in Helleday, 2003) (Figure 1).

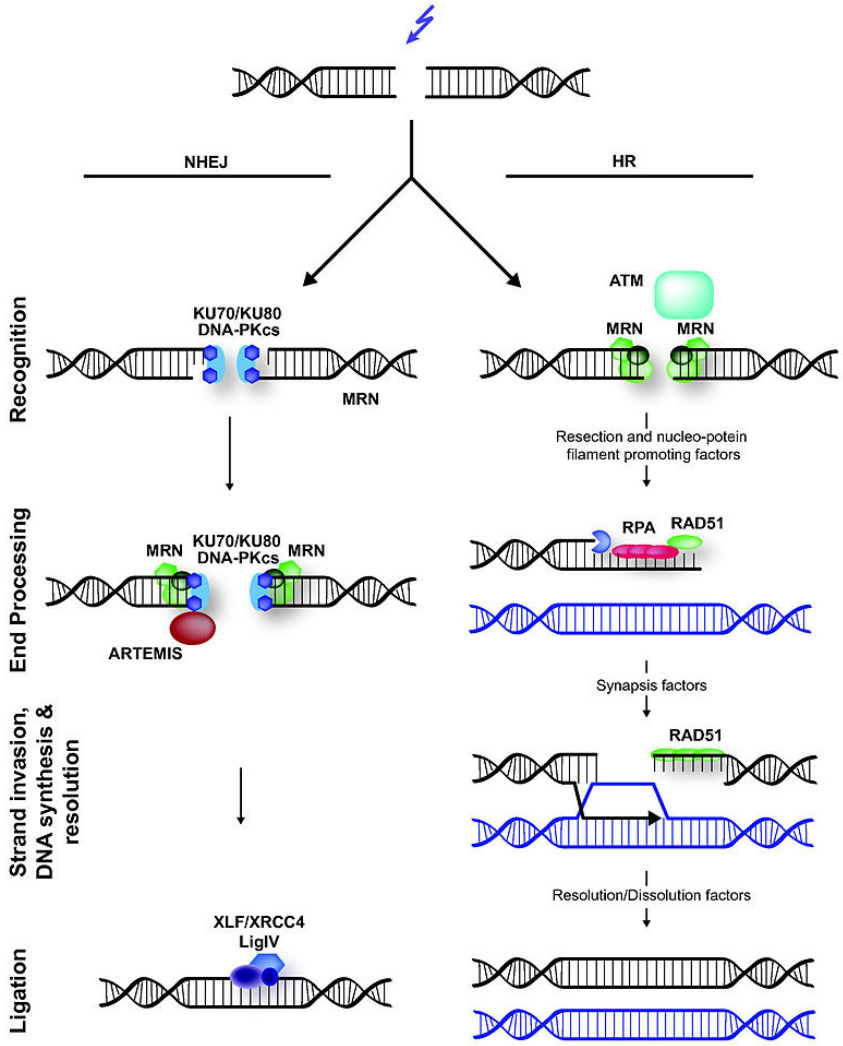


Figure 1: Non-homologous end joining and Homologous Recombination in mammals during DSP repair: Left:Homologous recombination repairs DSB with the homological sequence provided by a sister chromatid. After end processing homologous pairing is followed by DNA strand exchange, DNA synthesis and ligation. Right:Non-homologous end-joining mediated by the activity of the Ku70/80 dimer which brings together two DSB ends. The DNA ends are end-processed and further repaired by the activity of XRCC4/DNA ligase IV complex.
(From Lans et al., 2012)

**Mismatch repair**

Processes such as misincorporation of nucleotides, and base conversion that result in a loss of exact base complementarity are repaired by mismatch repair (MMR) (reviewed in Jiricny, 2006;

Li,2008). MMR is a highly conserved pathway among both prokaryotes and eukaryotes. The pathway usually consists of recognition of the mismatch followed by cleavage of the DNA in the vicinity of the mismatch. This is then followed by exonuclease mediated removal of the mismatch, re-synthesis of DNA, and ligation (Figure 2A).

**Base excision repair**

The individual bases in a DNA strand are also subject to damage via oxidation, alkylation and hydrolysis. This forms one of the main sources of DNA damage. Lesions such as these, are repaired by replacement of the modified base via Base Excision Repair (BER) (reviewed in Krokan and Bjoras, 2013) (Figure 2B). BER is initiated by specific base-glycosylases that recognize a base, and remove it from the DNA backbone, creating an abasic site. The DNA strand is then cleaved by the endonuclease APE1, followed by filling of the gap and ligation. Some methylated nucleotides can also be repaired by direct demethylation of the base, eg: $O^6$-methylguanine, is repaired through activity of $O^6$-methylguanine-DNA methyltransferase (MGMT) (reviewed in Gerson, 2004; Sharma et al., 2009)

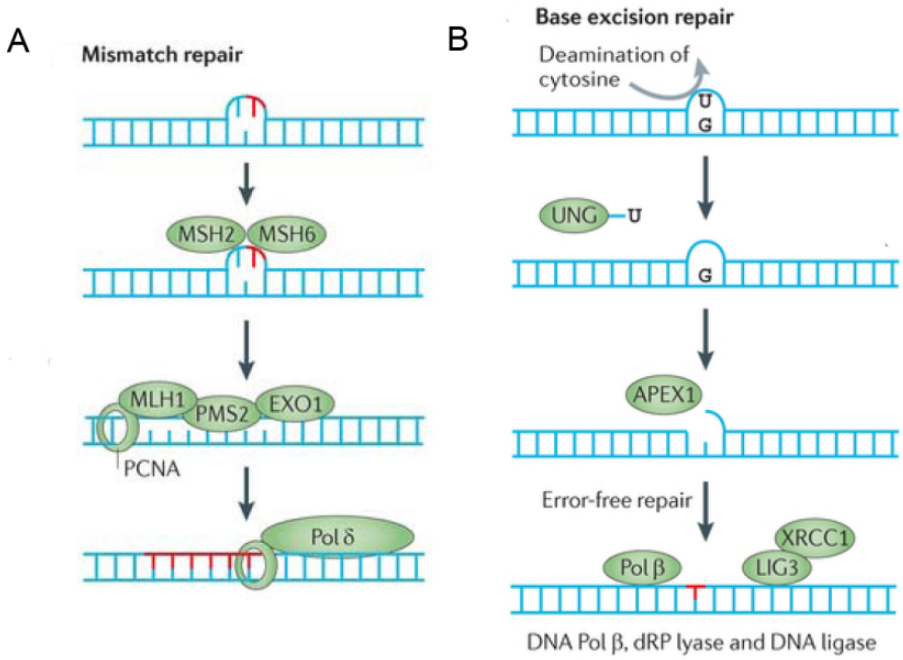


Figure 2: Mismatch and Base excision repair (A) Mismatch repair is initiated by the DNA mismatch recognition proteins MSH2 and MSH6; a segment of DNA is excised between the mismatch and a nearby nick by the MMR endonuclease PMS2 and exonuclease 1 (EXO1). The gap that is left in the DNA is filled by Pol δ.(b)BER is initiated by a number of specific base-glycosylases recognizing a modified nucleotide to create an abasic site (UNG). Further, DNA strand is cleaved by endonuclease APEX1, gap filling and ligation. Adpated from Helleday, 2003; Lans, 2012

**Nucleotide excision repair**

Nucleotide Excision Repair (NER) is a highly versatile DNA repair pathway that repairs helix distorting lesions. The main source of these type of lesions is exposure to UV light, that causes formation of cyclopyrimidine dimers (CPD) as well as 6'-4' photoproducts (reviewed in Franklin and Haseltine, 1986) . CPDs are formed more frequently, distort DNA structure to a larger extent, and usually block transcription and replication (Tung et al., 1996). They are repaired at a relatively slow rate, and complete removal of CPDs can take upto 48 hours (Han et al. 2016). 6'-4'photoproducts on the other hand, are less frequent, and do not lead to replication blocks. Thus, they can be highly mutagenic if unrepaired, and are repaired very rapidly (Kamiya et al. 1998). NER machinery also recognizes various other bulky DNA adducts such as benzo[a]pyrene derivatives and platinum adducts.

Mutations in the NER pathway lead to the *Xeroderma pigmentosum* (XP) spectrum of disorders (Cleaver 1968). XP is a rare autosomal-recessive genetic disorder, characterized by an inability to repair UV DNA damage. XP patients develop multiple base cell carcinomas and other skin malignancies at very young ages . The association of the NER defects and the phenotype of XP patients was demonstrated by Epstein and colleagues (Epstein et al., 1969). Subsequently, XP was found to consist of seven genetically heterogeneous groups: named as XPA, XPB, XPC, XPD, XPE, XPF, XPG (Arase et al., 1979; De Weerd-Kastelein et al.,1972). Primary fibroblast cells from XP patients are found to show defective DNA repair, as measured by unscheduled DNA synthesis (UDS) after exposure to UV.

Complementation studies done by various groups led to identification of the genes and proteins responsible for the various XP subtypes. This then led to the pioneering work of Aboussekhra and colleagues (Aboussekhra et al., 1995), who demonstrated the ability to reconstitute the NER reaction *in vitro*. Although the *in vitro* reaction requires over 30 different polypeptides, they do

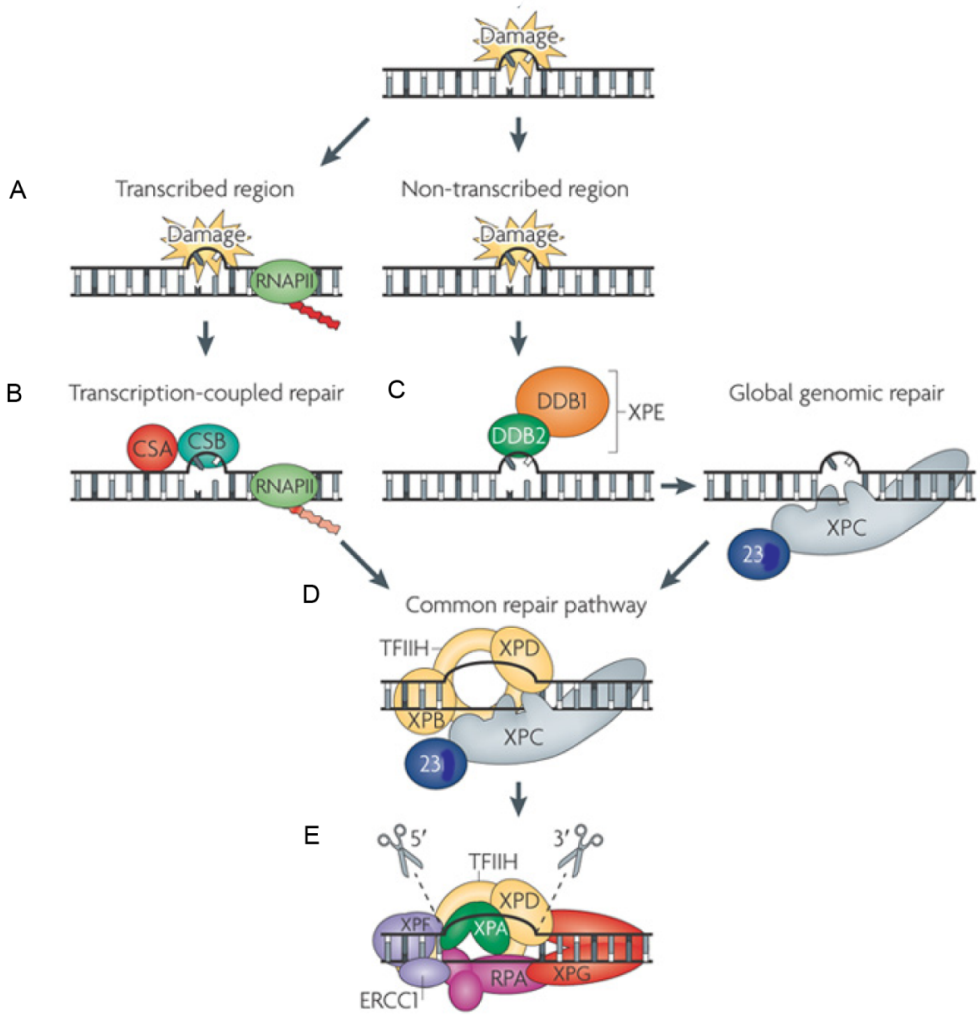


not reflect the complete assortment of proteins required for NER *in vivo*. The core repair pathway of NER can be divided in the following steps: lesion recognitnion, unwinding of the DNA and formation of the pre-incision complex, excision of the strand containing the lesion, and DNA synthesis and ligation (Figure 3). Depending on the position and recognition of the lesion, NER is further divided into two sub-pathways: Transcription couples NER (TC-NER) and global genomic NER (GG-NER).

Figure 3: Principal scheme of nucleotide excision repair pathway (A) NER is triggered by the detection of the DNA damage, usually mediated by exposure of DNA to UV-irradiation. (B) Transcription-coupled repair. DNA damage at the transcribed DNA strand is recognized by the stalling of RNApolII and further binding of CSA and CSB proteins (C) Global genome repair. DNA damage is recognized by DDB2 and further by XPC. (D)Formation of the pre-excision complex. TFIIH, including DNA helicases XPB and XPD, and XPA are recruited to the DNA damage site to form open DNA structure. (E) DNA lesions are excised by exonucleases XPF and XPG and the nick is ligated by DNA-polymerases and DNA ligases. Adapted from Cleaver et al., 2010.

### *Transcription-coupled NER*

UV damage occurs randomly throughout the genome. Lesions may be present in both transcribed and non-transcribed regions. Lesions in transcribed strands can cause stalling of RNA pol II and thus a global stalling of transcription, which is very taxing for the cell and needs to be quickly resolved. Early evidence showed that that repair in transcribed regions shows a different kinetics as compared to non-transcribed regions (Bohr et al., 1985). Subsequently, it was found that transcribed regions are indeed repaired at a faster rate (Mellon et al.,1987). The difference in repair kinetics between different genomic regions led to a further investigation to determine whether these two regions are indeed repaired by different pathways. Researchers found that although the core NER repair process is conserved between TC-NER and GG-NER, the recognition step of both pathways, and thus the resulting recruitment of the core repair machinery differs significantly. The main indication for a lesion in transcribed regions, is the physical stalling of RNA pol II. Stalled RNA pol II activates DNA repair pathways, and can further lead to cell cycle arrest or apoptosis. Recognition of stalled RNA pol II in response to UV lesions requires the activity of two additional proteins, CSA and CSB. Mutations in these proteins lead to Cockayne syndrome, which causes retarded growth and development, progressive neurodegeneration as well as other progeroid features. Fibroblasts from patients with defective CSA or CSB show only a minor impairment in NER however, which suggests two important distinctions. Firstly, GG-NER is able to compensate for defective TC-NER in a cell, leading to repair of lesions although with a slower kinetics. Secondly, given the diverse phenotypes in Cockayne syndrome patients, it is likely that CSA and CSB also play a role in other processes in the cell, and these indications are not a sole result of defective NER (Fousteri and Mullenders, 2008).

The mechanism of recognition of stalled RNA pol II has been extensively studied, leading to several hypotheses. One model suggests the reverse translocation of RNA pol II from the damage site followed by its removal from DNA and subsequent proteasomal degradation. *In vitro* data suggest that the CPD is incorporated into the active site of RNA pol II leading to its stalling. This is followed by removal of RNA pol II and cleavage of the misincorporated nucleotide in the transcript (Sigurdsson et al., 2010). It remains to be shown how this occurs *in vivo*, however recent research suggests that RNA pol II is likely retained at the damage site during the steps of lesion recognition (Fousteri and Mullenders, 2008 Schwertman et al.,2013. This is in agreement with the fact that recognition of stalled RNA pol II also requires presence of CSB, a DNA dependent ATPase (Troelstra et al., 1992). CSB then leads to recruitment of CSA, which leads to formation of the CSA-DDB1-CUL4-RBX1 ubiquitin E3 ligase complex (Fousteri et al., 2006; Henning et al., 1995). This complex leads to a chain of ubiquitylation events that regulate TC-NER (Groisman et al., 2003). The exact mechanism of recruitment of the core repair machinery viz. XPA and proteins further downstream through CSA and CSB is still unclear. However recent research suggests that this may involve the activity of additional proteins such as UVSSA/USP7 complex; XAB2 and HMGN1 (Birger et al., 2003; Fousteri and Mullenders, 2008; Nakatsu et al., 2000; Schwertman et al., 2013).

***Global genome NER***

GG-NER is a more universal pathway, and can directly recognize helix distorting lesions in the entire genome. Recognition via GGNER requires the proteins XPC and DDB2. XPC scans the DNA and recognizes structural deformation of the DNA helix (Hoogstraten et al., 2008). DDB2 assists this recognition in the context of chromatin. Interestingly, GG-NER, *in vitro* on a naked DNA template, does not require the presence of DDB2, suggesting that DDB2 has very specific role in recognition of a DNA lesion in the context of chromatin (Aboussekhra et al., 1995).

XPC forms a complex along with human Rad23 homologue HHR23A/B (RAD23A/B) and CENT2 (Araki et al., 2001; Masutani et al., 1994). The XPC-HHR23B dimer has a higher binding affinity to damaged DNA compared to non-damaged templates, and is dependent on small bubble structures (Sugasawa et al., 1998, Sugasawa, 2001). Surprisingly, XPC alone does not have a very high affinity to CPDs, presumably since they cause a relatively small helix distortion (Kusumoto et al., 2001). RAD23A and RAD23B have redundant functions in NER, it is proposed that their role is to stabilize XPC from proteolysis (Schauber et al., 1998). However,

overexpression of XPC does not completely rescue UV sensitivity in RAD23 deficient cells, suggesting another additional function. CENT2 is a component of the centrosome, and is shown to increase the DNA binding activity of XPC as part of the XPC-RAD23 complex (Nishi et al., 2005). The C-terminal domain of CENT2 interacts with XPC, while the N-terminal interacts with XPA (Nishi et al., 2013). This suggests a possible role in downstream recruitment of the repair machinery after XPC dependent lesion recognition.

The comparatively low efficiency of CPD recognition by XPC suggests the role for another protein to in recognition. A novel protein with specific binding to UV photoproducts was initially described by Feldburg and colleagues (Feldberg and Grossman, 1976), and this protein was found to be missing in cell extracts from XPE patients (Chu and Chang, 1988) and identified as DDB2/XPE. It was later identified that DDB2 in fact exists as a heterodimer consisting of the DDB1 and DDB2 proteins. (Keeney et al., 1993). UV-DDB complex has a high affinity to CPD and 6'-4' photoproducts ( Wittschieben et al., 2005). DDB1 has three WD40 B-propeller domains, and provides a binding platform for DDB2 (Angers et al., 2006; Scrima et al., 2008). DDB2 is docked to the damaged DNA is through the WD40 domains. Although NER *in vitro* can occur in the absence of DDB1/DDB2, their presence increases the efficiency of the reaction. DDB2 binding increases the XPC residency time at lesions (Luijsterburg et al., 2007), and overexpression of DDB2 leads to enhanced DNA damage recognition by (Fitch et al., 2003). All these observations suggest that DDB2 and XPC concertedly act to efficiently recognize a wide variety of DNA damage.

**Core NER repair**

NER mainly differs in the recognition of lesions depending on their genomic contexts. Thus, recognition occurs either via TC-NER (RNA pol II-CSA-CSB) or via direct recognition of DNA structural defects (XPC-DDB2). Recognition by both these mechanisms however leads to recruitment of the same downstream core repair machinery, and the lesion is repaired via a universal NER pathway.

The first step after lesion recognition is XPA mediated lesion verification. XPA is necessary in both GG-NER and TC-NER, and absence of XPA causes extremely severe defects in NER. XPA detects nucleotides with altered chemical structures, interacts with DNA and stabilizes 5' end of

the lesion site (Camenisch et al., 2006; Krasikova et al., 2010). XPA also promotes the recruitment of the ssDNA binding protein RPA.

Lesion verification by XPA is accompanied by recruitment of the multisubunit TFIIH complex (Coin et al., 2007; Li et al., 2015; Spangler et al., 2001). The main NER specific catalytic core of TFIIH consists of the helicases XPB and XPD. It is loaded at the 5'position of the lesion site and creates and open DNA structure by its helicase activity (Evans et al., 1997; Sugasawa, 2001). XPB interacts with XPC enabling its loading on DNA, followed by the binding of XPD to the unwound strand. XPD moves along DNA towards 3' end until it meets the DNA lesion, demarcating the damaged region (Mathieu et al., 2010; Sugasawa et al., 2009). XPA regulates the DNA helicase activity of TFIIH and stabilized the resulting open structure through RPA binding (Li et al., 2015; Sugasawa et al., 2009).

.

In addition to DNA stabilization, RPA is also involved in orienting the endonucleases XPG and ERCC1-XPF for accurate excision of the damaged DNA (de Laat et al., 1998). XPG is recruited through the binding with TFIIH (Dunand-Sauthier et al., 2005), whereas recruitment of ERCC1-XPF depends on the presence of XPA (Tsodikov et al., 2007). After recruitment of both XPG and XPF, the first nick is mediated by ERCC1-XPF at the 5'end, followed by the second nick by XPG at the 3' end. The first 5'incision already leads to gap-filling DNA synthesis thus preventing cytotoxicity triggered by ssDNA. Filling of the gap requires activity of replication associated proteins such as PCNA a, a DNA polymerase and a DNA ligase. Actively replicating cells employ DNA polε and DNA ligase 1, while quiescent cells use DNA polδ, DNA polκ, and a XRCC1-DNA ligase III complex (Moser et al., 2007; Ogi et al., 2010).

## DNA repair in the context of chromatin

The sequential molecular events as well as the proteins playing a role in these processes have been extensively characterized, both in the NER pathway, as well as in other DNA damage repair pathways. However, an important question that is still being answered, is how these repair pathways operate on a chromatin template. As seen in NER, GG-NER requires different recognition proteins from TC-NER. These recognition proteins also interact with histone modifiers and chromatin remodeling enzymes, in order to increase the accessibility of the chromatin template. The current model for the repair of DNA in a chromatin template is the

*Access-Repair-Restore* model (Smerdon, 1991; Green et al., 2002; Soria et al., 2012). This model proposes that chromatin is initially made less ordered, this is followed by binding of recognition and repair proteins, and finally re-setting of the chromatin to its original state. The restoring of chromatin structure is key to maintaining the epigenomic integrity of the cell.

One of the main defining factors of the chromatin landscape of a genomic region, is the histone composition of the chromatin. Histones, and thus nucleosomes can lead to changes in chromatin structure, DNA condensation, as well serve as signals for gene activity. Histone post translational modifications, as well as histone dynamics play an important role in modulation of the DNA damage response (Gurard-Levin et al., 2014; Bartholomew, 2013; Polo, 2014) Analogous to the difference in lesion recognition, GG-NER and TC-NER also differ in their chromatin modification strategies. The various mechanisms by which this occurs during both pathways is described below.

**Mechanisms of regulation of chromatin structure at site of DNA damage**

GG-NER and TC-NER differ in their requirements for modification of the surrounding chromatin. TC-NER occurs in actively transcribed regions which are normally open chromatin. Thus, it is relatively easy for the repair machinery to access the lesion. GG-NER on the other hand, recognizes lesions present throughout the genome. Many of these lesions are present in heterochromatin. Thus, the chromosome structure needs to be disorganized to enable access and recruitment of the repair machinery. Many of the strategies used for modification of chromatin structure are conserved between different processes such as gene activation and DNA repair. The two main strategies to change chromatin accessibility are:

1. Histone modifications
2. ATP dependent chromatin remodeling

Described below are how these strategies are specifically used by cells during NER.

**GG-NER**

**Histone modifications:**

a. Acetylation

Histone acetylation was one of the first histone modification to be discovered, and is usually associated with a more relaxed chromatin state (Kouzarides, 2007). The negatively charged acetyl moieties repel the negatively charged DNA backbone, thus leading to a loser chromatin structure. H4K16ac is one of the prominent histone marks that has a direct effect on chromatin structure and leads to decondensation (Shogren-Knaak et al., 2006). Induction of DNA damage leads to rapid acetylation of core histones, and promotes DNA repair (Ramanathan and Smerdon, 1989). Acetyl transferases such asMOF, GCN5 and TIP60 are associated with DNA damage (Ikura et al., 2000; Ikura et al., 2007; Lee et al., 2010; Li et al., 2010).

Acetylation has been shown to play a role during NER in yeast (Waters et al., 2015). Cells lacking Gcn5 show markedly lower levels of GG-NER as compared to wild-type cells. In mammalian cells, the UV-DDB complex is associated with p300 (Marteijn et al., 2015). Additionally, it has been shown to interact with the chromatin acetylating STAGA complex, which contains GCN5 (Marteijn et al., 2015) (Figure 4). This suggests that acetylation also plays a role in mammalian NER.

a. Methylation

Histone methylation is a mark usually associated with closed chromatin structure. For example, heterochromatin is marked by H3K9me3, and H4K20me3, while polycomb repressed genes show H3K27me3. Since NER recognition requires loosening of chromatin, there are no specific methylation marks associated with changing the chromatin structure during NER recognition. However, other repair pathways such as DSB repair are associated with chromatin compaction. through histone methylation of the chromatin surrounding the site of damage (Campbell et al., 2013). However, certain methylation marks potentially play a role in signaling event during NER. For eg: H4K20me2 is important in DSB as it recruits 53BP1to the sites of damage (Fradet-Turcotte et al., 2013). H4K20me2 also potentially has a role in NER.

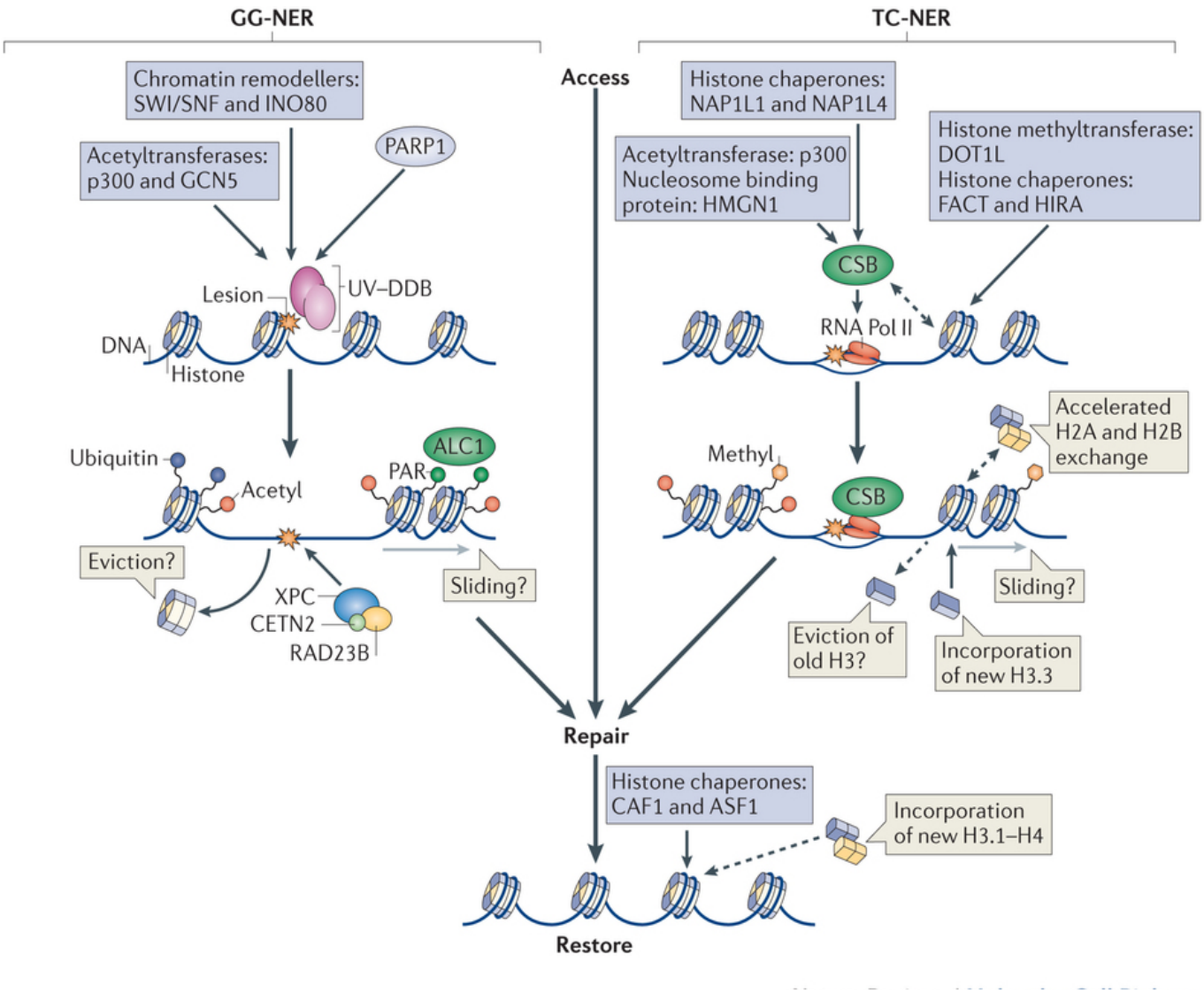


Figure 4: Chromatin dynamics in nucleotide excision repair. Global genome nucleotide excision repair (GG-NER; left) is stimulated by an open chromatin environment, which is promoted by the activity of several chromatin remodellers and histone modifications. Repair is stimulated by the activity of the UV–DDB (ultraviolet (UV) radiation–DNA damage-binding protein) complex, which ubiquitylates core histones and mediates chromatin poly(ADP-ribosyl)ation (PARylation) through its association with poly(ADP-ribosyl) polymerase 1 (PARP1); these processes result in chromatin decondensation. Furthermore, NER is stimulated by histone acetylation, perhaps induced by histone acetyltransferases p300 and GCN5, which are both recruited to UV-radiation-induced damage. The SWI/SNF and INO80 ATP-dependent chromatin remodelling complexes, which displace nucleosomes by histone eviction or sliding, promote repair by interacting with and stimulating the recruitment of GG-NER initiation factors. Amplified in liver cancer protein (ALC1) is an ATP-dependent chromatin remodelling protein that is recruited to PARylated chromatin and stimulates GG-NER. In transcription-coupled NER (TC-NER; right), the chromatin structure is altered by the activity of histone modifiers, histone chaperones and chromatin-remodelling proteins. Cockayne syndrome protein CSB remodels nucleosomes in vitro and this activity is stimulated by the histone chaperones nucleosome assembly protein 1-like 1 (NAP1L1) and NAP1L4, which interact with CSB. CSB attracts the histone acetyltransferase p300 and the nucleoseome binding protein high mobility group nucleosome-binding domain-containing protein 1 (HMGN1) to TC-NER complexes.(Marteijn et al., 2015)

b. Ubiquitination

Monoubiquitination of H2A is one of the most abundant histone modifications. Approximately 10% of nucleosomes contain an H2A ubiquitylated at lysine 119 (H2AK119ubi, further H2A-ubiquitin). This modification is normally present at transcriptionally repressed genomic loci (Stock et al., 2007). H2A is ubiquitinated by RING1B and RBF8 in response to UV-irradiation (Bergink et al., 2006; Marteijn et al., 2009). DDB2, one of the recognition proteins in GG-NER, is a component of a ubiquitin E3 ligase complex UV-CUL4. This complex ubiquitinates the core histones H2A, H3 and H4, as well as DDB2 and XPC (Guerrero-Santoro et al., 2008; Kapetanaki et al., 2006; Wang et al., 2006). Activity of the UV-CUL4 complex, is thought to facilitate H3 eviction from nucleosomes. Ubiquitination of histones H3 and H4 also facilitates nucleosome eviction *in vitro*. (Wang et al., 2006). H2A ubiquitination may also facilitate restoration of chromatin structure after repair completion (Adam et al., 2013).

c. Parylation

PARylation of proteins consists of addition of PAR (poly-(adenosine-ATP-ribose)) moieties at aspartate, glutamate and lysine of the target proteins. DDB2 is also responsible for induction of PARylation dependent chromatin decondensation (Luijsterburg et al., 2012). This role is independent of its role in ubiquitylation through the UV-CUL4 complex. Similar to ubiquitination, DDB2 is also PARylated itself, which enhances binding to damaged DNA and prevent ubiquitin dependent degradation. DDB2 induced PARylation occurs via activity of PARP1 ((poly(ADPribosyl) polymerase 1). PAR-chains, similar to acetyl moieties, have a strong negative charge and can dissociate histone-DNA interactions. This leads to a relaxation in chromatin structure (Poirier et al., 1982). It further leads to recruitment of the ATP dependent chromatin remodeler CHD1L (Pines et al., 2012). The negative charge on PAR chains can also attract DNA/RNA binding proteins and thus serve as a scaffold for docking of repair proteins.

**ATP dependent Chromatin remodeling**

ATP dependent chromatin remodeling is one of the major mechanisms of changing nucleosome distribution along DNA and this chromatin compaction. UV exposure causes mobilization of histones in damaged chromatin. This results in a reduced density of core and linker histones in the adjoining DNA. *In vitro* experiments have shown that a lowered nucleosome density leads to more efficient NER. Damage in SV40 minichromosomes was repaired at a much lower efficiency than lesions in naked DNA in in vitro experiments (Sugasawa et al., 1993)

Various ATP remodeling complexes have been implicated in NER, and specifically in GG-NER. CHD1L (also known as ALC1) is recruited to damage sites as a result of PARP1 mediated PARylation (Pines et al., 2012)). The INO80 complex potentially enhances repair by stimulating the recruitment of XPC and XPA via a DDB1 interaction (Jiang et al., 2010). Additionally, members of the SWI/SNF family of chromatin remodeling proeins lead to enhanced NER, however the exact mechanism remains to be determined (Hara and Sancar, 2002; Zhang et al., 2009; Zhao et al., 2009).

**TC-NER**

Transcription coupled NER recognized lesions in actively transcribing regions, and thus mostly in DNA in an open chromatin conformation. This differs greatly from the mostly closed chromatin environment in which GG-NER operates. In TC-NER, the recognition step is directly tied to chromatin remodeling. CSB, one of the proteins involved in recognition, contains a CSB a DNA dependent ATPase domain of the SNF2 family, that is required for its chromatin binding and repair functions (Muftouglou 2002; Selzer et al., 2002; Lake et al., 2010). *In vitro*, CSB along with the histone chaperones nucleosome assembly protein 1like 1 (NAP1L1) and NAP1L4 can remodel chromatin (Cho et al., 2013). It also additionally interacts with other chromatin proteins like p300 and HMGN1(Marteijn et al., 2015). It still remains to be determined whether CSB also performs this activity *in vivo*.

It is suggested that accelerated histone turnover at sites of damage stimulates TC-NER and resumption of transcription. The FACT complex was found to stimulate accelerated H2A and H2B exchange during TC-NER (Marteijn et al., 2015). Thus, even though TC-NER occurs in open chromatin, it is further regulated by a variety of chromatin modifications

## Spatial Nuclear organization of NER

Eukaryotic nuclei are organized into various functional compartments. Nuclear compartments include the nuclear periphery (nuclear lamina and nuclear pores), nucleoli, nuclear speckles and nuclear bodies like the PML bodies and Cajal bodies (Handwerger and Gall, 2006). The genome is organized inside the nucleus depending on its association with nuclear compartments (Kalousi and Soutoglou, 2016). The highly organized genome compartmentalization raises two important question related to DNA repair processes

1. Does the spatial location of the lesion affect DNA repair?
2. How does DNA damage affect the spatial organization of the nucleus?
3. Does Nucleoide Excision Repair also occur in a specific nuclear body?

I. Does the spatial location of the lesion affect DNA repair?

There have been a few recent insights into this question, however they have been mostly been studied in the context of DSB repair. Unlike UV damage, it is possible to induce a single DSBs in the genome of a cell, at specific genomic loci, using an I-SceI endonuclease based system (Bellaiche et al., 1999). This has enabled a greater insight into how lesion location affects pathway choice in DSB repair. Recent research has shown that the nuclear location of DSBs affects pathway choice (Kalousi and Soutoglou, 2016). Figure 5 summarizes what is known about repair of DSBs in various nuclear compartments.

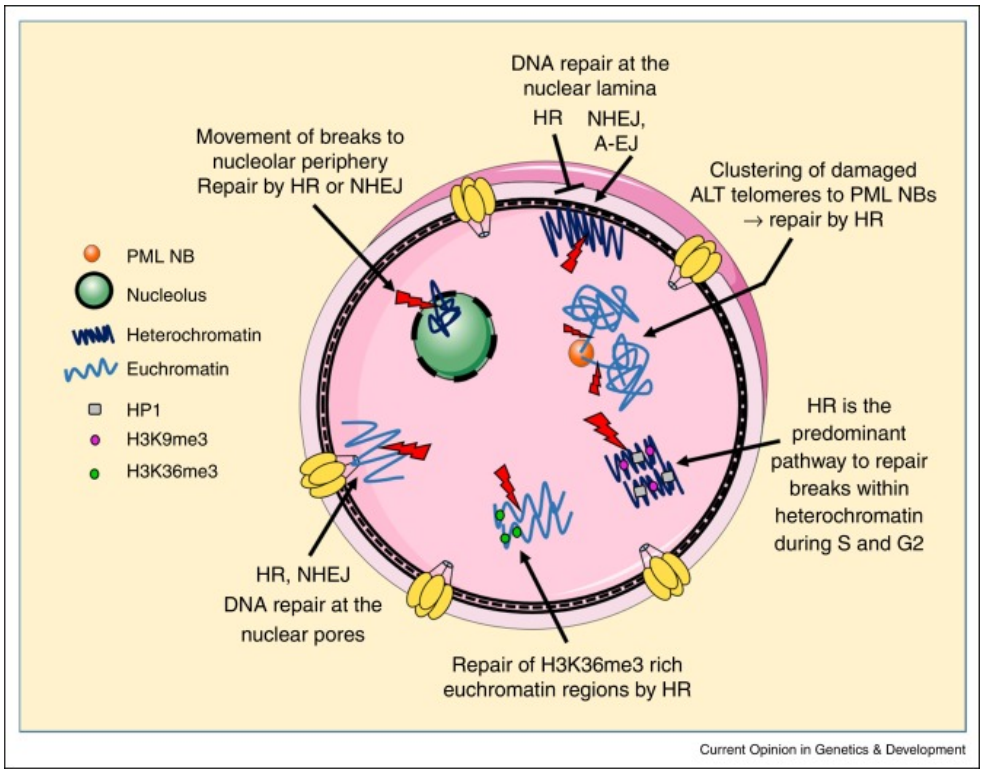


Figure 5: DNA Double Strand Break repair at distinct nuclear compartments of mammalian cells. Adapted from Kalousi and Soutoglou, 2016.

II. How does DNA damage affect the spatial organization of the nucleus?

The DNA damage response also has a global effect on the organization of the various nuclear compartments. The nucleolus as well as PML bodies are observed to undergo a reorganization, in response to both IR and UV irradiation. For example: PML nuclear bodies (NBs) have been proposed to sense DNA lesions and are known to reorganize to abut the sites of damage (Dellaire and Bazett-Jones, 2004; Varadaraj et al., 2007; Dellaire et al., 2006). Importantly, several proteins involved in DNA-damage repair, including Nbs1, are components of PML NBs and, in the presence of DNA damage, they are rapidly released from this NB and relocalize to the sites of DNA damage in order to facilitate lesion repair (reviewed in Warren and Shannahan, 2011) Furthermore, several studies have also shown that PML NBs relocate to nucleolar cap structures in the presence of DNA damage. Importantly, these nucleolar caps sequester Mdm2 (murine double minute 2) at the nucleolus to activate DNA-damage-induced p53 signaling (reviewed in Warren and Shannahan, 2011). Failure of these proteins to localize correctly in the presence of DNA damage, either at repair

foci or at sites distant to the lesion, results in inefficient DNA repair that promotes genomic instability. Various proteins are sequestered in, and released from the nucleolus in response to DNA damage. These processes play an important role in regulation of DNA repair, cell cycle and apoptosis.

III. Does Nucleotide Excision Repair also occur in a specific nuclear body?

Studies of DNA repair have shown that nuclear positioning and migration of the damaged DNA to specific repair centers is a central component of many repair pathways (Lisby et al. 2003; Therizols et al. 2006; Nagai et al. 2008; Misteli and Soutoglou 2009). During NER, there is evidence that the repair machinery is associated with the nuclear matrix, and that there is increased association of the damaged DNA with the nuclear matrix during repair (Koehler and Hanawalt 1996). However, no “repair centers” have so far been identified or spatially characterized in the process of NER. This is one of the questions that is addressed in this thesis.

## References


Aboussekhra, A., Biggerstaff, M., Shivji, M.K., Vilpo, J.A., Moncollin, V., Podust, V.N., Protic, M., Hubscher, U., Egly, J.M., and Wood, R.D. (1995). Mammalian DNA nucleotide excision repair reconstituted with purified protein components. Cell 80, 859-868.

Adam, S., Polo, S.E., and Almouzni, G. (2013). Transcription recovery after DNA damage requires chromatin priming by the H3.3 histone chaperone HIRA. Cell 155, 94-106.

Araki, M., Masutani, C., Takemura, M., Uchida, A., Sugasawa, K., Kondoh, J., Ohkuma, Y., and Hanaoka, F. (2001). Centrosome protein centrin 2/caltractin 1 is part of the xeroderma pigmentosum group C complex that initiates global genome nucleotide excision repair. The Journal of biological chemistry 276, 18665-18672.

Arase, S., Kozuka, T., Tanaka, K., Ikenaga, M., and Takebe, H. (1979). A sixth complementation group in xeroderma pigmentosum. Mutation research 59, 143-146.

Bartholomew B. (2013) Regulating the chromatin landscape: structural and mechanistic perspectives. Annu Rev Biochem.; 83:671–696.

Bellaiche Y, Mogila V, Perrimon N. (1999). I-SceI endonuclease, a new tool for studying DNA double-strand break repair mechanisms in Drosophila. Genetics. 152(3):1037-44.

Bergink, S., Salomons, F.A., Hoogstraten, D., Groothuis, T.A., de Waard, H., Wu, J., Yuan, L., Citterio, E., Houtsmuller, A.B., Neefjes, J., et al. (2006). DNA damage triggers nucleotide excision repair-dependent monoubiquitylation of histone H2A. Genes & development 20, 1343-1352.

Bergink, S., Toussaint, W., Luijsterburg, M.S., Dinant, C., Alekseev, S., Hoeijmakers, J.H., Dantuma, N.P., Houtsmuller, A.B., and Vermeulen, W. (2012). Recognition of DNA damage by XPC coincides with disruption of the XPC-RAD23 complex. The Journal of cell biology 196, 681-688.

Biochemical Society Transactions, 39 (6) 1780-1785;
Birger, Y., West, K.L., Postnikov, Y.V., Lim, J.H., Furusawa, T., Wagner, J.P., Laufer, C.S., Kraemer, K.H., and Bustin, M. (2003). Chromosomal protein HMGN1 enhances the rate of DNA repair in chromatin. The EMBO journal 22, 1665-1675.

Bohr, V.A., Okumoto, D.S., and Hanawalt, P.C. (1986). Survival of UV-irradiated mammalian cells correlates with efficient DNA repair in an essential gene. Proceedings of the National Academy of Sciences of the United States of America 83, 3830-3833.

Bohr, V.A., Smith, C.A., Okumoto, D.S., and Hanawalt, P.C. (1985). DNA repair in an active gene: removal of pyrimidine dimers from the DHFR gene of CHO cells is much more efficient than in the genome overall. Cell 40, 359-369.

Camenisch, U., Dip, R., Schumacher, S.B., Schuler, B., and Naegeli, H. (2006). Recognition of helical kinks by xeroderma pigmentosum group A protein triggers DNA excision repair. Nature structural & molecular biology 13, 278-284.

Campbell, S., Ismail, I.H., Young, L.C., Poirier, G.G., and Hendzel, M.J. (2013). Polycomb repressive complex 2 contributes to DNA double-strand break repair. Cell cycle 12, 2675-2683.

Chapman, J.R., Sossick, A.J., Boulton, S.J., and Jackson, S.P. (2012). BRCA1-associated exclusion of 53BP1 from DNA damage sites underlies temporal control of DNA repair. Journal of cell science 125, 3529-3534.

Cho I, Tsai PF, Lake RJ, Basheer A, Fan HY. (2013). ATP-dependent chromatin remodeling by Cockayne syndrome protein B and NAP1-like histone chaperones is required for efficient transcription-coupled DNA repair. PLoS Genetics

Chu, G., and Chang, E. (1988). Xeroderma pigmentosum group E cells lack a nuclear factor that binds to damaged DNA. Science 242, 564-567.

Cleaver, J.E. (1968). Defective repair replication of DNA in xeroderma pigmentosum. Nature 218, 652-656.

Coin, F., Oksenych, V., and Egly, J.M. (2007). Distinct roles for the XPB/p52 and XPD/p44 subcomplexes of TFIIH in damaged DNA opening during nucleotide excision repair. Molecular cell 26, 245-256.

De Bont, R., and van Larebeke, N. (2004). Endogenous DNA damage in humans: a review of quantitative data. Mutagenesis 19, 169-185.

de Laat, W.L., Appeldoorn, E., Jaspers, N.G., and Hoeijmakers, J.H. (1998). DNA structural elements required for ERCC1-XPF endonuclease activity. The Journal of biological chemistry 273, 7835-7842.

De Weerd-Kastelein, E.A., Keijzer, W., and Bootsma, D. (1972). Genetic heterogeneity of xeroderma pigmentosum demonstrated by somatic cell hybridization. Nature: New biology 238, 80-83.

Dellaire G., Bazett-Jones D.P.(2004) PML nuclear bodies: dynamic sensors of DNA damage and cellular stress. BioEssays 26:963–977.

Dellaire G., Ching R.W., Ahmed K., Jalali F., Tse K.C., Bristow R.G., Bazett-Jones D.P. (2006) Promyelocytic leukemia nuclear bodies behave as DNA damage sensors whose response to DNA double-strand breaks is regulated by NBS1 and the kinases ATM, Chk2, and ATR. J. Cell Biol. 175:55–66.

Dunand-Sauthier, I., Hohl, M., Thorel, F., Jaquier-Gubler, P., Clarkson, S.G., and Scharer, O.D. (2005). The spacer region of XPG mediates recruitment to nucleotide excision repair complexes and determines substrate specificity. The Journal of biological chemistry 280, 7030-7037.

Epstein, W.L., Fukuyama, K., and Epstein, J.H. (1969). Early effects of ultraviolet light on DNA synthesis in human skin in vivo. Archives of dermatology 100, 84-89.

Evans, E., Moggs, J.G., Hwang, J.R., Egly, J.M., and Wood, R.D. (1997). Mechanism of open complex and dual incision formation by human nucleotide excision repair factors. The EMBO journal 16, 6559-6573.

Feldberg, R.S., and Grossman, L. (1976). A DNA binding protein from human placenta specific for ultraviolet damaged DNA. Biochemistry 15, 2402-2408.

Fitch, M.E., Nakajima, S., Yasui, A., and Ford, J.M. (2003). In vivo recruitment of XPC to UV-induced cyclobutane pyrimidine dimers by the DDB2 gene product. The Journal of biological chemistry 278, 46906-46910.

Fousteri, M., and Mullenders, L.H. (2008). Transcription-coupled nucleotide excision repair in mammalian cells: molecular mechanisms and biological effects. Cell research 18, 73-84.

Fousteri, M., Vermeulen, W., van Zeeland, A.A., and Mullenders, L.H. (2006). Cockayne syndrome A and B proteins differentially regulate recruitment of chromatin remodeling and repair factors to stalled RNA polymerase II in vivo. Molecular cell 23, 471-482.

Fradet-Turcotte, A., Canny, M.D., Escribano-Diaz, C., Orthwein, A., Leung, C.C., Huang, H., Landry, M.C., Kitevski-LeBlanc, J., Noordermeer, S.M., Sicheri, F., and Durocher, D. (2013). 53BP1 is a reader of the DNA-damage-induced H2A Lys 15 ubiquitin mark. Nature 499, 50-54.

Franklin, W.A., and Haseltine, W.A. (1986). The role of the (6-4) photoproduct in ultraviolet light-induced transition mutations in E. coli. Mutation research 165, 1-7.

Gerson, S.L. (2004). MGMT: its role in cancer aetiology and cancer therapeutics. Nature reviews. Cancer 4, 296-307.

Green CM, Almouzni G. (2002) When repair meets chromatin. First in series on chromatin dynamics. EMBO Rep. 3:28–33.

Groisman, R., Kuraoka, I., Chevallier, O., Gaye, N., Magnaldo, T., Tanaka, K., Kisselev, A.F., Harel-Bellan, A., and Nakatani, Y. (2006). CSA-dependent degradation of CSB by the ubiquitin-proteasome pathway establishes a link between complementation factors of the Cockayne syndrome. Genes & development 20, 1429-1434.

Guerrero-Santoro, J., Kapetanaki, M.G., Hsieh, C.L., Gorbachinsky, I., Levine, A.S., and Rapic-Otrin, V. (2008). The cullin 4B-based UV-damaged DNA-binding protein ligase binds to UV-damaged chromatin and ubiquitinates histone H2A. Cancer research 68, 5014-5022.

Gurard-Levin ZA, Quivy J-P, Almouzni G. (2014) Histone chaperones: assisting histone traffic and nucleosome dynamics. Annu Rev Biochem. 83:487–517.

Han C, Srivastava AK, Cui T, Wang QE, Wani AA. (2016). Differential DNA lesion formation and repair in heterochromatin and euchromatin. Carcinogenesis.

Handwerger K.E., Gall J.G. (2006). Subnuclear organelles: new insights into form and function. Trends Cell Biol, 16, pp. 19–26

Hara, R. & Sancar, A. (2002). The SWI/SNF chromatin- remodeling factor stimulates repair by human excision nuclease in the mononucleosome core particle. Mol. Cell. Biol. **22**, 6779–6787

Helleday, T. (2003). Pathways for mitotic homologous recombination in mammalian cells. Mutation research 532, 103-115.

Helleday, T., Eshtad, S., and Nik-Zainal, S. (2014). Mechanisms underlying mutational signatures in human cancers. Nature reviews. Genetics 15, 585-598.

Henning, K.A., Li, L., Iyer, N., McDaniel, L.D., Reagan, M.S., Legerski, R., Schultz, R.A., Stefanini, M., Lehmann, A.R., Mayne, L.V., and Friedberg, E.C. (1995). The Cockayne syndrome group A gene encodes a WD repeat protein that interacts with CSB protein and a subunit of RNA polymerase II TFIIH. Cell 82, 555-564.

Hoogstraten, D., Bergink, S., Ng, J.M., Verbiest, V.H., Luijsterburg, M.S., Geverts, B., Raams, A., Dinant, C., Hoeijmakers, J.H., Vermeulen, W., and Houtsmuller, A.B. (2008). Versatile DNA damage detection by the global genome nucleotide excision repair protein XPC. Journal of cell science 121, 2850-2859.

Ikura, T., Ogryzko, V.V., Grigoriev, M., Groisman, R., Wang, J., Horikoshi, M., Scully, R., Qin, J., and Nakatani, Y. (2000). Involvement of the TIP60 histone acetylase complex in DNA repair and apoptosis. Cell 102, 463-473.

Ikura, T., Tashiro, S., Kakino, A., Shima, H., Jacob, N., Amunugama, R., Yoder, K., Izumi, S., Kuraoka, I., Tanaka, K., et al. (2007). DNA damage-dependent acetylation and ubiquitination of H2AX enhances chromatin dynamics. Molecular and cellular biology 27, 7028-7040.

Jiang, Y., Wang, X., Bao, S., Guo, R., Johnson, D.G., Shen, X., and Li, L. (2010). INO80 chromatin remodeling complex promotes the removal of UV lesions by the nucleotide excision repair pathway. Proceedings of the National Academy of Sciences of the United States of America 107, 17274-17279.

Jiricny, J. (2006). The multifaceted mismatch-repair system. Nature reviews. Molecular cell biology 7, 335-346.

Kalousi A, Soutoglou E. (2016) Nuclear compartmentalization of DNA repair. Current Opinion in Genetics and Development

Kamiya, H., Iwai, S., and Kasai, H. (1998). The (6-4) photoproduct of thymine-thymine induces targeted substitution mutations in mammalian cells. Nucleic acids research 26, 2611-2617.

Kapetanaki, M.G., Guerrero-Santoro, J., Bisi, D.C., Hsieh, C.L., Rapic-Otrin, V., and Levine, A.S. (2006). The DDB1-CUL4ADDB2 ubiquitin ligase is deficient in xeroderma pigmentosum group E and targets histone H2A at UV-damaged DNA sites. Proceedings of the National Academy of Sciences of the United States of America 103, 2588-2593.

Keeney, S., Chang, G.J., and Linn, S. (1993). Characterization of a human DNA damage binding protein implicated in xeroderma pigmentosum E. The Journal of biological chemistry 268, 21293-21300.

Koehler DR, Hanawalt PC. (1996). Recruitment of damaged DNA to the nuclear matrix in hamster cells following ultraviolet irradiation. Nucleic acids research **24**: 2877-2884.

Kouzarides, T. (2007). Chromatin modifications and their function. Cell 128, 693-705.

Krasikova, Y.S., Rechkunova, N.I., Maltseva, E.A., Petruseva, I.O., and Lavrik, O.I. (2010). Localization of xeroderma pigmentosum group A protein and replication protein A on damaged DNA in nucleotide excision repair. Nucleic acids research 38, 8083-8094.

Krokan, H.E., and Bjoras, M. (2013). Base excision repair. Cold Spring Harbor perspectives in biology 5, a012583.

Kusumoto, R., Masutani, C., Sugasawa, K., Iwai, S., Araki, M., Uchida, A., Mizukoshi, T., and Hanaoka, F. (2001). Diversity of the damage recognition step in the global genomic nucleotide excision repair in vitro. Mutation research 485, 219-227.

Lake, R. J., Geyko, A., Hemashettar, G., Zhao, Y. & Fan, H. Y. (2010). UV induced association of the CSB remodeling protein with chromatin requires ATP-dependent relief of N terminal autorepression. Mol. Cell 37, 235–246.

Lans, H, Marteijn , A. J., and Vermeulen, W., (2012). ATP-dependent chromatin remodeling in the DNA-damage response. Epigenetics & chromatin

Lee, H.S., Park, J.H., Kim, S.J., Kwon, S.J., and Kwon, J. (2010). A cooperative activation loop among SWI/SNF, gamma-H2AX and H3 acetylation for DNA double-strand break repair. The EMBO journal 29, 1434-1445.

Lee, K.K., and Workman, J.L. (2007). Histone acetyltransferase complexes: one size doesn't fit all. Nature reviews. Molecular cell biology 8, 284-295.

Li, C.L., Golebiowski, F.M., Onishi, Y., Samara, N.L., Sugasawa, K., and Yang, W. (2015). Tripartite DNA Lesion Recognition and Verification by XPC, TFIIH, and XPA in Nucleotide Excision Repair. Molecular cell 59, 1025-1034.

Li, G.M. (2008). Mechanisms and functions of DNA mismatch repair. Cell research 18, 85-98.

Lisby M, Mortensen UH, Rothstein R. (2003). Colocalization of multiple DNA double strand breaks at a single Rad52 repair centre. Nat Cell Biol **5**: 572-577.

Luijsterburg, M.S., Goedhart, J., Moser, J., Kool, H., Geverts, B., Houtsmuller, A.B., Mullenders, L.H., Vermeulen, W., and van Driel, R. (2007). Dynamic in vivo interaction of DDB2 E3 ubiquitin ligase with UV-damaged DNA is independent of damage-recognition protein XPC. Journal of cell science 120, 2706-2716.

Luijsterburg, M.S., Lindh, M., Acs, K., Vrouwe, M.G., Pines, A., van Attikum, H., Mullenders, L.H., and Dantuma, N.P. (2012). DDB2 promotes chromatin decondensation at UV-induced DNA damage. The Journal of cell biology 197, 267-281.

Marteijn, J.A., Bekker-Jensen, S., Mailand, N., Lans, H., Schwertman, P., Gourdin, A.M., Dantuma, N.P., Lukas, J., and Vermeulen, W. (2009). Nucleotide excision repair-induced H2A ubiquitination is dependent on MDC1 and RNF8 and reveals a universal DNA damage response. The Journal of cell biology 186, 835-847.

Marteijn, J.A., Lans, H., Vermeulen, W., and Hoeijmakers, J.H. (2014). Understanding nucleotide excision repair and its roles in cancer and ageing. Nature reviews. Molecular cell biology 15, 465-481.

Mathieu, N., Kaczmarek, N., and Naegeli, H. (2010). Strand- and site-specific DNA lesion demarcation by the xeroderma pigmentosum group D helicase. Proceedings of the National Academy of Sciences of the United States of America 107, 17545-17550.

Mellon, I., Spivak, G., and Hanawalt, P.C. (1987). Selective removal of transcription-blocking DNA damage from the transcribed strand of the mammalian DHFR gene. Cell 51, 241-249.

Misteli T, Soutoglou E. (2009). The emerging role of nuclear architecture in DNA repair and genome maintenance. Nature reviews Molecular cell biology **10**: 243-254.

Moser, J., Kool, H., Giakzidis, I., Caldecott, K., Mullenders, L.H., and Fousteri, M.I. (2007). Sealing of chromosomal DNA nicks during nucleotide excision repair requires XRCC1 and DNA ligase III alpha in a cell-cycle-specific manner. Molecular cell 27, 311-323.

Muftuoglu, M., Selzer, R., Tuo, J., Brosh, R. M. Jr & Bohr, V. A. (2002). Phenotypic consequences of mutations in the conserved motifs of the putative helicase domain of the human Cockayne syndrome group B gene. Gene 283, 27–40

Nagai S, Dubrana K, Tsai-Pflugfelder M, Davidson MB, Roberts TM, Brown GW, Varela E, Hediger F, Gasser SM, Krogan NJ. (2008). Functional targeting of DNA damage to a nuclear pore-associated SUMO-dependent ubiquitin ligase. Science **322**: 597-602.

Nakatsu, Y., Asahina, H., Citterio, E., Rademakers, S., Vermeulen, W., Kamiuchi, S., Yeo, J.P., Khaw, M.C., Saijo, M., Kodo, N., et al. (2000). XAB2, a novel tetratricopeptide repeat protein involved in transcription-coupled DNA repair and transcription. The Journal of biological chemistry 275, 34931-34937.

Nishi, R., Sakai, W., Tone, D., Hanaoka, F., and Sugasawa, K. (2013). Structure-function analysis of the EF-hand protein centrin-2 for its intracellular localization and nucleotide excision repair. Nucleic acids research 41, 6917-6929.

Ogi, T., Limsirichaikul, S., Overmeer, R.M., Volker, M., Takenaka, K., Cloney, R., Nakazawa, Y., Niimi, A., Miki, Y., Jaspers, N.G., et al. (2010). Three DNA polymerases, recruited by different mechanisms, carry out NER repair synthesis in human cells. Molecular cell 37, 714-727.

Pines, A., Vrouwe, M.G., Marteijn, J.A., Typas, D., Luijsterburg, M.S., Cansoy, M., Hensbergen, P., Deelder, A., de Groot, A., Matsumoto, S., et al. (2012). PARP1 promotes nucleotide excision repair through DDB2 stabilization and recruitment of ALC1. The Journal of cell biology 199, 235-249.

Poirier, G.G., de Murcia, G., Jongstra-Bilen, J., Niedergang, C., and Mandel, P. (1982). Poly(ADP-ribosyl)ation of polynucleosomes causes relaxation of chromatin structure. Proceedings of the National Academy of Sciences of the United States of America 79, 3423-3427.

Polo SE. (2014) Reshaping chromatin after DNA damage: the choreography of histone proteins. Journal of Molecular Biology

Ramanathan, B., and Smerdon, M.J. (1989). Enhanced DNA repair synthesis in hyperacetylated nucleosomes. The Journal of biological chemistry 264, 11026-11034.

Schauber, C., Chen, L., Tongaonkar, P., Vega, I., Lambertson, D., Potts, W., and Madura, K. (1998). Rad23 links DNA repair to the ubiquitin/proteasome pathway. Nature 391, 715-718.

Schwertman, P., Vermeulen, W., and Marteijn, J.A. (2013). UVSSA and USP7, a new couple in transcription-coupled DNA repair. Chromosoma 122, 275-284.

Selzer, R. R., Nyaga, S., Tuo, J., May, A., Muftuoglu, M., Christiansen, M., Bohr, V. A. (2002). Differential requirement for the ATPase domain of the Cockayne syndrome group B gene in the processing of UV-induced DNA damage and 8-oxoguanine lesions in human cells. Nucleic Acids Research, 30(3), 782–793.

Sharma, S., Salehi, F., Scheithauer, B.W., Rotondo, F., Syro, L.V., and Kovacs, K. (2009). Role of MGMT in tumor development, progression, diagnosis, treatment and prognosis. Anticancer research 29, 3759-3768.

Shiloh, Y., and Ziv, Y. (2013). The ATM protein kinase: regulating the cellular response to genotoxic stress, and more. Nature reviews. Molecular cell biology 14, 197-210.

Shogren-Knaak, M., Ishii, H., Sun, J.M., Pazin, M.J., Davie, J.R., and Peterson, C.L. (2006). Histone H4-K16 acetylation controls chromatin structure and protein interactions. Science 311, 844-847.

Sigurdsson, S., Dirac-Svejstrup, A.B., and Svejstrup, J.Q. (2010). Evidence that transcript cleavage is essential for RNA polymerase II transcription and cell viability. Molecular cell 38, 202-210.

Smerdon MJ. DNA repair and the role of chromatin structure. (1991). Curr Opin Cell Biol. 3:422– 428.

Sonoyama, T., Ui, M., Enomoto, T., Takio, K., Tanaka, K., van der Spek, P.J., Bootsma, D., and et al. (1994). Purification and cloning of a nucleotide excision repair complex involving the xeroderma pigmentosum group C protein and a human homologue of yeast RAD23. The EMBO journal 13, 1831-1843.

Soria G, Polo SE, Almouzni G. (2012) Prime, repair, restore: the active role of chromatin in the DNA damage response. Mol Cell.; 46:722–734.

Spangler, L., Wang, X., Conaway, J.W., Conaway, R.C., and Dvir, A. (2001). TFIIH action in transcription initiation and promoter escape requires distinct regions of downstream promoter DNA. Proceedings of the National Academy of Sciences of the United States of America 98, 5544-5549.

Stock, J.K., Giadrossi, S., Casanova, M., Brookes, E., Vidal, M., Koseki, H., Brockdorff, N., Fisher, A.G., and Pombo, A. (2007). Ring1-mediated ubiquitination of H2A restrains poised RNA polymerase II at bivalent genes in mouse ES cells. Nature cell biology 9, 1428-1435.

Stracker, T.H., and Petrini, J.H. (2011). The MRE11 complex: starting from the ends. Nature reviews. Molecular cell biology 12, 90-103.

Sugasawa, K. (2001). [Molecular mechanism of mammalian nucleotide excision repair]. Tanpakushitsu kakusan koso. Protein, nucleic acid, enzyme 46, 893-901.

Sugasawa, K., Akagi, J., Nishi, R., Iwai, S., and Hanaoka, F. (2009). Two-step recognition of DNA damage for mammalian nucleotide excision repair: Directional binding of the XPC complex and DNA strand scanning. Molecular cell 36, 642-653.

Sugasawa, K., Masutani, C. & Hanaoka, F. (1993) Cell-free repair of UV-damaged simian virus 40 chromosomes in human cell extracts. J. Biol. Chem. 268, 9098–9104.

Sugasawa, K., Ng, J.M., Masutani, C., Iwai, S., van der Spek, P.J., Eker, A.P., Hanaoka, F., Bootsma, D., and Hoeijmakers, J.H. (1998). Xeroderma pigmentosum group C protein complex is the initiator of global genome nucleotide excision repair. Molecular cell 2, 223-232.

Sugasawa, K., Okuda, Y., Saijo, M., Nishi, R., Matsuda, N., Chu, G., Mori, T., Iwai, S., Tanaka, K., Tanaka, K., and Hanaoka, F. (2005). UV-induced ubiquitylation of XPC protein mediated by UV-DDB-ubiquitin ligase complex. Cell 121, 387-400.

Therizols P, Fairhead C, Cabal GG, Genovesio A, Olivo-Marin JC, Dujon B, Fabre E. (2006). Telomere tethering at the nuclear periphery is essential for efficient DNA double strand break repair in subtelomeric region. The Journal of cell biology **172**: 189-199.

Troelstra, C., van Gool, A., de Wit, J., Vermeulen, W., Bootsma, D., and Hoeijmakers, J.H. (1992). ERCC6, a member of a subfamily of putative helicases, is involved in Cockayne's syndrome and preferential repair of active genes. Cell 71, 939-953.

Tsodikov, O.V., Ivanov, D., Orelli, B., Staresincic, L., Shoshani, I., Oberman, R., Scharer, O.D., Wagner, G., and Ellenberger, T. (2007). Structural basis for the recruitment of ERCC1-XPF to nucleotide excision repair complexes by XPA. The EMBO journal 26, 4768-4776.

Tung, B.S., McGregor, W.G., Wang, Y.C., Maher, V.M., and McCormick, J.J. (1996). Comparison of the rate of excision of major UV photoproducts in the strands of the human HPRT gene of normal and xeroderma pigmentosum variant cells. Mutation research 362, 65-74.

Varadaraj A., Dovey C.L., Laredj L., Ferguson B., Alexander C.E., Lubben N., Wyllie A.H., Rich T. (2007) Evidence for the receipt of DNA damage stimuli by PML nuclear domains. J. Pathol. 211:471–480.

Wang, H., Wang, L., Erdjument-Bromage, H., Vidal, M., Tempst, P., Jones, R.S., and Zhang, Y. (2004). Role of histone H2A ubiquitination in Polycomb silencing. Nature 431, 873-878.

Wang, H., Zhai, L., Xu, J., Joo, H.Y., Jackson, S., Erdjument-Bromage, H., Tempst, P., Xiong, Y., and Zhang, Y. (2006). Histone H3 and H4 ubiquitylation by the CUL4-DDB-ROC1 ubiquitin ligase facilitates cellular response to DNA damage. Molecular cell 22, 383-394.

Warren, D.T., Shanahan, C.M. (2011). Defective DNA-damage repair induced by nuclear lamina dysfunction is a key mediator of smooth muscle cell aging

Waters R, van Eijka P, Reeda, S. (2015). Histone modification and chromatin remodeling during NER. DNA Repair

Wittschieben, B.O., Iwai, S., and Wood, R.D. (2005). DDB1-DDB2 (xeroderma pigmentosum group E) protein complex recognizes a cyclobutane pyrimidine dimer, mismatches, apurinic/apyrimidinic sites, and compound lesions in DNA. The Journal of biological chemistry 280, 39982-39989.

Y., Watanabe, E., Mori, T., Iwai, S., Masutani, C., Sugasawa, K., and Hanaoka, F. (2005). Centrin 2 stimulates nucleotide excision repair by interacting with xeroderma pigmentosum group C protein. Molecular and cellular biology 25, 5664-5674.

Zhang, L., Zhang, Q., Jones, K., Patel, M. & Gong, F.(2009). The chromatin remodeling factor BRG1 stimulates nucleotide excision repair by facilitating recruitment of XPC to sites of DNA damage. Cell Cycle **8**, 3953–3959

Zhao Q1, Wang QE, Ray A, Wani G, Han C, Milum K, Wani AA. (2009). Modulation of nucleotide excision repair by mammalian SWI/SNF chromatin-remodeling complex. J. Biol. Chem. **284**, 30424–30432

Zimmermann, M., and de Lange, T. (2014). 53BP1: pro choice in DNA repair. Trends in cell biology 24, 108-117.

# Aims of the study

The main aim of this thesis is to determine the mechanisms of GG-NER recognition in a chromatin context, and the various methods of regulation of chromatin organization during NER. The specific aims are:

- Identify the role of ZRF1 and RING1B in NER
- Identifying the role of nuclear compartmentalization in NER
- Elucidate the role of DICER in NER
- Elucidate the link between lesion recognition and recruitment of repair proteins

# ZRF1 mediates remodeling of E3 ligases at DNA lesion sites during nucleotide excision repair

J Cell Biol. 2016 Apr 25;213(2):185-200.

# ZRF1 mediates remodeling of E3 ligases at DNA lesion sites during nucleotide excision repair

Ekaterina Gracheva,[1]* Shalaka Chitale,[1]* Thomas Wilhelm,[1] Alexander Rapp,[2] Jonathan Byrne,[1] Jens Stadler,[1] Rebeca Medina,[1] M. Cristina Cardoso,[2] and Holger Richly[1]

[1]*E. Gracheva and S. Chitale contributed equally to this paper.

Correspondence to Holger Richly: h.richly@imb-mainz.de

Abbreviations used in this paper: CPD, cyclobutane pyrimidine dimer; DSB, double-strand break; GG, global genome; NER, nucleotide excision repair; TC, transcription coupled; UDS, unscheduled DNA synthesis.

Laboratory of Molecular Epigenetics, Institute of Molecular Biology, 55128 Mainz, Germany [2]Department of Biology, Technische Universität Darmstadt, 64287 Darmstadt, Germany

Faithful DNA repair is essential to maintain genome integrity. Ultraviolet (UV) irradiation elicits both the recruitment of DNA repair factors and the deposition of histone marks such as monoubiquitylation of histone H2A at lesion sites. Here, we report how a ubiquitin E3 ligase complex speci c to DNA repair is remodeled at lesion sites in the global genome nucleotide excision repair (GG-NER) pathway. Monoubiquitylation of histone H2A (H2A-ubiquitin) is catalyzed pre- dominantly by a novel E3 ligase complex consisting of DDB2, DDB1, CUL4B, and RING1B (UV–RING1B complex) that acts early during lesion recognition. The H2A-ubiquitin binding protein ZRF1 mediates remodeling of this E3 ligase complex directly at the DNA lesion site, causing the assembly of the UV–DDB–CUL4A E3 ligase complex (DDB1–DDB2– CUL4A-RBX1). ZRF1 is an essential factor in GG-NER, and its function at damaged chromatin sites is linked to damage recognition factor XPC. Overall, the results shed light on the interplay between epigenetic and DNA repair recognition factors at DNA lesion sites.

## Introduction

Nucleotide excision repair (NER) constitutes one of the major DNA repair pathways. It handles various helix-distorting DNA lesions such as 6–4 photoproducts and cyclobutane pyrimidine dimers (CPDs), arising after exposure to UV light (de Laat et al., 1999). Impaired NER activity is associated with several ge- netic disorders such as *Xeroderma pigmentosum*, which is char- acterized by hypersensitivity to sunlight and a predisposition for skin cancer (Friedberg, 2001). Mammalian NER comprises two pathways that differ in the nature of recognizing DNA lesions. Transcription-coupled (TC) NER is con ned to regions of ac- tive transcription, where stalled RNA polymerase II triggers the DNA damage response. In contrast, global genome (GG) NER represents the transcription-independent recognition of lesions. The recognition step is followed by veri cation of the

lesion by the repair factor XPA and by the formation of the preexcision complex involving TFIIH and its helicase subunits XPB and XPD. Subsequently, the DNA lesion is excised by the endo- nucleases XPF and XPG, and the gap is lled by DNA poly- merases. (Fousteri and Mullenders, 2008; Marteijn et al., 2014).

In GG-NER DNA lesions are recognized by two well- described factors: XPC and DDB2. XPC represents a struc- ture speci c DNA binding factor, which speci cally binds helix-distorting structures (Sugasawa et al., 1998; Riedl et al., 2003). XPC forms a stable complex with the Rad23 homologs RAD23A or RAD23B, respectively, and centrin2 (Masutani et al., 1994; Araki et al., 2001). This trimeric complex binds to a variety of lesions, triggers NER activity, and rapidly dissoci- ates after binding damaged DNA (Sugasawa et al., 2001; Hoog- straten et al., 2008; Bergink et al., 2012). Ef cient recognition of CPDs and 6–4 photoproducts also requires the presence of DDB2 (XPE; Tang et al., 2000; Fitch et al., 2003; Moser et al., 2005; Luijsterburg et al., 2007; Nishi et al., 2009). Loss of func- tional DDB2 causes defective repair of CPDs, reduced repair of 6–4 photoproducts, and hypersensitivity to UV-induced skin cancer (Rapić-Otrin et al., 2003; Alekseev et al., 2005). DDB2 along with DDB1, the RING-domain protein RBX1, and either of the scaffold proteins CUL4A or CUL4B forms E3 ubiqui- tin ligase complexes (UV–DDB–CUL4A/B) that catalyze the monoubiquitylation of histones H2A, H3, and H4 (Shiyanov et al., 1999; Groisman et al., 2003; Angers et al., 2006; Wang et al., 2006; Guerrero-Santoro et al., 2008). Importantly, the UV–DDB–CUL4A complex catalyzes the polyubiquitylation of XPC, thereby increasing its af nity for DNA in vitro and contributing to recognition and stable binding of photolesions (Sugasawa et al., 2005).

A prominent histone modi cation present at DNA damage sites is ubiquitylation of histones H2A, H2AX, and H1 (Bergink et al., 2006; Mailand et al., 2007; Pan et al., 2011; Thorslund et al., 2015). At double-strand breaks (DSBs), ubiquitylation histones is catalyzed by the E3 ligases RNF168, RNF8, and RING1B (Doil et al., 2009; Pan et al., 2011; Mattiroli et al., 2012; Ui et al., 2015). During NER, H2A ubiquitylation is cat- alyzed by the E3 ligase RNF8 and the UV–DDB–CUL4A/B complexes (Bergink et al., 2006; Kapetanaki et al., 2006; Guer- rero-Santoro et al., 2008; Marteijn et al., 2009). Further, it was demonstrated that H2A ubiquitylation after UV irradiation de- pends on RING1B (Bergink et al., 2006). RING1B constitutes a subunit of the Polycomb group repressive complex 1 (PRC1), which catalyzes the monoubiquitylation of histone H2A at lysine 119 to silence genes during pluripotency (Wang et al., 2004; Morey and Helin, 2010). Interestingly, at DSBs, H2A ubiquitylation is dependent on the PRC1 subunits BMI-1 and RING1B (Ismail et al., 2010; Chagraoui et al., 2011; Ginjala et al., 2011; Pan et al., 2011). More recently, it was reported that PRC1 mediates DSB-induced gene silencing, linking PRC1 strongly to DSB repair (Ui et al., 2015). Still, it remains unclear how the E3 ligases cross talk and in which sequence they act during DNA repair.

We have previously shown that Zuotin-related factor 1 (ZRF1) binds monoubiquitylated histone H2A via its ubiqui- tin-binding domain and removes PRC1 from chromatin during

cellular differentiation (Richly et al., 2010). Given the signi - cance of H2A ubiquitylation in DNA repair, we have set out to study the roles of RING1B and ZRF1 in NER. Our results reveal that RING1B is the catalytic subunit of a novel DDB–cullin–E3 ligase complex, which ubiquitylates histone H2A early during NER. Further, we discovered that ZRF1 is a switch protein that remodels chromatin-bound E3 ligases during lesion recognition. Hence, our study sheds new light on the interplay of epi- genetic and DNA repair recognition factors at DNA lesion sites.

## Results

**RING1B mediates ubiquitylation of histone H2A after UV irradiation** To distinguish the functions of E3 ligases functioning after UV irradiation, we performed knockdown of RING1B (shRING1B), RNF168 (siRNF168), and the scaffold protein CUL4A (siCUL4A), which is a component of the UV–DDB–CUL4A E3 complex, in HEK293T cells. To assess the recruitment of the respective E3 ligases to chromatin, we cross-linked cells at the given time points after UV irradiation and isolated the chromatin fraction. We measured the relative intensities of H2A ubiquitin and H2A after probing Western blots with H2A antibodies. We observed that the reduction of RING1B hampered the increase of H2A ubiquitylation, whereas knockdown of the other E3 li- gases did not signi cantly alter H2A ubiquitin levels (Fig. 1 A; representative Western blots of the analysis: Figs. 1 B and S1, A and B). We also con rmed that RING1B speci cally catalyzes monoubiquitylation of lysine 119 at histone H2A after UV ir- radiation (Figs. 1 B and S1 C). Additionally, we con rmed that knockdown of CUL4A renders the UV–DDB–CUL4A E3 li- gase inactive (Fig. S1 A). To further assess whether RING1B is recruited to DNA damage sites, we performed microirradiation experiments with a 405-nm laser in cells expressing DDB2-GFP and RING1B-YFP fusion proteins (Fig. S1, D–F). We observed that both DDB2 and RING1B show a relatively weak, but sig- ni cant accumulation to sites of DNA damage, consistent with a previous observation demonstrating RING1B-mediated accu- mulation of H2A-ubiquitylation at DNA damage sites (Bergink

et al., 2006). Further, we did not observe any major difference in cellular ubiquitylation levels upon depletion of RING1B (Fig. S1, G and H) as suggested previously (Bergink et al., 2006). To link RING1B to the NER pathway, we investigated its func- tion performing UV irradiation experiments with the nematode *Caenorhabditis elegans* (Lans and Vermeulen, 2011; Craig et al., 2012). Compared with wild-type animals treated with a con- trol RNAi (N2/control), we observed a reduction of viability after UV irradiation of the RING1B mutant treated with control RNAi (VC31/control) and upon RNAi-mediated depletion of the NER factor XPC in wild-type worms (N2/*xpc-1*; Fig. 1 C). Knockdown of XPC in RING1B mutant strains (VC31/*xpc-1*) did not exhibit further reduction of viability, suggesting that RING1B is epistatic to XPC.

Given the function of PRC1 at DSBs, we next determined whether PRC1 plays a role in H2A ubiquitylation after UV irradiation. Knockdown of BMI-1 displayed only a slight effect on the recruitment of RING1B and the deposition of H2A ubiquitin (Fig. 1 D), which is likely a consequence of reduced RING1B and H2A-ubiquitin basal levels. A colony

formation assay showed that knockdown of either RING1B or BMI-1 ex- hibits a mild reduction of the colony formation potential. In- terestingly, simultaneous knockdown of both proteins showed additive reduction of the colony formation potential, suggesting that BMI-1 and RING1B likely exert different functions in the repair of UV-mediated DNA lesions (Fig. 1 E). Notably, we ob- served a similar relationship performing an epistasis analysis with the *C. elegans* orthologs of BMI-1 (*mig-32*) and RING1B (*spat-3*; Karakuzu et al., 2009; Fig. S1 I).

Collectively, these data suggest a critical role for RING1B in H2A-ubiquitylation in the NER pathway. Opposed to its function at DSBs, RING1B seems to catalyze the ubiquitylation reaction without its PRC1 binding partner BMI-1.

**RING1B and DDB2 cooperate in the ubiquitylation of histone H2A** Intrigued by the epistatic relationship of XPC and RING1B, we sought to nd out whether RING1B is linked to the NER machinery. We expressed $^{FLAG}$RING1B in HEK293T cells and performed af nity puri cations. As expected, RING1B binds the PRC1 subunit BMI-1 (Wang et al., 2004; Fig. 2 A). Inter- estingly, RING1B interacts robustly with DDB2, but not with other selected factors of the NER pathway (Figs. 2 A and S2 A). Immunoprecipitation of endogenous RING1B further veri ed the interaction of DDB2 with RING1B (Fig. 2 B). Likewise, pu- ri cations performed with $^{FLAG}$DDB2 displayed strong binding of RING1B and interaction with its well-characterized binding partners DDB1 and CUL4A (Shiyanov et al., 1999; Fig. 2 C).

Next, we examined whether DDB2 and BMI-1 interact with RING1B in a mutually exclusive manner. Immunoprecip- itating BMI-1 we observed binding of RING1B, but not DDB2 (Fig. S2 B). Overexpression of BMI-1 caused a slight increase in the BMI-1–RING1B interaction but a complete loss of DDB2-RING1B binding (Fig. S2 C). Depletion of BMI-1 had only a slight effect on the DDB2–RING1B interaction (Fig. S2 D). These data suggest that the majority of RING1B is associ- ated with BMI-1 rather than DDB2, which is in agreement with the general function of PRC1 in gene silencing.

To investigate a joint function of DDB2 and RING1B in DNA repair, we performed colony formation assays (Fig. 2 D). After depletion of DDB2 we observed reduced colony forma- tion potential, which is in agreement with a previous study



showing impaired survival of XPE patient fibroblasts after UV irradiation (Rapić-Otrin et al., 2003). Similarly, deple- tion of RING1B exhibited reduced colony formation po- tential. Simultaneous depletion of both proteins showed no further reduction of colony formation potential, suggesting that RING1B and DDB2 likely act in a common DNA re- pair pathway. To further support this finding, we analyzed skin biopsy specimens after staining with DDB2 and H2A ubiquitin or RING1B antibodies, respectively (Fig. S2, E, G, and I). We observed a clear correlation of DDB2 with both RING1B and H2A-

ubiquitin only in UV exposed skin sections as judged by single cell quantification of staining intensities (Fig. S2, F and H). Depletion of RING1B did not hamper the recruitment of DDB2 or BMI-1 to chroma- tin after UV irradiation (Fig. 2 E), implying divergent roles for RING1B and BMI-1 in UV-triggered DNA repair. Cells depleted of DDB2 as well as XPE patient fibroblasts exhib- ited reduced H2A ubiquitylation consistent with a previous study (Kapetanaki et al., 2006) and diminished recruitment of RING1B to chromatin (Figs. 2 F, 4 G, and S2 K). Nota- bly, knockdown of DDB2 did not impair BMI-1 recruitment to chromatin, further uncoupling BMI-1 from H2A ubiqui- tylation in NER (Figs. 2 F and S2 J).

In sum, these data suggest a functional interplay of DDB2 and RING1B in H2A ubiquitylation during NER.

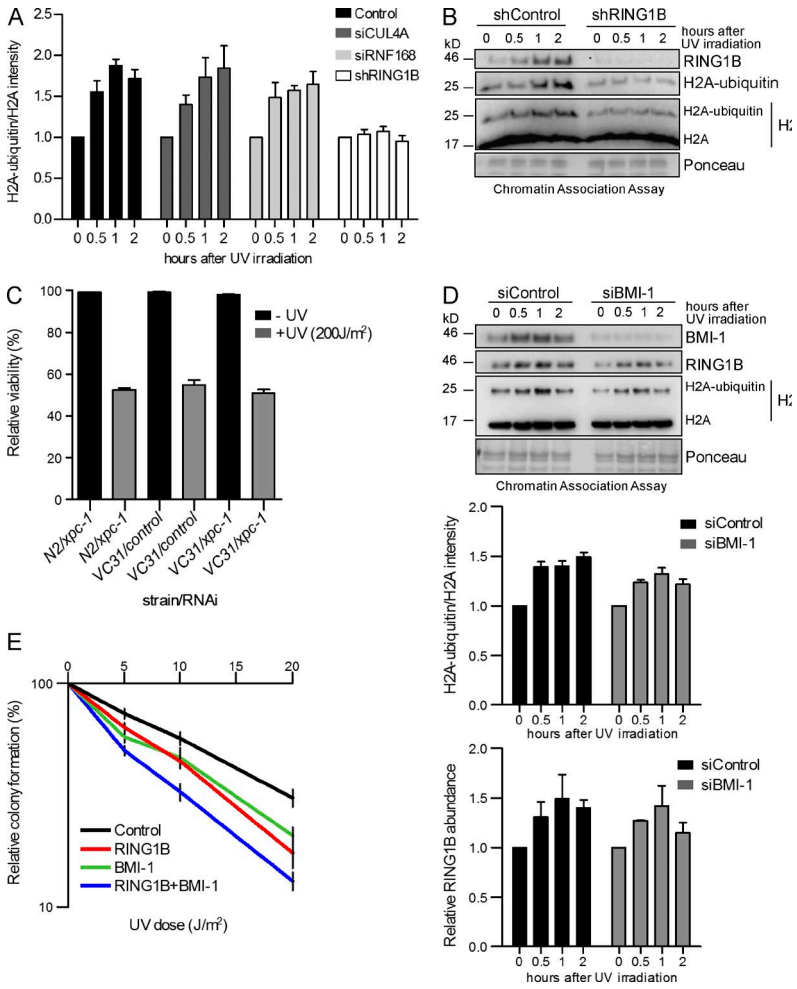


Figure 1. **Dissection of E3 ligase functions in UV-medi- ated DNA damage repair.** (A) Quantitative analysis of H2A-ubiquitylation levels. Immunoblots (as in B and Fig. S1, A and B) were probed with histone H2A antibody. The intensities of H2A and H2A-ubiquitin bands were quanti- ed by the ImageJ software. The graphs illustrate the rel- ative H2A ubiquitylation calculated as (H2A ubiquitin)/ (H2A +

H2A ubiquitin), normalized to Ponceau staining intensity after knockdown of the respective proteins (H2A ubiquitin/H2A). Values are normalized to the value from nonirradiated cells and are given as mean ± SEM ($n$ = 4). (B) Monoubiquitylation of histone H2A at lysine 119 after UV irradiation is mainly catalyzed by RING1B. Chroma- tin association assays of control and RING1B knockdown HEK293T cells after UV irradiation. De–cross-linked mate- rial of the respective time points was subjected to Western blotting and probed with the indicated antibodies. The speci city of the H2A-ubiquitin antibody was veri ed (Fig. S1 C). (C) Epistatic relationship of *xpc-1* and *spat- 3*. Wild-type nematodes (N2) or *spat-3* mutants (VC31) were fed with either control or *xpc-1* RNAi–producing bacteria. The relative viability was analyzed after UV ir- radiation (200 J/m$^2$). Values are given as mean ± SEM ($n$ = 3). (D) Impact of BMI-1 on RING1B-mediated H2A ubiquitylation after UV irradiation. Chromatin association assays of UV-irradiated HEK293T cells treated with siRNAs (control, *BMI-1*). De–cross-linked material of the respective time points was subjected to Western blotting and probed with the indicated antibodies. Relative intensities of H2A ubiquitin/H2A and RING1B abundance after BMI-1 de- pletion were measured. Values are given as mean ± SEM ($n$ = 4). (E) Epistatic relationship of RING1B and BMI-1 in response to UV irradiation. Relative colony formation po- tential of control or RING1B knockdown cell lines treated with siRNA was analyzed at different UV doses. Control cells were transfected with either control siRNA (control) or BMI-1 siRNA (*BMI-1*). RING1B knockdown cell lines were transfected with either control siRNA (*RING1B*) or BMI-1 siRNA (*RING1B* + *BMI-1*). Gene knockdown was con rmed by Western blots (not depicted). Values are given as mean ± SEM ($n$ = 9).

**RING1B forms a stable protein complex with CUL4B, DDB1, and DDB2** To reveal the composition of the putative RING1B-DDB2 E3 ligase complex, we expressed $^{FLAG}$DDB2 in HEK293T cells and performed puri cations in UV-irradiated and untreated cells (Fig. 3 A and Table S5). After elution of $^{FLAG}$DDB2 containing protein complexes with FLAG peptide, we subsequently used the eluate in immunoprecipitations with RING1B antibodies to speci cally purify RING1B-DDB2 containing protein com- plexes. The puri ed material was subjected to mass spectrom- etry, identifying DDB1 and CUL4B as the main interactors of RING1B and DDB2 (UV–RING1B complex in Fig. 3 A and Table S5). Furthermore, immunoprecipitations of endogenous DDB1 or RING1B as well as pull-downs with recombinant GST–RING1B and puri ed DDB1–DDB2 complexes con- rmed our ndings (Fig. S3, A–D). To verify the assembly of the UV–RING1B E3 ligase complex, we overexpressed $^{FLAG}$DDB1, $^{FLAG}$DDB2, and $^{FLAG}$RING1B with or without $^{FLAG\text{-}STREP}$CUL4B in HEK293T cells (Fig. 3 B). Af nity puri cations of CUL4B revealed speci c binding of DDB1, DDB2, and RING1B. We further analyzed the interactions of the subunits of the UV– RING1B complex in vitro by pull-down experiments with puri ed proteins (Fig. S3 E). Collectively, these experiments revealed that RING1B speci cally binds to CUL4B and DDB2 but shows no direct interaction with either CUL4A or DDB1

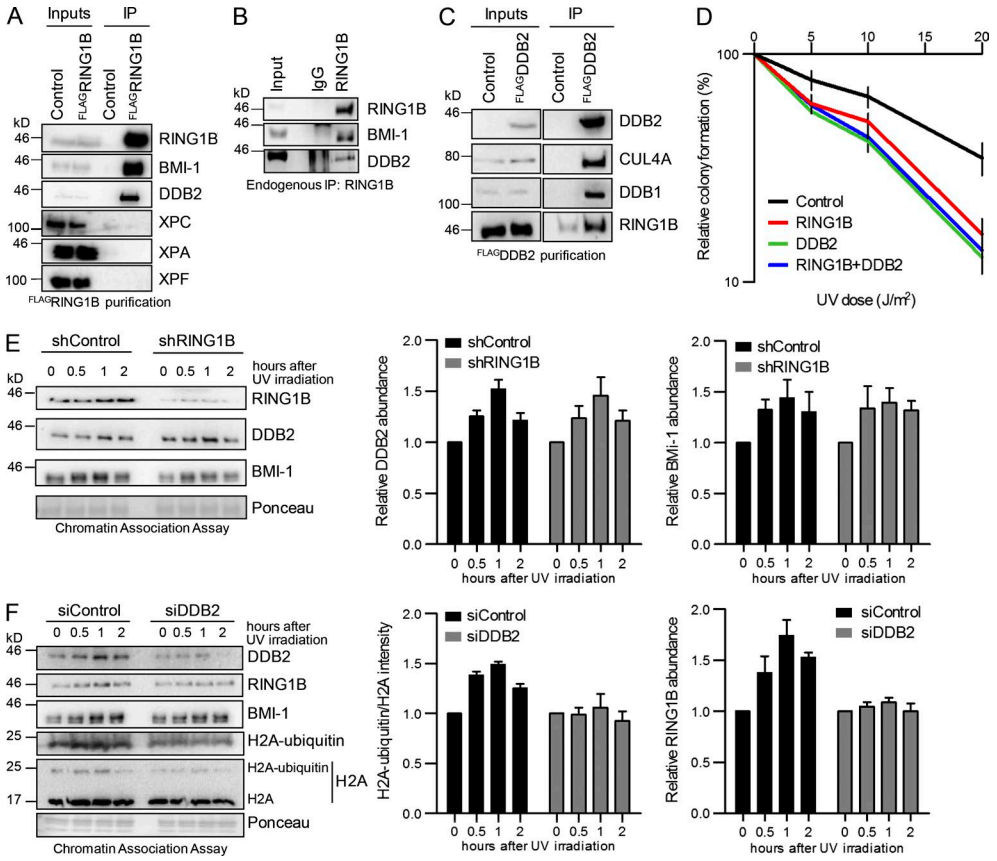


Figure 2. **RING1B and DDB2 cooperate in H2A ubiquitylation.** (A) RING1B interacts with DDB2. Control cells and cells expressing FLAGRING1B were irra- diated with UV light. After immunoprecipitation with FLAG-M2-Agarose the puri ed material was subjected to Western blotting and blots were incubated with the indicated antibodies. Inputs correspond to 3%. (B) Endogenous immunoprecipitations with RING1B antibodies after UV irradiation. Western blots of the precipitated material were incubated with the indicated antibodies. IgG lanes show unspeci c staining of the IgG heavy chains. (C) DDB2 associates with RING1B. Control cells and cells expressing FLAGDDB2 were irradiated with UV light. After immunoprecipitation with FLAG-M2-agarose, the puri ed material was subjected to Western blotting and blots were incubated with the indicated antibodies. Inputs correspond to 3%. (D) Epistatic relationship of RING1B and DDB2 in response to UV irradiation. Relative colony formation potential of control or RING1B knockdown cell lines treated with siRNA was analyzed at different UV dosages. Control cells were transfected with either control siRNA (control) or DDB2 siRNA (*DDB2*). RING1B knockdown cell lines were transfected with either control siRNA (*RING1B*) or DDB2 siRNA (*RING1B* + *DDB2*). Gene knockdown was con rmed by Western blots (not depicted). Values are given as mean ± SEM ($n$ = 6). (E) Knockdown of RING1B does not impair DDB2 recruitment. Chromatin association assays of control and RING1B knockdown HEK293T cells after UV irradiation. De–cross-linked material of the respective time points was subjected to Western blotting and probed with the indicated antibodies. The relative DDB2 and BMI-1 abundance was calculated. Values are given as mean ± SEM ($n$ = 3). (F) Knockdown of DDB2 shows reduced H2A-ubiquitylation but unaltered BMI-1 recruitment. Chromatin association assays of UV-irradiated HEK293T cells treated with siRNAs (control, *DDB2*). De–cross-linked material of the respective time points was subjected to Western blotting and probed with the indicated antibodies. The relative H2A-ubiquitylation and RING1B abundance was calculated. Values are given as mean ± SEM ($n$ = 4).

(Fig. S3, F–I). Additionally, to distinguish the UV–RING1B complex from the UV–DDB–CUL4B complex, we performed competition experiments. The E3 ligases RING1B and RBX1 compete for binding to CUL4B as judged by in vitro pull-down experiments with CUL4B (Fig. S3 J). Similarly, in pull-downs with recombinant RBX1 (Fig. S3, K and L) and in immunopre- cipitations of endogenous RBX1 after RING1B overexpression (Fig. S3 M), excess RING1B disrupted CUL4B-RBX1 binding.

Next, we set out to purify the UV–RING1B complex to test its ubiquitylation capacity in vitro. To this end, we over- expressed $^{FLAG}$DDB1, $^{FLAG}$DDB2, $^{FLAG}$RING1B, and $^{FLAG\text{-}STR\text{-}EP}$CUL4B in HEK293T cells (Fig. S3 N). After enriching for the FLAG-tagged proteins, we selectively puri ed the UV– RING1B complex. We subjected the puri ed material to col- loidal Coomassie staining (Fig. 3 C) and mass spectrometry (Table S4), which con rmed the speci c assembly of the UV– RING1B complex. Importantly, no contamination with chroma- tin components was found in the puri cation, ruling out that the assembly of the UV–RING1B complex was generated indi-

rectly through association with chromatin (Tables S5 and S6). Likewise, no other E3 ligases were identi ed in the af nity pu- ri cation, excluding unspeci c ubiquitylation events when test- ing the UV–RING1B complex in vitro. To explore whether the puri ed UV–RING1B complex catalyzes H2A ubiquitylation, we performed in vitro ubiquitylation assays with histone H2A (Fig. 3 D). Compared with control reactions, the UV–RING1B complex strongly increased the speci c monoubiquitylation of histone H2A over time. Similarly, the UV–RING1B complex caused monoubiquitylation of nucleosomes at histone H2A in ubiquitylation assays (Fig. 3 E).

In conclusion, we have identified a novel RING1B-contain- ing complex that catalyzes monoubiquitylation of histone H2A.

### ZRF1 tethers to the H2A-ubiquitin mark during UV-triggered DNA repair

Monoubiquitylated H2A is bound by ZRF1 during cellular dif- ferentiation (Richly et al., 2010). Interestingly, we observed that ZRF1 is recruited to chromatin after UV irradiation and its recruitment is dependent on RING1B (Fig. 4 A). Furthermore, the ubiquitin-binding domain of ZRF1 is required for its asso- ciation with chromatin after UV irradiation (Fig. 4 B). When inducing local UV damage by irradiation through a micropore membrane, we observed ZRF1 localizing to DNA lesions, which are marked by XPC and XPA (Fig. 4, C and D; and Fig. S4 A), further supporting a role for ZRF1 in UV-mediated DNA repair. We next addressed the association of ZRF1 with DNA lesions in the presence of the RING1B inhibitor PRT4165 (Is- mail et al., 2013). Under control conditions, we observed ZRF1 at DNA lesions (Fig. 4 E), whereas administration of the drug abolished H2A ubiquitylation (Fig. S4 B), unscheduled DNA synthesis (UDS) after UV irradiation (Fig. S4 C), and, most importantly, the presence of ZRF1 at the damage site (Figs. 4 E and S4 D). Similarly, ZRF1 recruitment to chromatin was hampered after depletion of the UV–RING1B complex sub- unit CUL4B or in XPE patient broblasts (Fig. 4, F and G). To investigate ZRF1 function in vivo, we analyzed human skin biopsy

specimens. ZRF1 and CPD antibody staining signals colocalized only when the skin was exposed to UV light (Fig. S4 E). In addition, single-cell analysis revealed that the relative ZRF1 intensities correlate with the relative intensities of CPDs upon irradiation (Fig. S4, E and F).

Collectively, these data suggest that ZRF1 plays a role in UV-triggered DNA repair and that it localizes to the damage site via binding of H2A-ubiquitin.

### ZRF1's function in NER is dependent on XPC

To explore whether ZRF1 interacts with NER factors, we performed affinity purifications after expressing $^{FLAG}$ZRF1 in

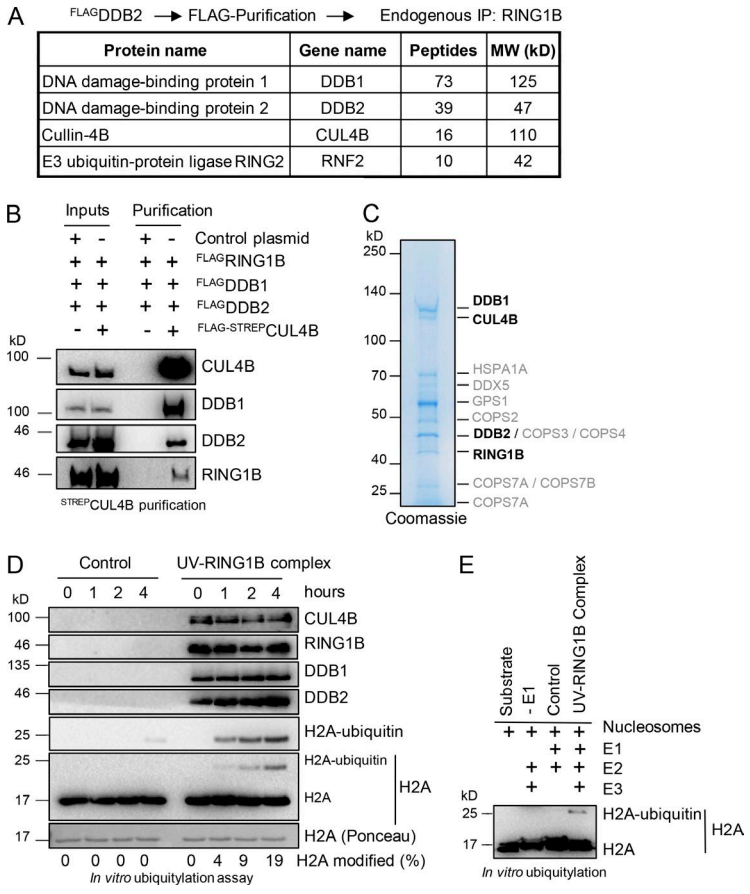


Figure 3. **H2A ubiquitylation after UV irradiation is performed by the UV–RING1B complex.** (A) Protein interaction partners of RING1B and DDB2. Mass spectrometry analysis after sequen- tial immunoprecipitations with FLAG and RING1B antibodies revealed DDB1 and CUL4B as main interaction partners of DDB2 and RING1B. A comprehensive list of the identi ed unique peptides after RING1B and control immunoprecipitations (with or without UV irradiation) is provided in Table S5. (B) Assem- bly of the UV–RING1B complex. Plasmids expressing $^{FLAG}$DDB1, $^{FLAG}$DDB2, and $^{FLAG}$RING1B were cotransfected in combination with either control plasmid or a plasmid encoding $^{FLAG\text{-}STREP}$CUL4B. After immunoprecipitation with STREP-Tactin beads, the puri ed material was subjected to Western

blotting and blots were incu- bated with the indicated antibodies. Inputs correspond to 5%. (C) Visualization of the UV–RING1B complex. Puri ed UV– RING1B complex was subjected to SDS gel electrophoresis and colloidal Coomassie staining. Mass spectrometry analysis revealed the presence of all four subunits (bold). A compre- hensive list of unique peptides is provided in Table S6. (D) The UV–RING1B complex catalyzes ubiquitylation of H2A in vitro. Ubiquitylation assays were performed with recombinant H2A, E1 (UBA1), E2 (UBCH5), and either GST (control) or the UV–RING1B complex. Reactions were performed at 37°C, and samples were taken at the indicated time points. Material of the respective time points was subjected to Western blotting and probed with the indicated antibodies. (E) The UV–RING1B complex catalyzes monoubiquitylation of nucleosomal H2A. Ubiquitylation assays were performed with recombinant nucleosomes, E1 (UBA1), E2 (UBCH5), and either GST (control) or UV-RING1B complex. Re- actions lacking E1 (−E1) were performed as additional controls. The ubiquitylation assays were performed at 37°C for 5 h, and samples or pure substrate (Substrate) were subjected to Western blotting and probed with H2A antibodies.

HEK293T cells (Fig. 5 A). We found the DNA lesion recogni- tion factor XPC interacting with ZRF1, but we did not observe binding of other selected NER factors. Likewise, we found XPC associated with ZRF1 in endogenous immunoprecipita- tions, con rming the interaction of both proteins (Fig. 5 B). To investigate the interplay between XPC and ZRF1, we analyzed the localization of ZRF1 to lesions sites using DDB2 as a dam- age marker. Interestingly, we observed reduced colocalization of ZRF1 and DDB2 in XPC patient broblasts (Figs. 5 C and S5 A). Next, we analyzed chromatin from XPC patient bro- blasts and control broblasts after UV irradiation (Fig. 5 D). We observed reduced levels of ZRF1 despite enhanced RING1B and H2A-ubiquitin levels. Accordingly, siRNA-mediated knockdown of XPC caused a drastic reduction of ZRF1 lev- els at chromatin after UV irradiation (Fig. S5 B). In contrast, chromatin isolated from XPA patient broblasts exhibited no reduction in H2A ubiquitylation, RING1B, and ZRF1 levels as compared with control broblasts (Fig. 5 E). These data sug- gest that H2A ubiquitylation via the UV–RING1B complex and subsequent ZRF1 recruitment predominantly occurs early during DDB2-mediated lesion recognition and likely before the assembly of the DNA incision complex (de Laat et al., 1999; Wakasugi and Sancar, 1999).

Next, we performed an epistasis analysis addressing the common functions of ZRF1 and XPC in NER. We observed a strong reduction in the colony formation potential after irradiat- ing ZRF1 knockdown cells or cells treated with siRNA directed against XPC, respectively (Fig. 5 F), consistent with previous observations in XPC patient broblasts (Bohr et al., 1986). Simultaneous knockdown of both factors did not signi cantly alter the colony formation potential compared with a single

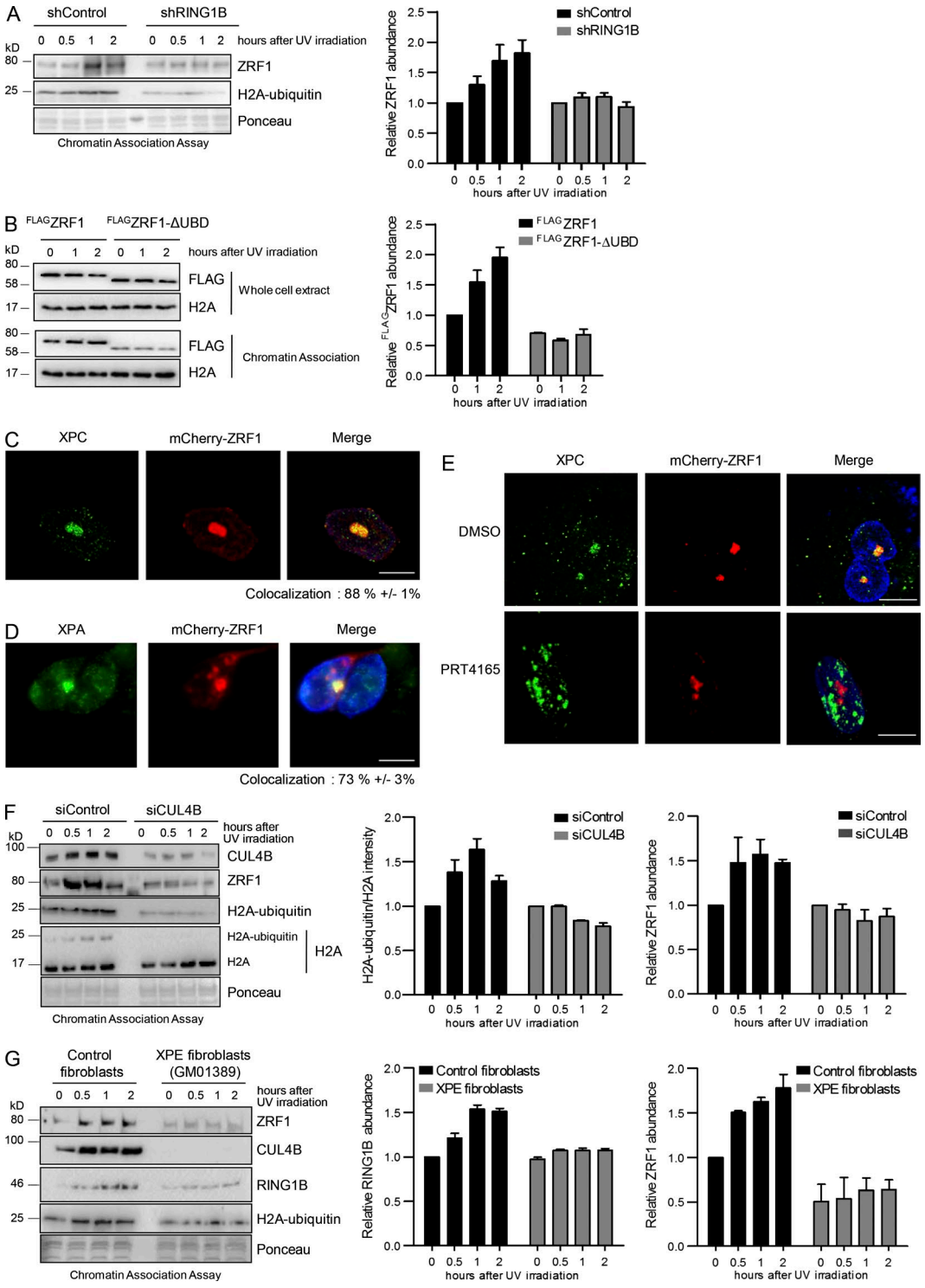


Figure 4. **Function of ZRF1 in UV-mediated DNA repair.** (A) ZRF1 is tethered to chromatin in a RING1B-dependent manner. Chromatin association assays of control and RING1B knockdown HEK293T cell lines after UV irradiation. De–cross-linked material of the respective time points was subjected to West- ern blotting and probed with the indicated antibodies. The relative ZRF1 abundance was calculated. Values are given as mean ± SEM ($n$ = 3). (B) The ubiquitin-binding domain (UBD) is important for tethering ZRF1 to chromatin after UV irradiation. HEK293T cells expressing FLAGZRF1 and FLAGZRF1-

ΔUBD were irradiated with UV light, and chromatin was isolated at the indicated time points. De-cross-linked material was subjected to Western blotting and blots were incubated with FLAG-antibody. The relative $^{FLAG}$ZRF1 abundance was calculated. Values are given as mean ± SEM ($n$ = 4). (C and D) ZRF1 localizes to DNA damage sites after UV irradiation. MRC5 broblasts expressing mCherry-ZRF1 were UV irradiated (100 J/m$^2$) through a micropore membrane (+ UV) 24 h after transfection. 30 min after irradiation, cells were preextracted and xed. DNA damage sites were visualized by staining with XPC (C) or XPA (D) antibody. The colocalization of ZRF1 with XPC amounts to 88% ± 1%. The colocalization of ZRF1 with XPA amounts to 73% ± −3%. Nonirradiated control and quanti cation of the ZRF1 localization at the damage sites are represented in Fig. S4 A. Bar, 10 µm. (E) Inhibition of RING1B affects recruitment of ZRF1 to DNA damage sites. MRC5 broblasts expressing mCherry-ZRF1 were treated with PRT4165 or DMSO. Cells were UV-irradiated (100 J/m$^2$) through a micropore membrane. 30 min after irradiation cells were preextracted and xed. DNA damage sites were visualized by XPC antibody staining. ZRF1 localization to DNA lesions after treatment with DMSO or PRT4165 was quanti ed (Fig. S4 B). Bar, 10 µm. (F) Depletion of CUL4B impacts H2A knockdown, suggesting that ZRF1 and XPC are likely epistatic in human cells. Additionally, we made similar observations in epistasis experiments using *C. elegans* (Fig. S5 C). To estimate the contribution of RING1B and ZRF1 in repairing UV-mediated DNA damage, we measured unscheduled DNA synthesis after UV irradiation and removal of CPDs in control broblasts, knockdown broblasts, and XPA broblasts (Fig. 6, A–C). In ZRF1 and RING1B knockdown cells, EdU incorporation was reduced to ∼40% when compared with control cells (Fig. 6 A). Similarly, the removal of CPDs was compromised in ZRF1 and RING1B knockdown broblasts (Fig. 6 B).

Further analysis of the DNA damage response in the *C. el- egans* germline, which is regarded a measure for GG-NER (Lans and Vermeulen, 2011; Craig et al., 2012), showed that RING1B (*spat-3*) and XPC (*xpc-1*) mutants were affected by UV irra- diation to a similar extent (Fig. 6 D). ZRF1 mutants (*dnj-11*) showed a stronger phenotype than XPC mutants (*xpc-1*), which is only surpassed by XPA mutants (xpa-1). We used a CSB mutant (*csb-1*) as a control strain, which is defective in TC-NER, but not in GG-NER. This mutant showed UV sensitivity com- parable to wild-type animals. We made similar ndings using RNAi-mediated knockdown of NER factors RING1B (*spat-3*) and ZRF1 (*dnaj-11*; Fig. S5 D). To analyze a potential function of RING1B and ZRF1 in TC-NER, we analyzed the relative lar- val stage stalling (L1 arrest; Lans and Vermeulen, 2011; Craig et al., 2012). After irradiation with increasing doses of UV light, worms were analyzed microscopically and by sorting on a large-particle sorter (Fig. 6 E; Fig. S5, E and F; and Table S1). Wild-type worms and XPC (*xpc-1*) and ZRF1 (*dnj-11*) mutants show larval arrest only at high doses of UV light, whereas CSB (*csb-1*) and XPA (*xpa-1*) mutants exhibit very strong pheno- types already at a low UV doses, in line with their defects in the TC-NER pathway (Fig. 6 E).

Collectively, we have identi ed ZRF1 and RING1B as potential players of GG-NER. ZRF1 recruitment to damaged chromatin is regulated by both its binding partner XPC and H2A ubiquitylation via the UV–RING1B complex.

**ZRF1 remodels E3 ligase complexes at the lesion site**

To explore the function of ZRF1 at damaged chromatin, we analyzed chromatin from ZRF1 knockdown cells after UV ir- radiation (Fig. 7 A). Upon depletion of ZRF1, we found en- hanced RING1B and H2A-ubiquitylation levels at chromatin consistent with a function of ZRF1 in dislocating RING1B from chromatin (Richly et al., 2010). We next addressed its potential role in dislodging other subunits of the UV–RING1B complex from chromatin. We noticed that depletion of ZRF1 did not alter the recruitment of DDB2 to chromatin (Fig. 7 B). Impor- tantly, however, we observed retention of CUL4B at chromatin, whereas recruitment of CUL4A was impaired. To determine the CUL4A levels at chromatin in control and ZRF1 knockdown cells, we expressed $^{FLAG}$H2AX and performed af nity puri - cations (Fig. 7 C). We observed constant levels of DDB2 but reduced levels of CUL4A in the coprecipitate puri ed from ZRF1 knockdown cells. Similarly, $^{FLAG}$DDB2 showed dimin- ished association with CUL4A when puri ed from ZRF1 knockdown cells (Fig. 7 D). These data suggest a potential function for ZRF1 in remodeling the UV–RING1B complex at the DNA damage sites. To follow up on this idea, we ana- lyzed whether the assembly of the UV–DDB–CUL4A com- plex was compromised in ZRF1 knockdown cells. To that end, we immunoprecipitated $^{HA}$RBX1 in control and ZRF1 knockdown cells (Fig. 7 E). In the coprecipitate, we noticed diminished levels of DDB2 and DDB1 but unaltered CUL4A binding upon ZRF1 knockdown, suggesting that ZRF1 me- diates the association of CUL4A–RBX1 with DDB1–DDB2. Next, we tested a function for ZRF1 in remodeling the UV– RING1B complex in vitro. In pull-down experiments with puri ed proteins, we had noticed that ZRF1, like CUL4B and RING1B, speci cally binds DDB2 (Fig. S3, F and G). Hence, we addressed whether ZRF1 competed with CUL4B, DDB1, and RING1B for binding to DDB2 (Fig. 7 F). In pull-downs with GFP-DDB2, we observed that increasing amounts of ZRF1 competes with CUL4B and RING1B bind- ing, whereas the DDB1–DDB2 interaction was unaltered. Experiments using similar amounts of CUL4A, RBX1, and DDB1 showed that ZRF1 did not hamper the interaction of CUL4A and RBX1 with DDB2 (Fig. 7 G).

Finally, to study ZRF1-mediated remodeling in vitro, we assembled the UV–RING1B complex and analyzed the replace- ment of CUL4B–RING1B with CUL4A–RBX1 (Fig. 7 H). The addition of puri ed CUL4A–RBX1 to immobilized UV– RING1B complexes (Fig. 7 H, lane 2) or GFP-loaded beads (lane 1) showed only minimal or no incorporation of CUL4A and RBX1 into the E3 ligase complex. In contrast, in the pres- ence of ZRF1, we noticed a signi cant replacement of CUL4B– RING1B by CUL4A–RBX1 (lane 3).

In sum, our data suggest that ZRF1 remodels E3 ligase complexes at the lesion site and that it mediates the assembly of the UV–DDB–CUL4A E3 ligase complex.

### ZRF1 regulates ubiquitylation of XPC

To confirm that ZRF1 mediates the assembly of the UV– DDB–CUL4A E3 ligase complex, we analyzed the poly- ubiquitylation of its substrate, XPC (Sugasawa et al., 2005). After UV irradiation of ZRF1 knockdown cells, we observed diminished polyubiquitylation of XPC when compared with control cells (Fig. 8 A). Similarly,

immunoprecipitations of ubiquitylated proteins after expressing $^{HA}$Ubiquitin in control, RING1B, and ZRF1 knockdown cells showed a signi cant re- duction of ubiquitylated XPC in knockdowns compared with control (Fig. 8 B). After expression of $^{HA}$XPC and $^{HIS}$Ubiq- uitin, we immunoprecipitated $^{HA}$XPC and analyzed its ubiq- uitylation status (Fig. 8 C). In agreement with our previous data, we observed a signi cant reduction of XPC ubiquityl- ation in both knockdown cell lines. Moreover, we expressed $^{HIS}$Ubiquitin in control, RING1B, and ZRF1 knockdown cell



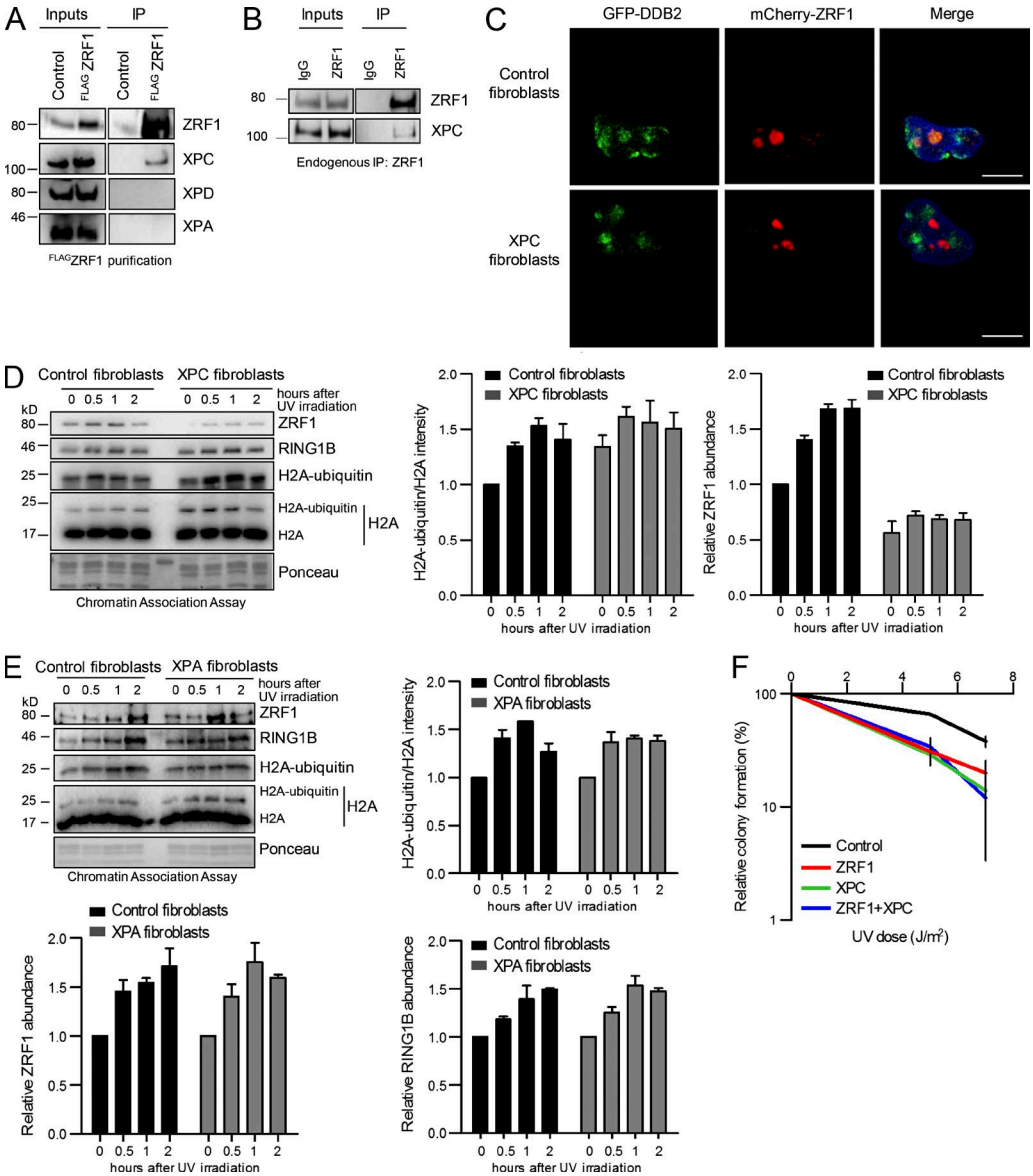


Figure 5. **ZRF1 interacts with XPC during UV-mediated DNA repair.** (A) ZRF1 speci cally binds to XPC. Control and $^{FLAG}$ZRF1-expressing cells were irra- diated with UV light. After immunoprecipitation with FLAG-M2-agarose, the puri ed material was subjected to Western blotting and blots were incubated

with the indicated antibodies. Inputs correspond to 4%. (B) Endogenous immunopreciptiations with ZRF1 antibodies. Precipitates were subjected to Western blotting, and blots were incubated with the indicated antibodies. Inputs correspond to 3%. (C) ZRF1 localization to DNA damage sites is dependent on XPC. Control broblasts and XPC patient broblasts expressing both mCherry-ZRF1 and DDB2-GFP were UV irradiated (100 J/m$^2$) through a micropore membrane. Thirty minutes after irradiation, cells were preextracted and xed. DNA damage sites were visualized by DDB2-GFP. (D) ZRF1 enriches at chromatin after UV irradiation in a XPC-dependent manner. Chromatin association assays with control broblasts (GM16248) and XPC patient broblasts (GM15983) after UV irradiation. De–cross-linked material of the respective time points was subjected to Western blotting and probed with the indicated antibodies. The relative H2A-ubiquitin and ZRF1 abundance was calculated. Values are given as mean ± SEM ($n$ = 3). (E) H2A ubiquitylation is not al- tered in XPA patient broblasts. Chromatin association assays with control broblasts (GM15876) and XPA broblasts (GM04312) after UV irradiation. De–cross-linked material of the respective time points was subjected to Western blotting and probed with the indicated antibodies. Relative intensities of H2A-ubiquitin/H2A, ZRF1 and RING1B abundance were measured. Values are given as mean ± SEM ($n$ = 3). (F) Epistasis analysis of ZRF1 and XPC. The relative colony formation potential of control or ZRF1 knockdown cell lines treated with control (Control; *ZRF1*) or XPC siRNA (*XPC*; *ZRF1+XPC*) was analyzed at different UV doses. Gene knockdown was con rmed by Western blots (not depicted). Values are given as mean ± SEM ($n$ = 3). ubiquitylation and ZRF1 recruitment. Chromatin association assays of UV irradiated HEK293T cells treated with siRNAs (control, *CUL4B*). De–cross-linked material of the respective time points was subjected to Western blotting and probed with the indicated antibodies. The relative H2A-ubiquitin and ZRF1 abundance was calculated. Values are given as mean ± SEM ($n$ = 3). (G) Tethering of ZRF1 to chromatin depends on DDB2 during NER. Chromatin asso- ciation assays in control broblasts (GM15876) and XPE (DDB2) broblasts (GM01389) after UV irradiation. De–cross-linked material of the respective time points was subjected to Western blotting and probed with the indicated antibodies. The relative RING1B and ZRF1 abundance was calculated. Values are given as mean ± SEM ($n$ = 3).

lines (Fig. 8 D). After UV irradiation of cells, we performed NiNTA pull-down experiments under denaturing conditions to enrich for ubiquitylated proteins. We observed strong ubiqui- tylation of XPC only in control cells, whereas XPC ubiquitylation levels in ZRF1 and RING1B knockdown cells were reduced. Collectively these experiments suggest that ZRF1 likely regulates XPC ubiquitylation by facilitating the assembly of the UV–DDB–CUL4A complex. RING1B in turn provides a tethering platform for ZRF1, thereby indirectly af- fecting the remodeling process.

Based on our results, we propose that H2A ubiquitylation by the UV–RING1B complex is catalyzed early during damage recognition (Fig. 8 E). Our data illustrate for the rst time how E3 ligase complexes are remodeled at the DNA lesion site. The pre- sented results suggest that ZRF1 acts as a switch protein that re- models E3 ligases at or close to the DNA damage site (Fig. 8 E).

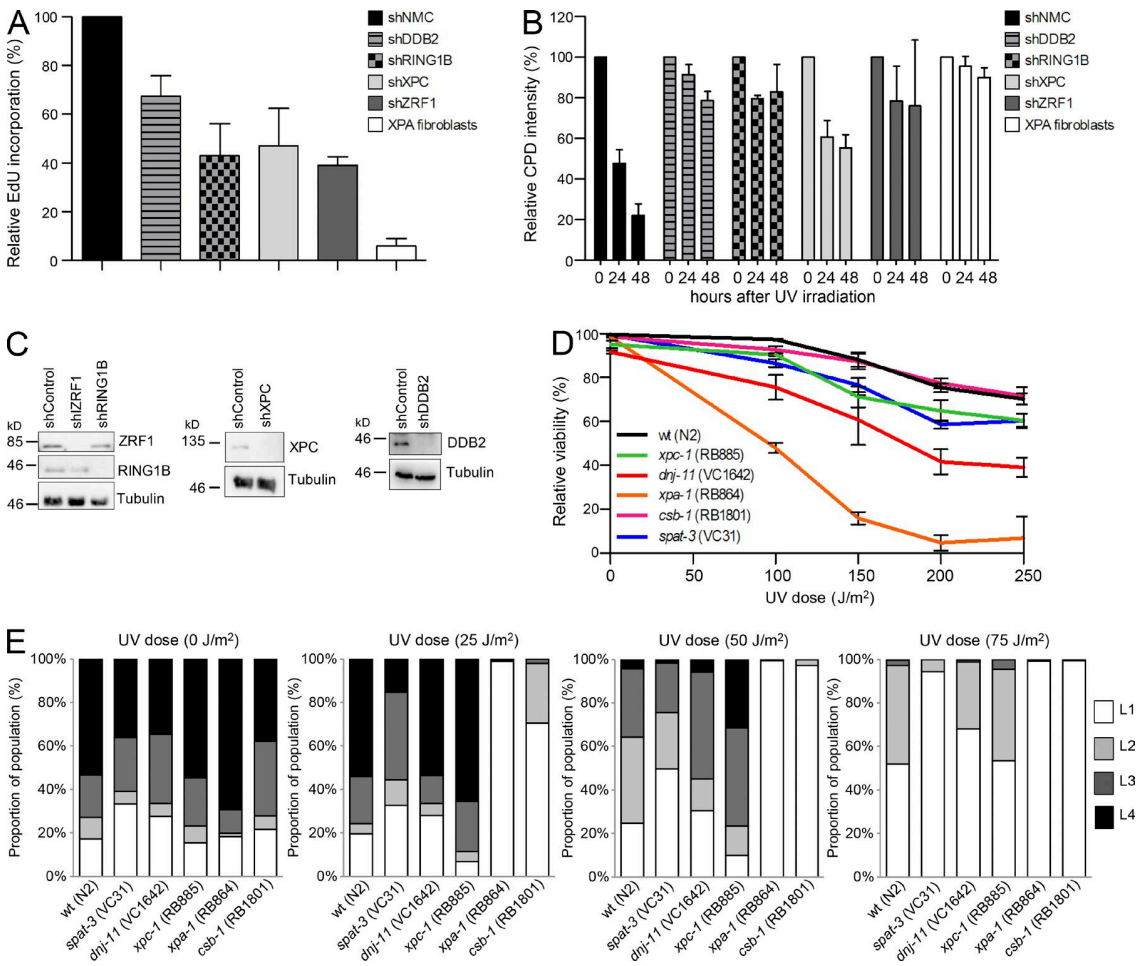


Figure 6. **ZRF1 and RING1B contribute to GG-NER.** (A) RING1B and ZRF1 knockdown broblasts are defective in UDS after UV irradiation. UDS was measured by EdU incorporation after UV treatment in MRC5 broblasts with shRNA-mediated knockdown of the indicated proteins. XPA broblasts were used as a positive control. Values are given as mean ± SEM. Data were acquired from three independent experiments (150–300 nuclei per sample). (B) RING1B and ZRF1 knockdown broblasts are defective in the removal of CPDs. The CPD removal was analyzed in MRC5 broblasts after knockdown of the indicated proteins in MRC5 broblasts and in XPA broblasts. Cells were irradiated with 10 J/m² and xed immediately or 24 or 48 h after irradiation and stained with CPD antibodies. The relative uorescence intensity was determined. Values are given as mean ± SEM. Data were acquired from three independent experiments (100–200 nuclei per sample). (C) MRC5 broblasts were treated with lentiviral particles containing the respective shRNA. Knock- down of the proteins levels was analyzed 48h after infection by Western blotting and incubation with the indicated antibodies. (D) *C. elegans* knockout mutants for ZRF1 (*dnj-11*) and RING1B (*spat-3*) show increased sensitivity toward UV irradiation. Late-L4 larval wild-type worms and the indicated mutants were irradiated with UV light at different doses, and the relative viability was determined by comparing hatched versus dead embryos (unhatched eggs). Values are given as mean ± SEM ($n = 3$). (E) *C. elegans* knockout mutants for dnj-11 and for spat-3 show only weak developmental arrest upon somatic UV irradiation. L1 larval worms were irradiated with UV light at different doses. Relative larval-stage stalling was determined after 60 h by using a large particle ow cytometer (BioSorter platform; Union Biometrica), assaying at least 1,000 worms per condition.

## Discussion

Monoubiquitylation of histone H2A is a hallmark of various DNA repair pathways. Nevertheless, it is still a matter of de- bate how and when different E3 ligases contribute to H2A ubiquitylation during the DNA damage response. Here, we have examined selected E3 ligases involved in UV-induced DNA damage repair. Our data point to RING1B as the main E3 ligase involved in H2A ubiquitylation at lysine 119 early during damage recognition in NER. Depletion of RNF168 or abrogation of UV–DDB–CUL4A E3 ligase function did not cause any signi cant changes in H2A ubiquitylation after UV irradiation. The UV–DDB–CUL4A E3 complex was previously shown to catalyze ubiquitylation of histone H2A (Kapetanaki et al., 2006). Our data show that the UV–DDB–CUL4A E3 ligase complex functions downstream of ZRF1, suggesting that it might ubiquitylate histone H2A at a later stage in the NER pathway (Fig. 7 D). Hence, we propose that the timing of E3 ligase action is an important feature of NER and other DNA repair pathways. In the same vein, it was demonstrated that RNF8-mediated H2A ubiquitylation is a relatively late event during NER (Marteijn et al., 2009). Our data extend this obser- vation, proposing that E3 ligases operate successively during the DNA damage response. In addition, E3 ligases target differ- ent lysines of histone H2A, adding another layer of complexity. For instance, at DSBs, RNF168 catalyzes the ubiquitylation of lysines 13 and 15 (Mailand et al., 2007; Mattiroli et al., 2012), whereas RING1B targets lysine 119 of histone H2A in both DSB repair and NER (Ui et al., 2015). However, understanding the concerted action and the substrate speci city of E3 ligases in DNA repair needs further investigation.

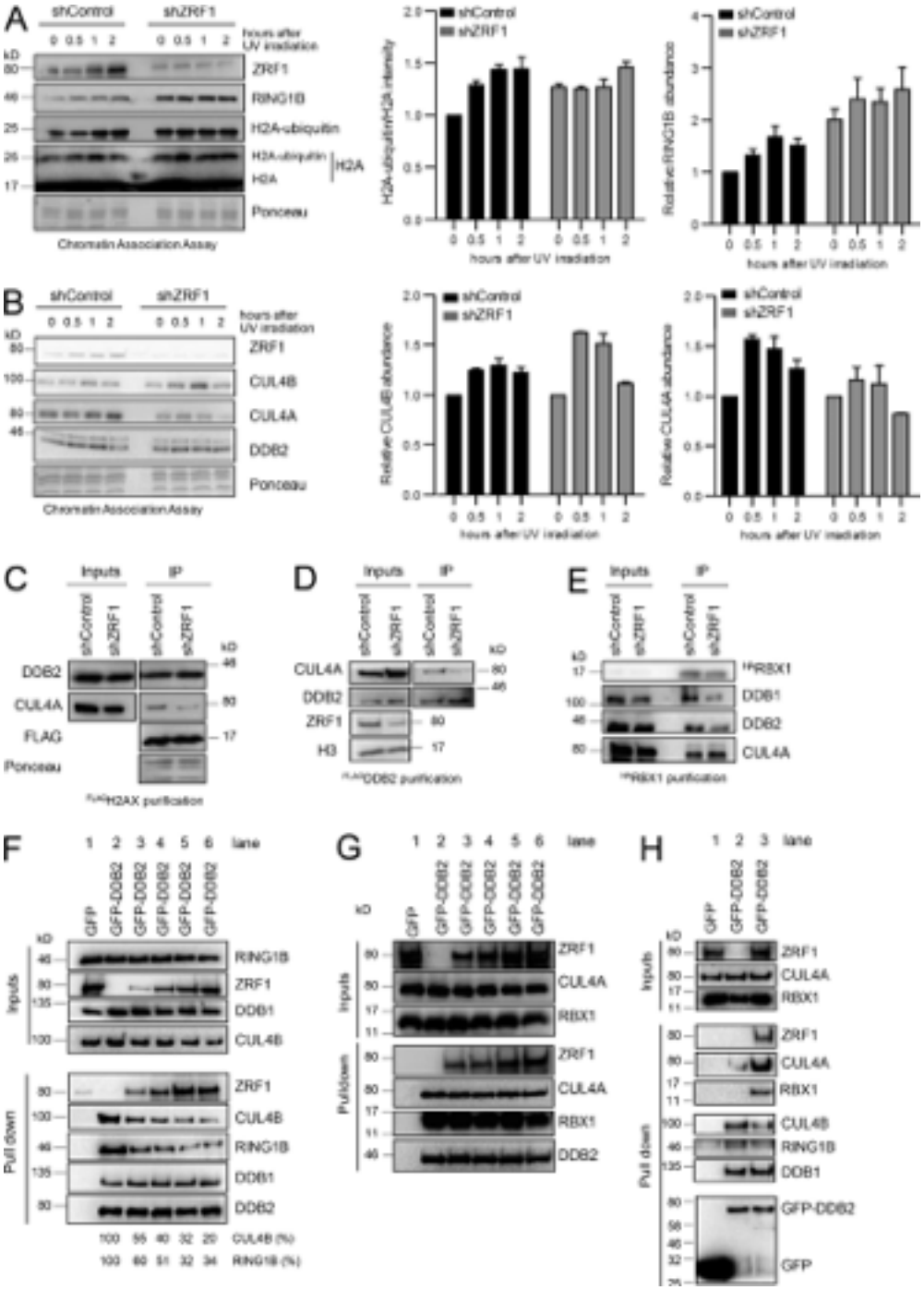


Figure 7. **ZRF1 facilitates the assembly of the UV–DDB–CUL4A E3 ligase complex.** (A) ZRF1 displaces RING1B from chromatin during NER. Chromatin association assays of control and ZRF1 knockdown HEK293T cell lines after UV irradiation. De–cross-linked material of the respective time points was sub- jected to Western blotting and probed with the indicated antibodies. The relative H2A ubiquitin and RING1B abundance was calculated. Values are given as mean ± SEM ($n$ = 3). (B) ZRF1 regulates chromatin association of CUL4A and CUL4B. Chromatin association assays of control and ZRF1 knockdown HEK293T cell lines after UV irradiation. De–cross-linked material of the respective time points was subjected to Western blotting and probed with the indi- cated antibodies. The relative CUL4B and CUL4A abundance was calculated. Values are given as mean ± SEM ($n$ = 3). (C) ZRF1 regulates CUL4A associa- tion with H2AX containing nucleosomes. Control cells and ZRF1 knockdown cells expressing $^{FLAG}$H2AX were irradiated with UV. After immunoprecipitation with FLAG-M2-agarose,

the puri ed material was subjected to Western blotting and blots were incubated with the indicated antibodies. Inputs correspond to 3%. (D) Knockdown of ZRF1 modulates CUL4A association with DDB2. Control cells and ZRF1 knockdown cells expressing $^{FLAG}$DDB2 were irradiated with UV light. After immunoprecipitation with FLAG-M2-agarose, the puri ed material was subjected to Western blotting and blots were incubated with the indicated antibodies. Inputs correspond to 3%. (E) Assembly of the UV–DDB–CUL4A E3 ligase is facilitated by ZRF1. Control cells and ZRF1 knockdown HEK293T cells expressing $^{HA}$RBX1 were irradiated with UV light. After immunoprecipitation with HA-speci c antibodies the precipitated material was sub- jected to Western blotting, and blots were incubated with the indicated antibodies. Inputs correspond to 5%. (F) ZRF1 competes with CUL4B and RING1B for DDB2 binding in vitro. GFP and GFP-DDB2 immobilized on beads were incubated with equimolar amounts of puri ed DDB1, CUL4B, and RING1B and increasing amounts of ZRF1. ZRF1 levels were doubled stepwise reaching an eightfold molar excess of ZRF1 over the other components (relative molarity ZRF1: DDB1–CUL4B–RING1B; lane 3, 1:1; lane 4, 2:1; lane 5, 4:1; lane 6, 8:1). Precipitated material was subjected to Western blotting and blots were blots were incubated with the indicated antibodies. Inputs correspond to 5%.

RING1B and H2A ubiquitylation have been implicated in UV-mediated DNA damage repair about a decade ago (Bergink et al., 2006). However, the molecular mechanism of RING1B function still remained unclear. RING1B controls the basal levels of the highly abundant H2A-ubiquitin mark (Matsui et al., 1979; Wang et al., 2004). Thus, it might affect the nuclear pool of free ubiquitin and thereby indirectly ubiquitin signaling during DNA repair (Dantuma et al., 2006). Additionally, it was reported that knockdown of RING1B decreases nuclear ubiquitin levels and thus indirectly reduces histone ubiquitylation at damaged chro- matin (Bergink et al., 2006). Our data refute these ideas, as we observe no global changes in the levels of ubiquitylated proteins in RING1B knockdown cells (Fig. S1, G and H). Thus, we rule out an indirect effect of RING1B knockdown, implying a DNA damage–speci c role of RING1B in H2A ubiquitylation. In particular, we provide evidence that RING1B constitutes a DNA damage–speci c E3 ligase, as it is speci cally recruited to DNA lesion sites induced by irradiation with a 405-nm laser (Fig. S1, D–F). This observation is also in agreement with a recent study demonstrating that RING1B is recruited to DSBs to promote local gene silencing (Ui et al., 2015). In light of these ndings, we addressed how RING1B interacts with the NER pathway, which is an essential DNA repair pathway implicated in repair of UV-mediated DNA damage. Previously, RING1B had been shown to mediate ubiquitylation of histones H2A and H2AX at DSBs together with its PRC1 binding partner, BMI-1 (Pan et al., 2011; Ui et al., 2015). After UV irradiation, RING1B seems to catalyze H2A ubiquitylation at lysine 119 independent of BMI-1, contrasting its function in DSB repair and during gene silencing. Our data indicate that RING1B binds to the DNA damage rec- ognition factor DDB2. Importantly, DDB2 determines whether RING1B is recruited to chromatin after UV irradiation, sug- gesting that DDB2 tethers RING1B to the damage site. DDB2 and RING1B represent subunits of a novel E3 ligase complex (UV–RING1B). In this complex, RING1B directly interacts with CUL4B (Fig. S3, E–I), which is in agreement with the common modular composition of cullin-RING E3 ligases (Petroski and Deshaies, 2005). The UV–RING1B complex is reminiscent of the well-described UV–DDB–CUL4A complex consisting of DDB1, DDB2, CUL4A, and RBX1 (Groisman et al., 2003). Our study suggests that DDB1–DDB2 might act as a platform that can either

accommodate CUL4B–RING1B or CUL4A– RBX1 modules, respectively. We have demonstrated that the UV–RING1B complex dramatically enhances ubiquitylation of histone H2A in vitro and in vivo. Hence, RING1B mediated monoubiquitylation at lysine 119 in DNA repair is performed by either the PRC1 complex or the UV–RING1B complex.

Because ZRF1 is one of the few known readers of H2A ubiquitin, we hypothesized that it would play a similar role in UV-mediated DNA repair as in cellular differentiation (Richly et al., 2010). In accordance, we observed that binding of ZRF1 to chromatin after UV irradiation depends both on presence of RING1B and its ability to bind H2A ubiquitin. More importantly, ZRF1 localizes to XPA and XPC foci after local irra- diation and knockdown of ZRF1 compromises DNA repair as seen by UDS and removal of CPD, describing ZRF1 as a new player in UV-mediated DNA repair. Drug-mediated inhibition of the RING1B activity signi cantly reduced ZRF1 colocaliza- tion with XPC, supporting a role for H2A ubiquitin in tethering ZRF1 to the damage site. On the other hand, UV irradiation– triggered recruitment of ZRF1 to chromatin depends on XPC. This close interplay between ZRF1 and XPC is further re ected by the interaction of both proteins and the epistasis analysis performed with either human cells or *C. elegans*, supporting a role for ZRF1 in GG-NER. In light of these ndings, we specu- late that XPC is probably involved in ZRF1's recruitment to the DNA damage site, whereas the H2A-ubiquitin mark is poten- tially needed to stably tether ZRF1 to chromatin. Most impor- tantly, ZRF1 mediates the remodeling of E3 ligase complexes at DNA damage sites (Fig. 7 D). Upon recruitment to chroma- tin, ZRF1 causes the exchange of the cullin-E3 ligase module, whereas DDB1 and DDB2 most probably remain bound to the lesion site. This observation does not exclude that UV–CUL4A complexes are generated independent of ZRF1. Still, our data re ect one plausible succession of events that take place at dam- aged chromatin. This function of ZRF1 is reminiscent of the Cand1 protein, which promotes the exchange of subunits from cullin–RING complexes (Pierce et al., 2013). We propose that ZRF1 acts in concert with other remodeling complexes or chap- erones at chromatin. In fact, ZRF1 was shown to cooperate with the HSP70 chaperone network during protein quality control (Qiu et al., 2006; Jaiswal et al., 2011). It remains to be tested whether ZRF1 cooperates with the HSP70 system, Cand1, or chromatin remodeling complexes during NER.

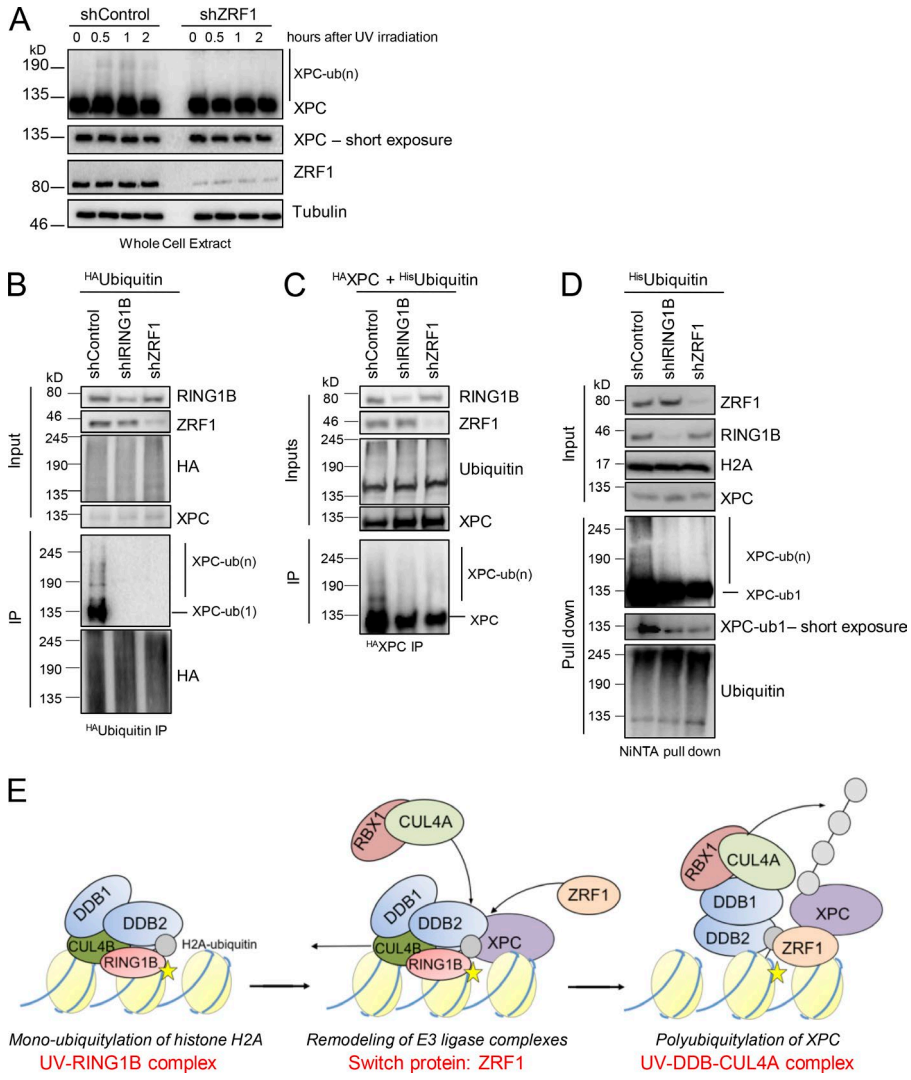


Figure 8. **ZRF1 regulates XPC ubiquitylation.** (A) ZRF1 facilitates XPC ubiquitylation after UV irradiation. Whole-cell extracts of control and ZRF1 knockdown HEK293T cells from the stated time points were subjected to Western blotting and probed with the indicated anti- bodies. (B) Role of RING1B and ZRF1 in XPC ubiquitylation. Control cells and RING1B and ZRF1 knockdown HEK293T cells expressing $^{HA}$Ubiquitin were irradiated with UV light. After immunoprecipitation with HA-speci c antibody, the precipitated material was subjected to Western blotting and blots were incubated with the indicated antibodies. Inputs corre- spond to 5%. (C) Control cells and RING1B and ZRF1 knockdown HEK293T cells express- ing $^{HA}$XPC and $^{HIS}$Ubiquitin were irradiated with UV light. After immunoprecipitation with HA-speci c antibody, the precipitated material was subjected to Western blotting and blots were incubated with the indicated antibodies. Inputs correspond to 5%. (D) Control cells and RING1B and ZRF1 knockdown HEK293T cells expressing HISUbiquitin were irradiated with UV and harvested 1 h after UV exposure. Ubiquitylated proteins were puri ed by NiNTA agarose under denaturing conditions, and Western blots of the puri ed material were in- cubated with the indicated antibodies. (E) The UV–RING1B complex and ZRF1 cooperate during NER. DNA lesions (yellow star) are rec- ognized by the UV-RING1B complex (DDB1– DDB2–CUL4B–RING1B), which catalyzes ubiquitylation of histone H2A (gray sphere). ZRF1 is recruited to the lesion site by XPC and tethers to the

H2A-ubiquitin mark. ZRF1 causes the assembly of the UV–DDB–CUL4A complex, which subsequently catalyzes ubiquitylation of XPC. incubated with the indicated antibodies. Inputs correspond to 10%. (G) ZRF1 does not compete with CUL4A and RBX1 for binding to DDB1–DDB2. GFP and GFP-DDB2 immobilized on beads were incubated with equimolar amounts of puri ed DDB1, CUL4A and RBX1 and increasing amounts of ZRF1. ZRF1 levels were doubled stepwise reaching an eightfold molar excess of ZRF1 (relative molarity ZRF1: DDB1–CUL4A–RBX1; lane 3, 1:1; lane 4, 2:1; lane 5, 4:1; lane 6, 8:1). Precipitated material was subjected to Western blotting and blots were incubated with the indicated antibodies. Inputs correspond to 10%. (H) ZRF1 mediates the formation of the UV-DDB-CUL4A complex in vitro. GFP and GFP-DDB2 were coupled to beads and incubated with CUL4B, DDB1 and RING1B. After washing, GFP and GFP-DDB2 (UV–RING1B complex) beads were incubated with an estimated vefold excess of puri ed CUL4A and RBX1 (lanes 1–3) over the retained UV–RING1B complex. Simultaneously, ZRF1 (lanes 1 and 3) or GST (lane 2) was added to the incubations in equim-olar amounts. The precipitated material was subjected to Western blotting and blots were incubated with the indicated antibodies. Inputs correspond to 5%.

## Materials and methods

### Cell lines and transfections

HEK293T and HEK293 cells were cultured in DMEM supple- mented with 10% FBS at 37°C and 5% $CO_2$. HeLa Kyoto cells sta- bly expressing cherry-PCNA were cultured in DMEM supplemented with 10% FCS and 1 μM/ml gentamycin and 2.5 μg/ml blastici- din. MRC5 (AG05965), normal skin broblasts (GM15876), XPE (GM01389), XPE (GM02415), XPC-complemented (GM16248), XPC (GM15983), XPA-complemented (GM15876), and XPA (GM04312 and GM00710) broblasts were purchased from Coriell Cell Repositories and cultured in DMEM, supplemented with 15% FBS. To generate cells stably expressing $^{FLAG}$RING1B, HEK293 cells were transfected with a pCMV-2b-RING1B-FLAG plasmid and selected with G148 for 14 d. The expression of $^{FLAG}$RING1B was veri ed by Western blot.

Transfection of HEK293T cells was either performed by the calcium phosphate coprecipitation method as described previously (Richly et al., 2010) or by Lipofectamine (Invitrogen) transfection. In- formation on the plasmids used is provided in Table S2.

### UV irradiation and drug treatment

Cells were irradiated with 10 J/m$^2$ UV-C using a CL-1000 UV cross- linker (UVP) unless stated otherwise. PRT4165 (Abcam) was used at a concentration of 50 μM as described in Ismail et al. (2013).

### Gene inactivation by shRNA/siRNA

HEK293T-shControl, HEK293T-shZRF1, and HEK293T-shRING1B were described previously and generated by transduction of HEK293T cells with retrovirus vector, containing shRNA against ZRF1 or RING1B (Richly et al., 2010). Gene knockdown in MRC5 broblasts was performed by introduction of MISSION pLKO.1-shRNA plas- mids (Sigma-Aldrich) targeting the respective gene using third gen- eration lentivirus system. Plasmids contained the following

sequences (Sigma-Aldrich): control (TRC1/1.5), ZRF1 (TRCN0000254058), RING1B (TRCN0000033697), DDB2 (TRCN0000083995), and XPC (TRCN0000307193).

The siRNA transfections were performed using Lipofect- amine 2000 according to the manufacturer's instructions (Invitro- gen). The following siRNAs were used in this study: control (SIC001; Sigma-Aldrich), CUL4A (esiRNA EHU011891; Sigma-Aldrich), RNF168 (SMARTpool D-011-22-(01–04); GE Healthcare), DDB2 (SASI_Hs01_00101645, SASI_Hs01_00101647; Sigma-Aldrich), BMI-1 (esiRNA EHU004421; Sigma-Aldrich), CUL4B (esiRNA EHU064911; Sigma-Aldrich), XPC (SASI_Hs01_00086530, SASI_

**Chromatin association assays**

HEK293T cells (unless stated otherwise) were irradiated with UV and cross-linked by formaldehyde at the indicated time points after UV irra- diation. Assays were essentially performed as published (Richly et al., 2010). In brief, cell pellets were resuspended in buffer A (100 mM Tris, pH 7.5, 5 mM $MgCl_2$, 60 mM KCl, 125 mM NaCl, 300 mM sucrose, 1% NP-40, and 0.5 mM DTT) and kept on ice for 10 min. After cen- trifuging nuclei pellet was lysed in a hypotonic solution (3mM EDTA, 0.2 mM EGTA, and 1 mM DTT) twice. The chromatin-containing pellet was solubilized in 2× Laemmli buffer, sonicated, and boiled to reverse cross-linking. Information on antibodies used for Western blots is provided in Table S4. All experiments were repeated at least three times. Band intensities from Western blots were measured as stated in the gure legends using ImageJ or ImageLab (Bio-Rad) software.

**Immunoprecipitations and af nity puri cations**

Cells were treated with UV and harvested 1 h after exposure unless stated otherwise. Cells were resuspended in buffer A (10 mM Hepes, pH 7.9, 1.5 mM $MgCl_2$, 10 mM KCl and 0.5 mM DTT, 1 mM PMSF, and protease inhibitors; Roche) and homogenized by 10 strokes in a Dounce homogenizer with a B-type pestle. After centrifugation, nuclei were resuspended in lysis buffer (20 mM Hepes, 150 mM NaCl, 2.5 mM EGTA, 2 mM EDTA, 0.1% Triton X-100, 0.5 mM DTT, 1 mM PMSF, and protease inhibitors; Roche) and soni ed using a Diagenode Bioruptor for 20 min on the high setting. To verify soni cation ef - ciency, DNA from the extracts analyzed by agarose gel electrophore- sis. Only samples containing DNA of 300 bp or smaller were used in the experiments. Protein extracts were then subjected to centrifugation (21,000 *g*, 4°C, 15 min), and the supernatant was incubated with anti- bodies overnight at 4°C. After incubation with protein A agarose beads for 2 h at 4°C, the immune complexes were washed extensively in lysis buffer and material retained on the beads was subjected to Western blotting. Information on antibodies used for immunoprecipitations and Western blots is provided in Table S4.

Af nity puri cations using FLAG-M2 agarose beads (Sigma- Aldrich) and Anti-HA Agarose beads (Sigma-Aldrich) were per- formed using the protocol stated for immunoprecipitations. Puri ca- tions involving the STREP tag were performed with STREP-Tactin beads (Iba LifeSciences) and Desthiobiotin (Sigma-Aldrich) accord- ing to the manufacturer's instructions. Puri cations involving the GFP tag were performed with GFP-Trap agarose beads (Chromo- Tek) according to the manufacturer's instructions. For puri cation of the proteins used in the in vitro experiments (Fig. S3 E: $^{FLAG\text{-}STR\ EP}$CUL4B, $^{FLAG}$DDB1, $^{FLAG}$RING1B, $^{FLAG}$ZRF1, $^{FLAG}$ZRF1, $^{HA}$RBX1, and

$^{HA}$CUL4A), the proteins were washed extensively on the beads with lysis buffer containing 1 M NaCl before elution with FLAG or HA peptide (Sigma-Aldrich).

**In vitro ubiquitylation assays**

In vitro ubiquitylation reactions were performed with 3 μg puri ed histone H2A (New England Biolabs, Inc.) or 5 μg recombinant nucle- osomes (Active Motif), 200 ng puri ed HIS-UBA1 (E1), 20 ng pu- ri ed GST-UBC5H (E2), 150 ng puri ed UV-RING1B (E3), or 150 ng GST (control) in UBAB buffer (25 mM Tris/HCl, pH 7.5, 50 mM NaCl, and 10 mM $MgCl_2$) supplemented with 20 mM ATP, 1.5 mg/ml ubiquitin, 10 mM DTT, and 1 U creatine phosphokinase. Reactions were kept at 37°C for the indicated times and subsequently sub- jected to Western blotting.

**Purification of recombinant proteins**

Proteins were puri ed as suggested by GE Healthcare (GST-tagged pro- teins) or QIAGEN (His-tagged proteins) after inducing BL21 bacterial strains transformed with the respective plasmids at an OD = 0.5 with 0.2 mM isopropyl-β-D-thiogalactoside for 4 h at 37°C or at 20°C for 14 h. The following recombinant proteins were purchased: H2A (New England Biolabs), Ubiquitin (Boston Biochem), nucleosomes (Active Motif), GST-RBX1 (Novus Biologicals), and RAD23A (Abcam).

**GST pull-downs**

Puri ed GST–proteins were bound in equimolar amounts to glutathi- one beads (Amersham) in binding buffer (20 mM Tris, pH 7.4, 150 mM NaCl, and 0.1% Triton X-100). Loaded beads were washed in the same buffer and used for incubation with puri ed proteins for 2 h at 4°C. After extensive washing in binding buffer, the retained material was subjected to Western blotting.

**Purification of ubiquitin conjugates from cells**

Cells expressing HIS-tagged ubiquitin were lysed in lysis buffer (8 M urea, 100 mM $NaH_2PO_4$, and 10 mM Tris, pH 8.0) 1 h after UV irra- diation. Ubiquitylated proteins were retained on NiNTA agarose after washing with wash buffer (8 M urea, 100 mM $NaH_2PO_4$, 10 mM Tris, pH 6.3, 300 mM NaCl, and 0.1% Triton X-100) and detected by West- ern blotting using the indicated antibodies.

**Fractionation of cell extracts**

HEK293T cells were harvested by trypsinization and the cell pellet was divided in two equal parts. One part was resuspended in Laemmli buf- fer and sonicated (whole-cell extract), and the other was washed twice with PBS and resuspended in buffer A (10 mM Hepes, pH 7.9, 10 mM KCl, 1.5 mM $MgCl_2$, 0.34 M sucrose, 10% glycerol, 1 mM DTT, pro- tease inhibitors, and 0.1% Triton X-100) and cells were incubated for 8 min on ice. Subsequently, cells were spun down (4°C, 1,300 *g*, 5 min). The supernatant (cytoplasmic fraction) was collected, precipitated with TCA, and resuspended in Laemmli buffer. Nuclei were washed twice with buffer A, resuspended in Laemmli buffer, and sonicated. Whole- cell extract, cytoplasmic, and nuclear fractions were subjected to West- ern blotting as indicated.

**Mass spectrometry analysis**

Mass spectrometry sample preparation, measurement and database search were performed as described previously (Bluhm et al., 2016). Gradient lengths of 45 or 105 min were chosen depending on the im- munoprecipitated material obtained. Raw les were processed with MaxQuant (version 1.5.2.8) and searched against the *Homo sapiens* UniProt database (February 25, 2012) using the Andromeda search en- gine integrated into MaxQuant and default settings were applied. Pro- teins with at least two peptides, one of them unique, count as identi ed.

**Fluorescence microscopy**

Experiments were performed with MRC5 broblasts and patient- derived broblasts. Cells were transfected with mCherry-ZRF1 and GFP-DDB2 expressing plasmids. Cells were exposed to localized UV damage (100 J/$m^2$) using a micropore membrane with 5-µm pore size as described previously (Katsumi et al., 2001). Preextraction was per- formed with CSK supplemented with 0.2% Triton X-100 at 30 min after UV and then xed in 4% PFA. Cells were stained with XPA (Novus Biologicals) or XPC (Cell Signaling Technology) antibodies overnight at 4°C. After washing, coverslips were incubated with Alexa Fluor 488 uorophore–conjugated secondary antibodies (Thermo Fisher Scienti c) and mounted in Vectashield with DAPI. Images were acquired with the LAS AF software (Leica Biosystems) using a TCS SP5 confocal microscope (Leica Biosystems) with a 63×/1.4 oil-immersion objective. For colocalization studies, ∼100 lesions were counted per condition.

**Imaging and microirradiation experiments**

For microirradiation, HeLa-Kyoto Cherry-PCNA cells were grown on cover slide dishes and transfected with the indicated constructs using polyethylenimine. Imaging and microirradiation experiments were performed using an UltraVIEW VoX spinning-disc confocal system (PerkinElmer) in a closed live-cell microscopy chamber (ACU; Perkin- Elmer) at 37°C with 5% $CO_2$ and 60% humidity, mounted on a Nikon TI microscope (Nikon). Images were taken with a CFI Apochromat 60×/1.45 NA oil immersion objective. GFP and Cherry or mRFP were imaged with 488 and 561 nm laser excitation and 527 ± 55 and 612 ± 70 nm (full width at half maximum) emission lters, respectively. For microirradiation, a preselected spot (1 µm diameter) within the nucleus was microirradiated for 1,200 ms with the 405-nm laser resulting in 1 mJ. Before and after microirradiation, confocal image series of one midnucleus z section were recorded in 2-s intervals. For evaluation of the accumulation kinetics between 4 and 12 cells were analyzed. Im- ages were rst corrected for cell movement (ImageJ plugin StackReg and transformation mode Rigid body), and mean intensity of the irradi- ated region was divided by mean intensity of the whole nucleus (both corrected for background) using ImageJ software. Maximal accumula- tion represents the highest ratio from each experiment.



**Microscopy on skin biopsy specimens**

Human skin sections were taken from material biopsied from patients who had given their written consent and were provided by R. Greinert and B. Volkmer (Dermatology Center Buxtehude, Buxtehude, Ger- many). Biopsy specimens were taken from either the cheek (UV ex- posed) or

groin (not exposed), and 7-μm cryosections were prepared after freezing in liquid nitrogen. The sections were mounted on glass slides and xed in 100% MeOH and 100% acetone for 10 min, each at −20°C. For immunostaining, the sections were rehydrated in PBS, and antigen retrieval was performed at 80°C in sodium citrate buffer (10 mM sodium citrate, pH 6.0) overnight. Then the sections were blocked in 4% BSA in PBS for 30 min before the rst antibody was applied in 1% BSA, 0.1% Triton X-100 in PBS (ZRF1; self-made), H2A ubiquitin (Cell Signaling Technology), RING1B (self-made; all diluted 1:100), and mouse DDB2 (1:20; Abcam). For CPD detection, DNA was additionally denatured for 3 min in 0.1 N NaOH/70% ethanol after the antigen retrieval followed by dehydration in 70%, 90%, and 100% ethanol. The CPD antibody (Kamiya) was used at a dilution of 1:100. Primary antibodies were incubated for 3 h at room temperature, followed by three washes in PBS. Secondary antibodies (anti–mouse IgG Alexa Fluor 488; Invitrogen; and anti–rabbit IgG-Cy3 and anti– rabbit IgG TexasRed; Jackson ImmunoResearch Laboratories, Inc.) were added at 1:500 for 1 h at room temperature. Sections were then washed three times in PBS and stained with 10 μM DAPI for 10 min before being mounted in Vectashield. Skin sections were imaged using an Axiovert 200 (ZEISS) equipped with a 40× Planneo uar 1.3 NA ob- jective lens and single channels were recorded with a black and white Axicam mRM (ZEISS). Quanti cation of signals on the single-cell level was performed using ImageJ. After selecting random nuclei in the DAPI channel, the mean and integrated intensities of the red and green channels were measured. All intensities are normalized to the DNA content of the corresponding nucleus. At least 200 nuclei were analyzed in at least three sections.

**Colony formation assay**

HEK293T control and knockdown cell lines were transfected with the respective siRNAs with Lipofectamine (Invitrogen) according to the manufacturer's protocol. Details on the respective transfections are given in the gure legends. Cells were plated on tissue culture plates at a density of 1,000 cells per plate 24 h after transfection. Cells were irradiated with the indicated UV dose 48 h after transfection. Colonies were counted 7 d after irradiation. Numbers of colonies formed after UV irradiation were normalized against the non-UV–treated control.

**UDS**

UDS experiments were performed as described previously (Jia et al., 2015). In brief, MRC5 broblasts were transduced with lentiviral par- ticles expressing the respective shRNAs. XPA broblasts were used as a positive control. After viral transduction, the cells were serum starved for 24 h, irradiated with UV light (20 J/$m^2$), and incubated with 10 μM EdU (Thermo Fisher Scienti c) for 2 h. Alexa Fluor 555 azide (Thermo Fisher Scienti c) was conjugated to EdU using the Click-reaction. The coverslips were mounted in Vectashield with DAPI. Images were acquired with the LAS AF software (Leica Bio- systems) using a AF-7000 wide eld microscope (Leica Biosystems) with a 63×/1.4 oil immersion objective and an ORCA CCD camera (Hamamatsu). Images were analyzed using ImageJ. DAPI was used to de ne nuclei, and EdU intensity within nuclei was measured after background subtraction. A total of 150–300 nuclei were analyzed per sample. Mean intensities of +UV and −UV conditions for all cells were calculated and used to estimate the DNA repair occurring in the particular sample.

**Removal of CPDs**

MRC5 broblasts were transduced with lentiviral particles express- ing the respective shRNAs. XPA broblasts were used as a positive control. 24 h after viral transduction, cells were replated on cover- slips, exposed to UV light, and xed at the indicated time points. Cells were stained with CPD antibody (Cosmo Bio) using the man- ufacturer's protocol, followed by incubation with Alexa Fluor 488 uorophore–conjugated secondary antibodies (Thermo Fisher Sci- enti c). The cells were mounted in Vectashield with DAPI, and im- ages were acquired with the LAS AF software (Leica Biosystems) using an AF-7000 wide eld microscope (Leica Biosystems) with a 63×/1.4 oil-immersion objective and an ORCA CCD camera (Ham- amatsu Photonics). Images were analyzed using ImageJ. DAPI was used to de ne nuclei, and CPD intensity within nuclei was mea- sured after background subtraction. 100–200 nuclei were analyzed per sample. Mean intensities of +UV and −UV conditions for all cells were calculated and used to estimate the DNA repair occurring in the particular sample.

**C. elegans culture**

Nematodes were cultured on agar plates at 20°C according to standard procedures. Strains were provided by the Caenorhabditis Genetics Cen- ter, which is funded by National Institutes of Health Of ce of Research Infrastructure Programs (P40 OD010440). The following strains were used: wild type (N2 Bristol), VC31/*spat-3* (gk22; WBGene00020496), DL74/*mig-32* (n4275; WBGene00008684), VC1642/*dnj-11* (gk1025; WBGene00001029), RB885/*xpc-1*(ok734; WBGene00022296), RB1801/*csb-1*(ok2335; WBGene00000803), and RB864/*xpa-1* (ok698; WBGene00006963). Mutant strains were outcrossed at least three times to the wild-type strain (N2).

**Measuring DNA damage response in the C. elegans germline**

The L4 survival assay was performed as described previously (Craig et al., 2012). In brief, late-L4 larval hermaphrodites were ir- radiated with different doses of UV light. The damage sensitivity of the meiotic pachytene cells of the germline was measured by de- termining the survival of embryos produced between 24 and 30 h after L4-stage irradiation.

**Measuring DNA damage response in the C. elegans soma via developmental arrest** The L1 development arrest assay was performed as described previ- ously (Craig et al., 2012). In brief, L1-stage worms were synchronized via starvation and irradiated with different doses of UV light. Relative larval-stage stalling was determined after 60 h, when control worms were fully fertile. Larval-stage scoring was done using a large-particle ow cytometer (BioSorter platform; Union Biometrica).

**RNAi via feeding**

Worms were fed at L1 larval stage with *Escherichia coli* feeding clones (HT115), which express dsRNAi targeted against a gene of interest. In brief a single colony of a clone was grown overnight in LB contain- ing 100 μg/ml ampicillin (37°C, 200 rpm). Subsequently the clone was induced for 1 h by adding 4 mM IPTG to the LB media. The induced bacteria then was spun down at room temperature and resuspended in nematode growth medium with 4 mM IPTG. L1 larval worms were directly grown in this medium at 20°C until they reached late L4 stage or early adulthood (50–60 h).

**Online supplemental material**

Fig. S1 shows the function of RING1B in H2A ubiquitylation during UV-triggered DNA repair and recruitment of RING1B to UV-mediated



DNA damage sites. Fig. S2 shows the BMI-1 independent interaction of RING1B–DDB2. RING1B, H2A ubiquitin, and DDB2 staining in human skin sections and H2A ubiquitin accumulation after UV irradiation in GM02415 broblasts. Fig. S3 shows interactions of UV–RING1B subunits and competition of RING1B and RBX-1 for binding to CUL4B. Fig. S4 shows a quanti cation of ZRF1 localization to DNA damage sites and its dependency on H2A ubiquitin. Fig. S5 shows the ZRF1 and XPC interplay and effect on UV sensitivity assays in *C. elegans*. Table S1 shows a data summary of developmental arrest assay in mutant strains. Table S2 lists plasmids used in this study. Table S3 lists the shRNA and siRNA sequences used for this study. Table S4 lists antibodies used in this study. Table S5 provides peptide numbers and protein names for all proteins identi ed in the mass spectrometry analysis after sequential immunoprecipitations with FLAG and RING1B antibodies. Table S6 provides peptide numbers and protein names for all proteins identi ed in the mass spectrometry analysis of puri ed UV–RING1B complex. Online supplemental material is available at http://www.jcb.org/cgi/content/full/jcb.201506099/DC1.

**Acknowledgments**

We thank the members of the Richly laboratory for comments on the manuscript. We thank M. Hanulova for help with processing data for UDS experiments. We thank S. Papaefstathiou, S. Schaffer, and S. Meyer for excellent technical work.

This work was supported by grants from the Boehringer Ingelheim Foun- dation and the Deutsche Forschungsgemeinschaft (RI-2413/1-1). M.C. Cardoso was supported by a grant from the Bundesministerium für Bildung und Forschung (02NUK017D). We thank the Institute of Molecu- lar Biology Proteomics and Microscopy core facilities for their expert as- sistance. *C. elegans* strains were kindly provided by the Caenorhabditis Genetics Center, which is funded by the National Institutes of Health Office of Research Infrastructure Programs (P40 OD010440).

The authors declare no competing nancial interests.

Submitted: 22 June 2015 Accepted: 16 March 2016

## Author Contribution

S.C. performed the following experiments:
1. Double purification and MS to identify the UV-RING1B complex.
2. All endogenous IPs
3. Immunofluorescence experiments
4. UDS experiments

## References

Alekseev, S., H. Kool, H. Rebel, M. Fousteri, J. Moser, C. Backendorf, F.R. de Gruijl, H. Vrieling, and

L.H. Mullenders. 2005. Enhanced DDB2 expression protects mice from carcinogenic effects of chronic UV-B irradiation. *Cancer Res*. 65:10298–10306. http://dx.doi.org/10.1158 /0008-5472.CAN-05-2295

Angers, S., T. Li, X. Yi, M.J. MacCoss, R.T. Moon, and N. Zheng. 2006. Molecular architecture and assembly of the DDB1-CUL4A ubiquitin li- gase machinery. *Nature*. 443:590–593.

Araki, M., C. Masutani, M. Takemura, A. Uchida, K. Sugasawa, J. Kondoh, Y. Ohkuma, and F. Hanaoka. 2001. Centrosome protein centrin 2/ caltractin 1 is part of the xeroderma pigmentosum group C complex that initiates global genome nucleotide excision repair. *J. Biol. Chem*. 276:18665–18672. http://dx.doi.org/10.1074/jbc.M100855200

Bergink, S., F.A. Salomons, D. Hoogstraten, T.A. Groothuis, H. de Waard, J. Wu, L. Yuan, E. Citterio, A.B. Houtsmuller, J. Neefjes, et al. 2006. DNA damage triggers nucleotide excision repair-dependent monoubiquitylation of histone H2A. *Genes Dev*. 20:1343–1352. http://dx.doi.org/10.1101/ gad.373706

Bergink, S., W. Toussaint, M.S. Luijsterburg, C. Dinant, S. Alekseev, J.H. Hoeijmakers, N.P. Dantuma, A.B. Houtsmuller, and W. Vermeulen. 2012. Recognition of DNA damage by XPC coincides with disruption of the XPC-RAD23 complex. *J. Cell Biol*. 196:681–688. http://dx.doi.org /10.1083/jcb.201107050

Bluhm, A., N. Casas-Vila, M. Scheibe, and F. Butter. 2016. Reader interactome of epigenetic histone marks in birds. *Proteomics*. 6:427-436. http://dx.doi .org/10.1002/pmic.201500217

Bohr, V.A., D.S. Okumoto, and P.C. Hanawalt. 1986. Survival of UV-irradiated mammalian cells correlates with ef cient DNA repair in an essential gene. *Proc. Natl. Acad. Sci. USA*. 83:3830–3833. http://dx.doi.org/10 .1073/pnas.83.11.3830

Chagraoui, J., J. Hébert, S. Girard, and G. Sauvageau. 2011. An anticlastogenic function for the Polycomb Group gene Bmi1. *Proc. Natl. Acad. Sci. USA*. 108:5284–5289. http://dx.doi.org/10.1073/pnas.1014263108

Craig, A.L., S.C. Moser, A.P. Bailly, and A. Gartner. 2012. Methods for studying the DNA damage response in the Caenorhabdatis elegans germ line. *Methods Cell Biol*. 107:321–352. http://dx.doi.org/10.1016/B978-0-12 -394620-1.00011-4

Dantuma, N.P., T.A. Groothuis, F.A. Salomons, and J. Neefjes. 2006. A dynamic ubiquitin equilibrium couples proteasomal activity to chromatin remodeling. *J. Cell Biol*. 173:19–26. http://dx.doi.org/10.1083/jcb .200510071

de Laat, W.L., N.G. Jaspers, and J.H. Hoeijmakers. 1999. Molecular mechanism of nucleotide excision repair. *Genes Dev*. 13:768–785. http://dx.doi.org /10.1101/gad.13.7.768

Doil, C., N. Mailand, S. Bekker-Jensen, P. Menard, D.H. Larsen, R. Pepperkok, J. Ellenberg, S. Panier, D. Durocher, J. Bartek, et al. 2009. RNF168 binds and ampli es ubiquitin conjugates on damaged chromosomes to allow accumulation of repair proteins. *Cell*. 136:435–446. http://dx.doi.org/10 .1016/j.cell.2008.12.041

Fitch, M.E., S. Nakajima, A. Yasui, and J.M. Ford. 2003. In vivo recruitment of XPC to UV-induced cyclobutane pyrimidine dimers by the DDB2 gene product. *J. Biol. Chem*. 278:46906–46910. http://dx.doi.org/10.1074/jbc .M307254200

Fousteri, M., and L.H. Mullenders. 2008. Transcription-coupled nucleotide excision repair in mammalian cells: molecular mechanisms and biological effects. *Cell Res*. 18:73–84. http://dx.doi.org/10.1038/cr.2008.6

Friedberg, E.C. 2001. How nucleotide excision repair protects against cancer. *Nat. Rev. Cancer*. 1:22–33. http://dx.doi.org/10.1038/35094000

Ginjala, V., K. Nacerddine, A. Kulkarni, J. Oza, S.J. Hill, M. Yao, E. Citterio, M. van Lohuizen, and S. Ganesan. 2011. BMI1 is recruited to DNA breaks and contributes to DNA damage-induced H2A ubiquitination and repair. *Mol. Cell. Biol*. 31:1972–1982. http://dx.doi.org/10.1128/MCB .00981-10

Groisman, R., J. Polanowska, I. Kuraoka, J. Sawada, M. Saijo, R. Drapkin, A.F. Kisselev, K. Tanaka, and Y. Nakatani. 2003. The ubiquitin ligase activity in the DDB2 and CSA complexes is differentially regulated by the COP9 signalosome in response to DNA damage. *Cell*. 113:357–367. http://dx.doi.org/10.1016/S0092-8674(03)00316-7

Guerrero-Santoro, J., M.G. Kapetanaki, C.L. Hsieh, I. Gorbachinsky, A.S. Levine, and V. Rapić-Otrin. 2008. The cullin 4B-based UV-damaged DNA-binding protein ligase binds to UV-damaged chromatin and ubiquitinates histone H2A. *Cancer Res*. 68:5014–5022. http://dx.doi.org /10.1158/0008-5472.CAN-07-6162

Hoogstraten, D., S. Bergink, J.M. Ng, V.H. Verbiest, M.S. Luijsterburg, B. Geverts, A. Raams, C. Dinant, J.H. Hoeijmakers, W. Vermeulen, and A.B. Houtsmuller. 2008. Versatile DNA damage detection by the global genome nucleotide excision repair protein XPC. *J. Cell Sci*. 121:2850– 2859. http://dx.doi.org/10.1242/jcs.031708

Ismail, I.H., C. Andrin, D. McDonald, and M.J. Hendzel. 2010. BMI1-mediated histone ubiquitylation promotes DNA double-strand break repair. *J. Cell Biol*. 191:45–60. http://dx.doi.org/10.1083/jcb.201003034

Ismail, I.H., D. McDonald, H. Strickfaden, Z. Xu, and M.J. Hendzel. 2013. A small molecule inhibitor of polycomb repressive complex 1 inhibits ubiquitin signaling at DNA double-strand breaks. *J. Biol. Chem*. 288:26944–26954. http://dx.doi.org/10.1074/jbc.M113.461699

Jaiswal, H., C. Conz, H. Otto, T. Wöl e, E. Fitzke, M.P. Mayer, and S. Rospert. 2011. The chaperone network connected to human ribosome-associated complex. *Mol. Cell. Biol*. 31:1160–1173. http://dx.doi.org/10.1128/MCB .00986-10

Jia, N., Y. Nakazawa, C. Guo, M. Shimada, M. Sethi, Y. Takahashi, H. Ueda, Y. Nagayama, and T. Ogi. 2015. A rapid, comprehensive system for assaying DNA repair activity and cytotoxic effects of DNA-damaging reagents. *Nat. Protoc*. 10:12–24. http://dx.doi.org/10.1038/nprot.2014 .194

Kapetanaki, M.G., J. Guerrero-Santoro, D.C. Bisi, C.L. Hsieh, V. Rapić-Otrin, and A.S. Levine. 2006. The DDB1-CUL4ADDB2 ubiquitin ligase is de cient in xeroderma pigmentosum group E and targets histone H2A at UV-damaged DNA sites. *Proc. Natl. Acad. Sci. USA*. 103:2588–2593. http://dx.doi.org/10.1073/pnas.0511160103



Karakuzu, O., D.P. Wang, and S. Cameron. 2009. MIG-32 and SPAT-3A are PRC1 homologs that control neuronal migration in Caenorhabditis elegans. *Development*. 136:943–953.

http://dx.doi.org/10.1242/dev.029363

Katsumi, S., N. Kobayashi, K. Imoto, A. Nakagawa, Y. Yamashina, T. Muramatsu, T. Shirai, S. Miyagawa, S. Sugiura, F. Hanaoka, et al.. 2001. In situ visualization of ultraviolet-light-induced DNA damage repair in locally irradiated human broblasts. *J. Invest. Dermatol*. 117:1156–1161. http://dx.doi.org/10.1046/j.0022-202x.2001.01540.x

Lans, H., and W. Vermeulen. 2011. Nucleotide excision repair in Caenorhabditis elegans. *Mol. Biol. Int*. 2011:542795. http://dx.doi.org/10.4061/2011/542795

Luijsterburg, M.S., J. Goedhart, J. Moser, H. Kool, B. Geverts, A.B. Houtsmuller, L.H. Mullenders, W. Vermeulen, and R. van Driel. 2007. Dynamic in vivo interaction of DDB2 E3 ubiquitin ligase with UV-damaged DNA is independent of damage-recognition protein XPC. *J. Cell Sci*. 120:2706– 2716. http://dx.doi.org/10.1242/jcs.008367

Mailand, N., S. Bekker-Jensen, H. Faustrup, F. Melander, J. Bartek, C. Lukas, and J. Lukas. 2007. RNF8 ubiquitylates histones at DNA double-strand breaks and promotes assembly of repair proteins. *Cell*. 131:887–900. http ://dx.doi.org/10.1016/j.cell.2007.09.040

Marteijn, J.A., S. Bekker-Jensen, N. Mailand, H. Lans, P. Schwertman, A.M. Gourdin, N.P. Dantuma, J. Lukas, and W. Vermeulen. 2009. Nucleotide excision repair-induced H2A ubiquitination is dependent on MDC1 and RNF8 and reveals a universal DNA damage response. *J. Cell Biol*. 186:835–847. http://dx.doi.org/10.1083/jcb.200902150

Marteijn, J.A., H. Lans, W. Vermeulen, and J.H. Hoeijmakers. 2014. Understanding nucleotide excision repair and its roles in cancer and ageing. *Nat. Rev. Mol. Cell Biol*. 15:465–481. http://dx.doi.org/10.1038/nrm3822

Masutani, C., K. Sugasawa, J. Yanagisawa, T. Sonoyama, M. Ui, T. Enomoto, K. Takio, K. Tanaka, P.J. van der Spek, D. Bootsma, et al. 1994. Puri cation and cloning of a nucleotide excision repair complex involv- ing the xeroderma pigmentosum group C protein and a human homo- logue of yeast RAD23. *EMBO J*. 13:1831–1843.

Matsui, S.I., B.K. Seon, and A.A. Sandberg. 1979. Disappearance of a structural chromatin protein A24 in mitosis: implications for molecular basis of chromatin condensation. *Proc. Natl. Acad. Sci. USA*. 76:6386–6390. http://dx.doi.org/10.1073/pnas.76.12.6386

Mattiroli, F., J.H. Vissers, W.J. van Dijk, P. Ikpa, E. Citterio, W. Vermeulen, J.A. Marteijn, and T.K. Sixma. 2012. RNF168 ubiquitinates K13-15 on H2A/H2AX to drive DNA damage signaling. *Cell*. 150:1182–1195. http://dx.doi.org/10.1016/j.cell.2012.08.005

Morey, L., and K. Helin. 2010. Polycomb group protein-mediated repression of transcription. *Trends Biochem. Sci*. 35:323–332. http://dx.doi.org/10 .1016/j.tibs.2010.02.009

Moser, J., M. Volker, H. Kool, S. Alekseev, H. Vrieling, A. Yasui, A.A. van Zeeland, and L.H. Mullenders. 2005. The UV-damaged DNA binding protein mediates ef cient targeting of the nucleotide excision repair complex to UV-induced photo lesions. *DNA Repair (Amst.)*. 4:571–582. http://dx.doi.org/10.1016/j.dnarep.2005.01.001

Nishi, R., S. Alekseev, C. Dinant, D. Hoogstraten, A.B. Houtsmuller, J.H. Hoeijmakers, W. Vermeulen, F. Hanaoka, and K. Sugasawa. 2009. UV-DDB-dependent regulation of nucleotide excision repair kinetics in

living cells. *DNA Repair (Amst.)*. 8:767–776. http://dx.doi.org/10.1016/j .dnarep.2009.02.004

Pan, M.R., G. Peng, W.C. Hung, and S.Y. Lin. 2011. Monoubiquitination of H2AX protein regulates DNA damage response signaling. *J. Biol. Chem*. 286:28599–28607. http://dx.doi.org/10.1074/jbc.M111.256297

Petroski, M.D., and R.J. Deshaies. 2005. Function and regulation of cullin-RING ubiquitin ligases. *Nat. Rev. Mol. Cell Biol*. 6:9–20. http://dx.doi.org/10 .1038/nrm1547

Pierce, N.W., J.E. Lee, X. Liu, M.J. Sweredoski, R.L. Graham, E.A. Larimore, M. Rome, N. Zheng, B.E. Clurman, S. Hess, et al. 2013. Cand1 promotes assembly of new SCF complexes through dynamic exchange of F box proteins. *Cell*. 153:206–215. http://dx.doi.org/10.1016/j.cell .2013.02.024

Qiu, X.B., Y.M. Shao, S. Miao, and L. Wang. 2006. The diversity of the DnaJ/ Hsp40 family, the crucial partners for Hsp70 chaperones. *Cell. Mol. Life Sci*. 63:2560–2570. http://dx.doi.org/10.1007/s00018-006-6192-6

Rapić-Otrin, V., V. Navazza, T. Nardo, E. Botta, M. McLenigan, D.C. Bisi, A.S. Levine, and M. Stefanini. 2003. True XP group E patients have a defective UV-damaged DNA binding protein complex and mutations in DDB2 which reveal the functional domains of its p48 product. *Hum. Mol. Genet*. 12:1507–1522. http://dx.doi.org/10.1093/hmg/ddg174

Richly, H., L. Rocha-Viegas, J.D. Ribeiro, S. Demajo, G. Gundem, N. Lopez- Bigas, T. Nakagawa, S. Rospert, T. Ito, and L. Di Croce. 2010. Transcriptional activation of polycomb-repressed genes by ZRF1. *Nature*. 468:1124–1128. http://dx.doi.org/10.1038/nature09574

Riedl, T., F. Hanaoka, and J.M. Egly. 2003. The comings and goings of nucleotide excision repair factors on damaged DNA. *EMBO J*. 22:5293–5303. http:// dx.doi.org/10.1093/emboj/cdg489

Shiyanov, P., A. Nag, and P. Raychaudhuri. 1999. Cullin 4A associates with the UV-damaged DNA-binding protein DDB. *J. Biol. Chem*. 274:35309– 35312. http://dx.doi.org/10.1074/jbc.274.50.35309

Sugasawa, K., J.M. Ng, C. Masutani, S. Iwai, P.J. van der Spek, A.P. Eker, F. Hanaoka, D. Bootsma, and J.H. Hoeijmakers. 1998. Xeroderma pigmentosum group C protein complex is the initiator of global genome nucleotide excision repair. *Mol. Cell*. 2:223–232. http://dx.doi.org/10 .1016/S1097-2765(00)80132-X

Sugasawa, K., T. Okamoto, Y. Shimizu, C. Masutani, S. Iwai, and F. Hanaoka. 2001. A multistep damage recognition mechanism for global genomic nucleotide excision repair. *Genes Dev*. 15:507–521. http://dx.doi.org/10 .1101/gad.866301

Sugasawa, K., Y. Okuda, M. Saijo, R. Nishi, N. Matsuda, G. Chu, T. Mori, S. Iwai, K. Tanaka, K. Tanaka, and F. Hanaoka. 2005. UV-induced ubiquitylation of XPC protein mediated by UV-DDB-ubiquitin ligase complex. *Cell*. 121:387–400. http://dx.doi.org/10.1016/j.cell.2005.02.035

Tang, J.Y., B.J. Hwang, J.M. Ford, P.C. Hanawalt, and G. Chu. 2000. Xeroderma pigmentosum p48 gene enhances global genomic repair and suppresses UV-induced mutagenesis. *Mol. Cell*. 5:737–744. http://dx.doi.org/10 .1016/S1097-2765(00)80252-X

Thorslund, T., A. Ripplinger, S. Hoffmann, T. Wild, M. Uckelmann, B. Villumsen, T. Narita, T.K. Sixma, C. Choudhary, S. Bekker-Jensen, and N. Mailand. 2015. Histone H1 couples initiation and ampli cation of

ubiquitin signalling after DNA damage. *Nature*. 527:389–393. http://dx .doi.org/10.1038/nature15401

Ui, A., Y. Nagaura, and A. Yasui. 2015. Transcriptional elongation factor ENL phosphorylated by ATM recruits polycomb and switches off transcription for DSB repair. *Mol. Cell*. 58:468–482. http://dx.doi.org/10.1016/j .molcel.2015.03.023

Wakasugi, M., and A. Sancar. 1999. Order of assembly of human DNA repair excision nuclease. *J. Biol. Chem*. 274:18759–18768. http://dx.doi.org/10 .1074/jbc.274.26.18759

Wang, H., L. Wang, H. Erdjument-Bromage, M. Vidal, P. Tempst, R.S. Jones, and Y. Zhang. 2004. Role of histone H2A ubiquitination in Polycomb silencing. *Nature*. 431:873–878. http://dx.doi.org/10.1038/nature02985

Wang, H., L. Zhai, J. Xu, H.Y. Joo, S. Jackson, H. Erdjument-Bromage, P. Tempst, Y. Xiong, and Y. Zhang. 2006. Histone H3 and H4 ubiquitylation by the CUL4-DDB-ROC1 ubiquitin ligase facilitates cellular response to DNA damage. *Mol. Cell*. 22:383–394. http://dx.doi.org/10.1016/j.molcel.2006 .03.035

# Nuclear Organization of Nucleotide Excision Repair is mediated by RING1B dependent H2A-ubiquitylation

Oncotarget (in Press)

# Nuclear Organization of Nucleotide Excision Repair is mediated by RING1B dependent H2A-ubiquitylation

Shalaka Chitale[1] and Holger Richly[1,*]

[1] Laboratory of Molecular Epigenetics, Institute of Molecular Biology (IMB), Mainz, Germany, Ackermannweg 4, 55128 Mainz, Germany

[*] Correspondence: h.richly@imb-mainz.de

## SUMMARY

One of the major cellular DNA repair pathways is Nucleotide Excision Repair (NER). It is the primary pathway for repair of various DNA lesions caused by exposure to ultraviolet (UV) light (de Laat et al. 1999; Fousteri and Mullenders 2008), such as cyclobutane pyrimidine dimers (CPDs) and 6-4 photoproducts. Although lesion-containing DNA associates with the nuclear matrix after UV irradiation (Koehler and Hanawalt 1996) it is still not understood how nuclear organization affects NER. Analyzing unscheduled DNA synthesis (UDS) indicates that NER preferentially occurs in specific nuclear areas, viz the nucleolus. Upon inducing localized damage, we observe migration of damaged DNA towards the nucleolus. Employing a LacR-based tethering system (Janicki et al. 2004) we demonstrate that H2A-ubiquitylation via the UV-RING1B complex (Gracheva et al. 2016) localizes chromatin close to the nucleolus. We further show that the H2A-ubiquitin binding protein ZRF1 resides in the nucleolus, and that it anchors ubiquitylated chromatin along with XPC. Our data thus provide insight into the sub-nuclear organization of NER and reveal a novel role for histone H2A-ubiquitylation.

## INTRODUCTION

Nucleotide Excision Repair (NER) is one of the major DNA repair pathways and handles various lesions such as cyclobutane pyrimidine dimers (CPDs) and 6-4 photoproducts, which occur after exposure to ultraviolet (UV) light (de Laat et al. 1999). Defects in NER cause genetic disorders such as *Xeroderma pigmentosum*, which constitutes hypersensitivity to sunlight and a predisposition for skin cancer (Friedberg 2001). Mammalian NER recognizes DNA lesions by two different pathways. Transcription-coupled NER (TC-NER) is limited to regions of active transcription, where RNA Polymerase II stalling elicits the DNA damage response. In contrast, transcription-independent recognition of lesions is handled by global genome NER (GG-NER) (Fousteri and Mullenders 2008; Marteijn et al. 2014). During GG-NER, lesions are detected by the proteins XPC and DDB2. XPC specifically recognizes structures that distort the DNA double-helix, binds damaged DNA, and rapidly dissociates upon triggering NER (Sugasawa et al. 2001; Hoogstraten et al. 2008; Bergink et al. 2012). Efficient recognition of CPDs and 6-4 photoproducts also requires DDB2 (XPE) (Tang et al. 2000; Fitch et al. 2003; Moser et al. 2005; Luijsterburg et al. 2007; Nishi et al. 2009). DDB2 along with DDB1, the RING-domain proteins RBX1 or RING1B, and either of the scaffold proteins CUL4A or CUL4B forms E3 ubiquitin ligase complexes (UV-DDB-CUL4A/B) and UV-RING1B. These complexes catalyze the mono-ubiquitylation of histones H2A, H3 and H4 as well as the polyubiquitylation of XPC (Shiyanov et al. 1999; Angers et al. 2006; Wang et al. 2006; Guerrero-Santoro et al. 2008).

Studies of DNA repair have shown that nuclear positioning and migration of the damaged DNA to specific repair centers is a central component of many repair pathways (Lisby et al. 2003; Therizols et al. 2006; Nagai et al. 2008; Misteli and Soutoglou 2009). In mammalian cells, nuclear organization during double-strand break (DSB) repair affects chromosome translocations (Roukos and Misteli 2014) and pathway choice (Lemaitre et al. 2014). During NER, the damage recognition factor DDB2 promotes local chromatin decondensation (Luijsterburg et al. 2012) and NER seems to involve large-scale chromatin rearrangements (Adam and Polo 2012). Additionally, it has been recently shown that heterochromatin impedes CPD removal, and this process is enabled by DDB2 (Han et al., 2002). Although lesion-containing DNA associates with the nuclear matrix after UV irradiation (Koehler and Hanawalt 1996) it is less well understood how nuclear organization affects NER.

Another important feature of DNA repair is H2A-ubiquitylation. At DSBs, ubiquitylation of H2A is carried out by the E3 ligases RNF168, RNF8, and RING1B, which facilitates signaling and accumulation of repair proteins (Doil et al. 2009; Pan et al. 2011; Mattiroli et al. 2012; Ui et al.

2015). Furthermore, it was demonstrated that the RING1B-catalyzed ubiquitylation through Polycomb-repressive complex 1 (PRC1) mediates DSB-induced gene silencing, highlighting an additional function of H2A-ubiquitylation in DNA repair (Ui et al. 2015). During NER H2A-ubiquitylation is catalyzed by the E3 ligase RNF8, the UV-DDB-CUL4 and UV-RING1B complexes (Bergink et al. 2006; Kapetanaki et al. 2006; Guerrero-Santoro et al. 2008; Marteijn et al. 2009; Gracheva et al. 2016). We have recently shown that ZRF1 is an essential factor in NER. ZRF1 binds the H2A-ubiquitin mark catalyzed by the UV-RING1B complex, and its presence at damaged chromatin depends on the recognition factor XPC (Gracheva et al. 2016).

Here we report that H2A-ubiquitylation via the UV-RING1B complex repositions chromatin close to the nucleolus. We provide further evidence that ZRF1 resides in the nucleolus and that H2A-ubiquitylation and its recognition by ZRF1 facilitate nucleolar DNA repair.

## RESULTS

### NER is partially routed to the nucleolus and involves reorganization of chromatin

In order to determine whether NER, similar to other DNA repair pathways, occurs in so called ”repair factories” we studied the nuclear distribution of repair. We visualized unscheduled DNA synthesis (UDS) in fibroblasts to determine whether DNA repair shows a bias in nuclear distribution. In order to analyze the distribution at various stages of repair, we pulsed the cells with EdU for 2 hours at various time points post UV exposure and measured the EdU incorporation in non S-phase cells (Figure S1A). Immediately after UV exposure, DNA repair occurred uniformly throughout the nucleus with no discernible patterns. However, at later time points after UV exposure, we observed repair occurring in specific nuclear foci (Figure 1A). These foci resembled nucleoli in size and number, and thus we performed a costaining with nucleophosmin (NPM- a marker for the nucleolus). We found that the repair foci indeed overlapped with nucleoli (Figure 1A). In order to measure the share of repair occurring in the nucleolus, we measured the mean EdU intensity in the nucleolus, nucleoplasm as well as in the whole nucleus. Using these values we calculated the Nucleolar Repair Index (NRI) as $(Nucleolus^{mean} - Nucleoplasm^{mean)}/Nucleus^{mean} \times 100$, where a positive NRI reflects an enrichment of DNA repair in the nucleolus. Interestingly, 8 hours after UV irradiation we started to observe an enrichment of EdU incorporation in the nucleolus as compared to the nucleoplasm, reflected

by a positive NRI, which increased with time reaching its maximum 24 hours post irradiation (Figure 1A). In non-irradiated cells we did not detect any EdU incorporation confirming that the incorporation was indeed a consequence of active DNA repair (Figure S1A). Additionally, we analyzed the images to determine whether the observed nucleolar EdU enrichment is a consequence of the underlying chromatin structure, specifically due to the presence of perinuclolar heterochromatin. We normalized the EdU signal by the DAPI signal, giving us a normalized image for EdU per DNA amount. We then measured the mean EdU intensity in the nucleolus, nucleoplasm as well as in the whole nucleus in the normalized image. Using these values we calculated the Nucleolar Repair Index (NRI). The NRI showed a similar increase in nucleolar signal as compared to the non-normalized EdU signal (Figure S1E), thus demonstrating that the enrichment seen is independent of the underlying chromatin structure.

Next, we wanted to determine if the measured nucleolar EdU incorporation is due solely to the repair of perinuclear heterochromatin or whether it predominantly reflects repair of non-nucleolar chromatin. To this end, we EdU-pulsed cells for 2 hours, at 0 and 10 hours after UV irradiation, and subsequently allowed the repair to proceed in EdU-free medium up to 24 hours. We chose the 10 hour time point, as we had observed an overall sufficient repair signal and enrichment of nucleolar repair at this time (Figure 1A). We noticed that, 12 hours after changing to EdU-free medium, the nucleolar enrichment of the EdU signal was lost and that it was once again evenly distributed within the nucleus for both the 0 and 10 hour time points (Figure 1B). This re-distribution of the repaired DNA suggests a dynamic relationship between the site of repair and the subsequent nuclear positioning of the repaired DNA. Notably, the redistribution of repaired DNA occurred even for DNA repaired immediately after UV damage, reflected by a decrease in the NRI. This further implies that nucleolar repair occurs throughout the repair process, but at later time points the majority of repair occurs in the nucleolus.

To further confirm whether the nucleolus acts as a repair center, we investigated whether the endogenous NER proteins relocated to the nucleolus upon UV irradiation. We observed a distinct enrichment of XPA, a critical NER protein (de Laat et al. 1999) in the nucleolus of pre-extracted U2OS and MRC5 cells, starting at 1 hour after UV irradiation (Figure 1C and S1E). Furthermore, we assessed the presence of selected DNA repair factors in purified nucleoli before and after UV irradiation (Figures 1D, S1B, S1C and S1D). We found repair proteins such as XPC, and XPB in nucleoli even in unexposed cells, while XPA levels increased post UV exposure. In the time course assayed, the total protein levels of XPA did not change, suggesting a

specific recruitment to the nucleolus (Figure S1D). In addition, we tested whether the proteins found in the nucleolus were also chromatin bound. To this end, we extracted purified nucleoli with increasing salt concentrations (Figure 1D). We found XPC, XPB, DDB2 and XPA associated to chromatin in nucleoli of irradiated cells.

Lastly, we wanted to assess if damaged DNA also translocates to the nucleolus. To this end, we inflicted localized damage on the cells through a micropore membrane. We marked the damaged DNA by XPA staining, and observed overlap of the lesions with the nucleoli. We observed that at 5 min post damage, ≈20% of lesions marked by XPA overlapped with a nucleolus, which could be due to random positioning of the micropore in the vicinity of the nucleolus. However at 1 hour post UV damage, ≈70% of cells show XPA signal with some degree of overlap with the nucleolus (Figure 1E), indicating an active change in positioning of the damaged DNA. Taken together our data suggest that GG-NER is carried out in part at the nucleolus and that it involves re-localization of the damaged DNA.

Figure 1. The nucleolus is a site of accumulation of NER proteins as well as active repair. (a) NER occurs in repair foci that colocalize with nuclophosmin (NPM-a nucleolar protein). (Left panel) Representative images of active repair foci indicated by EdU incorporation, at the indicated time points post UV exposure. Cells are costained with NPM to show nucleolar overlap of repair foci Scale bar- 5µm (Right panel) The graph shows the Nucleolar Repair Index (NRI) values of nucleoli from ≈100 non-S phase cells at the indicated time points post UV exposure. Statistical significance was calculated using a Mann-Whitney test. (b) DNA repaired in the nucleolus is later redistributed throughout the nucleus. (Top panel) The graph shows the Nucleolar Repair Index (NRI) values of nucleoli from ≈100 non-S phase cells, at the indicated time points post UV exposure, with or without extended repair upto 24 hours (extended) in EdU free medium. Statistical significance was calculated using a Mann Whitney test. (Bottom panel) Representative images of active repair indicated by EdU incorporation, at the indicated time points post UV exposure, stained either immediately after incorporation, or after extended repair in EdU free medium upto 24 hrs (extended). Scale bar- 5µm (c) XPA accumulates in the nucleolus post UV exposure. Immunofluorescence images showing staining of NPM and XPA in pre-extracted cells unexposed to UV, or 1 hour after exposure to a 20J/$m^2$ UV dose. Pre-extraction washes off unbound nuclear and cytoplasmic proteins and enables visualization of chromatin-associated proteins. In UV exposed cells, nucleolar XPA is seen in 73.57% ±10.13 cells. 60-80 cells were counted per replicate. n=3. Scale bar - 5µm (d) Nucleolar NER proteins are present in the chromatin fraction post UV exposure. Western blot showing sequential salt extraction fractions of nucleoli at the indicated timepoints post UV exposure. The pellet consists of the chromatin bound fraction. (e) Immunofluorescence images showing XPA distribution in pre-extracted MRC5 cells subjected to damage through a micropore of diameter 5 µm. Cells were fixed and stained at the indicated time points after UV damage. Lesions are marked by XPA staining. Nuclei are shown by DAPI staining, and nucleoli marked by Nucleophosmin (NPM). XPA signal shows overlap with NPM in 13%±6 nucleoli at 5 min timepoint, and increases to 71%±4 at 60 min timepoint. 30 cells measured per experiment. N=2. Scale bar - 5µm

Figure 1

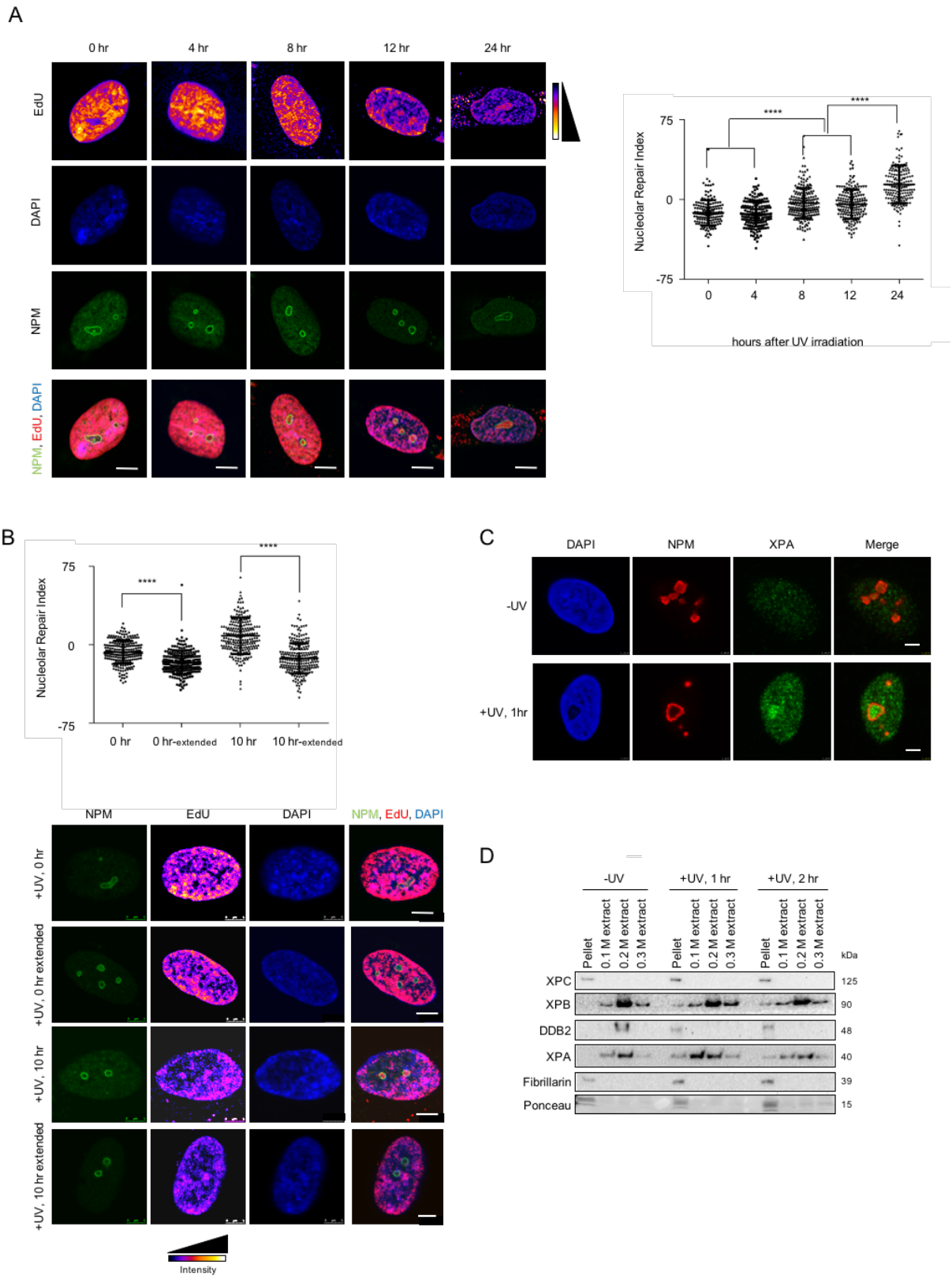
A
0 hr
4 hr
8 hr
12 hr
24 hr
EdU
DAPI
NPM
NPM, EdU, DAPI
Nucleolar Repair Index
75
0
-75
****
****
0
4
8
12
24
hours after UV irradiation
B
Nucleolar Repair Index
75
0
-75
****
****
0 hr
0 hr-extended
10 hr
10 hr-extended
NPM
EdU
DAPI
NPM, EdU, DAPI
+UV, 0 hr
+UV, 0 hr extended
+UV, 10 hr
+UV, 10 hr extended
Intensity
C
DAPI
NPM
XPA
Merge
-UV
+UV, 1hr
D
-UV
+UV, 1 hr
+UV, 2 hr
Pellet
0.1 M extract
0.2 M extract
0.3 M extract
kDa
XPC
XPB
DDB2
XPA
Fibrillarin
Ponceau
125
90
48
40
39
15

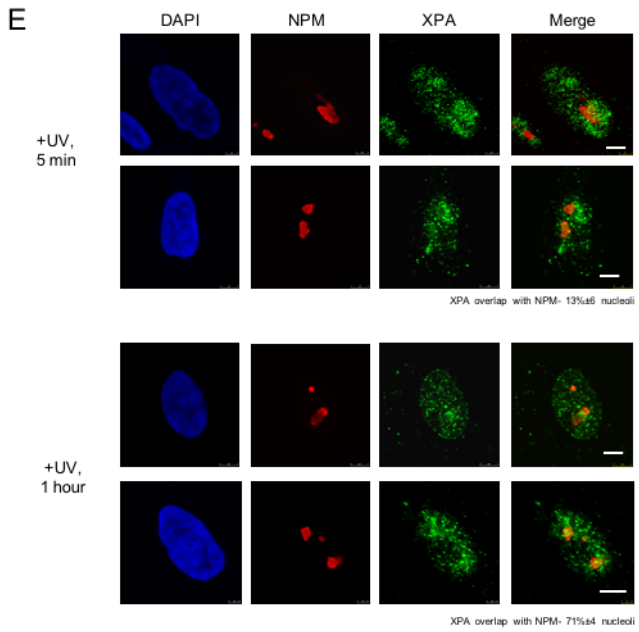


**DDB2 causes repositioning of chromatin to the vicinity of the nucleolus**

As lesion recognition is essential for subsequent repair, we wanted to determine if lesion recognition led to translocation of DNA to the nucleolus for repair. To directly assess the effect of binding of recognition proteins to DNA, we used a lactose repressor (LacR) based system for tethering proteins to a defined chromosome region *in vivo* (Belmont and Straight 1998; Janicki et al. 2004). We tethered mCherry-LacR fusions of DDB2, XPC and CSA to a heterochromatic locus in human U2OS 2-6-3 cells, containing 200 copies of a LacO containing cassette (total array size ≈ 4Mbp) (Janicki et al. 2004). We expressed mCherry-LacR-fusion and mCherry-LacR proteins in the U2OS 2-6-3 cell line and analyzed the nuclear positioning of the array. We observed a significant increase in the number of nucleolar arrays (distance from nucleolus 0 μm) upon tethering of DDB2 (Figure 2A), while tethering of XPC or CSA did not show a significant effect (Figures 2B and 2C). Representative images and the corresponding nucleolar distance are shown in Figure S2A. Our UDS data showed the nucleolus to be a site of active DNA repair. The LacO tethering system however, mimics the recognition and subsequent relocalization of chromatin to the nucleolus. In order quantify this dynamic process, we additionally determined if the tethered array was positioned overall closer to the nucleolus. The nucleolar distance was measured as the distance of the array to the closest nucleolus. Distances were measured for 100 randomly picked transfected cells per sample (Chubb et al. 2002)(Strongin et al. 2014) and the

mean nucleolar distance from at least 3 independent experiments was calculated. Tethering of DDB2 caused a relocation of the DNA array and positioned it closer to the nucleolus (mean ≈1μm). In comparison, the untethered control (mean ≈2μm) showed a random distribution of the array in agreement with a previous report (Manuelidis and Borden 1988) (Figure 2D). Tethering of XPC-LacR or CSA-LacR did not significantly relocate the array to the vicinity of the nucleolus (Figures 2E and 2F). It has been previously reported that tethered DDB2 recruits GFP tagged DDB1 and CUL4A (Luijsterburg et al. 2012). We additionally confirmed the functionality of tethered DDB2 by staining with DDB1 antibodies, as well as by showing recruitment of XPC-GFP to the array (Figure S2B). In addition we verified that tethered CSA-LacR co-localized with its binding partner DDB1 (Groisman et al. 2003; Lee and Zhou 2007) (Figure S2D). Expression of mCherry-LacR-DDB2 also results in an excess of unbound nuclear protein. To confirm that the repositioning is indeed a consequence of the tethered DDB2, and not an effect of global DDB2 overexpression, we expressed DDB2-EGFP in cells containing mCherry-LacR and DDB2-LacR tethered arrays. Overexpression of DDB2-EGFP caused no relocation of the control array and did not impair repositioning by the tethered DDB2-LacR (Figure 2G). Indirect tethering of DDB2-EGFP through a GFP binding protein (GBP)-LacR system (Rothbauer et al. 2008; Zolghadr et al. 2008; Herce et al. 2013) also led to a similar re-localization (Figure S2C). Altogether, these data suggest that specifically DDB2 is important for repositioning the array close to the nucleolus. Importantly, the repositioning of the array occurs only through components of the GG-NER pathway, which is in agreement with the later time points at which an enrichment of nucleolar repair is observed (Bohr et al. 1985; Mellon et al. 1987)

Figure 2

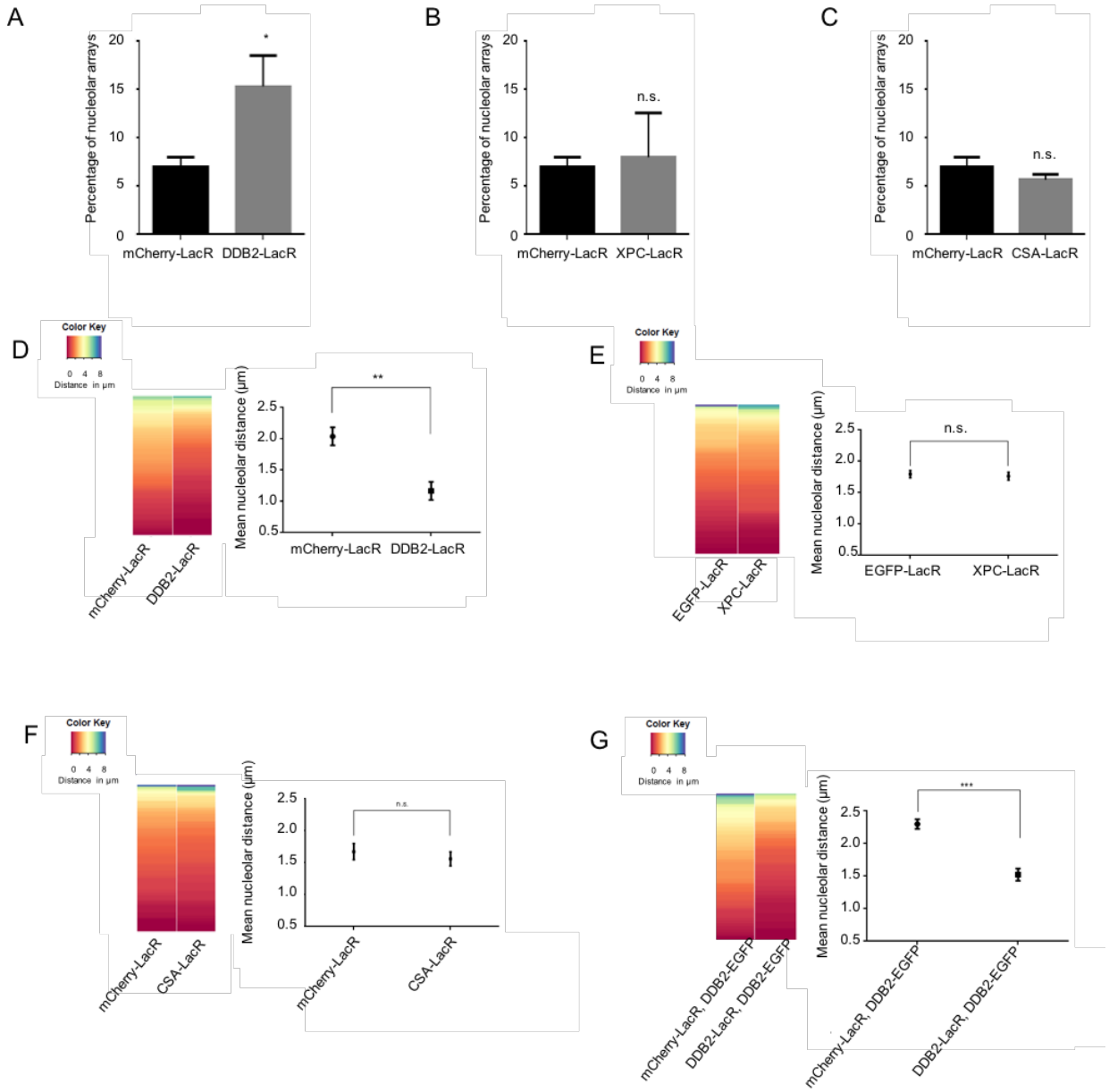


Figure 2. DDB2 tethering causes repositioning of a LacO array to the nucleolus. (a) Quantification of nucleolar arrays (distance from nucleolus=0µm) in control (mCherry-LacR) and DDB2 (DDB2-LacR) tethered arrays. 90-100 cells were counted per experiment. The graph shows the mean ±SD. (n=3). Significance was determined by an unpaired t-test. (b) Quantification of nucleolar arrays (distance from nucleolus=0µm) in control (mCherry-LacR) and XPC (XPC-LacR) tethered arrays. 90-100 cells were counted per experiment. The graph shows the mean ±SD. (n=3). Significance was determined by an unpaired t-test. (c) Quantification of nucleolar arrays (distance from nucleolus=0µm) in control (mCherry-LacR) and CSA (CSA-LacR) tethered arrays. 90-100 cells were counted per experiment. The graph shows the mean ±SD. (n=3). Significance was determined by an unpaired t-test. (d) (Left panel) Heat map showing the distribution of the nucleolar distance of the array in 100 cells. Control arrays (mCherry-LacR)

and DDB2 tethered arrays (DDB2-LacR) were analyzed. The distribution of the control array differs significantly from the DDB2 array as judged by a KS test. (p value≤ 0.0001). (Right panel) Mean nucleolar distance of the array in control and DDB2 conditions. The mean nucleolar distance of each replicate was calculated from measurements of nucleolar distance in 100 cells. The graph shows the average of the means from 3 independent experiments ±SD. Statistical significance was determined using an unpaired t-test. (e) Tethering of XPC does not cause repositioning of the LacO array. (Left panel) Heat map showing the distribution of the nucleolar distance of the array in 100 cells. Control arrays (mCherry-LacR) and XPC tethered arrays (XPC-LacR) were analyzed. The distribution of the control array is not significantly different compared to the XPC tethered array as judged by the KS test. (Right panel) Mean nucleolar distance of the array in control and XPC conditions. The mean nucleolar distance of each replicate was calculated from measurements of nucleolar distance in 100 cells. The graph shows the average of the means from 3 independent experiments ±SD. Statistical significance was determined using an unpaired t-test. (f) Tethering of CSA does not cause repositioning of the LacO array. (Left panel) Heat map showing the distribution of the nucleolar distance of the array in 100 cells with control arrays (mCherry-LacR) and CSA tethered arrays (CSA-LacR). Distribution of the control array does not significantly differ from the CSA-tethered array as judged by KS test. (Right panel) Mean nucleolar distance of the array in control and CSA conditions. The mean nucleolar distance of each replicate was calculated from measurements of nucleolar distance in 100 cells. The graph shows the average of the means from 3 independent experiments ±SD. Statistical significance was determined using an unpaired t-test. (g) Repositioning of the array is specifically an effect of local DDB2 tethering. DDB2-EGFP was expressed in cells with mCherry-LacR and DDB2-LacR tethered arrays (Left panel) Heat map showing the distribution of the distance between the array and the nucleolus in 100 cells. Expression of DDB2-EGFP does not affect the distribution of the mCherry-LacR array. The distribution of the control array differs significantly from the DDB2 array as judged by a KS test. (p value≤ 0.0001). (Right panel) Mean nucleolar distance of the array in the corresponding cells. The mean nucleolar distance of each replicate was calculated from measurements of nucleolar distance in 100 cells. The graph shows the average of the means from 3 independent experiments ±SD. Statistical significance was determined using an unpaired t-test.

## Nucleolar repositioning requires presence of a functional UV-RING1B complex and H2A-K119 ubiquitylation

DDB2 is known to form various ubiquitin E3 ligase complexes that catalyze the ubiquitylation of histones and other DNA repair factors during NER (Sugasawa et al. 2005; Angers et al. 2006; Kapetanaki et al. 2006; Guerrero-Santoro et al. 2008; Gracheva et al. 2016). Each complex harbors the DDB2-DDB1 heterodimer, while the cullins and the E3 ligases vary between the complexes. To establish whether the repositioning of the array requires the formation of a functional DDB2 complex, we tethered two naturally occurring point mutations of DDB2 to the array, $DDB2^{D370Y}$ and $DDB2^{L350P}$ (Figure 3A). These mutants lack the ability to bind DDB1 and were previously shown to abolish the formation of a functional E3 ligase complex (Figure S3A) (Luijsterburg et al. 2012). As opposed to DDB2-LacR, neither of the tethered DDB2 mutants

caused re-localization of the array to the nucleolus. This implies that a functional E3 ligase complex is required for the re-localization of the array.

Given the localization phenotype of the DDB2 mutants (Figure 3A) we reasoned that the catalytic activity of the UV-DDB-CUL4 complexes or the UV-RING1B complex might form the basis for the repositioning of the array. To distinguish the E3 ligase complexes we tethered either RING1B-LacR (UV-RING1B complex) or RBX1-LacR (UV-DDB-CUL4A/4B complexes) to the array (Figure 3B). We noticed that only RING1B but not RBX1 repositioned the array to the proximity of the nucleolus (Figure 3B), even though both E3 ligases caused ubiquitylation of the array (Figure S3B). Furthermore, we did not observe repositioning when binding an enzymatically inactive RING1B mutant (RING1B$^{R70C}$-LacR) (Figure 3C) (Wang et al. 2004), although RING1B$^{R70C}$ retained the ability to recruit DDB2-EGFP, similar to RBX1 and RING1B (Figure S3C). Notably, while both RING1B and RBX1 caused ubiquitylation when tethered to the array (Figure S3B), only RING1B generated a prominent H2A-K119 ubiquitin mark (Figure 3D).

Figure 3

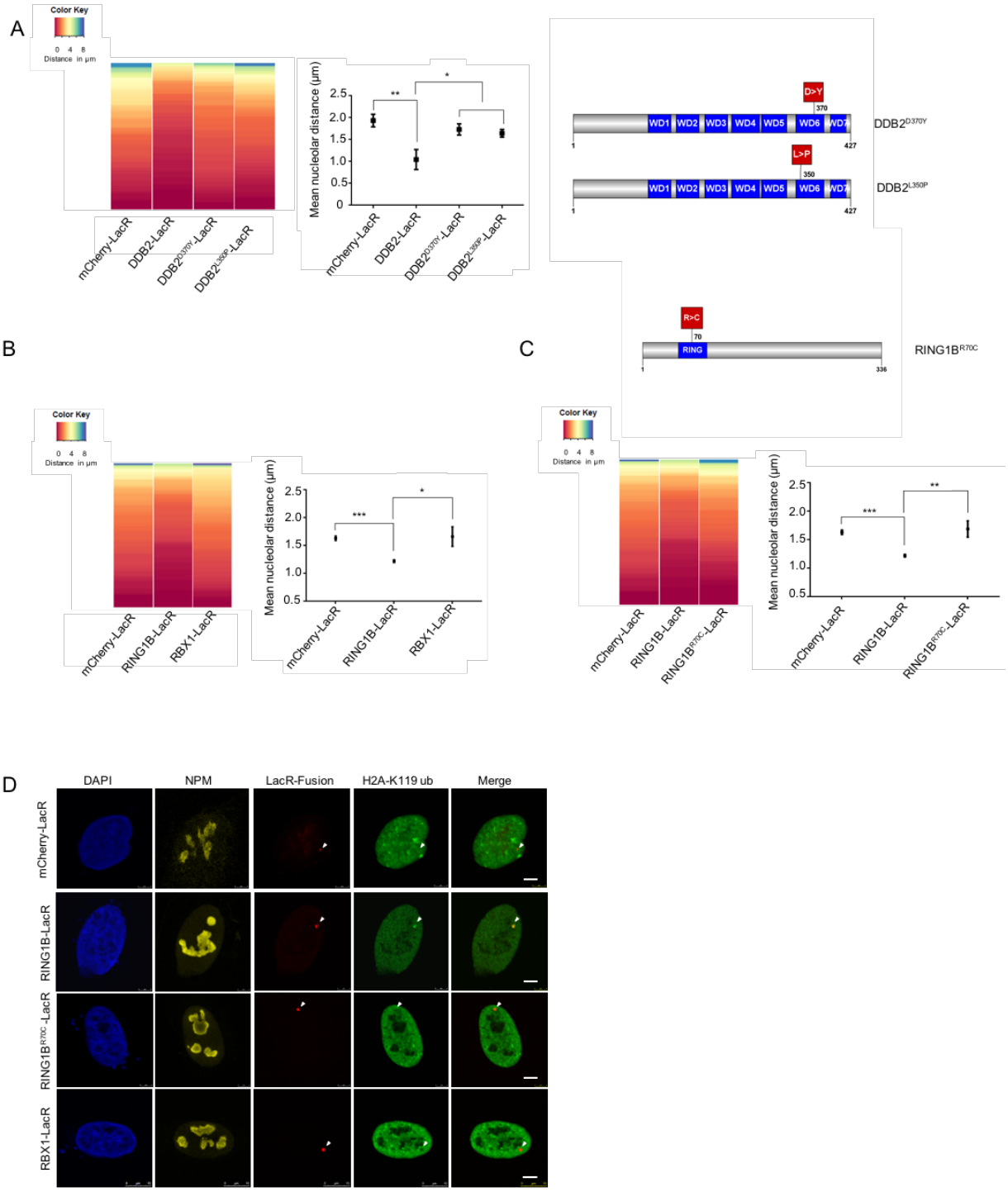
A
Color Key
0 4 8
Distance in µm
Mean nucleolar distance (µm)
mCherry-LacR
DDB2-LacR
DDB2D370Y-LacR
DDB2L350P-LacR
B
RING1B-LacR
RBX1-LacR
C
D>Y
370
L>P
350
WD1
WD2
WD3
WD4
WD5
WD6
WD7
DDB2D370Y
DDB2L350P
R>C
70
RING
RING1BR70C
RING1BR70C-LacR
D
DAPI
NPM
LacR-Fusion
H2A-K119 ub
Merge

Figure 3. Repositioning of the array is dependent on formation of a functional UV-DDB complex (a) Tethering of DDB2 mutants does not lead to repositioning of the LacO array. (Left panel) Heat map showing the distribution of the nucleolar distance of the array in 100 cells. Distances were measured in control arrays (mCherry-LacR) and DDB2-LacR, $DDB2^{D370Y}$-LacR and $DDB2^{L350P}$-LacR tethered arrays. Relocalization of DDB2 differs significantly from the control array as judged by a KS test. (p value$\leq$ 0.0001). Tethering $DDB2^{D370Y}$-LacR or $DDB2^{L350P}$-LacR does not differ significantly from the control. (Middle panel) Mean nucleolar distance of the array in control, DDB2-LacR, $DDB2^{D370Y}$-LacR and $DDB2^{L350P}$-LacR tethered conditions. The mean nucleolar distance of each replicate was calculated from measurements of nucleolar distance in 100 cells. The graph shows the average of the means from 3 independent experiments ±SD. Statistical significance was determined using an unpaired t-test. (Right panel) Graphical representation of the DDB2 point mutations used in this study. (b) RING1B, but not RBX1 tethering does not lead to repositioning of the array. (Left panel) Heat map showing the distribution of nucleolar distance of the array in 100 cells. Control arrays (mCherry-LacR), RING1B-LacR and RBX1-LacR tethered arrays were analyzed. The distribution of the RING1B-LacR array differs significantly when compared to the control array as judged by the KS test (p value$\leq$ 0.001). (Right panel) Mean nucleolar distance in mCherry-LacR, RING1B-LacR and RBX1-LacR tethered arrays. The mean nucleolar distance of each replicate was calculated from measurements of nucleolar distance in 100 cells. The graph shows the average of the means from 3 independent experiments ±SD. Statistical significance was determined using an unpaired t-test. (c) $RING1B^{R70C}$-LacR tethering does not cause repositioning of the array. (Top panel) Graphical illustration of the RING1B point mutation used in this study (Left panel) Heat map showing distribution of distance of the array from the nucleolus in 100 cells with mCherry-LacR, RING1B-LacR or $RING1B^{R70C}$-LacR tethered arrays. RING1B-LacR differs significantly from the control as judged by a KS test (p value$\leq$ 0.001). (Right panel) Mean nucleolar distance of the array in mCherry-LacR, RING1B-LacR and $RING1B^{R70C}$-LacR tethered cells. The mean nucleolar distance of each replicate was calculated from measurements of nucleolar distance in 100 cells. The graph shows the average of the means from 3 independent experiments ±SD. Statistical significance was determined using an unpaired t-test. (d) Tethering of RING1B causes deposition of a prominent H2A-K119 ubiquitin mark. H2A-K119 ubiquitin antibody staining in cells with tethered RING1B-LacR, RBX1-LacR or $RING1B^{R70C}$-LacR. Scale bar - 5µm. H2A-K119 ub signal was observed to colocalize with RING1B LacR in 70/100 cells. Colocalization was seen in 0/100 cells for mCherry-LacR, RBX1-LacR and $RING1B^{R70C}$-LacR.

Next, we performed experiments expressing RING1B (RING1B-EGFP), RBX1 (RBX1-EGFP) or the RING1B mutant ($RING1B^{R70C}$-EGFP) in combination with DDB2-LacR in the U2OS 2-6-3 cell line. We observed recruitment of all EGFP tagged E3 ligases to the DDB2-LacR array, further confirming the formation of an E3 ligase complex (Figure S4A). Expression of RING1B-EGFP did not significantly change the localization observed with tethered DDB2-LacR alone

(Figure 4A). However, simultaneous expression of RING1B$^{R70C}$-EGFP or RBX1-EGFP caused an increase in the mean distance from the nucleolus suggesting they might compete with functional endogenous RING1B for binding DDB2-LacR thereby precluding the generation of the UV-RING1B complex. Next we assessed whether RING1B depletion affected the repositioning of the array. Depletion of RING1B (shRING1B) in the U2OS 2-6-3 cell line caused a reduction of DDB2 mediated re-localization (Figures 4C and S4D) when compared to control cells (shNMC) (Figure 4B). Finally, we wanted to confirm that the loss of the repositioning occurs due to absence of H2A-ubiquitylation, and not due to absence of functional RING1B. Hence, we performed a double tethering experiment with the H2A-ubiquitin specific deubiquitinase USP16 (Joo et al. 2007). Simultaneous tethering of RING1B and USP16 to the array completely eliminated the H2A-K119 mark from the array (Figures S4B and S4C). Importantly, simultaneous tethering of USP16 and DDB2 to the array provoked a total loss of the re-localization observed for DDB2 alone (Figure 4D). Thus, our data suggest that absence of H2A-K119-ubiquitylation prevents the re-localization of the array to the nucleolus in spite of presence of a functional UV-DDB complex.

Figure 4. Repositioning of the array is dependent on H2A K119 ubiquitin mark set by RING1B (a) DDB2-LacR mediated repositioning can be attenuated by competition between E3 ligases. (Left panel) Heat map showing distribution of nucleolar distance of the array in 100 cells. Cells with DDB2-LacR tethered arrays, expressing EGFP, RING1B-EGFP, RBX1-EGFP or RING1B$^{R70C}$-EGFP were analyzed as shown. (Right panel) Mean nucleolar distance of the DDB2-LacR tethered arrays in cells expressing EGFP, RING1B-EGFP, RBX1-EGFP or RING1B$^{R70C}$-EGFP as shown. The mean nucleolar distance of each replicate was calculated from measurements of nucleolar distance in 100 cells. The graph shows the average of the means from 3 independent experiments ±SD. Statistical significance was determined using an unpaired t-test. (b,c) Knockdown of RING1B abolishes repositioning of a DDB2-LacR tethered array. (Left panel) Heat map showing distribution of the nucleolar distance of the array in 100 cells. mCherry-LacR or DDB2-LacR tethered arrays were analyzed in a control (shNMC) or RING1B knockdown (shRING1B) background. There was no significant difference between the control and DDB2-LacR tethered array in the shRING1B cells as judged by a KS test. (Right panel) Mean nucleolar distance of the control and DDB2-tethered array in shNMC or shRING1B cells. The mean nucleolar distance of each replicate was calculated from measurements of nucleolar distance in 100 cells. The graph shows the average of the means from 3 independent experiments ±SD. Statistical significance was determined using an unpaired t-test. (d) Co-tethering of USP16-LacR abolishes repositioning of a DDB2-LacR tethered array. (Left panel) Heat map showing nucleolar distance of the array in 100 cells. EGFP-DDB2-LacR (base tethering) was co-tethered to the array along with either mCherry-LacR or mCherry-LacR-USP16. Co-tethering of USP16 leads to a significant repositioning of the array as judged by a KS test (p value$\leq$ 0.0001). (Right panel) Mean nucleolar distance of the DDB2-LacR tethered array with mCherry-LacR and USP16 LacR co-tethering. The mean nucleolar distance of each replicate was calculated from measurements of nucleolar distance in 100 cells. The graph shows the average of the means from 3 independent experiments ±SD. Statistical significance was determined using an unpaired t-test.

Figure 4

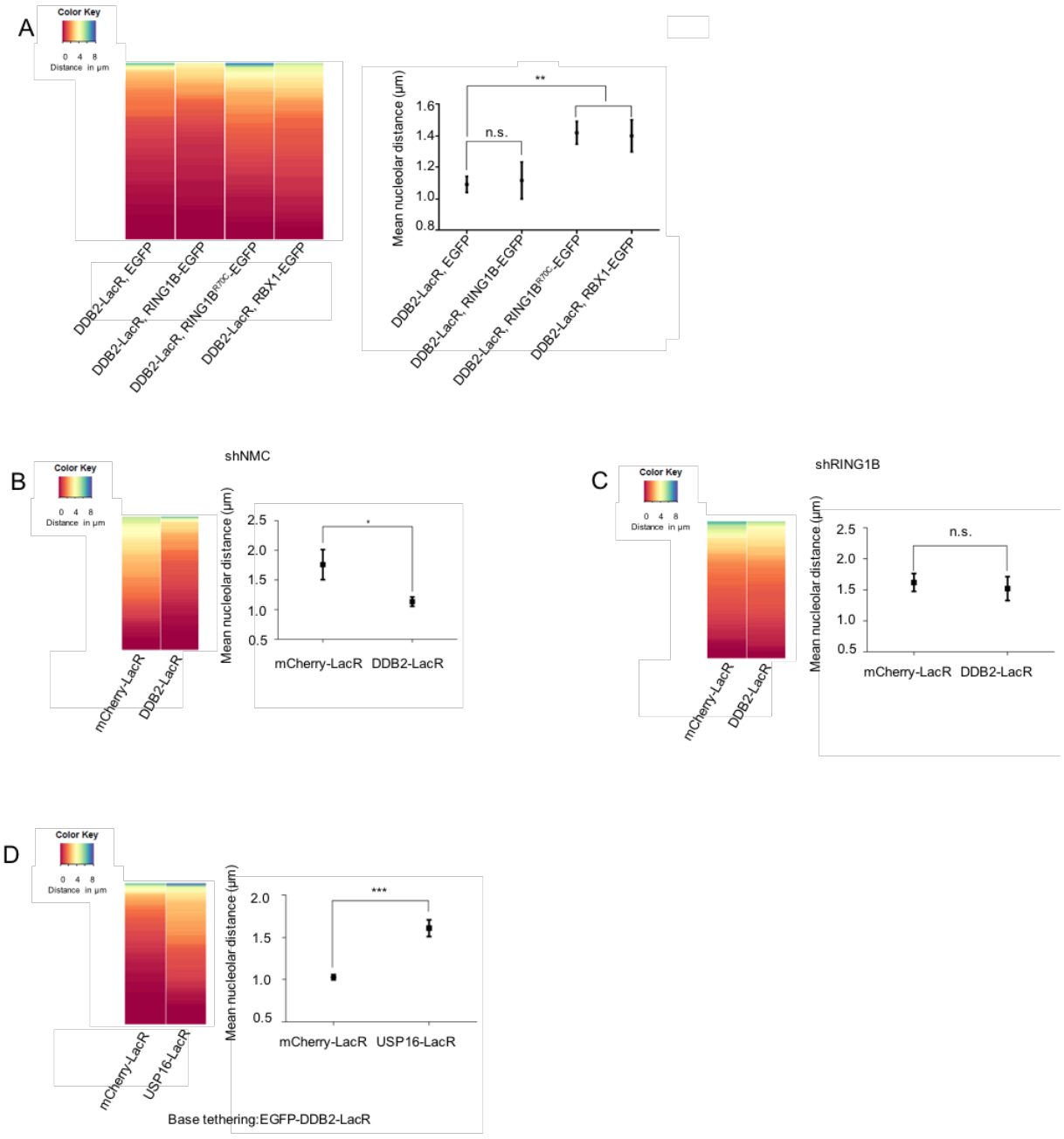


**ZRF1 is present in the nucleolus and facilitates relocalization of chromatin**

As the UV-RING1B complex is required for relocalization of the array to the vicinity of the nucleolus, we next asked how the DNA is anchored at the nucleolus for repair. ZRF1, a reader of the H2A-ubiquitin mark, was recently shown to be essential for NER. ZRF1 requires both H2A-ubiquitylation and XPC to bind to damaged chromatin (Gracheva et al. 2016). Investigating the

nuclear distribution of ZRF1 after pre-extraction of U2OS cells, we detected ZRF1 in the nucleolus as seen by simultaneous Nucleophosmin (NPM) staining (Figure 5A). Similarly, EGFP tagged ZRF1 showed nucleolar localization (Figure S5A). In agreement with these findings we detected NPM in immunoprecipitations of endogenous ZRF1 as well as ectopically expressed $ZRF1^{FLAG}$ (Figure 5B, S5B). Furthermore, immunoprecipitations of FLAG-tagged ZRF1 followed by mass spectroscopy indicated that it associates with many nucleolar proteins, including Nucleophosmin, Fibrillarin and Nucleolin (Figure 5C, Supplemental Table 1). We did not detect any major changes in the interaction partners of ZRF1 in control versus irradiated cells (Figure S1C and Supplemental Table 1), suggesting that the bulk of ZRF1 is constitutively present in the nucleolus. Next, we explored if chromatin-associated ZRF1 also localized to the nucleolus. Upon tethering ZRF1, the LacO array showed a nucleolar positioning in ≈ 90 % of the analyzed cells (Figures 5D and 5E). Importantly, tethered mCherry-LacR-ZRF1 was able to bind XPC-GFP, in agreement with our recent findings (Gracheva et al. 2016 ) thus confirming functional activity of tethered ZRF1 (Figure S5D). Collectively these data show that a randomly distributed DNA locus is repositioned to the nucleolus upon ZRF1 binding.

We next assessed if loss of ZRF1 affected the nucleolar positioning of a DDB2 tethered array. To this end we created ZRF1 U2OS 2-6-3 knockdown cell lines (Figure S5F). However, when analyzing the knockdown cells, we observed only insufficient depletion of nucleolar ZRF1 whereas the cytoplasmic protein levels were reduced significantly (data not shown). In order to circumvent the lack of sufficient knockdown of nucleolar ZRF1, we next analyzed the repositioning of the array after knockdown of XPC. In absence of XPC, ZRF1 cannot bind chromatin even in presence of H2A-ubiquitylation (Gracheva et al. 2016). Depletion of XPC resulted in a complete loss of the re-localization phenotype when utilizing a DDB2-tethered array (Figures 5F and S5E). The data suggests that ZRF1 is a strong candidate to tether damaged DNA to the nucleolus. It presumably interacts with H2A-ubiquitin at the damage site via its Ubiquitin-binding domain in a XPC dependent manner.

Figure 5

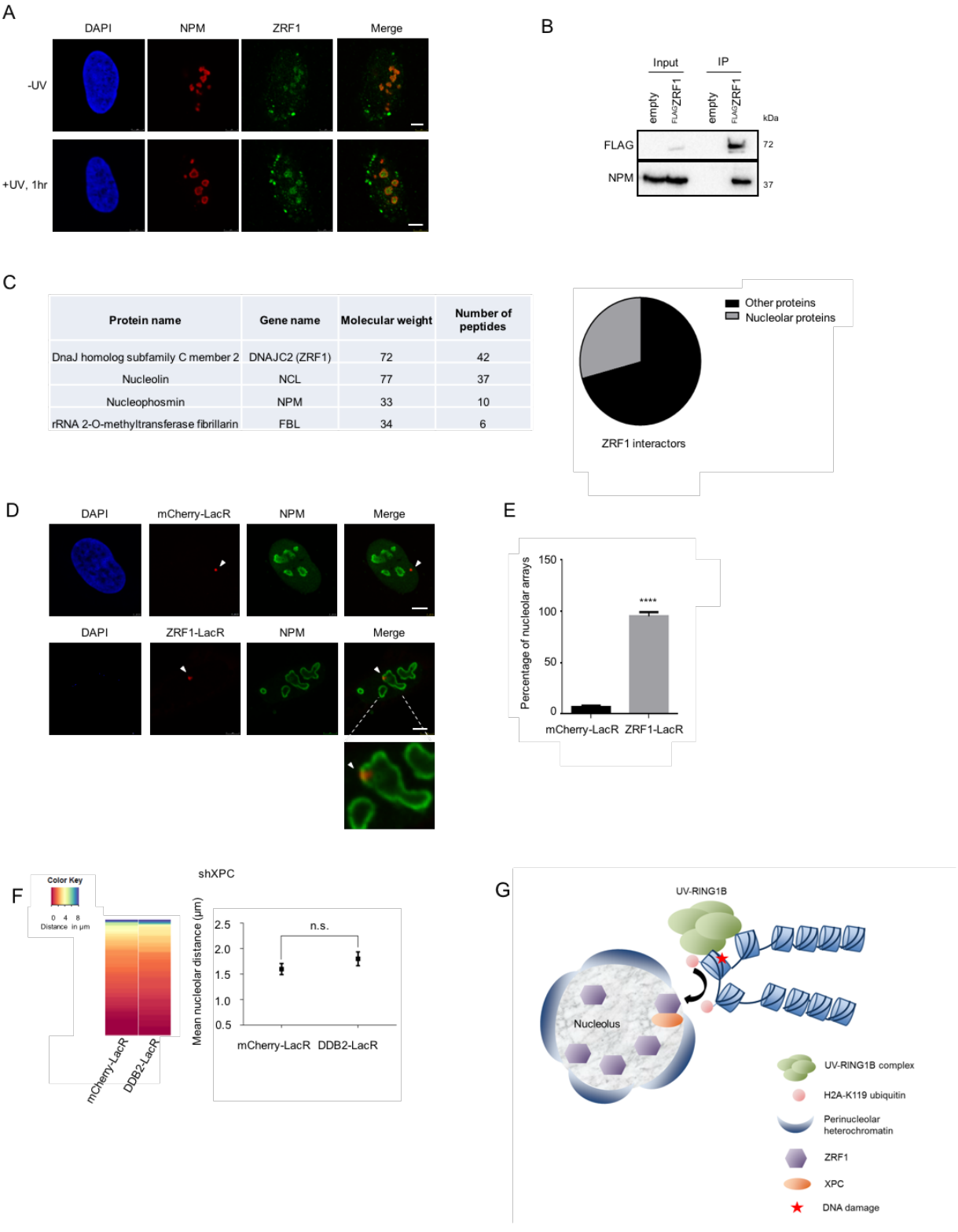
A
DAPI
NPM
ZRF1
Merge
-UV
+UV, 1hr
B
Input
IP
empty
FLAG-ZRF1
kDa
FLAG
NPM
72
37
C
Protein name
Gene name
Molecular weight
Number of peptides
DnaJ homolog subfamily C member 2
DNAJC2 (ZRF1)
72
42
Nucleolin
NCL
77
37
Nucleophosmin
NPM
33
10
rRNA 2-O-methyltransferase fibrillarin
FBL
34
6
Other proteins
Nucleolar proteins
ZRF1 interactors
D
DAPI
mCherry-LacR
NPM
Merge
DAPI
ZRF1-LacR
NPM
Merge
E
Percentage of nucleolar arrays
150
100
50
0
****
mCherry-LacR
ZRF1-LacR
F
Color Key
0 4 8
Distance in µm
mCherry-LacR
DDB2-LacR
shXPC
Mean nucleolar distance (µm)
2.5
2.0
1.5
1.0
0.5
n.s.
mCherry-LacR
DDB2-LacR
G
UV-RING1B
Nucleolus
UV-RING1B complex
H2A-K119 ubiquitin
Perinucleolar heterochromatin
ZRF1
XPC
DNA damage

Figure 5. ZRF1 is present in the nucleolus and causes relocalization of chromatin (a) ZRF1 localizes to nucleoli. Immunofluorescence images showing intra-nuclear distribution of ZRF1 in pre-extracted control cells and cells exposed to UV irradiation. Nucleoli are marked by Nucleophosmin (NPM). Pre-extraction washes off unbound nuclear and cytoplasmic proteins and enables visualization of chromatin-associated proteins. Scale bar -5µm (b) ZRF1 interacts with NPM. Purifications from HEK293T cells transfected with either empty vector or $^{FLAG}$ZRF1, show specific interaction of NPM with ZRF1 (c) ZRF1 interacts with major components of the nucleolus. $^{FLAG}$ZRF1, along with its interactors, was purified from HEK293T cells and the purified material was subjected to mass spectrometry. Multiple components of the nucleolus were found to interact with ZRF1. (Left panel) the table shows peptide numbers for selected proteins in the FLAG purification. (Right panel) 30% of all interacting proteins were found to be nucleolar, as assessed by comparison with the nucleolar protein database NOPdb (http://lamondlab.com/NOPdb3.0/). (d) Tethering of ZRF1 to a LacO array leads to repositioning of the array. Representative images of mCherry-LacR-ZRF1 or mCherry-LacR tethered LacO arrays. Nucleoli are marked by Nucleophosmin (NPM). Scale bar -5µm (e) Quantification of nucleolar arrays (distance from nucleolus=0µm) in control (mCherry-LacR) and ZRF1 (ZRF1-LacR) tethered arrays. 90-100 cells were counted per experiment. The graph shows the mean ±SD. (n=3). Significance was determined by an unpaired t-test. (f) Knockdown of XPC abolishes repositioning of a DDB2-LacR tethered array. (Left panel) Heat map showing distribution of the nucleolar distance of the array in 100 cells. mCherry-LacR or DDB2-LacR tethered arrays were analyzed in a XPC knockdown (shXPC) background. There was no significant difference between the control and DDB2-LacR tethered array in the shXPC cells as judged by a KS test. (Right panel) Mean nucleolar distance of the control and DDB2-tethered array in shXPC cells. The mean nucleolar distance of each replicate was calculated from measurements of nucleolar distance in 100 cells. The graph shows the average of the means from 3 independent experiments ±SD. Statistical significance was determined using an unpaired t-test. (g) The figure shows a representative model for nucleolar tethering of damaged DNA via H2A K119 ubiquitylation, thereby leading to its repair.

## DISCUSSION

NER is one of the most prominent DNA repair pathways. In order to investigate if NER occurs in defined repair centers, we used a modified UDS protocol to look at the nuclear distribution of repair occurring at various time points after UV irradiation. We observed appearance of specific repair foci starting from 8 hours and lasting up to 24 hours after UV exposure, which overlapped with nucleoli. Upon quantification, we observed that repair in the nucleolus occurs at all the measured timepoints (0- 24 hours), however at later timepoints the majority of the repair consists of nucleolar repair (Figure 1A). These relatively late time points of DNA repair are in agreement with the timing observed for the removal of CPDs, specifically from heterochromatin in a DDB2 dependent manner (Bykov et al., 1999; Zhao et al., 2002; Han et al. 2016). We also observed translocation of the repaired DNA out of the nucleolus at both early and late timepoints (Figure 1B), implying that it is non-nucleolar DNA that is actively brought to the nucleolus for repair. In addition, upon irradiation through a micropore, we observed a migration of the damaged DNA towards the nucleolus (Figure 1E). Additionally we see accumulation of XPA in the nucleolus

very early after UV damage, which implies the presence of functional repair machinery. Interestingly, loss of NPM causes reduced NER (Wu et al., 2002a) whereas its overexpression increases survival and NER capacity (Wu et al., 2002b) supporting a role for the nucleolus in NER. In line with these observations, our data suggest that the nucleolus might facilitate NER by organizing repair through tethering of damaged chromatin (Figure 5G).

In order to determine the mechanism of translocation of damaged DNA to the nucleolus for repair, we used a tethering system to mimic a lesion (Bergink S et al., 2012; Ziani S et al., 2014). Tethering two subunits of the UV-RING1B complex (DDB2 or RING1B) we observe a re-localization of the array close to the nucleolus (mean ≈1µm). Experiments in different systems such as flies, yeast as well as mammalian cells have demonstrated that chromatin undergoes rapid motion in a radius of 0.5-1µm (Chubb et al., 2002; Heun et al., 2001; Marshall et al., 1997; Vazquez et al., 2001) making our repositioning functionally relevant. RING1B is most widely known as a component of PRC1 and for its role in gene silencing during development. RING1B specifically catalyzes ubiquitylation of H2A at lysine 119. Here, we show that during NER, H2A-K119 ubiquitylation plays a definite role in tethering damaged chromatin to the nucleolus. This tethering is facilitated by XPC, and probably uses nucleolar ZRF1 as the anchor. We have shown previously that ubiquitylation at H2A-K119 precedes RBX1-mediated ubiquitylation (Gracheva et al. 2016) thereby initiating a ubiquitin signaling cascade. Since ZRF1 is responsible for exchanging the E3 ligases at the damage site (Gracheva et al. 2016), it is likely that this remodeling occurs at the nucleolus, too. Recently it was shown that many of the PRC1 related functions of RING1B are independent of its E3 ligase activity (Eskeland et al., 2010; Illingworth et al., 2015). However, its function in NER requires functional catalytic activity. Thus, our data propose a novel function for RING1B catalyzed H2A-ubiquitylation in nuclear chromatin organization (Figure 5G).

ZRF1 is one of the few known readers of H2A-K119 ubiquitin. ZRF1 function has been shown to actively displace RING1B not only in NER but also in the course of cellular differentiation. Upon differentiation of cells, ZRF1 is present at the promoters of many developmental genes such as HOX genes. In this study, we show that tethering ZRF1 to chromatin relocates the chromatin to the nucleolus. This finding creates an interesting repercussion for ZRF1-mediated transcriptional activation. We speculate that the activation of developmental loci by ZRF1 might also potentially involve their migration to the nucleolus.

The nucleolus, along with the nuclear lamina, is considered an important nuclear structure that binds specific genomic regions and plays a major role in the three-dimensional organization of the genome (Padeken and Heun, 2014). In addition, about half of the nucleolar proteome consists of proteins involved in functions other than ribosome biogenesis, viz. regulation tumor suppressor and proto-oncogene activities, cell-cycle control, DNA replication, DNA repair, and stress signaling (Anderson et al., 2002). A potential function of relocation to the nucleolus may be to aid in chromatin remodeling. Ribosome biogenesis and chromatin remodeling, both involve regulation of nucleic acid-protein interactions, and the nucleolus contains much of the machinery required for this process. Notably, Nucleophosmin functions as a histone chaperone and as a sink for histones (Keck and Pemberton, 2012).

In conclusion, we propose a novel role for RING1B mediated H2A-ubiquitylation in sub-nuclear localization of NER. ZRF1, in combination with XPC, presumably tethers the damaged chromatin to the nucleolus, and facilitates repair. It remains to be seen which fraction of NER occurs in the nucleolus, and how the decision is made for a lesion to be repaired there. Another interesting open question is whether the recognition and tethering of chromatin bearing the H2A-ubiquitylation mark by ZRF1 is a central mechanism playing a role in other cellular processes.

## EXPERIMENTAL PROCEDURES

### Cell culture and cell lines

HEK293T, U2OS and U2OS 2-6-3 cells were cultured in DMEM supplemented with 10% FBS at 37°C and 5% CO2. U2OS 2-6-3 medium was additionally supplemented with 100 µg/ml Hygromycin to maintain stable insertion of the LacO cassette. Normal skin fibroblasts (GM15876) were purchased from the Coriell Cell Repositories and cultured in DMEM, supplemented with 15% FBS.

Transfection of U2OS 2-6-3 and HEK293T cells was performed by Lipofectamine 2000 (Invitrogen) transfection according to manufacturer's instructions. Information on the plasmids used in this study is provided in the supplementary information.

### Lentiviral transduction

Gene knockdown in U2OS 2-6-3 cells was performed by introduction of MISSION pLKO.1-shRNA plasmids (Sigma-Aldrich) targeting the respective gene using the 3rd generation lentivirus system. Plasmids contained the following sequences (Sigma): non-mammalian control

(NMC) (TRC1/1.5), RING1B (TRCN0000033697), XPC (TRCN0000307193), ZRF1 (TRCN0000254058).

**Immunofluorescence**

Cells were fixed in 4%PFA for 10 min at room temperature. Pre-extraction with CSK buffer (10mM PIPES pH- 7.4, 100mM NaCl, 300mM sucrose, 3mM $MgCl_2$) containing 0.2% Triton-X, for 5 min on ice, was performed prior to fixation when indicated. Cells were incubated overnight with primary antibody at 4 °C. Subsequently cells were incubated with Alexa-fluorophore-conjugated secondary antibodies (Life Technologies). The mounting was carried out in Vectashield with DAPI (Vector Laboratories).

Micropore irradiation experiments were performed on MRC5 fibroblasts. Cells were exposed to localized UV damage (100 J/m2) using a micropore membrane with 5-µm pore size as described previously (Katsumi et al., 2001).

**Measurement and statistical analysis of array distributions**

For tethering experiments, nucleolar distances were measured in 100 randomly picked transfected cells per sample. All cells with visible tethered array were used, consisting of all levels of LacR-fusion protein expression. Nucleolar distance was measured as the distance of the array, to the closest NPM marked nucleolus. Distributions of nucleolar distances for control and test sample were compared by the Kolmogorov-Smirnov (KS) test. For each experiment, mean nucleolar distances were calculated from a minimum of three independent experiments, each showing a significant difference in distributions as indicated by the KS test. The respective means were then compared by an unpaired t-test. All statistical tests were performed using GraphPad Prism.

**UDS experiments**

UDS experiments were performed as described elsewhere (Jia et al. 2015). Briefly, fibroblasts were serum starved for 24 hours, irradiated with UV light ($20J/m^2$) and incubated with 10µM EdU (Thermo Fisher) for 2 hours at the indicated time point after UV exposure. At this stage, the cells were then fixed and further processed to visualize localization of repaired DNA. In experiments tracking re-distribution of repaired DNA, medium was replaced by EdU free medium, and repair was allowed to proceed till 24 hours post UV. Cells were then fixed and processed for further staining. Alexa-555-azide (Thermo Fisher) was conjugated to EdU using the click-reaction. The cells were additionally incubated with Nucleophosmin antibodies, followed by Alexa-488 secondaries (anti-mouse) before mounting in Vectashield with DAPI.

**Microscopy and image analysis**

Images were acquired with the LAS AF software (Leica) using a TCS SP5 confocal microscope (Leica) with a 63x/1.4 oil immersion objective. The following lasers were used: 50 mW UV diode (405 nm), 65 mW argon, 20 mW DPSS (561 nm) and 10 mW HeNe (633 nm).

Analysis of nuclear distribution of UDS was carried out by a self-written Fiji/ImageJ macro. Briefly, single z-planes with nucleoli in focus were captured for each cell. Single channel fluorescence images (NPM-488, DAPI) were smoothed, threshholded and converted to binary masks. DAPI was used as a nuclear mask, while NPM was used as a nucleolar mask and a combination of the two (nuclear-nucleolar) served as the nucleoplasmic mask. The binary masks were used to measure the mean intensity for the nucleus, nucleolus, and nucleoplasm in the corresponding EdU image. These values were used to calculate the Nucleolar Repair Index as $(Nucleolus^{mean} - Nucleoplasm^{mean)}/Nucleus^{mean} \times 100$. NRI was calculated for all the nucleoli from ≈ 100 cells per time point.

**FLAG purifications**

Cells were UV irradiated ($20J/m^2$) and harvested 1 hour after exposure (unless stated otherwise). FLAG affinity purifications were performed using FLAG-M2 agarose beads as already published (Richly et al. 2010).

**Mass spectrometry**

Mass-spectrometry sample preparation, measurement and database search were performed as described elsewhere (Bluhm et al. 2015). Gradient lengths of 45 or 105 min were chosen depending on the IP material obtained. Raw files were processed with MaxQuant (version 1.5.2.8) and searched against the *Homo sapiens* Uniprot database (25. February 2012) using the Andromeda search engine integrated into MaxQuant and default settings were applied. Proteins with at least 2 peptides, one of them unique, count as identified.

**Purification of nucleoli**

Nucleolar purification was performed as previously described (Liang et al. 2012) with slight modifications. Roche's complete Protease Inhibitor Cocktail (PI) was added to all solutions and the entire protocol was performed on ice. Briefly, cells were scraped off in Solution I (0.5M Sucrose, 3mM $MgCl_2$ +PI), chilled to -20 °C to quench metabolic activities, pelleted, and washed once more with Solution I. Washed cells were resuspended in 1ml Solution I and sonicated for 7 cycles (10s on/10s off) in a Bioruptor (Diagenode). Sonicated cells were checked under a microscope to ensure efficient cell lysis. Cell lysate was then layered over 1.4 ml of Solution II

(1M Sucrose, 3mM Mg $Cl_2$ +PI) and centrifuged at 1800g for 10 min at 4 °C. The supernatant was carefully removed and the nucleolar pellet was resuspended in Laemmli buffer and boiled, or subjected to subsequent salt extraction.

**Nucleolar fractionation**

Purified nucleoli were incubated with Salt Extraction buffer I (50mM Tris pH 7.5, 0,05%NP40, 0.1M NaCl + PI) for 10 min on ice. Nucleoli were centrifuged at 2800g for 5 min and the supernatant was saved as the 0.1M salt soluble fraction. Similar extractions were performed sequentially with Salt Extraction buffer II (50mM Tris pH 7.5, 0,05%NP40, 0.2M NaCl + PI) and Salt Extraction Buffer III (50mM Tris pH 7.5, 0,05%NP40, 0.3M NaCl + PI). After the last extraction the remaining pellet was saved as chromatin bound fraction. Laemmli buffer was added to the samples and they were boiled for 10 min. Subsequently the samples were analysed by SDS-PAGE and western blotting. Histones were found to be prominently in the insoluble fraction, thus verifying that it represents the chromatin bound fraction.

**UV irradiation:**

Cells were irradiated with 20J/$m^2$ UV-C using a CL-1000 UV-crosslinker (UVP) unless stated otherwise.

**Plasmids and antibodies:**

mCherry-LacR-DDB2, mCherry-LacR-DDB2$^{D370Y}$, mCherry-LacR-DDB2$^{L350P}$, EGFP-DDB2, EGFP- DDB2$^{D370Y}$, EGFP- DDB2$^{L350P}$ were kindly provided by Nico Dantuma. XPC-GFP was gifted by Cristina Cardoso. GBP-LacR was obtained from Heinrich Leonhardt. mCherry-LacR-nostop was a gift from Vassilis Roukos.

mCherry-LacR-RING1B, mCherry-LacR-CSA, mCherry-LacR-RBX1, mCherry-LacR-RING1B$^{R70C}$, mCherry-LacR-ZRF1, mCherry-TetR-USP16, EGFP-LacR-RING1B, EGFP-LacR-DDB2, EGFP-ZRF1, EGFP-NLS-ZRF1, EGFP-RING1B, EGFP-RING1B$^{R70C}$, EGFP-RBX1, FLAG-ZRF1 were cloned. For details please contact the authors.

Antibodies used in this study were: XPA (Genetech), XPC (Abcam), DDB2 (MyBioSource), XPB (Santa Cruz Biotechnology), Fibrillarin (Thermo Scientific), ZRF1 (Novus Biologicals), Nucleophosmin (Abcam ab10530), DDB1 (Bethyl), Ubiquitin (clone P4D1, Cell Signalling).

## REFERENCES

Adam S, Polo SE. 2012. Chromatin dynamics during nucleotide excision repair: histones on the move. *International journal of molecular sciences* **13**: 11895-11911.

Angers S, Li T, Yi X, MacCoss MJ, Moon RT, Zheng N. 2006. Molecular architecture and assembly of the DDB1-CUL4A ubiquitin ligase machinery. *Nature* **443**: 590-593.

Belmont AS, Straight AF. 1998. In vivo visualization of chromosomes using lac operator-repressor binding. *Trends in cell biology* **8**: 121-124.

Bergink S, Salomons FA, Hoogstraten D, Groothuis TA, de Waard H, Wu J, Yuan L, Citterio E, Houtsmuller AB, Neefjes J et al. 2006. DNA damage triggers nucleotide excision repair-dependent monoubiquitylation of histone H2A. *Genes & development* **20**: 1343-1352.

Bergink S, Toussaint W, Luijsterburg MS, Dinant C, Alekseev S, Hoeijmakers JH, Dantuma NP, Houtsmuller AB, Vermeulen W. 2012. Recognition of DNA damage by XPC coincides with disruption of the XPC-RAD23 complex. *The Journal of cell biology* **196**: 681-688.

Bluhm A, Casas-Vila N, Scheibe M, Butter F. 2015. Reader interactome of epigenetic histone marks in birds. *Proteomics*.

Bohr VA, Smith CA, Okumoto DS, Hanawalt PC. 1985. DNA repair in an active gene: removal of pyrimidine dimers from the DHFR gene of CHO cells is much more efficient than in the genome overall. *Cell* **40**: 359-369.

Chubb JR, Boyle S, Perry P, Bickmore WA. 2002. Chromatin motion is constrained by association with nuclear compartments in human cells. *Current biology : CB* **12**: 439-445.

de Laat WL, Jaspers NG, Hoeijmakers JH. 1999. Molecular mechanism of nucleotide excision repair. *Genes & development* **13**: 768-785.

Doil C, Mailand N, Bekker-Jensen S, Menard P, Larsen DH, Pepperkok R, Ellenberg J, Panier S, Durocher D, Bartek J et al. 2009. RNF168 binds and amplifies ubiquitin conjugates on damaged chromosomes to allow accumulation of repair proteins. *Cell* **136**: 435-446.

Fitch ME, Nakajima S, Yasui A, Ford JM. 2003. In vivo recruitment of XPC to UV-induced cyclobutane pyrimidine dimers by the DDB2 gene product. *The Journal of biological chemistry* **278**: 46906-46910.

Fousteri M, Mullenders LH. 2008. Transcription-coupled nucleotide excision repair in mammalian cells: molecular mechanisms and biological effects. *Cell research* **18**: 73-84.

Friedberg EC. 2001. How nucleotide excision repair protects against cancer. *Nature reviews Cancer* **1**: 22-33.

Gracheva E, Chitale S, Wilhelm T, Rapp A, Byrne J, Stadler J, Medina R, Cardoso MC, Richly H. 2016. ZRF1 mediates Remodeling of E3 ligases at DNA lesion sites during Nucleotide Excision Repair. *Journal of Cell Biology*.

Groisman R, Polanowska J, Kuraoka I, Sawada J, Saijo M, Drapkin R, Kisselev AF, Tanaka K, Nakatani Y. 2003. The ubiquitin ligase activity in the DDB2 and CSA complexes is differentially regulated by the COP9 signalosome in response to DNA damage. *Cell* **113**: 357-367.

Guerrero-Santoro J, Kapetanaki MG, Hsieh CL, Gorbachinsky I, Levine AS, Rapic-Otrin V. 2008. The cullin 4B-based UV-damaged DNA-binding protein ligase binds to UV-damaged chromatin and ubiquitinates histone H2A. *Cancer research* **68**: 5014-5022.

Herce HD, Deng W, Helma J, Leonhardt H, Cardoso MC. 2013. Visualization and targeted disruption of protein interactions in living cells. *Nature communications* **4**: 2660.

Hoogstraten D, Bergink S, Ng JM, Verbiest VH, Luijsterburg MS, Geverts B, Raams A, Dinant C, Hoeijmakers JH, Vermeulen W et al. 2008. Versatile DNA damage detection by the global genome nucleotide excision repair protein XPC. *Journal of cell science* **121**: 2850-2859.

Janicki SM, Tsukamoto T, Salghetti SE, Tansey WP, Sachidanandam R, Prasanth KV, Ried T, Shav-Tal Y, Bertrand E, Singer RH et al. 2004. From silencing to gene expression: real-time analysis in single cells. *Cell* **116**: 683-698.

Jia N, Nakazawa Y, Guo C, Shimada M, Sethi M, Takahashi Y, Ueda H, Nagayama Y, Ogi T. 2015. A rapid, comprehensive system for assaying DNA repair activity and cytotoxic effects of DNA-damaging reagents. *Nature protocols* **10**: 12-24.

Joo HY, Zhai L, Yang C, Nie S, Erdjument-Bromage H, Tempst P, Chang C, Wang H. 2007. Regulation of cell cycle progression and gene expression by H2A deubiquitination. *Nature* **449**: 1068-1072.

Kapetanaki MG, Guerrero-Santoro J, Bisi DC, Hsieh CL, Rapic-Otrin V, Levine AS. 2006. The DDB1-CUL4ADDB2 ubiquitin ligase is deficient in xeroderma pigmentosum group E and targets histone H2A at UV-damaged DNA sites. *Proceedings of the National Academy of Sciences of the United States of America* **103**: 2588-2593.

Koehler DR, Hanawalt PC. 1996. Recruitment of damaged DNA to the nuclear matrix in hamster cells following ultraviolet irradiation. *Nucleic acids research* **24**: 2877-2884.

Lee J, Zhou P. 2007. DCAFs, the missing link of the CUL4-DDB1 ubiquitin ligase. *Molecular cell* **26**: 775-780.

Lemaitre C, Grabarz A, Tsouroula K, Andronov L, Furst A, Pankotai T, Heyer V, Rogier M, Attwood KM, Kessler P et al. 2014. Nuclear position dictates DNA repair pathway choice. *Genes & development* **28**: 2450-2463.

Liang YM, Wang X, Ramalingam R, So KY, Lam YW, Li ZF. 2012. Novel nucleolar isolation method reveals rapid response of human nucleolar proteomes to serum stimulation. *Journal of proteomics* **77**: 521-530.

Lisby M, Mortensen UH, Rothstein R. 2003. Colocalization of multiple DNA double-strand breaks at a single Rad52 repair centre. *Nat Cell Biol* **5**: 572-577.

Luijsterburg MS, Goedhart J, Moser J, Kool H, Geverts B, Houtsmuller AB, Mullenders LH, Vermeulen W, van Driel R. 2007. Dynamic in vivo interaction of DDB2 E3 ubiquitin ligase with UV-damaged DNA is independent of damage-recognition protein XPC. *Journal of cell science* **120**: 2706-2716.

Luijsterburg MS, Lindh M, Acs K, Vrouwe MG, Pines A, van Attikum H, Mullenders LH, Dantuma NP. 2012. DDB2 promotes chromatin decondensation at UV-induced DNA damage. *The Journal of cell biology* **197**: 267-281.

Manuelidis L, Borden J. 1988. Reproducible compartmentalization of individual chromosome domains in human CNS cells revealed by in situ hybridization and three-dimensional reconstruction. *Chromosoma* **96**: 397-410.

Marteijn JA, Bekker-Jensen S, Mailand N, Lans H, Schwertman P, Gourdin AM, Dantuma NP, Lukas J, Vermeulen W. 2009. Nucleotide excision repair-induced H2A ubiquitination is dependent on MDC1 and RNF8 and reveals a universal DNA damage response. *The Journal of cell biology* **186**: 835-847.

Marteijn JA, Lans H, Vermeulen W, Hoeijmakers JH. 2014. Understanding nucleotide excision repair and its roles in cancer and ageing. *Nature reviews Molecular cell biology* **15**: 465-481.

Mattiroli F, Vissers JH, van Dijk WJ, Ikpa P, Citterio E, Vermeulen W, Marteijn JA, Sixma TK. 2012. RNF168 ubiquitinates K13-15 on H2A/H2AX to drive DNA damage signaling. *Cell* **150**: 1182-1195.

Mellon I, Spivak G, Hanawalt PC. 1987. Selective removal of transcription-blocking DNA damage from the transcribed strand of the mammalian DHFR gene. *Cell* **51**: 241-249.

Misteli T, Soutoglou E. 2009. The emerging role of nuclear architecture in DNA repair and genome maintenance. *Nature reviews Molecular cell biology* **10**: 243-254.

Moser J, Volker M, Kool H, Alekseev S, Vrieling H, Yasui A, van Zeeland AA, Mullenders LH. 2005. The UV-damaged DNA binding protein mediates efficient targeting of the nucleotide excision repair complex to UV-induced photo lesions. *DNA repair* **4**: 571-582.

Nagai S, Dubrana K, Tsai-Pflugfelder M, Davidson MB, Roberts TM, Brown GW, Varela E, Hediger F, Gasser SM, Krogan NJ. 2008. Functional targeting of DNA damage to a nuclear pore-associated SUMO-dependent ubiquitin ligase. *Science* **322**: 597-602.

Nishi R, Alekseev S, Dinant C, Hoogstraten D, Houtsmuller AB, Hoeijmakers JH, Vermeulen W, Hanaoka F, Sugasawa K. 2009. UV-DDB-dependent regulation of nucleotide excision repair kinetics in living cells. *DNA repair* **8**: 767-776.

Pan MR, Peng G, Hung WC, Lin SY. 2011. Monoubiquitination of H2AX protein regulates DNA damage response signaling. *The Journal of biological chemistry* **286**: 28599-28607.

Richly H, Rocha-Viegas L, Ribeiro JD, Demajo S, Gundem G, Lopez-Bigas N, Nakagawa T, Rospert S, Ito T, Di Croce L. 2010. Transcriptional activation of polycomb-repressed genes by ZRF1. *Nature* **468**: 1124-1128.

Rothbauer U, Zolghadr K, Muyldermans S, Schepers A, Cardoso MC, Leonhardt H. 2008. A versatile nanotrap for biochemical and functional studies with fluorescent fusion proteins. *Molecular & cellular proteomics : MCP* **7**: 282-289.

Roukos V, Misteli T. 2014. The biogenesis of chromosome translocations. *Nat Cell Biol* **16**: 293-300.

Shiyanov P, Nag A, Raychaudhuri P. 1999. Cullin 4A associates with the UV-damaged DNA-binding protein DDB. *The Journal of biological chemistry* **274**: 35309-35312.

Strongin DE, Groudine M, Politz JC. 2014. Nucleolar tethering mediates pairing between the IgH and Myc loci. *Nucleus* **5**: 474-481.

Sugasawa K, Okamoto T, Shimizu Y, Masutani C, Iwai S, Hanaoka F. 2001. A multistep damage recognition mechanism for global genomic nucleotide excision repair. *Genes & development* **15**: 507-521.

Sugasawa K, Okuda Y, Saijo M, Nishi R, Matsuda N, Chu G, Mori T, Iwai S, Tanaka K, Hanaoka F. 2005. UV-induced ubiquitylation of XPC protein mediated by UV-DDB-ubiquitin ligase complex. *Cell* **121**: 387-400.

Tang JY, Hwang BJ, Ford JM, Hanawalt PC, Chu G. 2000. Xeroderma pigmentosum p48 gene enhances global genomic repair and suppresses UV-induced mutagenesis. *Molecular cell* **5**: 737-744.

Therizols P, Fairhead C, Cabal GG, Genovesio A, Olivo-Marin JC, Dujon B, Fabre E. 2006. Telomere tethering at the nuclear periphery is essential for efficient DNA double strand break repair in subtelomeric region. *The Journal of cell biology* **172**: 189-199.

Ui A, Nagaura Y, Yasui A. 2015. Transcriptional elongation factor ENL phosphorylated by ATM recruits polycomb and switches off transcription for DSB repair. *Molecular cell* **58**: 468-482.

Wang H, Wang L, Erdjument-Bromage H, Vidal M, Tempst P, Jones RS, Zhang Y. 2004. Role of histone H2A ubiquitination in Polycomb silencing. *Nature* **431**: 873-878.

Wang H, Zhai L, Xu J, Joo HY, Jackson S, Erdjument-Bromage H, Tempst P, Xiong Y, Zhang Y. 2006. Histone H3 and H4 ubiquitylation by the CUL4-DDB-ROC1 ubiquitin ligase facilitates cellular response to DNA damage. *Molecular cell* **22**: 383-394.

Zolghadr K, Mortusewicz O, Rothbauer U, Kleinhans R, Goehler H, Wanker EE, Cardoso MC, Leonhardt H. 2008. A fluorescent two-hybrid assay for direct visualization of protein interactions in living cells. *Molecular & cellular proteomics : MCP* **7**: 2279-2287.

## ACKNOWLEDGEMENTS

This work was supported by grants from the Boehringer Ingelheim Foundation and the DFG (RI-2413/1-1). We are grateful to the IMB microscopy and proteomics facilities for their expert help and assistance, particularly Dr. Maria Hanulova for assisting with the image analysis and macros. We would like to thank Nico Dantuma, Cristina Cardoso,

and Vassilis Roukos for plasmids used in this study. We thank the members of the Richly laboratory for comments on the manuscript and Ekaterina Gracheva for assistance with cell lines.

**AUTHOR CONTRIBUTIONS**

S.C and H.R conceived of the study and wrote the manuscript. S.C performed all experiments and analyzed the data.

**COMPETING FINANCIAL INTERESTS**

The authors declare no competing financial interests.

## SUPPLEMENTARY FIGURES

Figure S1. NER is routed to the nucleolus. (a) Immunofluorescence images showing EdU incorporation (green) in control cells unexposed to UV (-UV), non-S phase cells showing post-damage repair activity (+UV, repair) and S phase cells. Nuclei are demarcated by DAPI staining, and nucleoli marked by Nucleophosmin (NPM). (b) Assessment of purity of nucleolar fractions. (Top panel) bright field image showing nucleoli in cell lysate. (Bottom panel) Coomassie staining of extracts from: whole cells, cytoplasmic and nucleoplasmic fraction (Cyto+NP) and nucleolar fraction. Western blots showing the purity of nucleolar fractions. Fibrillarin was used as a marker for the nucleolus and Tubulin as a marker for the Cyto+NP fraction. (c) Western blot images to show specificity of XPA antibody. Cell extracts from XPA deficient fibroblasts (XPA patient cells) and MRC5 fibroblasts were loaded on a gel and blotted for XPA. (d) XPA is enriched in the nucleolus post UV exposure. (Top panel) Western blots showing levels of the indicated proteins in either whole cell extracts, or nucleolar fractions at the stated time points after UV exposure.(Bottom panels) The XPA band intensity was normalized to Fibrillarin as a loading control, and the normalized band intensity was plotted. The graph shows Mean±SEM, N=3 (e) (Left panel) Representative images of active repair foci indicated by EdU incorporation, at the indicated time points post UV exposure. The figure additionally shows the image generated after normalization of the EdU signal with respect to DAPI signal (Ratio). Cells are costained with NPM to show nucleolar overlap of repair foci Scale bar- 5μm. (Right panel; Figure 1B) The graph shows the Nucleolar Repair Index (NRI) values of nucleoli from ≈100 non-S phase cells at the indicated time points post UV exposure. NRI values were calculated with respect to the normalized EdU image (Ratio). Statistical significance was calculated using a Mann-Whitney test. (f) Immunofluorescence images showing XPA distribution at the indicated time point post UV. Nucleoli are marked by Nucleophosmin (NPM)

Supplemental Figure 1

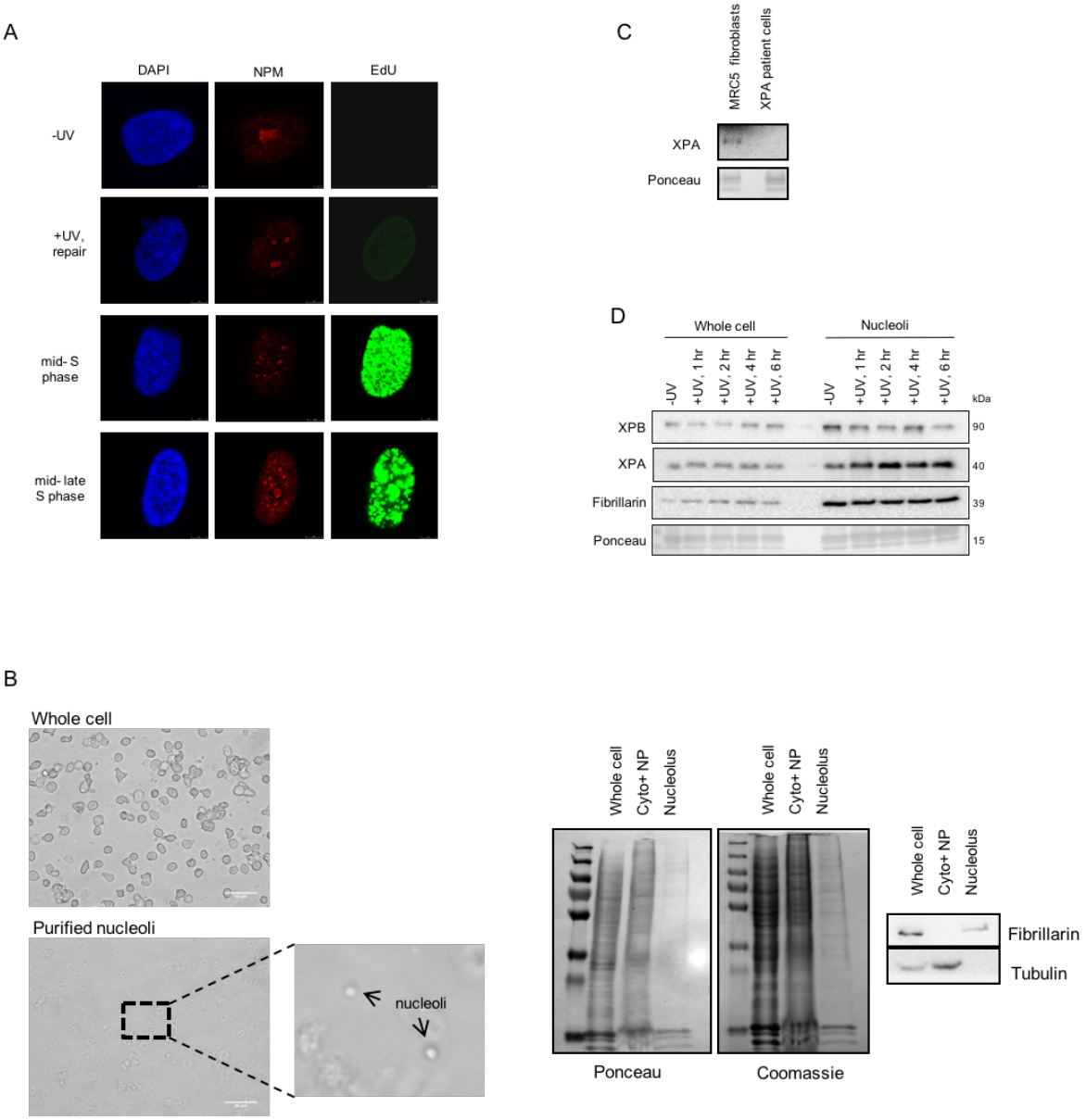

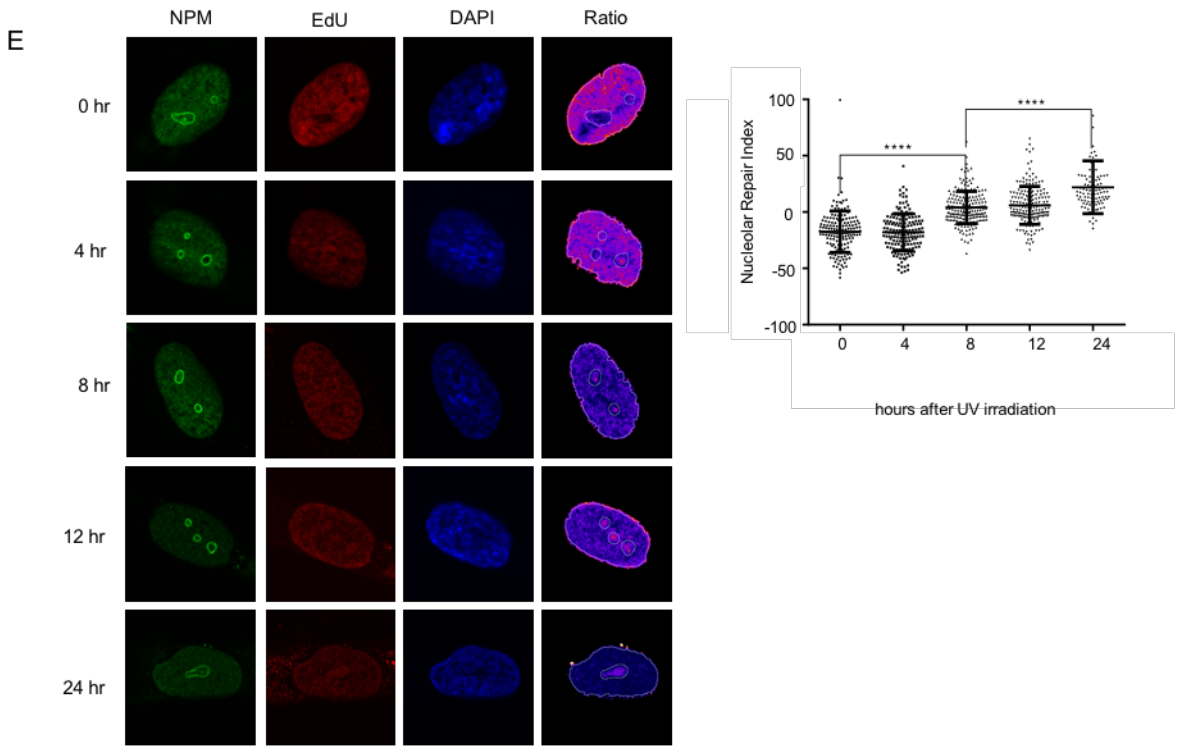
E
NPM
EdU
DAPI
Ratio
0 hr
4 hr
8 hr
12 hr
24 hr
Nucleolar Repair Index
100
50
0
-50
-100
****
****
0
4
8
12
24
hours after UV irradiation

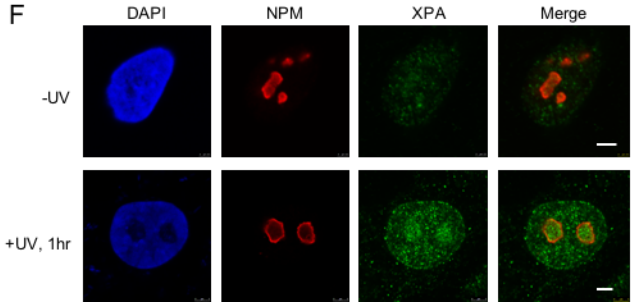
F
DAPI
NPM
XPA
Merge
-UV
+UV, 1hr

Supplemental Figure 2

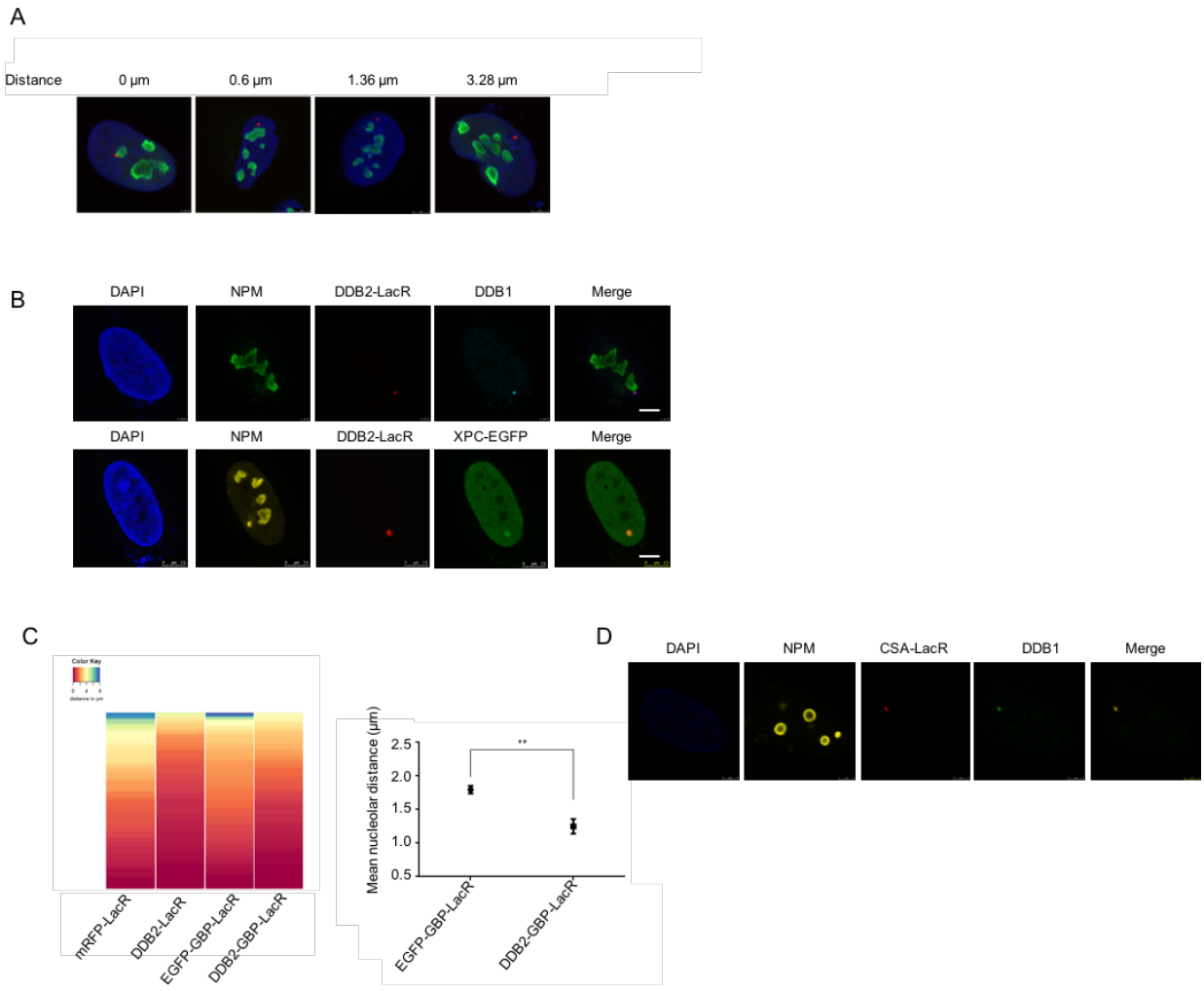


Figure S2. Tethering of DDB2 leads to relocalization of the LacO array. (a) Representative immunofluorescence images showing the position of a LacO array with respect to the nucleolus. The corresponding nucleolar distance is indicated. Nucleoli are marked by NPM. Scale bar- 5 µm (b) Tethered DDB2-LacR shows co-localization with endogenous DDB1 and XPC-EGFP. Immunofluorescence images showing the recruitment of endogenous DDB1 or XPC-GFP to an mCherry-LacR-DDB2 tethered array. Nucleoli are marked by NPM. Scale bar- 5 µm (c) DDB2 shows a similar effect on the array distribution when tethered indirectly. (Left panel) Heat map showing the distribution of the nucleolar distance of the array in 100 cells expressing either EGFP or DDB2-EGFP along with GFP-binding protein (GBP)-LacR. DDB2-EGFP tethering leads to a significant difference in distribution of the array when compared to EGFP tethering as judged by a KS test. (p value≤ 0.0001). (Right panel) Mean nucleolar distance of the array in EGFP-GBP-LacR and DDB2-GBP-LacR arrays. The mean nucleolar distance of each replicate was calculated from measurements of nucleolar distance in 100 cells. The graph shows the

average of the means from 3 independent experiments ±SD. Statistical significance was determined using an unpaired t-test. (d) Tethering CSA-LacR can bind DDB1. Immunofluorescence image showing colocalization of tethered CSA-LacR with endogenous DDB1. Scale bar- 5 µm

Supplemental Figure 3

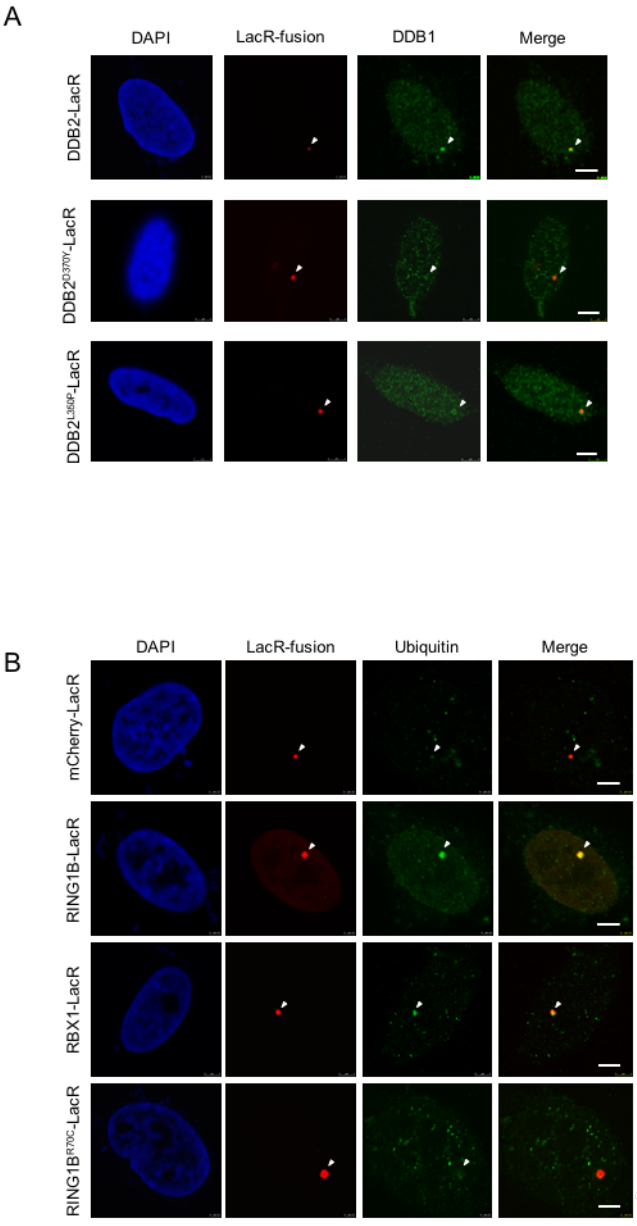

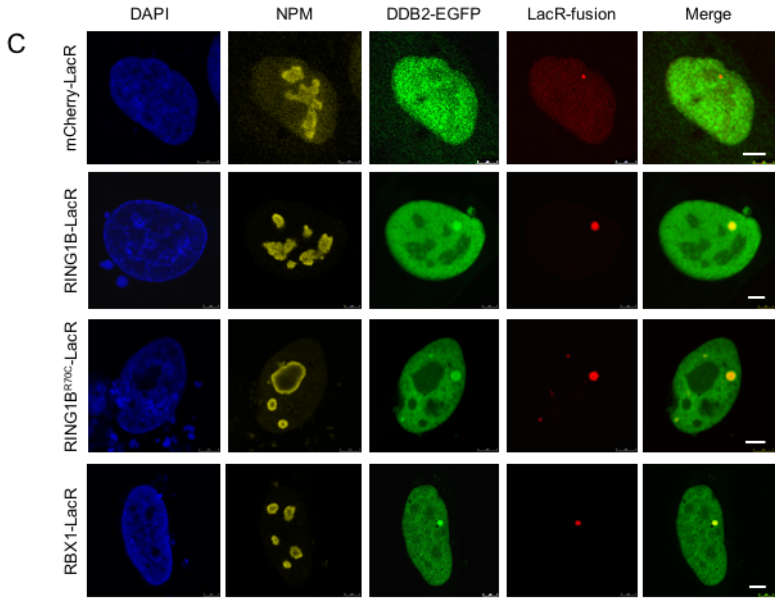


Figure S3. UV-DDB E3 ligase complexes are formed at the LacO array.
(a) Immunofluorescence images showing recruitment of endogenous DDB1 to tethered DDB2-LacR, DDB2$^{D370Y}$-LacR and DDB2$^{L350P}$-LacR tethered arrays. Scale bar- 5 µm (b) Tethered RING1B and RBX1 facilitate ubiquitylation at the array. Immunofluorescence images showing accumulation of ubiquitin at the array tethered with the respective proteins. The observed co-localization was seen in 50/50 cells imaged for all conditions. Scale bar- 5 µm. (c) Tethered RING1B, RING1B$^{R70C}$ and RBX1 all show recruitment and binding of DDB2-EGFP. Immunofluorescence images showing co-localization of DDB2-EGFP with the respective tethered proteins. Nucleoli are marked by NPM. Colocalization was assessed in cells showing comparable expression levels of the EGFP and the LacR fusion proteins. Colocalization was observed in 0/30 cells for mCherry-LacR, 30/30 cells for RBX1-LacR, 26/30 cells for RING1B$^{R70C}$-LacR and 27/30 cells for RING1B-LacR. Scale bar- 5 µm

Supplemental Figure 4

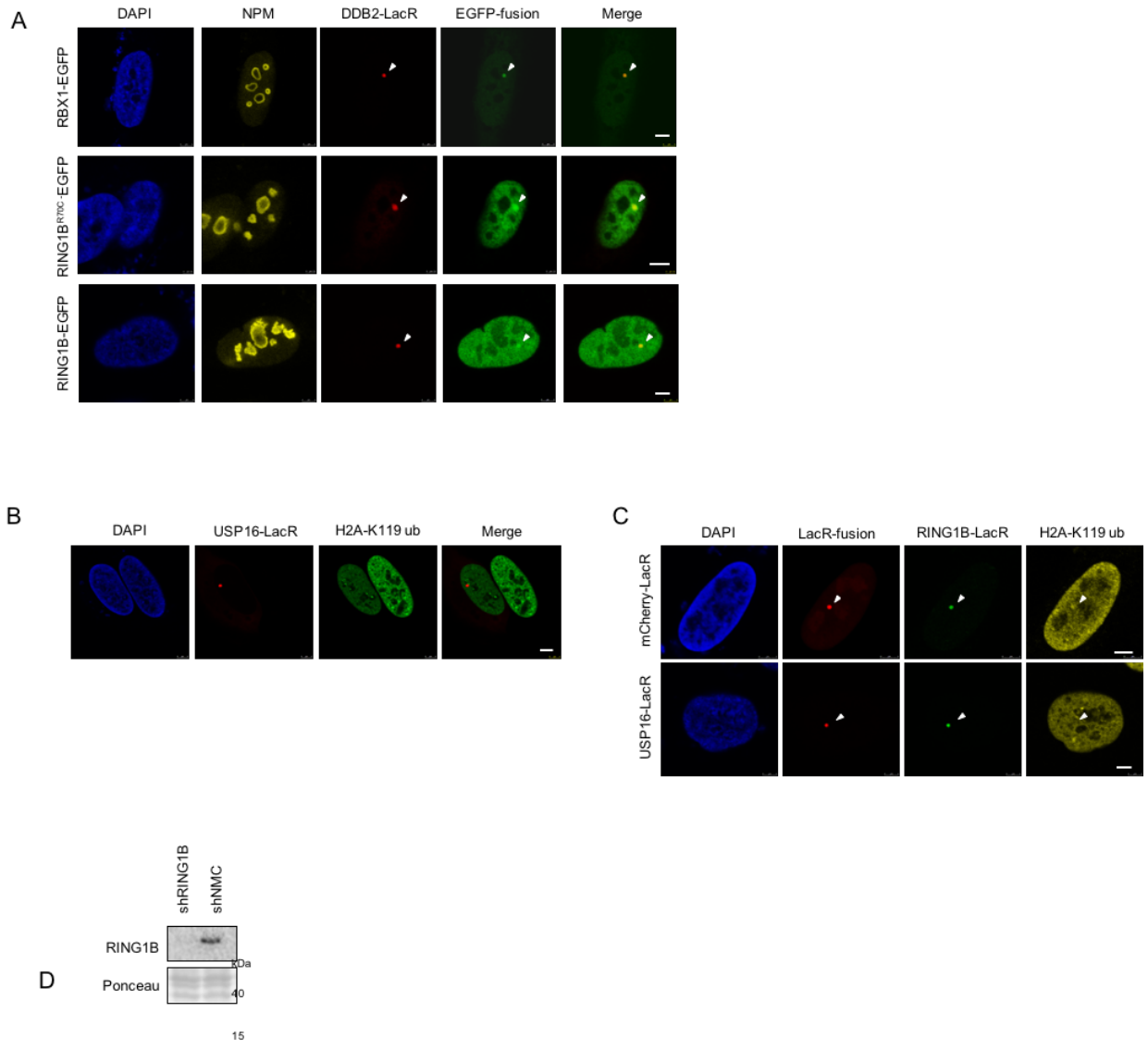


Figure S4. RING1B mediated H2A-ubiquitylation is required for relocation of array

(a) Tethered DDB2 shows recruitment of RING1B-EGFP, RING1B$^{R70C}$-EGFP and RBX1-EGFP. Immunofluorescence images showing recruitment of the respective EGFP tagged proteins to a DDB2-LacR tethered array. Nucleoli are marked by NPM. Colocalization was assessed in cells showing comparable expression levels of the EGFP and the LacR fusion proteins. Colocalization was observed in 30/30 cells for RBX1-EGFP, 25/30 cells for RING1B$^{R70C}$ and 27/30 cells for RING1B-EGFP. Scale bar- 5 µm (b) Expression of USP16-LacR leads to overall loss of H2A-K119 ubiquitylation. Immunofluorescence images showing reduced H2A-K119 ubiquitin levels both, at the array, as well as in the entire nucleus of cells expressing mCherry-USP16-LacR. Absence of H2A-K119 signal at the tethered USP16-LacR array was observed in 50/50 cells. Scale bar- 5 µm. (c) Co-tethering of USP16-LacR leads to loss of the RING1B-LacR catalyzed H2A K119 mark.

Immunofluorescence images showing the distribution of H2A-K119 ubiquitylation after co-tethering of EGFP-LacR-RING1B with either mCherry-LacR or mCherry-LacR-USP16. Absence of H2A-K119 signal at the double tethered RING1B-LacR, USP16-LacR array was observed in 50/50 cells Scale bar- 5 µm. (d) Western blot showing knockdown of RING1B in shRING1B cells compared to control (shNMC).

Supplemental Figure 5

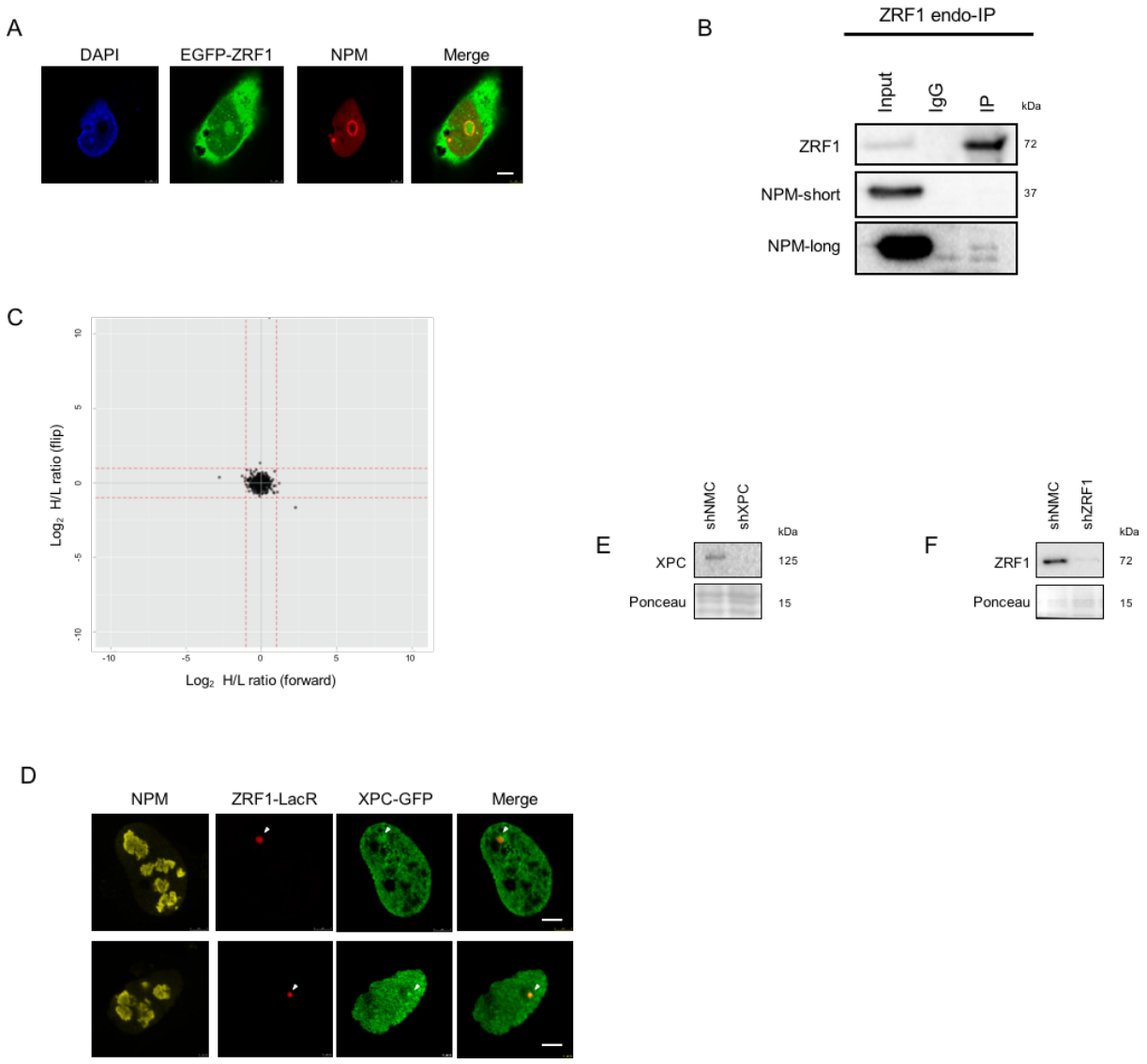

Figure S5. Nucleolar functions of ZRF1. (a) The distribution of EGFP tagged ZRF1 matches the distribution of endogenous ZRF1. Immunofluorescence images showing intracellular localization of EGFP-ZRF1 in non pre-extracted cells. Nucleoli are marked by NPM staining. Scale bar- 5 μm. (b) Endogenous ZRF1 interacts with NPM. Immunoprecipitation of endogenous ZRF1 showed co-immunoprecipitation of NPM (c) Scatterplots depicting SILAC heavy/light (H/L) ratios for proteins identified in both the "forward" (light lysates from unexposed cells, heavy lysates from UV exposed cells) and "flip" (heavy lysates from unexposed cells, light lysates from UV exposed cells) of $ZRF1^{FLAG}$ purifications. Almost all proteins show a ratio ≤2 (shown by dotted red lines) indicating no identification of differentially bound proteins. (d) Tethered ZRF1 binds XPC. Immunofluorescence images showing interaction of XPC-GFP in cells with array bound ZRF1-LacR, confirming functionality of both expressed proteins. Scale bar- 5 μm. (e) Western blot showing knockdown of XPC in shXPC cells compared to control (shNMC). (f) Western blot showing knockdown of ZRF1 in shZRF1 cells compared to control (shNMC).

# DICER and ZRF1 contribute to chromatin decondensation during nucleotide excision repair

**DICER and ZRF1 contribute to chromatin decondensation during nucleotide excision repair**

Shalaka Chitale[1,2] and Holger Richly[1,*]

[1] Laboratory of Molecular Epigenetics, Institute of Molecular Biology (IMB), Ackermannweg 4, 55128 Mainz, Germany

[2] Faculty of Biology, Johannes Gutenberg University, 55099 Mainz, Germany

[*] Correspondence: h.richly@imb-mainz.de

## ABSTRACT

Repair of damaged DNA relies on the recruitment of DNA repair factors in a well orchestrated manner. As a prerequisite, the chromatin needs to be decondensed by chromatin remodelers to allow for binding of repair factors and for DNA repair to occur. Recent studies have implicated members of the SWI/SNF and INO80 families as well as PARP1 in nucleotide excision repair (NER). In this study, we report that the endonuclease DICER is implicated in chromatin decondensation during NER. In response to UV irradiation, DICER is recruited to chromatin in a ZRF1-mediated manner. The H2A-ubiquitin binding protein ZRF1 and DICER together impact on the chromatin conformation via PARP1. Moreover, DICER-mediated chromatin decondensation is independent of its catalytic activity. Taken together, we describe a novel function of DICER at chromatin and its interaction with the ubiquitin signalling cascade during GG-NER.

## INTRODUCTION

Nucleotide excision repair (NER) represents a major DNA repair pathway, which removes helix distorting DNA lesions such as 6-4 photoproducts and cyclobutane pyrimidine dimers (CPDs) from chromatin (1). Mammalian NER comprises of two subpathways that vary in the mechanism of DNA lesion recognition. Transcription-coupled NER (TC-NER) is carried out at regions of active transcription, where stalled RNA Polymerase II elicits the DNA damage response. Global genome NER (GG-NER) carries out the transcription-independent repair of DNA lesions. The recognition step of both subpathways is followed by verification of the lesion, and by the generation of the pre-excision complex consisting of TFIIH and its helicase subunits XPB and XPD. Subsequently, the lesion is excised by the endonucleases XPF and XPG and the gap is refilled by DNA polymerases (2,3).

Another important feature of DNA repair and a hallmark of the DNA damage response is H2A-ubiquitylation. Ubiquitin signaling has been extensively studied at DNA double strand breaks. The E3 ligases RNF168, RNF8 and RING1B were reported to catalyze H2A-ubiquitylation thereby facilitating accumulation of repair proteins (4-7). During NER, H2A-ubiquitylation is catalyzed by the E3 ligase RNF8, the UV-DDB-CUL4 and UV-RING1B complexes (8-12). We have recently shown that ZRF1 is an essential factor in NER (12). ZRF1 interacts with the H2A-ubiquitin mark generated by the UV-RING1B complex. Its presence at damaged chromatin depends on XPC, a structure specific DNA binding factor, which specifically binds helix-distorting structures (12-14). At the lesion site, ZRF1 mediates the specific exchange of the cullin and E3 ligase subunits from the UV-RING1B complex, converting it into the DDB-CUL4A E3 ligase complex (12,15). However, it is currently not known whether ZRF1 interacts with other components of chromatin signaling during the DNA damage response.

The endoribonuclease DICER contributes to the DNA damage response by generating small non-coding RNAs that entail the sequence of the damaged locus (16-19). At DNA double strand breaks DICER seems to be essential for the activation of the DNA damage response and checkpoint control (16). More recently, it was demonstrated that DICER is necessary for the recruitment of the mediators MDC1 and 53BP1 (20). However, insights into the molecular mechanism of DICER at DSBs are still relatively sparse. Apart from its specific regulatory function at DSBs, DICER is involved in the formation of heterochromatin (21). Here we report

that DICER plays an essential role in NER and that, in contrast to its role in gene regulation, it facilitates the decondensation of damaged chromatin.

## MATERIALS AND METHODS

### Unscheduled DNA synthesis

UDS experiments were performed as described previously (22). Briefly, MRC5 fibroblasts were transfected with siRNAs, serum starved for 24 hours, irradiated with UV light (20J/$m^2$) and incubated with 10μM EdU (Thermo Fisher) for 2 hours. Alexa-488-azide (Thermo Fisher) was conjugated to EdU using the Click-reaction. The coverslips were mounted in Vectashield with DAPI. Images were acquired with the LAS AF software (Leica) using a AF-7000 widefield microscope (Leica) with a 63x/1.4 oil immersion objective and an ORCA CCD camera (Hamamatsu). Images were analyzed using ImageJ. DAPI was used to define nuclei, and EdU intensity within nuclei was measured after background subtraction. 150-300 nuclei were analyzed per sample. Mean intensities of +UV and –UV conditions for all cells were calculated, and used to estimate the DNA repair occurring in the particular sample.

### Recovery of RNA synthesis (RRS) assay

RRS assay was performed as described previously (22). Briefly, MRC5 cells were transfected with siRNAs, irradiated with UV light (11 J/$m^2$), and incubated in DMEM containg 1%FBS for 12 hours. This was followed by 2 hour incubation with EU (Sigma) and subsequent fixation. Alexa-488-azide (Thermo Fisher) was conjugated to EU using the Click-reaction. The coverslips were mounted in Vectashield with DAPI. Images were acquired with the LAS AF software (Leica) using a AF-7000 widefield microscope (Leica) with a 63x/1.4 oil immersion objective and an ORCA CCD camera (Hamamatsu). Images were analyzed using ImageJ as described (22).

### *C. elegans* culture

Nematodes were cultured on agar plates at 20°C according to standard procedures. Mutant strains were outcrossed at least three times to the wildtype strain (N2) to clear the genetic background prior to analysis. Some strains were provided by the CGC, which is funded by NIH Office of Research Infrastructure Programs (P40 OD010440*)*.

**Measuring DNA damage response in the *C.elegans* germ line**

The L4 survival assay was carried out as described (23). Briefly, late-L4 larval hermaphrodites were irradiated with different doses of UV light. The damage sensitivity of the meiotic pachytene cells of the germline was measured by determining the survival of embryos produced between 24 and 30 hours post L4 stage irradiation.

**Measuring DNA damage response in the *C.elegans* soma via developmental arrest**

The L1 development arrest assay was carried out as described (23). Briefly, L1 staged worms were synchronized via starvation and irradiated with different doses of UV-C light. Relative larval-stage stalling was determined after 60 hours, when control worms were fully fertile.

**Cell lines and transfections**

HEK293T, U2OS and U2OS 2-6-3 cells were cultured in DMEM supplemented with 10% FBS at 37°C and 5% CO2. The medium for U2OS 2-6-3 cells was additionally supplemented with 100 µg/ml Hygromycin to maintain stable insertion of the LacO cassette. The HEK293 T-REx cell lines shScrambled (containing non-targeting shRNA; #2800272) and shDICER (containing anti-DICER shRNA; #2800353) were a gift from Petr Svoboda and have been described in (24). Normal skin fibroblasts (GM15876), MRC-5 fibroblasts, XP-A patient cells and CS-A patient cells were purchased from the Coriell Cell Repositories and cultured in DMEM, supplemented with 15% FBS.

Transfection of U2OS 2-6-3 and HEK293T cells was performed by Lipofectamine 2000 (Invitrogen) transfection according to manufacturer's instructions. Plasmids used were mCherry-LacR-ZRF1, mCherry-LacR-DICER, mCherry-LacR-DICER$^{44ab}$, EGFP-LacR and EGFP-LacR-DDB2. Information on cloning strategies available on request. Control and DICER siRNA was purchased from Dharmacon (siGENOME SMARTpool). Control and PARP1 esiRNAs were purchased from Sigma.

**Plasmid transfection in MRC-5 cells was performed using a Nucleofector 2b (Lonza), Kit:R, program V-020.**

**UV irradiation and drug treatment**

Cells were irradiated with 20J/$m^2$ UV-C using a CL-1000 UV-crosslinker (UVP) unless stated otherwise. Micropore irradiation experiments were performed on MRC5 fibroblasts. Cells were exposed to localized UV damage (100 J/m2) using a micropore membrane with 3-μm pore size as described previously (25).

PARP inhibitor treatment was performed as described in (26). Briefly, 5mM IPTG was added to the cells before and during transfection with the mCherry-LacR-fusion plasmid. IPTG was washed out 24 hours post transfection, and replaced with medium containing 1 μM PARP inhibitor (KU-0058948). Cells were incubated with inhibitor for 16 hours, followed by fixation and staining.

**Immunofluorescence**

Cells were fixed in 4%PFA for 10 min at room temperature. When indicated, pre-extraction with CSK buffer (10mM PIPES pH- 7.4, 100 mM NaCl, 300mM sucrose, 3 mM $MgCl_2$) containing 0.2% Triton-X was performed for 5 min on ice prior to fixation. Cells were incubated overnight with primary antibody at 4 °C. Subsequently cells were incubated with Alexa-fluorophore-conjugated secondary antibodies (Life Technologies). The mounting was carried out in Vectashield with DAPI (Vector Laboratories). CPD staining (TDM-2 CosmoBio) was performed according to the manufacturer's protocol, prior to incubation with primary antibodies. Antibodies used in this study were: anti-DICER (Cell Signalling), anti-ZRF1 (Novus Biologicals).

**Chromatin association assays**

HEK293T cells (unless stated otherwise) were irradiated with UV and crosslinked by formaldehyde at the indicated time points after UV irradiation. Assays were essentially performed as published (27).

**Mass spectrometry**

Mass-spectrometry sample preparation, measurement and database search were performed as described elsewhere (28). Gradient lengths of 45 or 105 min were chosen depending on the IP

material obtained. Raw files were processed with MaxQuant (version 1.5.2.8) and searched against the *Homo sapiens* Uniprot database (25. February 2012) using the Andromeda search engine integrated into MaxQuant and default settings were applied. Proteins with at least 2 peptides, one of them unique, count as identified.

**FLAG purifications**

Cells were UV irradiated (20J/$m^2$) and harvested 1 hour after exposure (unless stated otherwise). FLAG affinity purifications were performed using FLAG-M2 agarose beads as already published (27).

**RNAseA digestion**

RNAse digestion was performed based on protocols described in (29,30).Briefly, cells were permeabilized in CSK buffer (10mM PIPES pH 7.4, 100mM NaCl, 300mM sucrose, 3mM $MgCl_2$) containing 0.5% Triton-X and protease inhibitors for 2 min. This was followed by treatment with 1mg/ml RNAse at RT for 10 min. Cells were then washed once in PBS followed by formaldehyde fixation (for chromatin association assays) or PFA fixation (for immunofluorescence experiments).

**MNase digestion and assessment of chromatin condensation**

Micrococcal nuclease was obtained from New England Biolabs. MNase digestion was performed as described in (31) with certain modifications. Cells were harvested at specified time points after UV treatment and washed once with Permeabilization Solution I (150 mM sucrose, 80 mM KCl, 35 mM HEPES, pH 7.4, 5 mM $K_2HPO_4$, 5 m $MMgCl_2$, 0.5 mM $CaCl_2$). Cells were permeabilized in Permeabilization Solution I containing 0.2% Triton X-100 for 2 min. Cells were resuspended in 1ml Permeabilization Solution II (150 mM sucrose,50 mM Tri-HCl, pH 7.5 , 50 mM NaCl, 2 mM $CaCl_2$) containing 7.5 or 15 units of MNAse and incubated for 5 min at RT. This was followed by cell lysis with TNES (10 mM Tris-HCl, pH 7.4, 0.1M NaCl, 1 mM EDTA, 1%SDS), RNAse A treatment and Proteinase-K digestion as described. DNA was purified using a Qiaquick PCR purification kit and loaded on a 1.5% Agarose gel. DNA bands were labeled 1-8 from high to low molecular weight. Band intensity was measured using ImageLab (BioRad). Intensities

were normalized to the band of highest intensity for each sample, and a graph of relative band intensity vs band number was plotted.

## RESULTS

### DICER is essential for nucleotide excision repair and is recruited to DNA damage sites

DICER has been previously implicated in DNA damage pathways and is thought to play a role in preventing DNA damage by maintaining heterochromatin structure (32,33) as well as indirectly through microRNA mediated regulation of DNA damage checkpoints (34-36). Specifically, it was shown that knockdown of DICER results in miRNA dependent hypersensitivity to UV irradiation (37). In order to differentiate between more global effects of DICER on DNA damage repair and a potentially more specific role in nucleotide excision repair, we performed unscheduled DNA synthesis (UDS) assays. We analyzed EdU incorporation specifically in non-S phase MRC-5 fibroblasts exposed to UV damage. Under these conditions the EdU incorporation reflects the efficiency of the core DNA repair process. As a reference we addressed UDS in XP-A and CS-A patient fibroblasts (Figure 1A). We observed about a 40% decrease of EdU incorporation in DICER knockdown cells as compared to control cells (Figure 1A). This finding suggested that DICER is required for nucleotide excision repair. Next, we wanted to elucidate whether DICER plays a role in either the GG-NER or the TC-NER subpathway. To this end, we monitored the recovery of RNA synthesis (RRS) after exposure to UV damage. Cells deficient specifically in TC-NER (XP-A and CS-A patient fibroblasts) show an impaired recovery, while depletion of GG-NER proteins does not affect the recovery of RNA synthesis. We observed that DICER knockdown cells showed no impairment of RNA synthesis. In contrast XP-A and CS-A deficient fibroblasts showed impaired RRS. (Supplementary Figure 1A). Additionally, we performed survival assays in *C. elegans*. In *C.elegans*, DNA repair in the germ line occurs mainly via GG-NER during early development, while TC-NER is the main NER subpathway employed during larval development (38). Upon UV treatment of a DICER mutant (*dcr-1*), we observed a substantial decrease in egg hatching comparable to that observed in a XPA deficient strain (*xpa-1*), which is essential for survival following UV treatment (39) (Supplementary Figure 1B). In contrast, upon irradiation of L1 larvae, we observed no significant developmental arrest in the DICER mutant (Supplementary Figure 1C). However, we observed a developmental arrest in both XPA (*xpa-1*) and CSB (*csb-1*) deficient worms, which are deficient in total NER and TC-

NER, respectively (Supplementary Figure 1C). Taken together these data imply that DICER plays a more prominent role in GG-NER.

Next, we wanted to determine if DICER is recruited to chromatin after UV irradiation. To this end we performed chromatin association assays in HEK293T cells treated with either control or DICER siRNAs followed by UV irradiation (Figure 1B, Supplementary Figure 1D). We found that DICER is specifically recruited to chromatin after UV irradiation. Additionally, to verify if DICER is localized to the site of DNA damage we performed micropore irradiation experiments. Normal fibroblasts were irradiated through a micropore to generate localized damage, and then stained with CPD and DICER antibodies (Figure 1C). We observed that DICER was recruited to the DNA damage locus in about 50% of the lesions. These data together suggest that DICER represents an essential factor in nucleotide excision repair in human cells and in *C. elegans*.

Figure 1

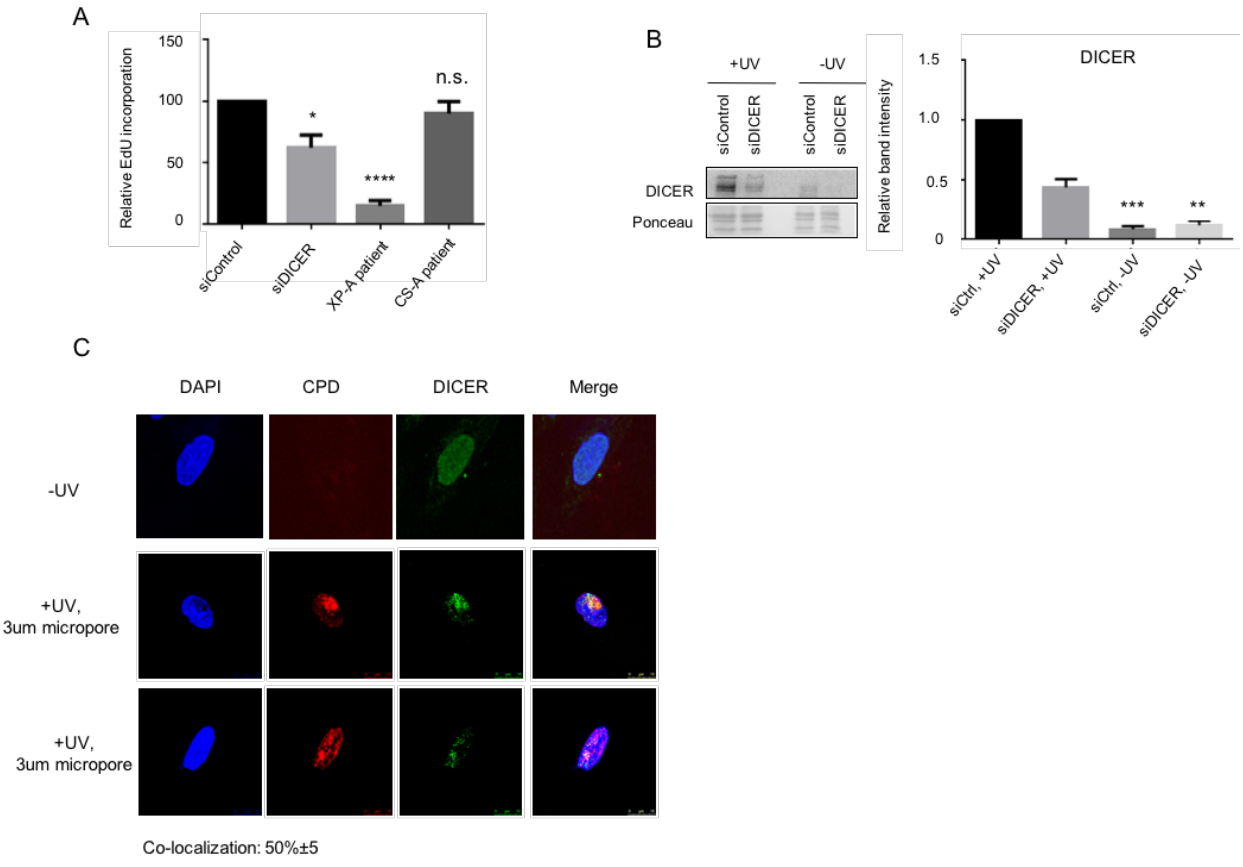


Figure 1. DICER is essential for nucleotide excision repair. (a) Knockdown of DICER results in impaired NER. The graph shows relative EdU incorporation as a measure of unscheduled DNA synthesis (UDS) in

control (siControl), DICER knockdown (siDICER) , XP-A patient fibroblasts (XP-A patient) and CS-A patient fibroblasts (CS-A patient) cells. Mean ± SD, n=3. (b) DICER is recruited to chromatin after UV damage. (Left panel) The blot shows DICER levels in the chromatin fraction in control (siControl) and DICER knockdown (siDICER) cells in UV unexposed cells and 1 hour after UV exposure. (Right panel) Quantification of Figure 1B. The graph shows the relative band intensities for DICER, normalized to a loading control for control and DICER knockdown cells in -/+UV conditions. (c) DICER is recruited to UV lesions. Immunofluorescence images showing DICER recruitment to DNA lesions (marked by CPD) in cells subjected to irradiation through a 3 μm micropore. Recruitment was observed at 50% ±5 lesions, quantified from 30 cells each. N=2

**DICER interacts with ZRF1 and its recruitment to chromatin is dependent on ZRF1**

In order to further investigate the function of DICER in NER, we expressed FLAG tagged DICER in HEK293T cells and performed immunoprecipitations followed by mass spectroscopy (Supplemental Table 1). We observed that DICER interacts strongly with ZRF1. We further confirmed this interaction by immunoblotting the aforementioned immunoprecipitated material (Figures 2A and 2B). The interaction of the two proteins was recapitulated in reverse immunoprecipitation experiments using FLAG tagged ZRF1 as well (Supplementary Figure 2A). We additionally assessed the nuclear distribution of chromatin bound ZRF1 and DICER in both UV unexposed and UV exposed cells. We found that DICER co-localized with ZRF1 foci at chromatin after UV damage, further confirming the interaction of the two proteins (Supplementary Figure 2B). Next we assessed the functional interplay of DICER, ZRF1 and the E3 ligase RING1B, which is essential for ZRF1 recruitment to the damage site (12). To this end we transfected HEK293T cells and HEK293T cell lines expressing short hairpin RNAs (shRNAs) targeting RING1B and ZRF1 with control or DICER siRNA pools followed by UV irradiation (Figure 2C). We observed that knockdown of both ZRF1 and RING1B had an adverse effect on recruitment of DICER to chromatin. These data suggest that RING1B dependent mono-ubiquitylation of H2A and hence tethering of ZRF1 are a prerequisite for DICER recruitment to chromatin. In contrast, siRNA mediated knockdown of DICER did not affect recruitment of RING1B or ZRF1 (Figure 2C, Supplementary Figure 2D), suggesting that DICER probably plays a role downstream of ZRF1.

Figure 2

A

| Protein name | Gene name | Molecular weight | Number of peptides |
|---|---|---|---|
| Endoribonuclease Dicer | DICER1 | 255 | 85 |
| DnaJ homolog subfamily C member 2 | ZRF1 | 65 | 11 |

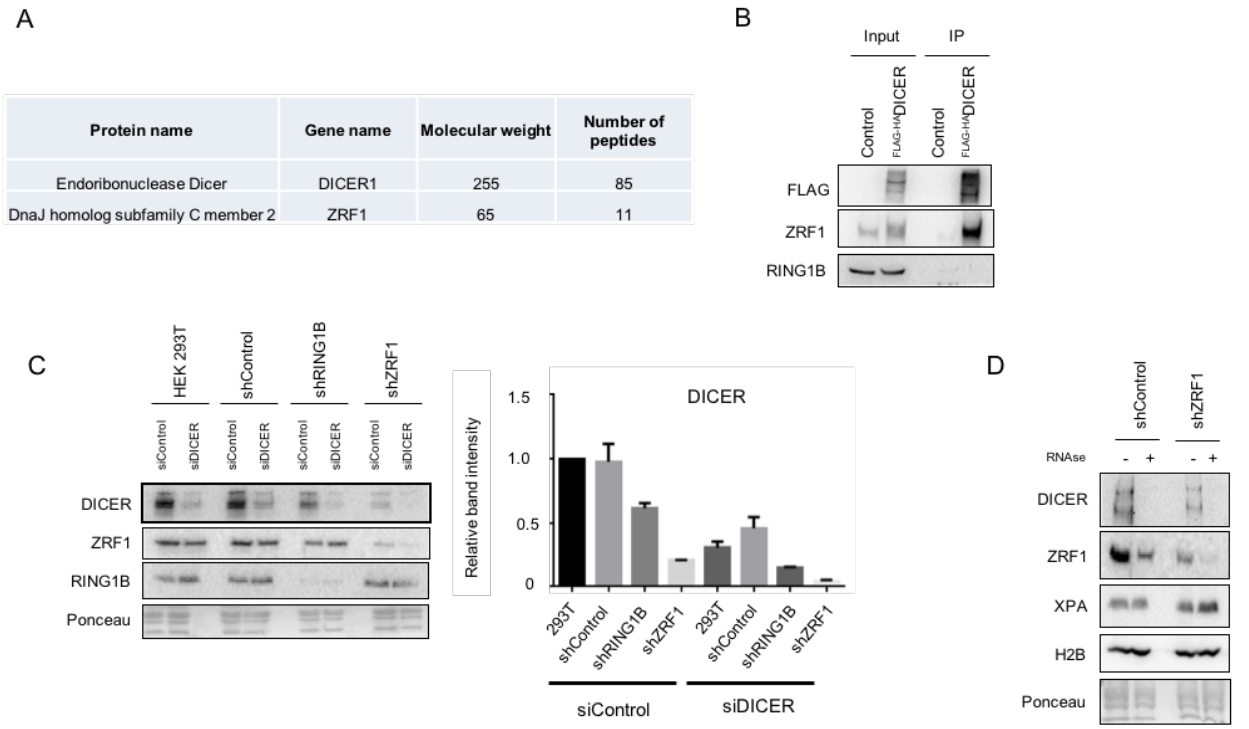


Figure 2. DICER interacts with ZRF1 and is recruited to chromatin in a ZRF1 dependent manner. (a) $^{FLAG\text{-}HA}$DICER along with its interactors, was purified from HEK293T cells and the purified material was subjected to mass spectrometry. Strong interaction was seen with ZRF1. The table shows the number of peptides identified by mass spectroscopy for DICER and ZRF1. (b) Western blot showing co-immunoprecipitation of ZRF1 in a $^{FLAG\text{-}HA}$DICER purification. (c) (Top panel) The blot shows levels of the indicated proteins in chromatin fractions from cells 1 hour post UV exposure. Control and DICER siRNA was transfected into the indicated stable shRNA knockdown cell lines. (Bottom panel) Quantification of Figure 2C. The graph shows the relative band intensities for DICER, normalized to a loading control for control and DICER knockdown cells in the indicated knockdown cell lines in -+UV conditions.(d) RNAse treatment leads to loss of DICER and ZRF1 from chromatin. The blot shows levels of the indicated proteins in the chromatin fraction from cells subjected to RNAse treatment.

**DICER and ZRF1 interactions with chromatin are RNA dependent**

DICER contributes to the generation of heterochromatin and it is known to bind and process RNA (16,17,40). Hence, we next examined whether the association of DICER with chromatin observed after UV irradiation was mediated by RNA. To this end, we irradiated HEK293T cell lines (shControl and shZRF1), permeabilized them and subsequently treated them with RNAseA, prior to cross-linking and chromatin purification (Figure 2D). Upon RNAseA treatment, DICER

was completely lost from the chromatin fraction whereas ZRF1 levels at chromatin were dramatically reduced in control cells. Next we assessed the levels of XPA, a core NER protein involved in damage verification. XPA levels at chromatin were unaffected upon RNAse digestion (Figure 2D). Similarly, we assessed the chromatin bound levels of ZRF1 and DICER by immunofluorescence in presence and absence of RNAseA. We found that RNAse treatment completely disrupted the previously observed foci of ZRF1 and DICER in UV exposed cells (Supplementary Figures 2B and 2C). These data suggest that DICER and ZRF1 association with chromatin is dependent on RNA.

Considering the RNA dependent association of both DICER and ZRF1 with chromatin, we further examined whether their interaction with each other, is also RNA dependent. To this end, we immunoprecipitated FLAG-tagged DICER and ZRF1, and subsequently incubated the beads in presence or absence of RNAseA. We did not observe a significant change in the ZRF1-DICER interaction upon RNAseA treatment (Supplementary Figure 2E). We additionally performed a SILAC experiment involving a selective degradation of dsRNA and ssRNA species to quantitatively determine the effect of RNAseA treatment on DICER-ZRF1 interaction. We found no dependence of the DICER-ZRF1 interaction on RNA (data not shown). Collectively, these data suggest that DICER and ZRF1 are associated with chromatin in a RNA dependent fashion.

**DICER and ZRF1 are required for chromatin decondensation after UV damage**

We next addressed the potential functions of DICER and ZRF1 in NER. DICER is known to play a role in establishing heterochromatin by processing small RNAs that maintain a condensed chromatin configuration (40). ZRF1 mediates remodeling of multiprotein complexes at chromatin (12,15,41) and might interact with chromatin remodeling complexes (15). Thus, we hypothesized that DICER and ZRF1 might impact on the chromatin conformation. We additionally performed a purification of FLAG tagged ZRF1, followed by mass spectroscopy to identify its interactors. Upon examining the interactors of both ZRF1 and DICER, we found several chromatin remodelers (Figures 3A and 3B). Notably, a strong interactor of both ZRF1 and DICER was PARP1, which is known to play a role in chromatin decondensation during NER (42). The *Access-Prime-Repair* model of DNA damage repair suggests that chromatin decondensation precedes DNA repair and is required for access of the repair machinery to the lesion site. We therefore performed MNAse assays to determine the chromatin conformation in both unexposed cells and 1 hour after UV irradiation. Knockdown of ZRF1 did not show a significant effect on

chromatin structure in unexposed cells (Figures 3C and 3D). In agreement with the known role of DICER in heterochromatin maintenance, we observed that unexposed shDICER cells had a much more decondensed chromatin structure than the control cells (shScrambled) indicated by a more efficient MNase digestion, and thus higher levels of DNA of lower molecular weight (Figures 3E and 3F). In contrast, upon exposure to UV, we noticed a shift in chromatin structure towards a more condensed state in both ZRF1 and DICER knockdown cells (Figures 3C, 3D, 3E and 3F, Supplementary Figure 3A, 3B, 3C and 3D), reflected by an increase in DNA of high molecular weight. The chromatin condensation observed in ZRF1 knockdown cells is concurrent with our earlier observation that ZRF1 is required for eviction of RING1B from chromatin (27). Prolonged binding of RING1B causes elevated H2A-ubiquitin levels, which are also a marker for condensed chromatin. Thus, also given the physical interaction of DICER and ZRF1 we speculate that both together are required for efficient de-compaction of chromatin after UV exposure.

Figure 3: DICER and ZRF1 play a role in chromatin remodeling post UV exposure. (a,b) DICER and ZRF1 interact with various chromatin remodelers. $^{FLAG\text{-}HA}$DICER or $^{FLAG}$ZRF1 along with its interactors, was purified from HEK293T cells and the purified material was subjected to mass spectrometry. Multiple proteins with chromatin remodeling functions were found to interact with DICER and ZRF1. The table shows peptide numbers for selected proteins obtained by affinity purification. (c, d, e, f) ZRF1 and DICER play a role in chromatin decondensation post UV exposure. Quantification of band intensities of MNAse digested chromatin from UV exposed cells in the indicated control and knockdown cells. Band numbers 1 to 8 depict DNA of high to low molecular weight. The graph shows the mean band intensity ±SD calculated from 3 independent experiments.

Figure 3

A

| Protein name | Gene name | Molecular weight | Number of peptides |
|---|---|---|---|
| Endoribonuclease Dicer | DICER1 | 255 | 103 |
| Zuotin-related factor 1 | DNAJC2 | 77 | 20 |
| SWI/SNF-related matrix-associated actin-dependent regulator of chromatin subfamily A member 5 | SMARCA5 | 116.78 | 21 |
| Poly [ADP-ribose] polymerase I | PARP1 | 113.08 | 11 |

B

| Protein name | Gene name | Molecular weight | Number of peptides |
|---|---|---|---|
| Zuotin-related factor 1 | DNAJC2 | 77 | 41 |
| Endoribonuclease Dicer | DICER1 | 255 | 17 |
| SWI/SNF-related matrix-associated actin-dependent regulator of chromatin subfamily A member 5 | SMARCA5 | 116.78 | 18 |
| Poly [ADP-ribose] polymerase I | PARP1 | 113.08 | 14 |

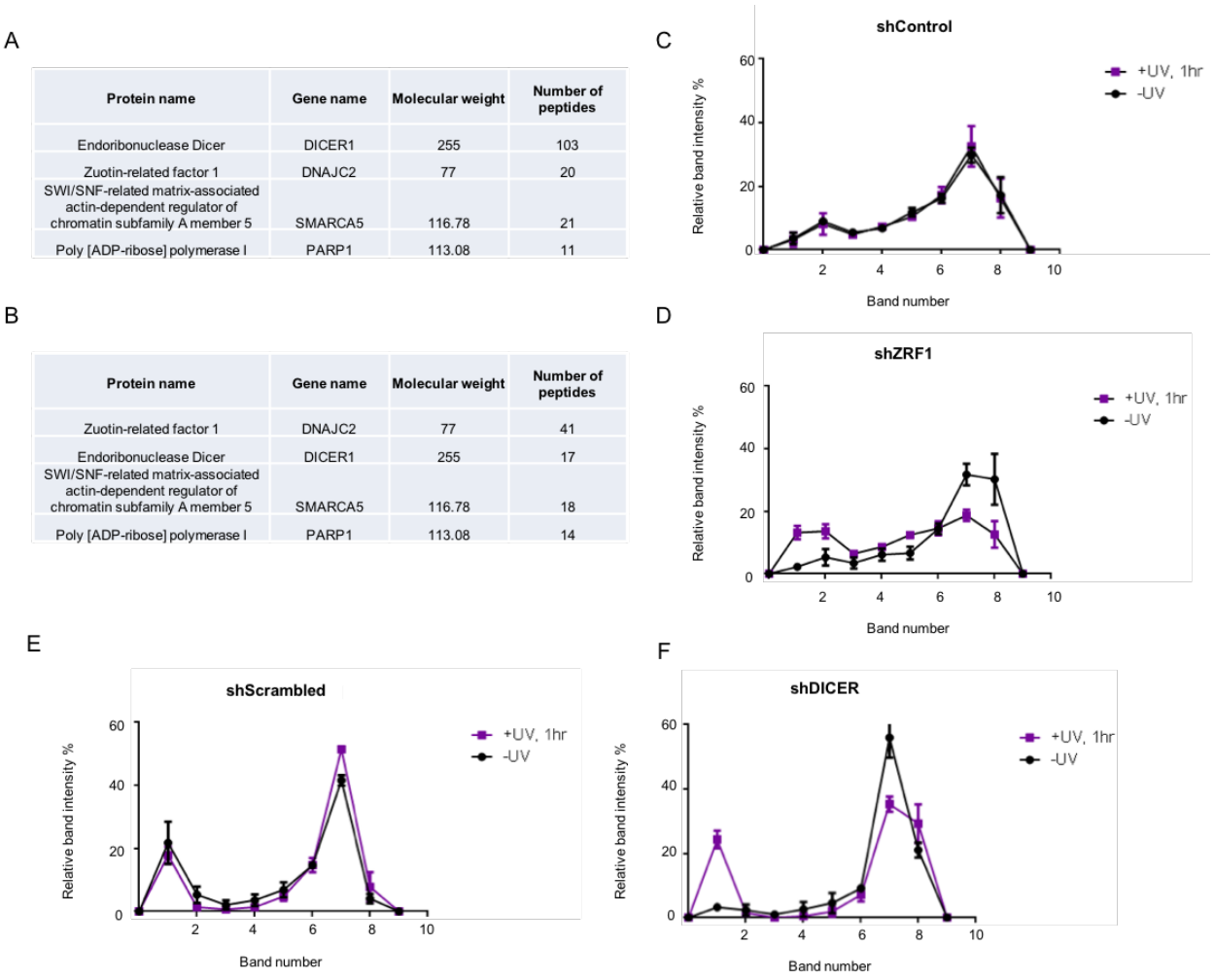


In order to determine whether the effect on chromatin decondensation is direct or indirect, we made use of a LacO tethering system in U2OS 2-6-3 cells (43) to directly examine the effect of ZRF1 or DICER tethering to a chromatin array. The LacO array in 2-6-3 cells is known to be heterochromatinized under normal conditions, and the size of the array is used as a common marker for the state of condensation/de-condensation of the chromatin array (43). We found that tethering of ZRF1 led to an increase in the array size compared to the mCherry-LacR tethered control array (Figures 4A and 4B). Similarly, tethering of DICER also led to an increase in size of the chromatin array (Figures 4A and 4B). Interestingly, DICER had an even stronger effect on array size than ZRF1 alone. This might suggest that the ZRF1-mediated decondensation occurs

potentially by function of DICER. In order to further dissect the role of DICER and ZRF1 in regulating array size, we tethered ZRF1-LacR to the array in control and DICER knockdown cells. We found that knockdown of DICER reduced the ZRF1 dependent increase in array size (Figure 4C). However, co-tethering of ZRF1 and DICER did not further increase the size of the array as compared to tethering of DICER alone (Supplementary Figure S4A). These data together suggest that DICER and ZRF1 are potentially involved in chromatin decondensation via similar mechanisms, and that ZRF1 acts in a DICER dependent manner.

DICER has been described to play a role in the establishment of heterochromatin via processing of small RNAs (44). Recently, it was also shown that DICER contributes to acetylation of histones via small RNA mediated recruitment of TIP60 (45). Hence, we wanted to determine whether the effect of DICER on chromatin decondensation was also dependent on the RNA processing activity of DICER. Thus, we generated a completely inactive DICER mutant (DICER$^{44ab}$) (46). We tethered DICER$^{44ab}$ –LacR to chromatin, and analyzed the array size as a measure of chromatin decondensation (Figures 4A and 4D). Surprisingly, we found that the array size was similar when tethering either wildtype or mutant DICER. Thus, it seems that the potential role of DICER in chromatin decondensation is unrelated to its ribonuclease activity.

In order to confirm these findings, we compared the activity of wildtype and mutant DICER on chromatin in UV exposed cells. We expressed either mCherry-DICER or mCherry- DICER$^{44ab}$ in shDICER cells (Supplementary Figure 4B) and then performed an MNase assay on unexposed cells and and after UV exposure. We found that expression of wildtype DICER was able to reverse the overall decondensation of chromatin observed in unexposed DICER knockdown cells (Figures 3F and 4E). In contrast, the cells expressing DICER$^{44ab}$ retained the decondensed state observed in unexposed shDICER cells suggesting that the catalytic function of DICER is essential for maintenance of heterochromatin in unchallenged cells (Figure 4F). However, upon exposure to UV light, we did not observe a shift towards a more condensed state in either wildtype or mutatant DICER expressing cells. (Figures 3F, 4E and 4F). Thus both wildtype DICER and the inactive mutant were able to rescue the chromatin conformation phenotype of DICER knockdown cells in response to UV damage. This suggests that the catalytic activity of DICER might be dispensible for the observed conformational changes after UV irradiation. In order to evaluate whether the catalytic activity of DICER is essential for NER, we expressed mCherry-DICER or mCherry- DICER$^{44ab}$ in MRC-5 cells, and performed a UDS assay. We

found that expression of the enzymatically inactive DICER mutant did not have a detrimental effect on repair activity, as measured by UDS (Supplementary Figure 4C). These data together point towards a potential role of DICER in NER that is independent of its catalytic activity.

Figure 4: ZRF1 or DICER tethering facilitates decondensation of a chromatin array. (a) Representative immunofluorescence images showing the size of the LacO array after tethering of mCherry-LacR (control), ZRF1-LacR, DICER-LacR or DICER$^{44ab}$-LacR. (b, c, d) The graph shows the distribution (Min to Max) of percentage of nuclear area occupied by the specified tethered array in the specified knockdown conditions. Array size was measured in 50-100 cells from two independent experiments. Statistical significance was assessed by an unpaired t-test. (e,f) Quantification of band intensities of MNAse digested chromatin from UV exposed cells in shDICER cells expressing either wildtype or mutant DICER. Band numbers 1 to 8 depict DNA of high to low molecular weight. The graph shows the mean band intensity ±SD calculated from 3 independent experiments.

Figure 4

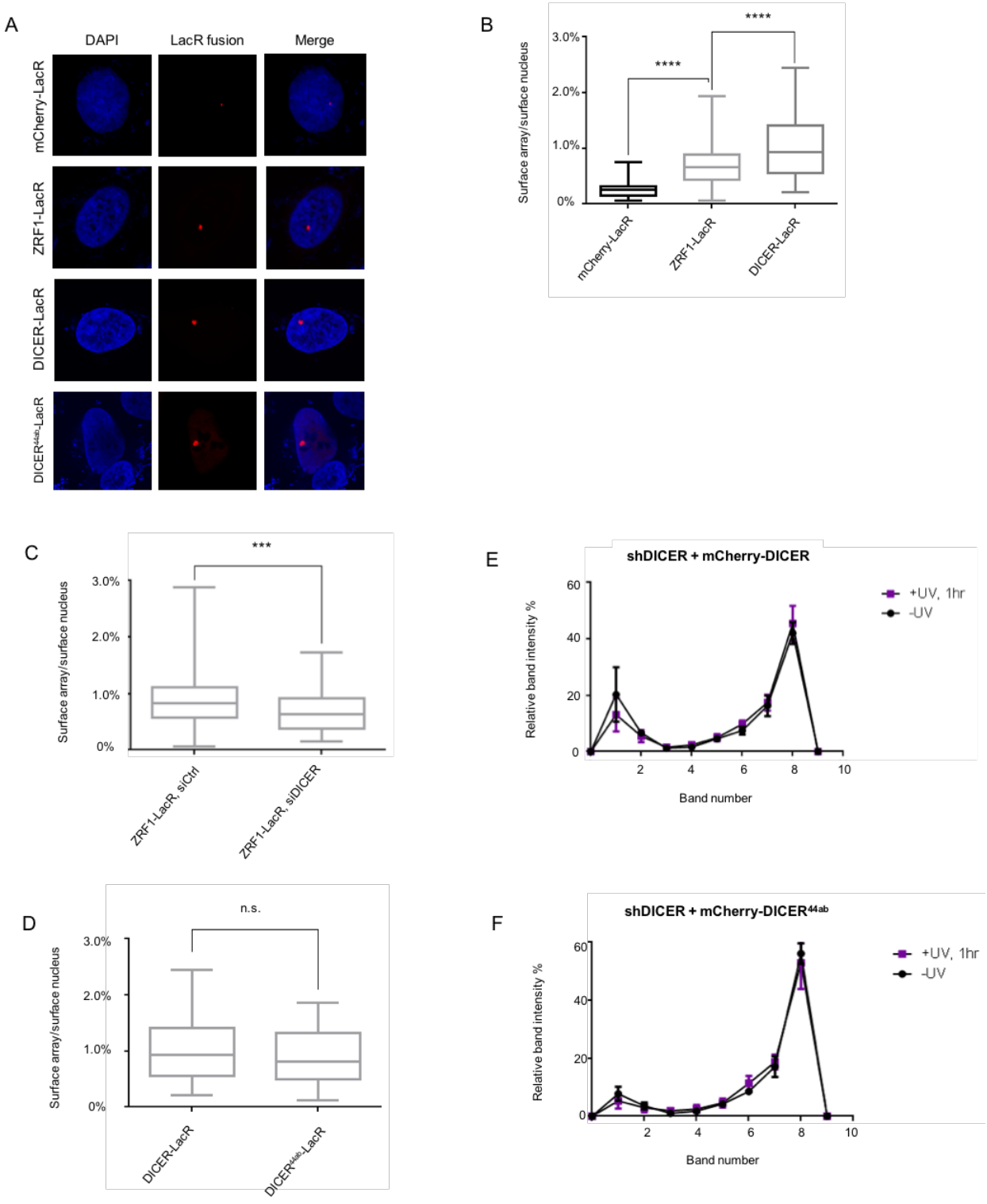
A
DAPI
LacR fusion
Merge
mCherry-LacR
ZRF1-LacR
DICER-LacR
DICER44ab-LacR
B
Surface array/surface nucleus
3.0%
2.0%
1.0%
0%
****
****
mCherry-LacR
ZRF1-LacR
DICER-LacR
C
***
Surface array/surface nucleus
3.0%
2.0%
1.0%
0%
ZRF1-LacR, siCtrl
ZRF1-LacR, siDICER
D
n.s.
Surface array/surface nucleus
3.0%
2.0%
1.0%
0%
DICER-LacR
DICER44ab-LacR
E
shDICER + mCherry-DICER
Relative band intensity %
60
40
20
0
2
4
6
8
10
Band number
+UV, 1hr
-UV
F
shDICER + mCherry-DICER44ab
Relative band intensity %
60
40
20
0
2
4
6
8
10
Band number
+UV, 1hr
-UV

It has been previously reported that DDB2 facilitates decondensation of chromatin upon tethering to a chromatin array (26). Since DDB2, ZRF1 and DICER operate in the GG-NER pathway, we wanted to determine whether the decondensation mediated by DDB2 also occurs in a DICER dependent manner, and vice versa. To this end we performed an experiment to co-tether DDB2 with either DICER or ZRF1, followed by measuring the size of the array. Notably, we found that co-tethering of DDB2 leads to an increase in both the ZRF1 and DICER mediated decondensation (Figures 5A, 5B, 5C and 5D). This additive effect suggests that chromatin decondensation via DDB2 or DICER/ZRF1 is in fact initiated independently of each other. In order to substantiate this finding, we measured the array size of the DDB2 tethered chromatin array in control and DICER knockdown cells. We found that knockdown of DICER did not affect the DDB2 mediated chromatin decondensation (Supplementary Figure 5A). We additionally assayed the DICER mediated decondensation in control and DDB2 knockdown cells. We found that knockdown of DDB2 had no effect on the DICER mediated decondensation (Supplementary Figure 5B) supporting that DICER and DDB2 might potentially contribute to decondensation of chromatin independently.

Figure 5: Co-tethering of ZRF1 or DICER with DDB2 increases array decondensation. (a,c) Representative images showing size of the LacO array after double tethering of mCherry-LacR-ZRF1 or mCherry-LacR-DICER with either EGFP-LacR (control) or EGFP-LacR-DDB2. (b,d) The graph shows the distribution (Min to Max) of percentage of nuclear area occupied by the specified tethered array. Array size was measured in 50-100 cells from two independent experiments. Statistical significance was assessed by an unpaired t-test.

Figure 5

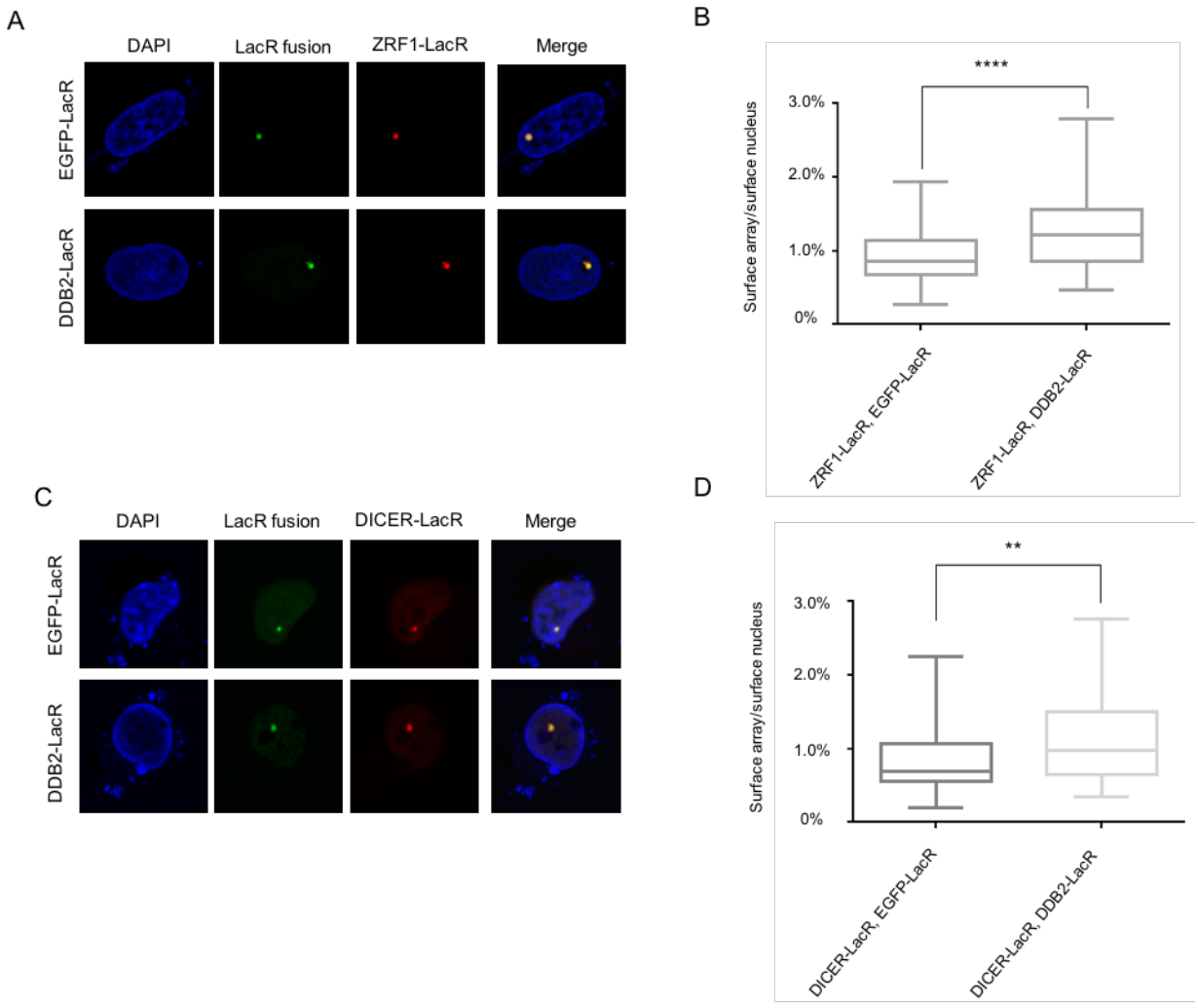


**DICER and ZRF1 mediated decondensation requires PARP activity**

Finally, we wanted to determine a potential mechanism by which ZRF1 and DICER might lead to decondensation of chromatin. It is well established that DDB2 decondenses chromatin in a PARP1-dependent manner (26) and that efficient NER requires parylation (3). In line with these findings and in agreement with our interaction data (Figures 3A and 3B), we examined whether ZRF1 and DICER mediated decondensation is also PARP dependent. To this end, we incubated DICER or ZRF1-LacR expressing cells with IPTG, followed by an IPTG release to enable chromatin binding of the LacR-fusion protein and treatment with a PARP inhibitor (KU-0058948). We subsequently fixed the cells after a 16 hour incubation with PARP inhibitor and

measured the array size. We found that inhibitor treatment reduced ZRF1 mediated chromatin decondensation (Figure 6A). Similarly, PARPi treatment also reduced DICER mediated chromatin decondensation (Figure 6B). In order to further confirm the role of PARP in the activity of ZRF1 and DICER, we measured the size of the ZRF1 or DICER tethered array in control and PARP1 knockdown cells. Similar to the effect of the PARP inhibitor, knockdown of PARP1 also significantly reduced the ability of ZRF1 and DICER to cause an increase in array size (Figure 6C). Next, we wanted to determine if the PARP1 mediated impact on the array size is also linked to UV damage repair. To this end, we treated HEK293T cells with either DMSO or PARPi and assessed the condensation state of chromatin before and after UV exposure. Similar to the effect observed for ZRF1 and DICER knockdown, treatment with PARP inhibitor also caused an increase in condensed chromatin in UV exposed cells. In contrast, administration of DMSO did not have any significant effect on the chromatin state (Figures 6D and 6E). Lastly, we directly assessed the effect of PARP1 depletion on UDS. We found that knockdown of PARP1 also reduced the repair dependent EdU incorporation after UV damage (Supplementary Figure 6A). Thus, PARP1 plays an important role in maintenance of chromatin state during NER.

In sum, our data provide evidence for a novel role of DICER in cooperation with ZRF1 and PARP1 in altering the chromatin conformation during nucleotide excision repair.

Figure 6: ZRF1 and DICER mediated decondensation is dependent on PARP. (a,b) (Left panel) Representative images showing the specified tethered array under specified treatment conditions. (Right panel) The graph shows the distribution (Min to Max) of percentage of nuclear area occupied by the specified tethered array, after treatment with vehicle (DMSO) or PARP inhibitor (PARPi). Array size was measured in 50-100 cells from two independent experiments. Statistical significance was assessed by an unpaired t-test. (c) The graph shows the distribution (Min to Max) of percentage of nuclear area occupied by the specified tethered array, after treatment in either control (esiControl) or PARP1 knockdown (esiPARP1) conditions. Array size was measured in 50-100 cells from two independent experiments. Statistical significance was assessed by an unpaired t-test. (d,e) Quantification of band intensities of MNAse digested chromatin from UV exposed cells in 293T cells treated with either DMSO or PARP inhibitor (PARPi). Band numbers 1 to 8 depict DNA of high to low molecular weight. The graph shows the mean band intensity ±SD calculated from 3 independent experiments.

Figure 6

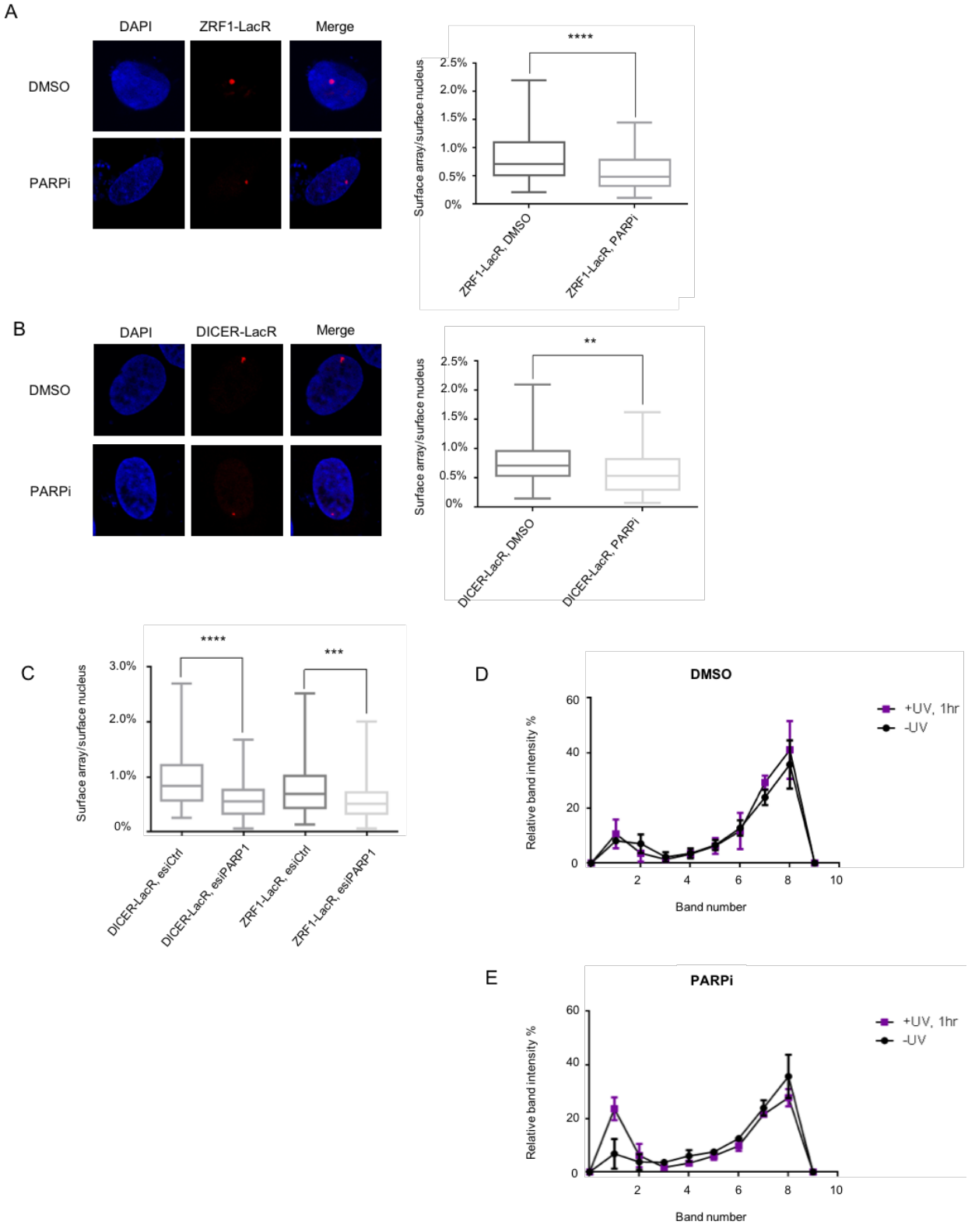
A
DAPI
ZRF1-LacR
Merge
DMSO
PARPi
****
Surface array/surface nucleus
2.5%
2.0%
1.5%
1.0%
0.5%
0%
ZRF1-LacR, DMSO
ZRF1-LacR, PARPi
B
DAPI
DICER-LacR
Merge
DMSO
PARPi
**
Surface array/surface nucleus
2.5%
2.0%
1.5%
1.0%
0.5%
0%
DICER-LacR, DMSO
DICER-LacR, PARPi
C
****
***
Surface array/surface nucleus
3.0%
2.0%
1.0%
0%
DICER-LacR, esiCtrl
DICER-LacR, esiPARP1
ZRF1-LacR, esiCtrl
ZRF1-LacR, esiPARP1
D
DMSO
+UV, 1hr
-UV
Relative band intensity %
60
40
20
0
2
4
6
8
10
Band number
E
PARPi
+UV, 1hr
-UV
Relative band intensity %
60
40
20
0
2
4
6
8
10
Band number

## DISCUSSION

The endoribonuclease DICER is most well-known for its role in miRNA processing and RNAi mediated silencing via the RITS complex (21,44). Both these functions involve processing of RNAs by DICER to form short double-stranded RNA fragments. Additionally, DICER has also been shown to bind to rDNA (47). In this case, DICER was observed to bind to both active and inactive genes but its effect on the chromatin conformation remained uncertain. Furthermore, DICER was shown to operate at DSBs (16,17). Although the exact mechanism of dsRNAs produced by DICER in DSB repair stays elusive, it was recently reported that dsRNAs facilitate the recruitment of mediators of DNA damage signalling to chromatin (20). We assessed whether DICER also plays a role in other DNA damage pathways. Our data employing human cell lines and *C. elegans* unequivocally show that DICER is an essential player in NER. Reduction of DICER levels significantly reduces the incorporation of EdU in UDS assays and UV irradiated dcr-1 strains show a severe germ line phenotype causing high mortality. In contrast, DICER depletion does not affect RRS, thus linking DICER preferentially to the GG-NER pathway. These findings are in agreement with the observed interaction of DICER and ZRF1, which is an important player in the GG-NER branch (12,15), and their localization to DNA damage sites.

Apart from its remodeling function at the DNA damage site (12), the H2A-ubiquitin binding protein ZRF1 is important for recruiting DICER to chromatin after UV irradiation. This further suggests that DICER is functionally linked to the ubiquitin signalling cascade during damage recognition. Interestingly, the binding of both proteins to chromatin seems to be RNA-dependent. In contrast, the interaction of both factors is not stabilized by RNA as judged by immunoprecipitation experiments involving RNAse digestion. Hence, RNA is probably not a scaffold for a putative protein complex consisting of ZRF1 and DICER but rather important for maintaining or recruiting these factors at chromatin. However, the exact role and nature of this RNA is still unclear.

Our mass spectroscopy experiments revealed a strong association of both ZRF1 and DICER with chromatin remodeling factors, and most notably with PARP1. In agreement with a potential function in chromatin remodeling, we observed a strong impact on the chromatin conformation after UV irradiation upon knockdown of ZRF1 or DICER. Likewise, when tethering both proteins to a genomic locus we observed a significant increase in size of the locus, implying a role in the decondensation of the locus. The decondensation seems to be carried out primarily by

DICER, since knockdown of DICER also reduces the ZRF1 dependent decondensation. Hence, it appears that both proteins are involved in the decondensation of chromatin, which is an important prerequisite for DNA repair. ZRF1 had been linked to remodeling of protein complexes previously (12,15), however, here we provide evidence that it might play an additional role in chromatin remodeling during NER. DICER had been demonstrated to be involved in the formation of heterochromatin during gene silencing but whether it impacts on chromatin remodeling during DSB repair is still unknown. Here, we provide experimental evidence for a novel function of DICER which promotes the decondensation of chromatin. Consistent with their interaction with PARP1, ZRF1 and DICER mediated chromatin decondensation is entirely abolished when adding PARP inhibitors or when knocking down PARP1. This finding further substantiates potential functions of DICER and ZRF1 in chromatin remodeling. Interestingly, we found that DICER mediated chromatin decondensation is independent of its ribonuclease activity. Thus, even though the recruitment of DICER and ZRF1 to chromatin may potentially involve RNA, the decondensation activity likely does not.

Taken together our data highlight a novel and unexpected common role for ZRF1 and DICER during NER. DICER, apart from its catalytic function, harbors multiple domains that might be involved in recruitment of factors that drive the decondensation of chromatin. One potential candidate for such a function is evidently PARP1. Moreover, though speculative, the helicase activity of DICER might be involved in the decondensation process. Clearly, our study foreshadows also an RNA-independent chromatin remodeling function for DICER at DSBs, where the relationship of dsRNAs produced by DICER and its potential role in chromatin remodeling might be studied in more detail. Future research will certainly unveil the underlying molecular mechanisms.

**ACKNOWLEDGEMENTS**

We are grateful to the IMB microscopy facility for their expert help and assistance. We thank the members of the Richly laboratory for comments on the manuscript.

**FUNDING**

This work was supported by grants from the Boehringer Ingelheim Foundation and the DFG (RI-2413/1-1).

## REFERENCES

1. de Laat, W.L., Jaspers, N.G. and Hoeijmakers, J.H. (1999) Molecular mechanism of nucleotide excision repair. *Genes & development*, **13**, 768-785.

2. Fousteri, M. and Mullenders, L.H. (2008) Transcription-coupled nucleotide excision repair in mammalian cells: molecular mechanisms and biological effects. *Cell research*, **18**, 73-84.

3. Marteijn, J.A., Lans, H., Vermeulen, W. and Hoeijmakers, J.H. (2014) Understanding nucleotide excision repair and its roles in cancer and ageing. *Nature reviews. Molecular cell biology*, **15**, 465-481.

4. Doil, C., Mailand, N., Bekker-Jensen, S., Menard, P., Larsen, D.H., Pepperkok, R., Ellenberg, J., Panier, S., Durocher, D., Bartek, J. *et al.* (2009) RNF168 binds and amplifies ubiquitin conjugates on damaged chromosomes to allow accumulation of repair proteins. *Cell*, **136**, 435-446.

5. Mattiroli, F., Vissers, J.H., van Dijk, W.J., Ikpa, P., Citterio, E., Vermeulen, W., Marteijn, J.A. and Sixma, T.K. (2012) RNF168 ubiquitinates K13-15 on H2A/H2AX to drive DNA damage signaling. *Cell*, **150**, 1182-1195.

6. Pan, M.R., Peng, G., Hung, W.C. and Lin, S.Y. (2011) Monoubiquitination of H2AX protein regulates DNA damage response signaling. *The Journal of biological chemistry*, **286**, 28599-28607.

7. Ui, A., Nagaura, Y. and Yasui, A. (2015) Transcriptional elongation factor ENL phosphorylated by ATM recruits polycomb and switches off transcription for DSB repair. *Molecular cell*, **58**, 468-482.

8. Bergink, S., Salomons, F.A., Hoogstraten, D., Groothuis, T.A., de Waard, H., Wu, J., Yuan, L., Citterio, E., Houtsmuller, A.B., Neefjes, J. *et al.* (2006) DNA damage triggers nucleotide excision repair-dependent monoubiquitylation of histone H2A. *Genes & development*, **20**, 1343-1352.

9. Kapetanaki, M.G., Guerrero-Santoro, J., Bisi, D.C., Hsieh, C.L., Rapic-Otrin, V. and Levine, A.S. (2006) The DDB1-CUL4ADDB2 ubiquitin ligase is deficient in xeroderma pigmentosum group E and targets histone H2A at UV-damaged DNA sites. *Proceedings of the National Academy of Sciences of the United States of America*, **103**, 2588-2593.

10. Marteijn, J.A., Bekker-Jensen, S., Mailand, N., Lans, H., Schwertman, P., Gourdin, A.M., Dantuma, N.P., Lukas, J. and Vermeulen, W. (2009) Nucleotide excision repair-induced H2A

ubiquitination is dependent on MDC1 and RNF8 and reveals a universal DNA damage response. *The Journal of cell biology*, **186**, 835-847.

11. Guerrero-Santoro, J., Kapetanaki, M.G., Hsieh, C.L., Gorbachinsky, I., Levine, A.S. and Rapic-Otrin, V. (2008) The cullin 4B-based UV-damaged DNA-binding protein ligase binds to UV-damaged chromatin and ubiquitinates histone H2A. *Cancer Res*, **68**, 5014-5022.

12. Gracheva, E., Chitale, S., Wilhelm, T., Rapp, A., Byrne, J., Stadler, J., Medina, R., Cardoso, M.C. and Richly, H. (2016) ZRF1 mediates remodeling of E3 ligases at DNA lesion sites during nucleotide excision repair. *The Journal of cell biology*, **213**, 185-200.

13. Riedl, T., Hanaoka, F. and Egly, J.M. (2003) The comings and goings of nucleotide excision repair factors on damaged DNA. *The EMBO journal*, **22**, 5293-5303.

14. Sugasawa, K., Ng, J.M., Masutani, C., Iwai, S., van der Spek, P.J., Eker, A.P., Hanaoka, F., Bootsma, D. and Hoeijmakers, J.H. (1998) Xeroderma pigmentosum group C protein complex is the initiator of global genome nucleotide excision repair. *Molecular cell*, **2**, 223-232.

15. Papadopoulou, T. and Richly, H. (2016) On-site remodeling at chromatin: How multiprotein complexes are rebuilt during DNA repair and transcriptional activation. *BioEssays : news and reviews in molecular, cellular and developmental biology*.

16. Francia, S., Michelini, F., Saxena, A., Tang, D., de Hoon, M., Anelli, V., Mione, M., Carninci, P. and d'Adda di Fagagna, F. (2012) Site-specific DICER and DROSHA RNA products control the DNA-damage response. *Nature*, **488**, 231-235.

17. Wei, W., Ba, Z., Gao, M., Wu, Y., Ma, Y., Amiard, S., White, C.I., Rendtlew Danielsen, J.M., Yang, Y.G. and Qi, Y. (2012) A role for small RNAs in DNA double-strand break repair. *Cell*, **149**, 101-112.

18. Michalik, K.M., Bottcher, R. and Forstemann, K. (2012) A small RNA response at DNA ends in Drosophila. *Nucleic acids research*, **40**, 9596-9603.

19. Gao, M., Wei, W., Li, M.M., Wu, Y.S., Ba, Z., Jin, K.X., Li, M.M., Liao, Y.Q., Adhikari, S., Chong, Z. *et al.* (2014) Ago2 facilitates Rad51 recruitment and DNA double-strand break repair by homologous recombination. *Cell Res*, **24**, 532-541.

20. Francia, S., Cabrini, M., Matti, V., Oldani, A. and d'Adda di Fagagna, F. (2016) DICER, DROSHA and DNA damage response RNAs are necessary for the secondary recruitment of DNA damage response factors. *Journal of cell science*, **129**, 1468-1476.

21. Holoch, D. and Moazed, D. (2015) RNA-mediated epigenetic regulation of gene expression. *Nature Reviews Genetics*, **16**, 71-84.

22. Jia, N., Nakazawa, Y., Guo, C., Shimada, M., Sethi, M., Takahashi, Y., Ueda, H., Nagayama, Y. and Ogi, T. (2015) A rapid, comprehensive system for assaying DNA repair activity and cytotoxic effects of DNA-damaging reagents. *Nature protocols*, **10**, 12-24.

23. Craig, A.L., Moser, S.C., Bailly, A.P. and Gartner, A. (2012) Methods for studying the DNA damage response in the Caenorhabdatis elegans germ line. *Methods in cell biology*, **107**, 321-352.

24. Schmitter, D., Filkowski, J., Sewer, A., Pillai, R.S., Oakeley, E.J., Zavolan, M., Svoboda, P. and Filipowicz, W. (2006) Effects of Dicer and Argonaute down-regulation on mRNA levels in human HEK293 cells. *Nucleic acids research*, **34**, 4801-4815.

25. Katsumi, S., Kobayashi, N., Imoto, K., Nakagawa, A., Yamashina, Y., Muramatsu, T., Shirai, T., Miyagawa, S., Sugiura, S., Hanaoka, F. *et al.* (2001) In situ visualization of ultraviolet-light-induced DNA damage repair in locally irradiated human fibroblasts. *J Invest Dermatol*, **117**, 1156-1161.

26. Luijsterburg, M.S., Lindh, M., Acs, K., Vrouwe, M.G., Pines, A., van Attikum, H., Mullenders, L.H. and Dantuma, N.P. (2012) DDB2 promotes chromatin decondensation at UV-induced DNA damage. *The Journal of cell biology*, **197**, 267-281.

27. Richly, H., Rocha-Viegas, L., Ribeiro, J.D., Demajo, S., Gundem, G., Lopez-Bigas, N., Nakagawa, T., Rospert, S., Ito, T. and Di Croce, L. (2010) Transcriptional activation of polycomb-repressed genes by ZRF1. *Nature*, **468**, 1124-1128.

28. Bluhm, A., Casas-Vila, N., Scheibe, M. and Butter, F. (2015) Reader interactome of epigenetic histone marks in birds. *Proteomics*.

29. Martini, E., Roche, D.M., Marheineke, K., Verreault, A. and Almouzni, G. (1998) Recruitment of phosphorylated chromatin assembly factor 1 to chromatin after UV irradiation of human cells. *The Journal of cell biology*, **143**, 563-575.

30. Maison, C., Bailly, D., Peters, A.H., Quivy, J.P., Roche, D., Taddei, A., Lachner, M., Jenuwein, T. and Almouzni, G. (2002) Higher-order structure in pericentric heterochromatin involves a distinct pattern of histone modification and an RNA component. *Nature genetics*, **30**, 329-334.

31. Zaret, K. (2005) Micrococcal nuclease analysis of chromatin structure. *Curr Protoc Mol Biol*, **Chapter 21**, Unit 21 21.

32. Peng, J.C. and Karpen, G.H. (2009) Heterochromatic genome stability requires regulators of histone H3 K9 methylation. *PLoS genetics*, **5**, e1000435.

33. Tang, K.F., Ren, H., Cao, J., Zeng, G.L., Xie, J., Chen, M., Wang, L. and He, C.X. (2008) Decreased Dicer expression elicits DNA damage and up-regulation of MICA and MICB. *The Journal of cell biology*, **182**, 233-239.

34. Mudhasani, R., Zhu, Z., Hutvagner, G., Eischen, C.M., Lyle, S., Hall, L.L., Lawrence, J.B., Imbalzano, A.N. and Jones, S.N. (2008) Loss of miRNA biogenesis induces p19Arf-p53 signaling and senescence in primary cells. *The Journal of cell biology*, **181**, 1055-1063.

35. Teta, M., Choi, Y.S., Okegbe, T., Wong, G., Tam, O.H., Chong, M.M., Seykora, J.T., Nagy, A., Littman, D.R., Andl, T. *et al.* (2012) Inducible deletion of epidermal Dicer and Drosha reveals multiple functions for miRNAs in postnatal skin. *Development*, **139**, 1405-1416.

36. Kraemer, A., Anastasov, N., Angermeier, M., Winkler, K., Atkinson, M.J. and Moertl, S. (2011) MicroRNA-mediated processes are essential for the cellular radiation response. *Radiat Res*, **176**, 575-586.

37. Pothof, J., Verkaik, N.S., van, I.W., Wiemer, E.A., Ta, V.T., van der Horst, G.T., Jaspers, N.G., van Gent, D.C., Hoeijmakers, J.H. and Persengiev, S.P. (2009) MicroRNA-mediated gene silencing modulates the UV-induced DNA-damage response. *The EMBO journal*, **28**, 2090-2099.

38. Lans, H. and Vermeulen, W. (2015) Tissue specific response to DNA damage: C. elegans as role model. *DNA Repair (Amst)*, **32**, 141-148.

39. Astin, J.W., O'Neil, N.J. and Kuwabara, P.E. (2008) Nucleotide excision repair and the degradation of RNA pol II by the Caenorhabditis elegans XPA and Rsp5 orthologues, RAD-3 and WWP-1. *DNA Repair (Amst)*, **7**, 267-280.

40. Holoch, D. and Moazed, D. (2015) Small-RNA loading licenses Argonaute for assembly into a transcriptional silencing complex. *Nature structural & molecular biology*, **22**, 328-335.

41. Papadopoulou, T., Kaymak, A., Sayols, S. and Richly, H. (2016) Dual role of Med12 in PRC1-dependent gene repression and ncRNA-mediated transcriptional activation. *Cell cycle*, **15**, 1479-1493.

42. Robu, M., Shah, R.G., Petitclerc, N., Brind'Amour, J., Kandan-Kulangara, F. and Shah, G.M. (2013) Role of poly(ADP-ribose) polymerase-1 in the removal of UV-induced DNA lesions by nucleotide excision repair. *Proceedings of the National Academy of Sciences of the United States of America*, **110**, 1658-1663.

43. Janicki, S.M., Tsukamoto, T., Salghetti, S.E., Tansey, W.P., Sachidanandam, R., Prasanth, K.V., Ried, T., Shav-Tal, Y., Bertrand, E., Singer, R.H. *et al.* (2004) From silencing to gene expression: real-time analysis in single cells. *Cell*, **116**, 683-698.

44. Wilson, R.C. and Doudna, J.A. (2013) Molecular mechanisms of RNA interference. *Annu Rev Biophys*, **42**, 217-239.

45. Wang, Q. and Goldstein, M. (2016) Small RNAs Recruit Chromatin-Modifying Enzymes MMSET and Tip60 to Reconfigure Damaged DNA upon Double-Strand Break and Facilitate Repair. *Cancer Res*, **76**, 1904-1915.

46. Zhang, H., Kolb, F.A., Jaskiewicz, L., Westhof, E. and Filipowicz, W. (2004) Single processing center models for human Dicer and bacterial RNase III. *Cell*, **118**, 57-68.

47. Sinkkonen, L., Hugenschmidt, T., Filipowicz, W. and Svoboda, P. (2010) Dicer is associated with ribosomal DNA chromatin in mammalian cells. *PloS one*, **5**, e12175.

## Supplementary data

Supplemental Figure 1. DICER is essential for nucleotide excision repair. (a) Recovery of RNA synthesis (RRS) assay showing levels of EU incorporation in the indicated cells in unexposed cells and cells exposed to UV damage. The EU intensity is normalized to the intensity of the –UV condition for each cell type. DICER mutants show impaired survival after UV exposure. (b) The graph shows the percentage of eggs hatched after exposure to the indicated UV dose in the wildtype (N2) and mutant *C.elegans* strains. (c) DICER mutants do not show developmental arrest after UV exposure. The graph shows the percentage of larvae that successfully develop from L1 to L2 stage after exposure to the indicated UV dose in the wildtype (N2) and mutant *C.elegans* strains. Quantification of Figure 1B. The graph shows the relative band intensities for DICER, normalized to a loading control for control and DICER knockdown cells in -/+UV conditions.

Supplementary Figure 1

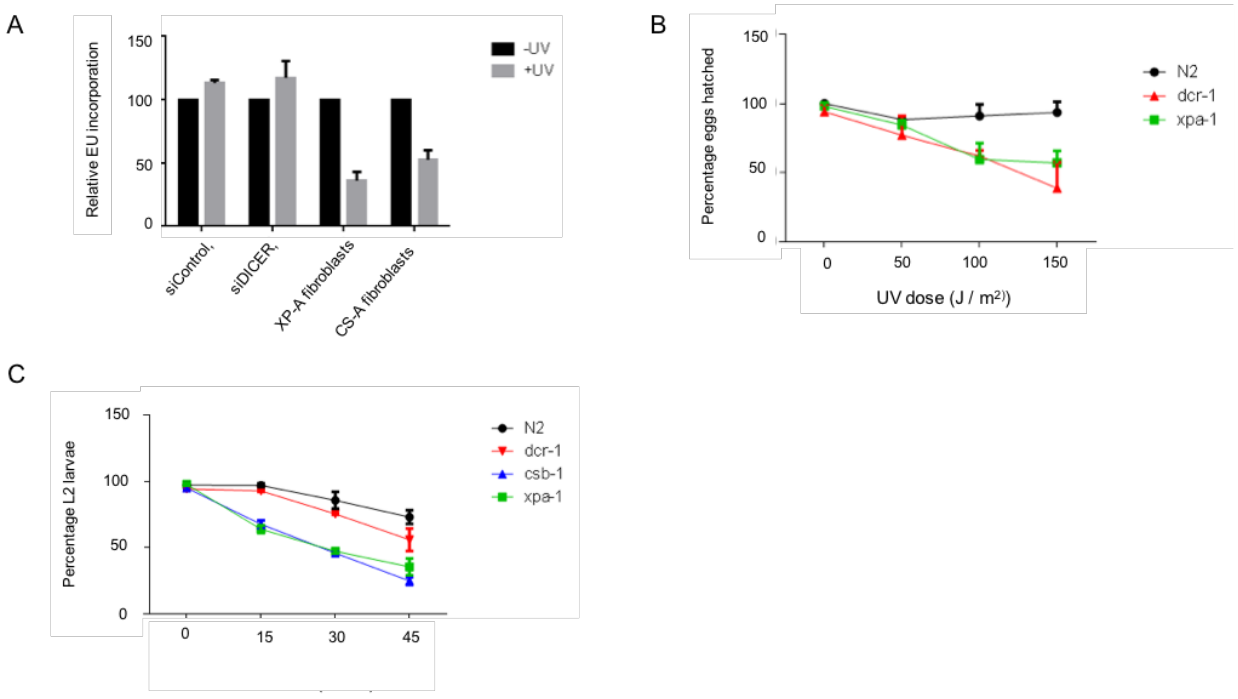

Supplemental Figure 2. DICER interacts with ZRF1. (a) Western blot showing co-immunoprecipitation of DICER in a $^{FLAG}$ZRF1 purification. (b) Immunofluorescence images showing the distribution of ZRF1 and DICER in unexposed cells and 1 hour after UV exposure. Pre-extraction was performed before staining to visualize only chromatin bound protein. (c) Immunofluorescence images showing the distribution of chromatin bound ZRF1 and DICER in RNAse treated and untreated cells, 1 hour after UV exposure. (d) DICER-ZRF1 interaction is not dependent on RNA. $^{FLAG\text{-}HA}$DICER (left) and $^{FLAG}$ZRF1 (right) purifications were subjected to RNAse treatment and the presence of ZRF1 and DICER, respectively, was examined in the co-precipitate. The blot shows the ZRF1 and DICER levels in purifications from control and transfected cells in -/+RNAse conditions.

Supplementary Figure 2

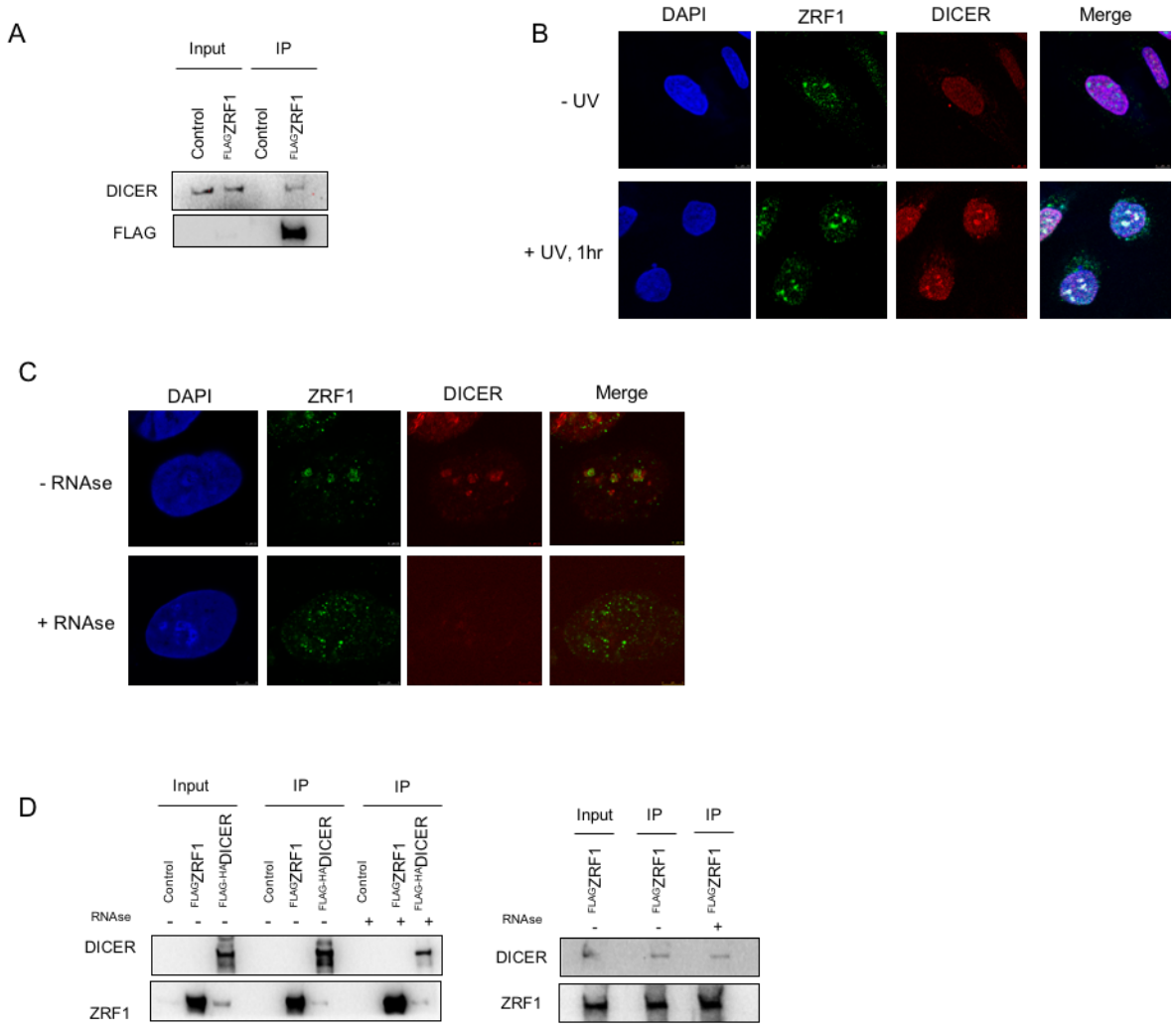

Supplemental Figure 3. ZRF1 and DICER play a role in chromatin rearrangements during NER. (a, b) Representative agarose gel showing MNase digested chromatin from the indicated knockdown cell lines. Band numbers are indicated on the left. Band number 1-8 represent high to low mol wt. DNA. (c, d) Quantification of band intensities of MNAse digested chromatin from UV exposed cells in the indicated knockdown cells. Band number 1 to 8 depicts DNA of high to low molecular wt. The graph shows the mean band intensity ±SD calculated from 3 independent experiments. The band intensities were normalized to the intensities for the –UV conditions in all the indicated cell lines.

Supplementary Figure 3

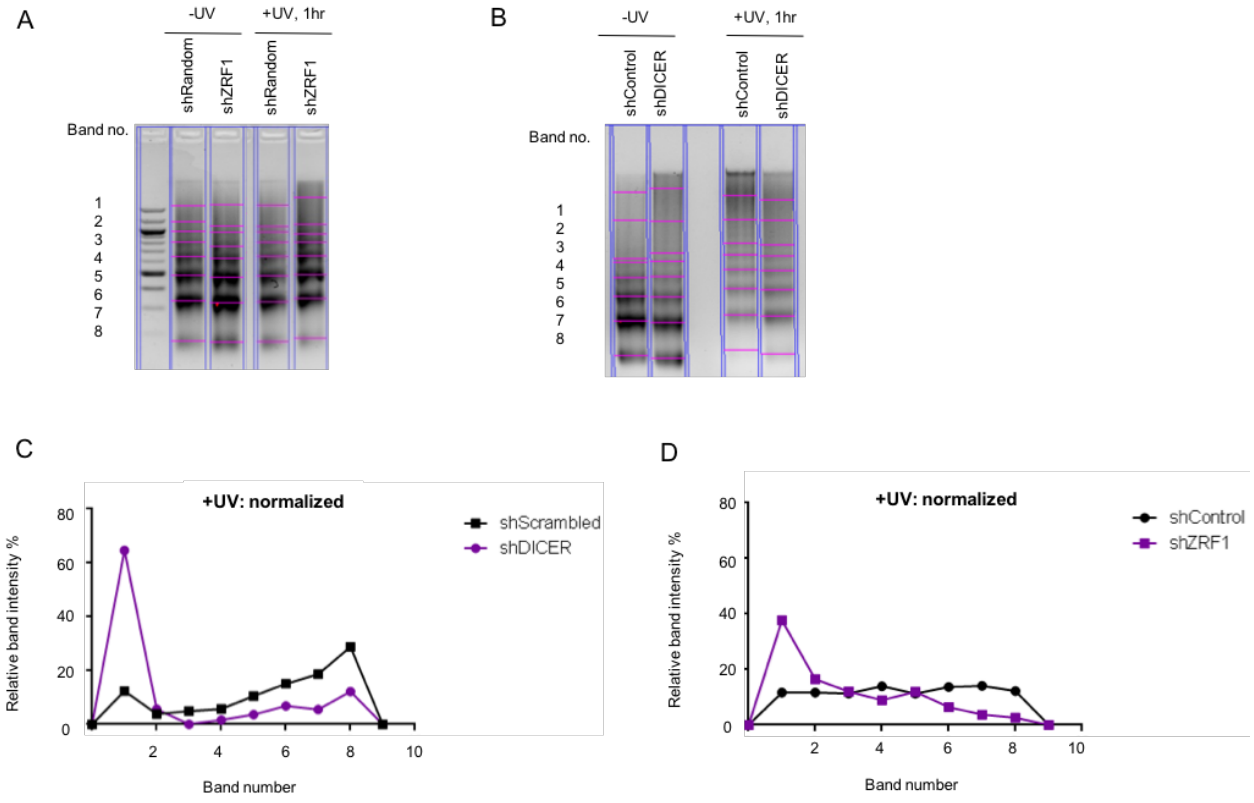

Supplementary Figure 4

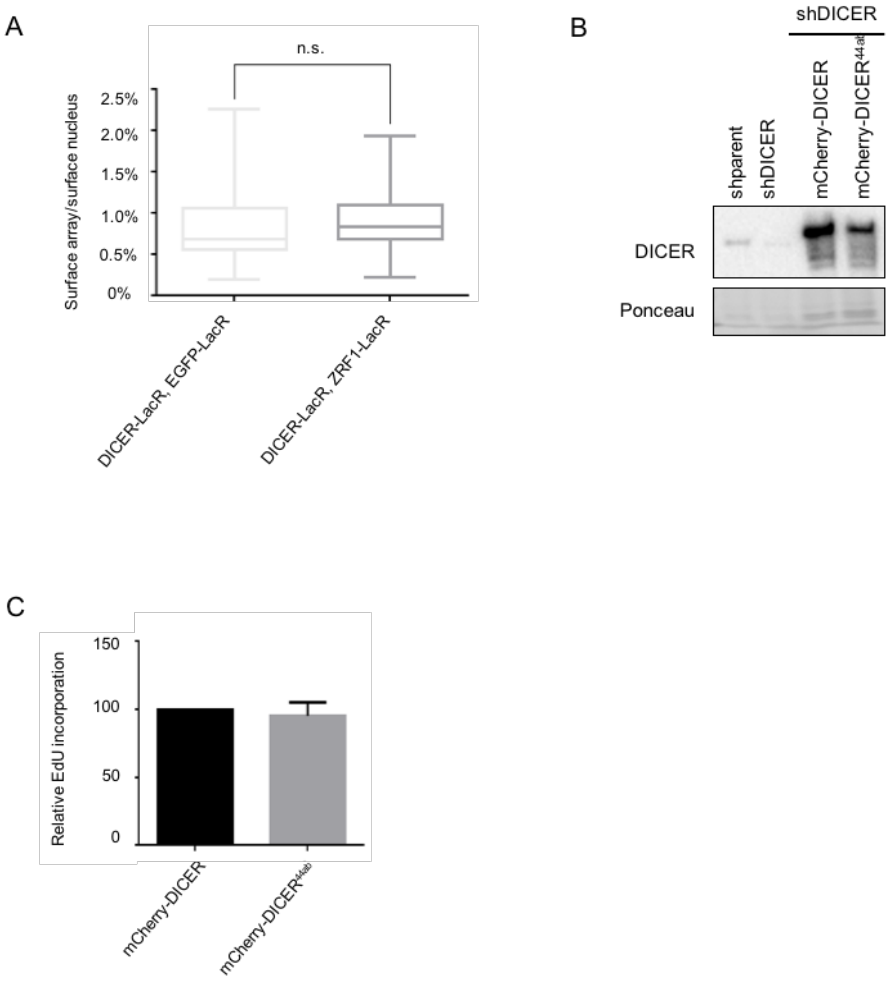


Supplemental Figure 4. (a) The graph shows the distribution (Min to Max) of percentage of nuclear area occupied by co-tethering of either DICER-LacR and EGFP-LacR, or DICER-LacR and ZRF1-LacR. Array size was measured in 50-100 cells from two independent experiments. Statistical significance was assessed by an unpaired t-test. (b) Western blot showing the levels of DICER, and mCherry tagged forms of DICER in the indicated cells (c) The graph shows the relative EdU incorporation after UV exposure in cells expressing either DICER or DICER$^{44ab}$ .

Supplementary Figure 5

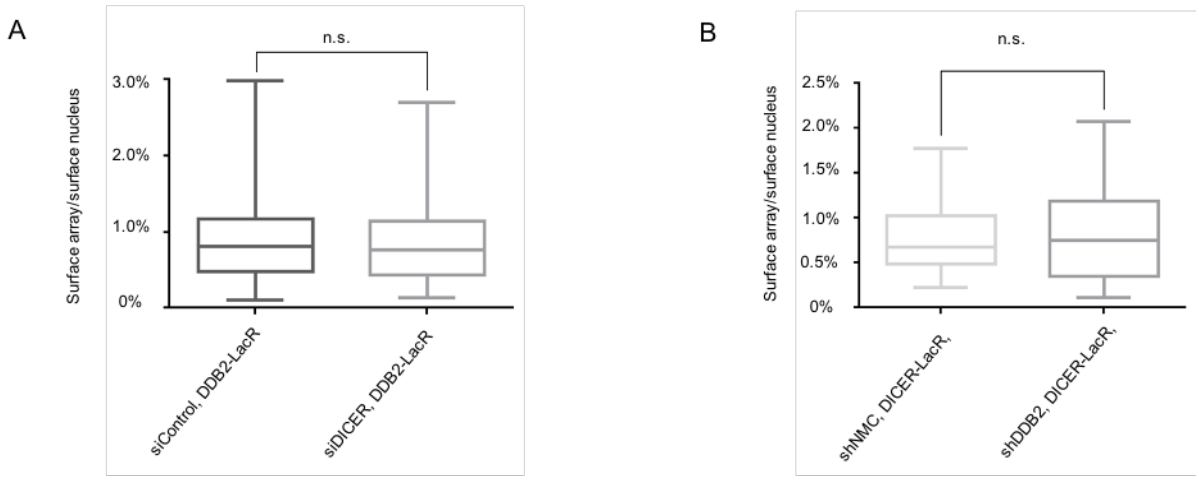


Supplemental Figure 5. DICER and DDB2 impact on the chromatin conformation independently of each other. (a) The graph shows the distribution (Min to Max) of percentage of nuclear area occupied by the DDB2 tethered array, in control (sicontrol) and DICER knockdown (siDICER) cells. Array size was measured in 50-100 cells from two independent experiments. Statistical significance was assessed by an unpaired t-test. (b) The graph shows the distribution (Min to Max) of percentage of nuclear area occupied by the DICER tethered array, in control (shNMC) and DDB2 knockdown (shDDB2) cells. Array size was measured in 50-100 cells from two independent experiments. Statistical significance was assessed by an unpaired t-test.

Supplementary Figure 6

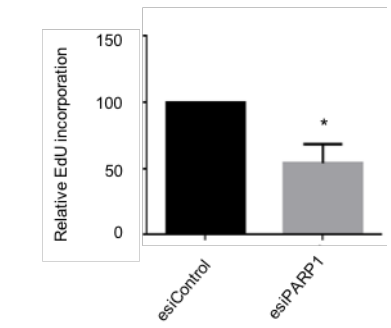


Supplemental Figure 6. (a) The graph shows the relative EdU incorporation after UV exposure in either MRC-5 control (esicontrol) or PARP1 knockdown (esiPARP1) cells .

# XPA recruitment to DNA damage sites is mediated by DICER and MMSET-catalyzed dimethylation of H4K20

**XPA recruitment to DNA damage sites is mediated by DICER and MMSET-catalyzed dimethylation of H4K20**

Shalaka Chitale[1,2] and Holger Richly[1,#]

[1] Laboratory of Molecular Epigenetics, Institute of Molecular Biology (IMB), Ackermannweg 4, 55128 Mainz, Germany

[2] Faculty of Biology, Johannes Gutenberg University, 55099 Mainz, Germany

[#] Correspondence: h.richly@imb-mainz.de

## INTRODUCTION

Nucleotide excision repair (NER) is one of the most versatile DNA repair pathways in the cell and handles a number of helix distorting lesions, caused by both intrinsic and extrinsic factors. The main types of lesions repaired by NER are photoproducts and pyrimidine dimers, which are caused by exposure to UV light (de Laat et al., 1999) Depending on the genomic location of the lesion, NER operates in two sub-pathways. Transcriptional coupled NER (TC-NER) recognizes lesions in transcriptionally active genes, while global genomic NER (GG-NER) deals with lesions in any chromatin environment. The recognition of the lesion is followed by lesion verification, unwinding of the DNA, excision of the lesion containing strand, and refilling of the DNA gap (de Laat et al., 1999; Fousteri and Mullenders, 2008; Marteijn et al., 2014). One of the critical factors linking lesion recognition to actual repair in both sub pathways is the DNA binding zinc-finger containing protein XPA. Cells lacking XPA are completely deficient in both TC- and GG-NER (Kim et al., 1995). XPA patients are characterized by central nervous system disorders (Enokido et al., 1997; Kohji et al., 1998), clinical skin defects and are very susceptible to UV light induced skin tumors (Kraemer, 1994). In both the GG and TC-NER pathways, XPA is recruited to chromatin by the TFIIH complex (Feltes and Bonatto, 2015; Yang et al., 2006). This recruitment occurs together with the recruitment of RPA. RPA bind the ssDNA to stabilize

the repair bubble, while XPA shows a high affinity for ssDNA-dsDNA junctions. Along with interacting with most of NER proteins, XPA also interacts with certain NER regulating proteins such as PARP1 (King et al., 2012). XPA is parylated and can stimulate PARP1 activity. However, parylated XPA has a lower affinity towards DNA (Fischer et al., 2014). PARP inhibition can also inhibit recruitment of XPA to DNA lesions. Considering its interactions with both the NER repair bubble and various NER proteins, there is strong support for the idea that XPA functions as a scaffold protein. In addition, it may also be responsible for linking NER to other cellular processes such as cell cycle regulation. Since XPA plays a central role in NER, research into inhibiting or enhancing its recruitment has many therapeutic applications (Sugitani et al., 2016).

One of the main constraints of GG-NER is the recognition and repair of a lesion in a chromatin context. One prominent histone mark involved in many DNA repair pathways is histone H2A ubiquitylation. In the context of NER, H2A-ubiquitylation is catalyzed by the E3 ligase RNF8, the UV-DDB-CUL4 and UV-RING1B complexes (Bergink et al., 2006; Gracheva et al., 2016; Guerrero-Santoro et al., 2008; Kapetanaki et al., 2006; Marteijn et al., 2009). We have recently demonstrated that the H2A-ubiquitin binding protein ZRF1 is an essential factor in GG-NER that mediates the remodeling of E3 ligase multiprotein complexes (Gracheva et al., 2016) and contributes to the sub-nuclear localization of GG-NER (Chitale and Richly, 2017 *in Press*). More recently we have shown that during GG-NER ZRF1 operates in concert with the endoribonuclease DICER. DICER is most well known for its role in the RNAi pathway and has been shown to play a role in the establishment of heterochromatin (Holoch and Moazed, 2015; Wilson and Doudna, 2013). DICER is recruited to sites of DNA damage, and cells lacking DICER show impaired GG-NER. Importantly, we found that contrary to its function in heterochromatin formation, DICER is involved in chromatin decondensation during NER. This function of DICER is independent of its riboendonuclease activity and occurs upon association of DICER with chromatin. This points towards a DICER function relatively early in the NER pathway probably enabling the repair machinery to better access the lesion.

During DSB repair H2A-ubiquitylation is linked to the methylation of histone H4. The vast majority of H4K20me2 at chrmatin is set by the di/trimethylases SUV4-20H1 and SUV4-20H2 (Schotta et al., 2004; Schotta et al., 2008). More recently the enzymes SETD8 (Milite et al., 2016;

Panier and Boulton, 2014) and MMSET/WHSC1 (Pei et al., 2011; Wang and Goldstein, 2016; Zimmermann and de Lange, 2014) were reported to affect the methylation status of H4K20 during DSB repair. SETD8 represents a member of the SET domain containing methyltransferases. It catalyzes the monomethylation of histone H4 Lys20 (H4K20) a modification that may be involved modulating chromatin compaction (Lu et al., 2008). Moreover, methylation of H4K20 was reported to be essential for the recruitment of the signalling factor 53BP1 (Dulev et al., 2014). In particular, H4K20 dimethylation (H4K20me2) via MMSET and H2A-ubiquitylation together were suggested to provide a binding platform for 53BP1 (Fradet-Turcotte et al., 2013). Interestingly, small RNAs produced by DICER where demonstrated to recruit MMSET to sites of DSBs suggesting a potential interplay of both factors in DNA repair pathways (Wang and Goldstein, 2016). Given our previous findings linking DICER to GG-NER we sought to investigate a potential function for DICER and MMSET during GG-NER.

Here, we show a novel role for MMSET in GG-NER. MMSET is recruited to chromatin in a DICER dependent manner setting the H4K20me2 mark in response to UV damage. We further provide evidence that H4K20me2 is responsible for the recruitment of XPA in the GG-NER pathway.

# RESULTS

### DICER is associated with setting of H4K20me2 during NER

One essential mechanism of establishing and maintaining chromatin states, as well as controlling the binding of chromatin associated proteins, is mediated by histone modifications. Several histone modifications such as H2AX-phosphorylation, H2A-ubiquitylation and histone methylation are implicated in playing both structural and tethering roles in nucleotide excision repair (Li, 2012; Bergink et al., 2006). We had previously observed that DICER can initiate chromatin decondensationin a PARP1 dependent manner. n order to identify novel histone modifications that may be associated with this process, we microscopically screened selected histone marks to monitor whether tethering of DICER at chromatin affected their levels (Figure S1A). We observed that tethering of DICER to chromatin set a prominent H4K20me2 mark at the chromatin array (Figure 1A). Next, we wanted to determine whether this setting of H4K20me2 is

relevant to NER. We observed that H4K20me2 showed a very significant change in its nuclear distribution upon UV damage, and that it formed specific nuclear foci (Figures 1B and S1B). These foci overlapped with nucleoli, as seen by a co-staining with nucleophosmin, a nucleolar marker. The presence of nucleolar H4K20me2 was further confirmed by biochemical purification of nucleoli (Supplementary Figure 1C). Surprisingly, we did not observe a significant change in global H4K20me2 levels after UV irradiation (Supplementary Figure 1D) suggesting that chromatin decorated with H4K20me2 is relocalized during the DNA damage response. In order to assess the permanence of H4K20me2 foci, we quantified the number of cells showing specific foci at various timepoints post UV exposure (Figure 1C). We found that the H4K20me2 foci were formed as soon as 1-2 hours after UV exposure and were retained up to 24 hours post UV damage. Next, we wanted to determine whether the H4K20me2 foci are formed during NER. To this end, we analysed the formation of H4K20me2 foci in cells after knocking down DDB2 or XPC, the two main GG-NER lesion recognition proteins. (Figure 1D). We found that DDB2 knockdown cells (shDDB2) showed impaired formation of H4K20me2 foci after UV damage. In contrast, foci formation occurred normally in XPC knockdown cells (shXPC). Finally, we wanted to confirm whether the global changes in H4K20me2 in response to UV damage and NER, were indeed linked to the presence of DICER at chromatin. To this end, we assessed the formation of H4K20me2 foci in DICER knockdown cells. We observed that the foci formation was severely impaired in absence of DICER comparable to the reduction of H4K20me2 foci after DDB2 depletion (Figure 1E). Collectively, these data point at H4K20me2 foci being formed specifically during lesion recognition via DDB2.

Figure 1

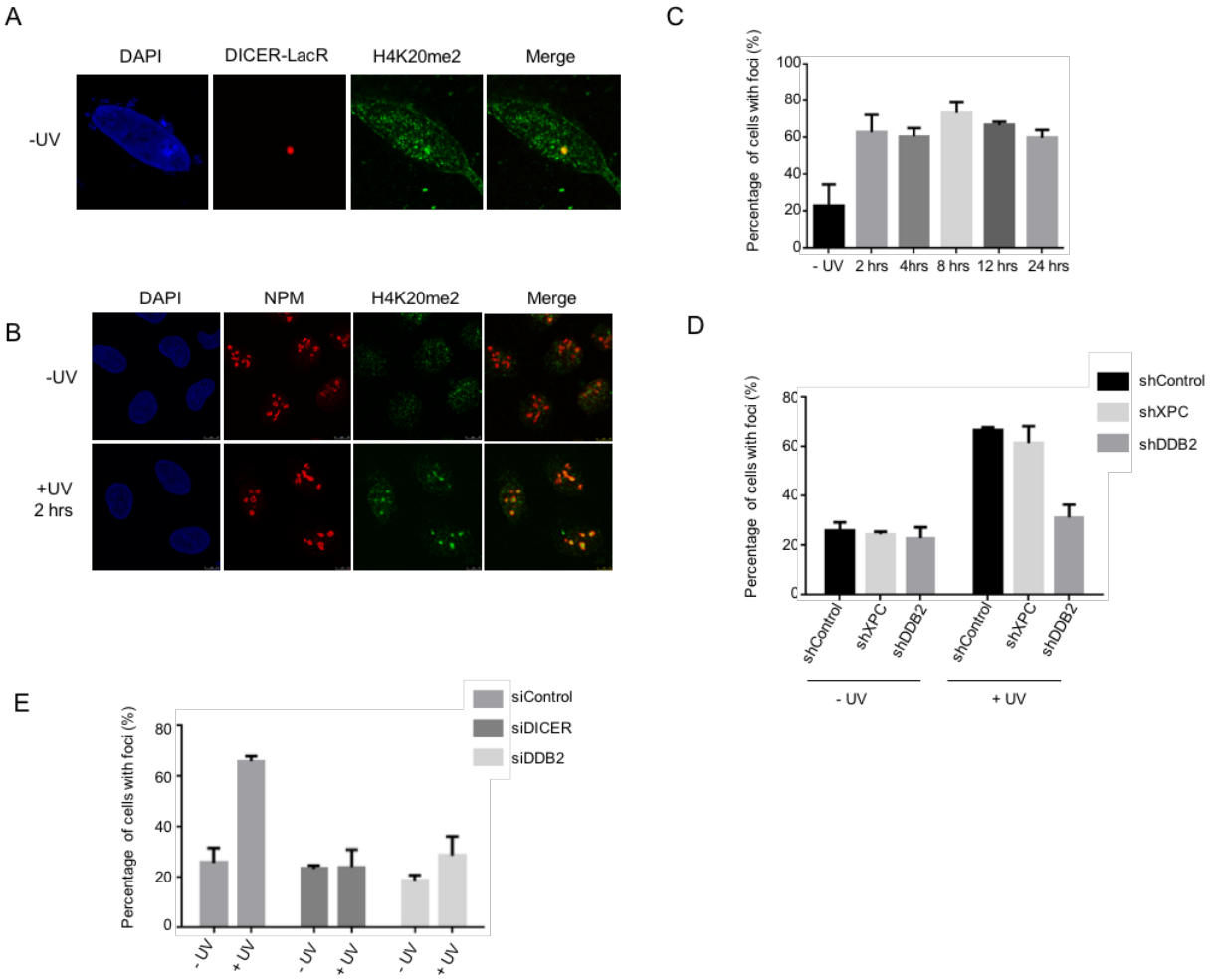


Figure 1: DICER and UV exposure results in formation of H4K20me2 foci: (a) Immunofluorescence images showing 2-6-3 cells with a tethered DICER-LacR chromatin array, and H4K20me2 distibution. (b) UV exposure results in formation of H4K20me2 foci which overlap with the nucleolus. Immunofluorescence images showing nuclear distributon of H4K20me2 in UV unexposed and UV exposed U2OS cells. Nucleoli are marked by Nucleophosmin (NPM). (c) H4K20me2 foci are maintained upto 24 hrs post UV exposure. The graph shows the percentage of U2OS cells showing nucleolar foci of H4K20me2 at various timepoints post UV exposure (Mean ± SEM). Cells were counted from 3 independent experiments, with 200 cells counted per experiment. (d, e) Formation of H4K20me2 foci is dependent on NER. The graph shows the percentage of cells showing nucleolar foci of H4K20me2 in unexposed U2OS cells (-UV) and 2 hours after UV exposure (+UV) in the indicated knockdown cell lines. (Mean ± SEM). Cells were counted from 3 independent experiments, with 200 cells counted per experiment.

**H4K20me2 is catalyzed by MMSET during NER**

We next wanted to determine whether H4K20me2 is set by a particular histone methyl transferase in response to UV exposure, and which specific enzyme sets this mark. H4K20me2 is a histone modification known to play a role in double strand break repair (DSB), where it provides a tethering platform for binding of 53BP1 (Fradet-Turcotte et al., 2013). In DSB repair, SETD8 and MMSET have been implicated in setting of the H4K20me2 mark.

Thus, we next addressed a potential role of SETD8 and MMSET in setting of H4K20me2 during NER. Therefore, we assessed the appearance of H4K20me2 foci in cells after depletion of SETD8 or MMSET, respectively, after UV irradiation. We found that siRNA mediated knockdown of SETD8 did not affect the appearance of H4K20me2 foci formation, whereas knockdown of MMSET resulted in a dramatic loss of foci (Figure 2A). Since our previous data linked the appearance of H4K20me2 foci to lesion recognition via DDB2, we additionally determined whether MMSET is also an essential factor of NER. To this end we measured the levels of unscheduled DNA synthesis (UDS) in control as well as SETD8 (siSETD8) and MMSET (siMMSET) knockdown cells (Figure 2B). We observed a modest effect on UDS upon SETD8 knockdown, as evidenced by decreased EdU incorporation post UV damage. In contrast, knockdown of MMSET had a stronger effect and resulted in about a 50% decrease of EdU incorporation. Having confirmed that MMSET is indeed required for efficient NER, we wanted to determine if MMSET has a direct role at the sites of DNA damage. Thus, we induced localized DNA damage in cells using a micropore membrane and analyzed recruitment of MMSET to the sites of damage (Figure 2C). We found recruitment of MMSET to about 40% of lesions marked by DDB2 30 minutes after UV damage. This further points towards a role for MMSET in NER.

MMSET has been shown to catalyze H4K20me2 in the context of DSB repair. In light of this finding, we wanted to further study its function during NER. Hence, we utilized a U2OS cell line (U2OS 2-6-3) containing a stably integrated LacO array, around 4MB in size (Janicki et al., 2004). We expressed a mCherry-LacR-MMSET fusion protein in these cells to selectively tether the MMSET protein to the LacO array and then assessed the presence of H4K20me2 at the array by immunofluorescence (Figure 2D). Surprisingly, we found that in unexposed cells MMSET was able to set the H4K20me2 mark in only about 20% of tethered arrays, consistent with the enzymatic function of MMSET. However, after exposure to UV irradiation we observed a

prominent H4K20me2 mark in about 70% of the arrays. This suggests that MMSET mediated catalysis of H4K20me2 is enhanced after UV damage. In contrast, tethering of SETD8-LacR coincided with H4K20me2 in only about 30% of the analyzed cells after exposure to UV light (Figure S2A). We next asked whether UV-dependent H4K20 methylation required the function of NER factors. To this end, we monitored the presence of H4K20me2 at the array in UV exposed cells employing various knockdown backgrounds. We found that, in line with our earlier data, knockdown of DDB2 resulted in a decreased ability of MMSET to catalyze the H4K20me2 mark, while knockdown of XPC had no effect (Figure 2E). Finally, we assessed the role of DICER in setting of H4K20me2. Again we found that knockdown of DICER impaired the ability of MMSET to set the H4K20me2 mark in response to UV (Figure 2F). Collectively, these data suggest a specific MMSET function in response to UV damage.

Figure 2

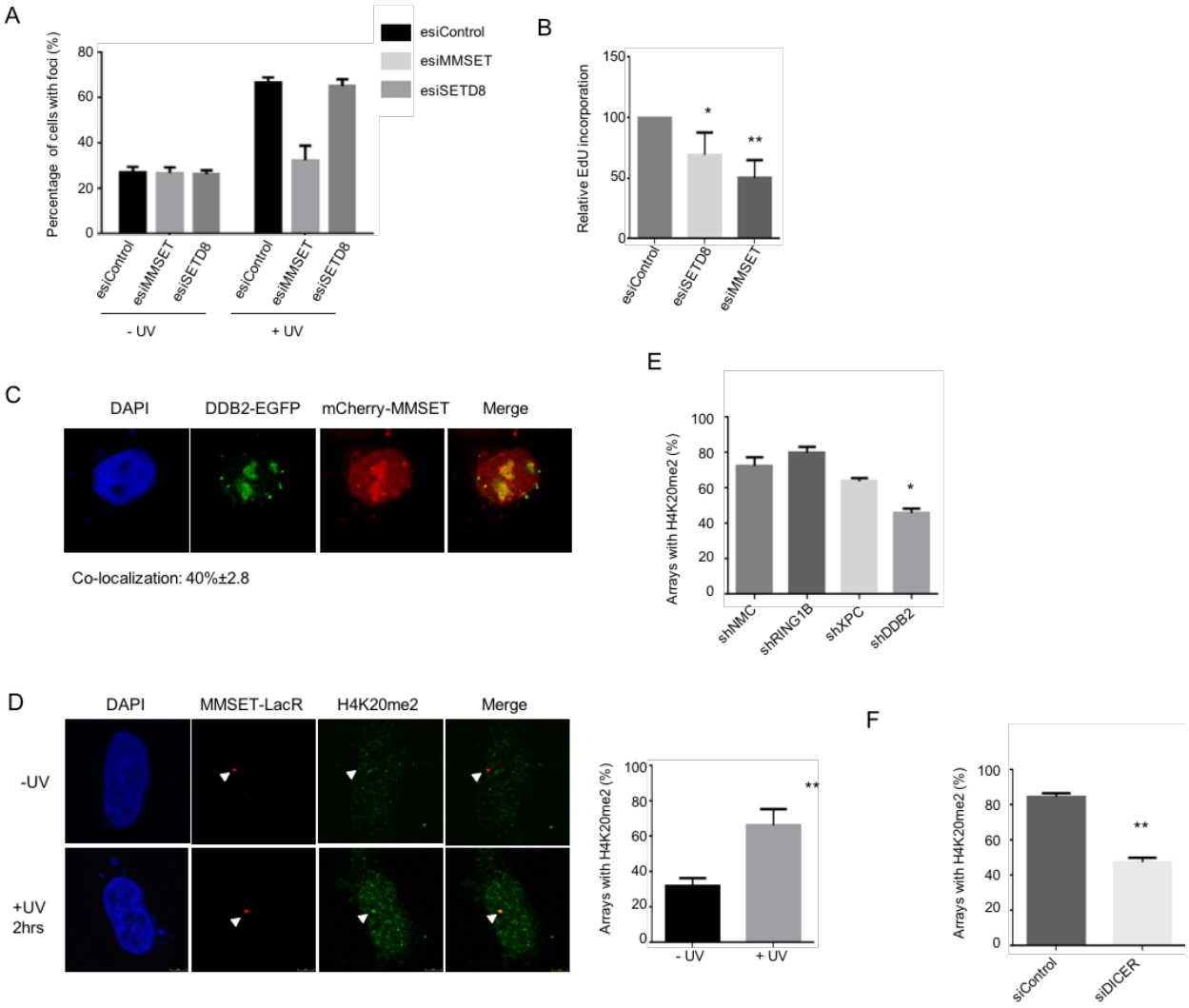


Figure 2: Formation of H4K20me2 foci is mediated by MMSET: (a) H4K20me2 foci are set by MMSET. The graph shows the percentage of cells showing nucleolar foci of H4K20me2 in unexposed cells (-UV) and 2 hours after UV exposure (+UV) in U2OS cells transfected by the indicated esiRNA. (Mean ± SEM). Cells were counted from 3 independent experiments, with 200 cells counted per experiment. (b) MMSET is required for efficient NER. The graph shows relative EdU incorporation as a result of unscheduled DNA synthesis, in MRC5 cells transfected with the indicated esiRNAs. (Mean ± SEM) EdU intensity was measured in 3 independent experiments, with 200 cells counted per experiment. (c) MMSET is recruited to the site of UV damage. Immunofluorescence images showing distribution of DDB2-EGFP and mCherry-MMSET in U2OS cells subjected to damage through a 3 μm micropore membrane. The damage sites are marked by DDB2-EGFP. MMSET is recruited to ≈ 40% of lesions, 30 min after UV exposure. (d) MMSET tethered to a chromatin array can set the H4K20me2 mark after UV exposure. (Left panel) Immunofluorescence images showing H4K20me2 distribution in U2OS 2-6-3 cells, expressing mCherry-LacR-MMSET (MMSET-LacR). The lacO array is visualized by binding of MMSET-LacR. (Right panel) The graph shows a quantification of the number of

arrays showing an H4K20me2 mark in unexposed cells (-UV) and 2hours post UV exposure (+UV). (Mean ± SEM) Co-localization was measured from 3 independent experiments, 30 cells per experiments. (e,f) The graph shows a quantification of the number of MMSET-LacR arrays showing H4K20me2 in cells transfected with the indicated siRNAs 2hours post UV exposure. (Mean ± SEM) Co-localization was measured from 3 independent experiments, 30 cells per experiments

**MMSET is recruited to chromatin by DICER**

Having established a role for MMSET in setting H4K20me2 we next wanted to determine how MMSET is recruited to chromatin, and whether it interacts with any known NER proteins. Thus, we performed an immunoprecipitation after expressing HA-tagged MMSET in cells (Figure 3A). We found that MMSET interacts robustly with DICER and ZRF1 but not with XPA, a core NER protein (Figure 3A). Reverse immunoprecipitation experiments, using FLAG-ZRF1 or FLAG-DICER in combination with HA-MMSET (Supplementary Figure 3A) recapitulated the interaction of MMSET with DICER, but not ZRF1. This suggests potentially a stronger interaction with DICER than with ZRF1. We next wanted to determine if any of these factors specifically recruits MMSET to chromatin. We tethered either DDB2-LacR, ZRF1-LacR or DICER-LacR to the LacO array while co-expressing MMSET-EGFP. DDB2 did not recruit MMSET in neither unexposed nor UV exposed cells corroborating the lack of interaction observed in the immunoprecipitation (Figures 3A and Supplementary Figure 3B). ZRF1 tethering was not sufficient to recruit MMSET to chromatin (Figure 3B). This further confirmed that the MMSET-ZRF1 interaction was potentially not as robust. In contrast, chromatin tethered DICER showed a strong recruitment of MMSET in both unexposed and exposed cells (Figures 3A and 3C). We have previously shown that ZRF1 and DICER interact strongly and that DICER is recruited to chromatin in a UV dependent manner. During DSB repair MMSET is recruited to the damage site via small RNAs generated by DICER (Wang and Goldstein, 2016). Hence, we wanted to determine whether during GG-NER the recruitment of MMSET occurred similarly via DICER catalyzed generation of small RNAs. We generated a double mutant of DICER (DICER$^{44ab}$) that was previously reported to lack the endoribonuclease activity. Tethering of DICER$^{44ab}$ to the LacO locus recruited MMSET to a similar extent as wildtype DICER (Figure 3D). Thus, the recruitment of MMSET to chromatin in the context of NER seems to be independent of the endoribonuclease function of DICER. These data suggest that DICER plays an essential role in recruiting MMSET to the DNA damage site.

Figure 3

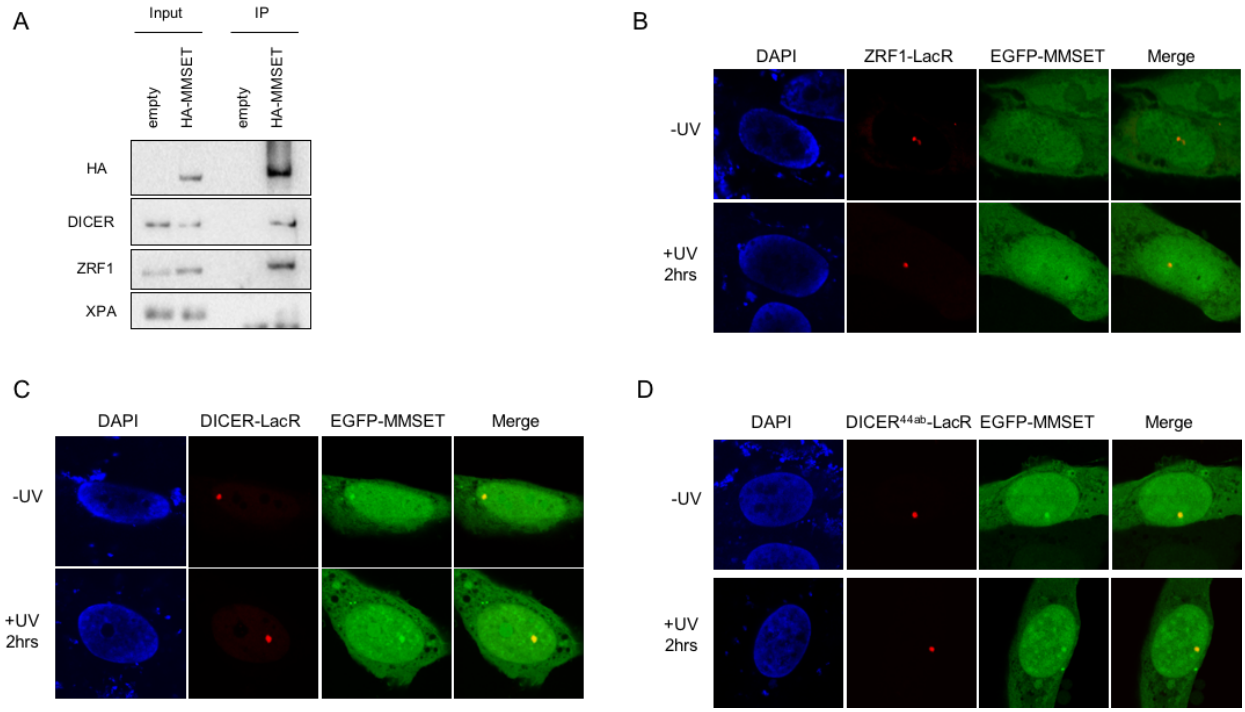


Figure 3: MMSET is recruited to chromatin by DICER: (a) MMSET interacts with ZRF1 and DICER. Western blot showing HA immunoprecipitations from cells transfected with either empty plasmid or HA-MMSET. (b) ZRF1 alone cannot recruit MMSET to chromatin. Immunofluorescence images showing distribution of EGFP-MMSET in cells with ZRF1-LacR tethered arrays, in both UV unexposed and exposed cells. (c) DICER recruits MMSET to chromatin. Immunofluorescence images showing distribution of EGFP-MMSET in cells with DICER-LacR tethered arrays, in both UV unexposed and exposed cells. (d) DICER$^{44ab}$ can also recruit MMSET to chromatin. Immunofluorescence images showing distribution of EGFP-MMSET in cells with DICER$^{44ab}$-LacR tethered arrays, in both UV unexposed and exposed cells..

**H4K20me2 provides a tethering platform for XPA recruitment**

It has previously been shown that H4K20me2 is essential to recruit 53BP1 to the damage site during DSB repair (Botuyan et al., 2006; Tuzon et al., 2014). Thus, we next addressed if H4K20me2 could provide a tethering platform for any of the downstream repair factors during NER. As expected from our previous data (Supplementary Figure 3B), we found that MMSET could not recruit DDB2 in UV exposed cells (Supplementary Figure 4A). Similarly, we did not observe any recruitment of either XPC or RING1B to an MMSET-LacR tethered array in UV exposed cells (Supplementary Figures 4B and 4C). Interestingly, we found that XPA was strongly recruited to the MMSET tethered array in UV exposed cells. In contrast, we observed

only minimal XPA recruitment in UV unexposed cells (Figure 4A). We had observed earlier that chromatin tethered MMSET predominantly sets the H4K20me2 mark only upon UV exposure (Figure 2C). This, along with our previous data showing that XPA does not directly interact with MMSET, led us to hypothesize that XPA might be recruited to chromatin by the H4K20me2 mark, rather than by MMSET itself. Additionally, we assayed the recruitment of XPF, a protein further downstream of XPA. We found a very mild recruitment of XPF compared to that of XPA in UV exposed cells (Supplementary Figure 4D), suggesting as specific recruitment of XPA by H4K20me2. We had previously observed that DICER is able to recruit MMSET to chromatin in a UV independent manner. Thus, we assessed whether DICER is also able to recruit XPA. Contrary to the UV dependent XPA recruitment by MMSET, DICER was able to recruit XPA to chromatin in both unexposed and exposed cells (Figure 4B). This fit in well with our data that DICER was also able to recruit MMSET and set the H4K20me2 mark, also in UV unexposed cells. Similarly, the DICER mutant lacking the riboendonuclease activity was also able to recruit XPA to chromatin (Supplementary Figure 4E). Next, we addressed whether MMSET or DICER are necessary for recruitment of XPA to damage sites. We assessed XPA recruitment to localized sites of UV damage in control and MMSET MRC5 knockdown cells (Figures 4C and S4F). Depletion of MMSET led to a significant reduction in XPA recruitment to the damage site (Figure 4C). Further, depletion of MMSET in 293T cells exhibited a drastic reduction of XPA levels at chromatin after UV irradiation (Figures S4E and S4F).

Our data so far pointed to a role for MMSET catalyzed setting of the H4K20me2 mark in the recruitment of XPA. To further support our findings, we next examined whether XPA or a multiprotein complex harboring XPA shows an affinity for H4K20me2. To this end we performed peptide pulldowns from nuclear extracts of 293T cells expressing GFP-XPA utilizing H4, H4K20me2 and H3K27me2 peptides (Figure 4D). We observed highly specific binding of 53BP1 to H4K20me2 in good agreement with previous studies (Botuyan et al., 2006; Tuzon et al., 2014). Importantly, we noticed a specific recruitment of XPA to H4K20me2 and to a lesser extent to H3K27me2. Taken together, our data suggests that XPA is recruited to the DNA damage site by both DICER and MMSET mediates H4K20 dimethylation.

Figure 4

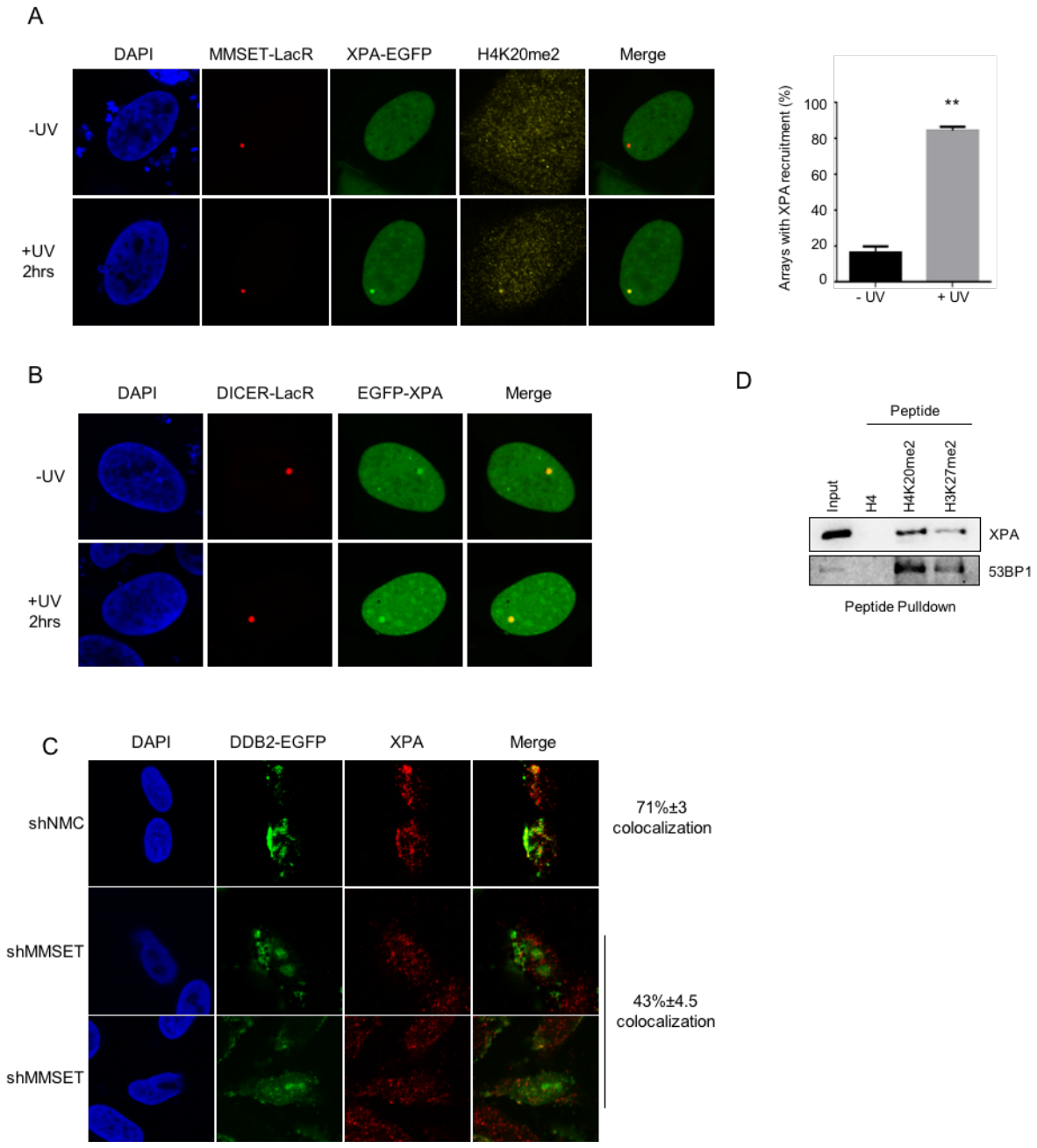


Figure 4: MMSET mediated H4K20me2 is required for recruitment of XPA: (a) MMSET mediated H4K20me2 recruits XPA to chromatin. (Left panel) Immunofluorescence images showing distribution of XPA-EGFP and H4K20me2 in cells with MMSET-LacR tethered arrays, in both UV unexposed and exposed cells. (Right panel) The graph shows a quantification of the number of arrays showing XPA-EGFP recruitment in unexposed cells (-UV) and 2hours post UV exposure (+UV). (Mean ± SEM) Co-localization was measured from 3 independent experiments, 30 cells per experiments (b) DICER can recruit XPA to chromatin. Immunofluorescence images showing distribution of XPA-EGFP in cells with DICER-LacR tethered arrays. Co-localization was observed in 20/20 cells in both -/+UV conditions. (c) MMSET is required for XPA recruitment to localized sites of DNA damage. Immunofluorescence images showing distribution of DDB2-EGFP and XPA in U2OS cells subjected to damage through a 3 μm

micropore membrane. The damage sites are marked by DDB2-EGFP. XPA recruitment was quantified in both control (shNMC) and MMSET knockdown (shMMSET) cell lines. (d) Western blots showing levels of select proteins that bind to the indicated modified peptide.

## DISCUSSION

Timed recruitment of DNA repair factors is an essential determinant of damage recognition and for the transition to downstream events of repair. Although we have learned much about how the NER machinery operates it is still largely unknown how the chromatin environment, and in particular histone marks, contribute to the different steps of NER. To gain a better understanding of the implications of histone marks during NER, we examined whether there is a global change in selected histone modifcations after UV damage. We found a striking formation of H4K20me2 foci in response to UV irradiation. H4K20me2 has previously been linked to the repair of DSBs, where it provides a binding platform for 53BP1 (Botuyan et al., 2006; Tuzon et al., 2014). Employing DDB2 knockdown cell lines we found a significant reduction in H4K20me2 foci linking the nuclear organization of this histone mark to NER.

To identify the H4K20 methylase that operates in the GG-NER subpathway we analyzed whether SETD8 and MMSET had an impact on H4K20me2 foci formation and if their knockdown affected DNA repair. Both enzymes had previously been shown to play a role during DSB repair (Lukas et al., 2011; Milite et al., 2016; Pei et al., 2011). Knockdown of MMSET nearly abolished the generation of H4K20me2 foci and evoked a significant reduction of EdU incorporation in UDS assays. In contrast, knockdown of SETD8 exhibited a relatively minor impact on DNA repair, and did not significantly alter the nuclear H4K20me2 pattern. Thus, in the context of NER, MMSET is responsible for setting of the H4K20me2 mark. By employing a LacO tethering system, we determined that MMSET exhibited a very low basal methylation activity at chromatin, and its H4K20me2 specific activity was stimulated after UV exposure. We were further able to determine that the UV dependent activity of MMSET in catalyzing the H4K20me2 mark depends both on recognition of the lesion via DDB2, and possibly by binding of DICER. This could suggest that upon UV inflicted DNA damage MMSET either associates with factors, which stimulate setting of only the H4K20me2 mark or that more substrate is made available, potentially as a consequence of chromatin rearrangements. To gain insight into potential interactors of MMSET we performed immunoprecipitations that indicated that MMSET associates with ZRF1 and DICER, but only DICER robustly recruits it to chromatin. Notably,

DICER is involved in recruiting MMSET to chromatin irrespective of its catalytic activity, which supports a novel non-catalytic role for DICER at chromatin. Interestingly, chromatin array tethered DICER recruits MMSET even in non-irradiated cells suggesting a stable interaction of DICER with MMSET in unchallenged cells. We have previously shown that ZRF1 and DICER are recruited to chromatin only in response to UV exposure. These data together suggest that DICER recruitment to chromatin might be accompanied by MMSET and that DICER triggers the modulation of MMSET activity and the setting of the H4K20me2 mark.

When assessing the function of MMSET catalyzed H4K20 dimethylation we observed a high and significant increase in XPA recruitment to the LacO array only after UV irradiation. Interestingly, in similar experiments we found that H4K20me2 is set only after exposure to UV light (Figure 2C) suggesting that the setting of H4K20me2 and recruitment of XPA coincide. Additionally, MMSET shows no interaction with XPA itself, further pointing towards an H4K20me2 dependent recruitment. These data are buttressed by a diminished recruitment of XPA to locally induced DNA damage in MMSET knockdown cells (Figure 4D). Our peptide pulldown experiments clearly indicate that XPA shown an affinity for the H4K20me2 mark. However, XPA itself does not contain any characterized methyl-binding domain. Thus, it remains to be determined how it exactly interacts with H4K20me2. It is possible that it associates with chromatin as part of a multi-protein complex capable of reading the H4K20me2 mark.

XPA is a critical factor of NER that serves in both sub-pathways, TC-NER and GG-NER. The recruitment of XPA to the DNA damage site has been discussed controversially over the last years since XPA was demonstrated to have a function during lesion recognition and in the damage verification step. Given the strong phenotypes of XPA deficient mice and the high susceptibility for cancer upon mutation of XPA alleles a molecular mechanism of XPA recruitment should be of paramount interest. We have delineated here a molecular understanding of how XPA is recruited to the DNA damage site during GG-NER (Figure 4X). It will now be interesting to find out whether XPA is recruited to the damage in the TC-NER pathway by a similar mechanism and in particular, a specific histone modification.

## REFERENCES


Bergink, S., Salomons, F.A., Hoogstraten, D., Groothuis, T.A., de Waard, H., Wu, J., Yuan, L., Citterio, E., Houtsmuller, A.B., Neefjes, J.*, et al.* (2006). DNA damage triggers nucleotide excision repair-dependent monoubiquitylation of histone H2A. Genes & development *20*, 1343-1352.

Botuyan, M.V., Lee, J., Ward, I.M., Kim, J.E., Thompson, J.R., Chen, J., and Mer, G. (2006). Structural basis for the methylation state-specific recognition of histone H4-K20 by 53BP1 and Crb2 in DNA repair. Cell *127*, 1361-1373.

de Laat, W.L., Jaspers, N.G., and Hoeijmakers, J.H. (1999). Molecular mechanism of nucleotide excision repair. Genes & development *13*, 768-785.

Dulev, S., Tkach, J., Lin, S., and Batada, N.N. (2014). SET8 methyltransferase activity during the DNA double-strand break response is required for recruitment of 53BP1. EMBO reports *15*, 1163-1174.

Enokido, Y., Inamura, N., Araki, T., Satoh, T., Nakane, H., Yoshino, M., Nakatsu, Y., Tanaka, K., and Hatanaka, H. (1997). Loss of the xeroderma pigmentosum group A gene (XPA) enhances apoptosis of cultured cerebellar neurons induced by UV but not by low-K+ medium. Journal of neurochemistry *69*, 246-251.

Feltes, B.C., and Bonatto, D. (2015). Overview of xeroderma pigmentosum proteins architecture, mutations and post-translational modifications. Mutat Res Rev Mutat Res *763*, 306-320.

Fischer, J.M., Popp, O., Gebhard, D., Veith, S., Fischbach, A., Beneke, S., Leitenstorfer, A., Bergemann, J., Scheffner, M., Ferrando-May, E.*, et al.* (2014). Poly(ADP-ribose)-mediated interplay of XPA and PARP1 leads to reciprocal regulation of protein function. FEBS J *281*, 3625-3641.

Fousteri, M., and Mullenders, L.H. (2008). Transcription-coupled nucleotide excision repair in mammalian cells: molecular mechanisms and biological effects. Cell research *18*, 73-84.

Fradet-Turcotte, A., Canny, M.D., Escribano-Diaz, C., Orthwein, A., Leung, C.C., Huang, H., Landry, M.C., Kitevski-LeBlanc, J., Noordermeer, S.M., Sicheri, F.*, et al.* (2013). 53BP1 is a reader of the DNA-damage-induced H2A Lys 15 ubiquitin mark. Nature *499*, 50-54.

Gracheva, E., Chitale, S., Wilhelm, T., Rapp, A., Byrne, J., Stadler, J., Medina, R., Cardoso, M.C., and Richly, H. (2016). ZRF1 mediates remodeling of E3 ligases at DNA lesion sites during nucleotide excision repair. The Journal of cell biology *213*, 185-200.

Guerrero-Santoro, J., Kapetanaki, M.G., Hsieh, C.L., Gorbachinsky, I., Levine, A.S., and Rapic-Otrin, V. (2008). The cullin 4B-based UV-damaged DNA-binding protein ligase binds to UV-damaged chromatin and ubiquitinates histone H2A. Cancer Res *68*, 5014-5022.

Holoch, D., and Moazed, D. (2015). Small-RNA loading licenses Argonaute for assembly into a transcriptional silencing complex. Nature structural & molecular biology *22*, 328-335.

Janicki, S.M., Tsukamoto, T., Salghetti, S.E., Tansey, W.P., Sachidanandam, R., Prasanth, K.V., Ried, T., Shav-Tal, Y., Bertrand, E., Singer, R.H.*, et al.* (2004). From silencing to gene expression: real-time analysis in single cells. Cell *116*, 683-698.

Kapetanaki, M.G., Guerrero-Santoro, J., Bisi, D.C., Hsieh, C.L., Rapic-Otrin, V., and Levine, A.S. (2006). The DDB1-CUL4ADDB2 ubiquitin ligase is deficient in xeroderma pigmentosum group E and targets histone H2A at UV-damaged DNA sites. Proceedings of the National Academy of Sciences of the United States of America *103*, 2588-2593.

Kim, J.K., Patel, D., and Choi, B.S. (1995). Contrasting structural impacts induced by cis-syn cyclobutane dimer and (6-4) adduct in DNA duplex decamers: implication in mutagenesis and repair activity. Photochem Photobiol *62*, 44-50.

King, B.S., Cooper, K.L., Liu, K.J., and Hudson, L.G. (2012). Poly(ADP-ribose) contributes to an association between poly(ADP-ribose) polymerase-1 and xeroderma pigmentosum complementation group A in nucleotide excision repair. The Journal of biological chemistry *287*, 39824-39833.

Kohji, T., Hayashi, M., Shioda, K., Minagawa, M., Morimatsu, Y., Tamagawa, K., and Oda, M. (1998). Cerebellar neurodegeneration in human hereditary DNA repair disorders. Neurosci Lett *243*, 133-136.

Kraemer, K.H. (1994). Nucleotide excision repair genes involved in xeroderma pigmentosum. Jpn J Cancer Res *85*, inside front cover.

Lu, X., Simon, M.D., Chodaparambil, J.V., Hansen, J.C., Shokat, K.M., and Luger, K. (2008). The effect of H3K79 dimethylation and H4K20 trimethylation on nucleosome and chromatin structure. Nature structural & molecular biology *15*, 1122-1124.

Lukas, J., Lukas, C., and Bartek, J. (2011). More than just a focus: The chromatin response to DNA damage and its role in genome integrity maintenance. Nat Cell Biol *13*, 1161-1169.

Marteijn, J.A., Bekker-Jensen, S., Mailand, N., Lans, H., Schwertman, P., Gourdin, A.M., Dantuma, N.P., Lukas, J., and Vermeulen, W. (2009). Nucleotide excision repair-induced H2A

ubiquitination is dependent on MDC1 and RNF8 and reveals a universal DNA damage response. Journal of Cell Biology *186*, 835-847.

Marteijn, J.A., Lans, H., Vermeulen, W., and Hoeijmakers, J.H. (2014). Understanding nucleotide excision repair and its roles in cancer and ageing. Nature reviews Molecular cell biology *15*, 465-481.

Milite, C., Feoli, A., Viviano, M., Rescigno, D., Cianciulli, A., Balzano, A.L., Mai, A., Castellano, S., and Sbardella, G. (2016). The emerging role of lysine methyltransferase SETD8 in human diseases. Clin Epigenetics *8*, 102.

Panier, S., and Boulton, S.J. (2014). Double-strand break repair: 53BP1 comes into focus. Nature reviews Molecular cell biology *15*, 7-18.

Pei, H., Zhang, L., Luo, K., Qin, Y., Chesi, M., Fei, F., Bergsagel, P.L., Wang, L., You, Z., and Lou, Z. (2011). MMSET regulates histone H4K20 methylation and 53BP1 accumulation at DNA damage sites. Nature *470*, 124-128.

Schotta, G., Lachner, M., Sarma, K., Ebert, A., Sengupta, R., Reuter, G., Reinberg, D., and Jenuwein, T. (2004). A silencing pathway to induce H3-K9 and H4-K20 trimethylation at constitutive heterochromatin. Genes & development *18*, 1251-1262.

Schotta, G., Sengupta, R., Kubicek, S., Malin, S., Kauer, M., Callen, E., Celeste, A., Pagani, M., Opravil, S., De La Rosa-Velazquez, I.A.*, et al.* (2008). A chromatin-wide transition to H4K20 monomethylation impairs genome integrity and programmed DNA rearrangements in the mouse. Genes & development *22*, 2048-2061.

Sugitani, N., Sivley, R.M., Perry, K.E., Capra, J.A., and Chazin, W.J. (2016). XPA: A key scaffold for human nucleotide excision repair. DNA Repair (Amst) *44*, 123-135.

Tuzon, C.T., Spektor, T., Kong, X., Congdon, L.M., Wu, S., Schotta, G., Yokomori, K., and Rice, J.C. (2014). Concerted activities of distinct H4K20 methyltransferases at DNA double-strand breaks regulate 53BP1 nucleation and NHEJ-directed repair. Cell reports *8*, 430-438.

Wang, Q., and Goldstein, M. (2016). Small RNAs Recruit Chromatin-Modifying Enzymes MMSET and Tip60 to Reconfigure Damaged DNA upon Double-Strand Break and Facilitate Repair. Cancer Res *76*, 1904-1915.

Wilson, R.C., and Doudna, J.A. (2013). Molecular mechanisms of RNA interference. Annu Rev Biophys *42*, 217-239.

Yang, Z., Roginskaya, M., Colis, L.C., Basu, A.K., Shell, S.M., Liu, Y., Musich, P.R., Harris, C.M., Harris, T.M., and Zou, Y. (2006). Specific and efficient binding of xeroderma

pigmentosum complementation group A to double-strand/single-strand DNA junctions with 3'- and/or 5'-ssDNA branches. Biochemistry *45*, 15921-15930.

Zimmermann, M., and de Lange, T. (2014). 53BP1: pro choice in DNA repair. Trends Cell Biol *24*, 108-117.

## Supplementary Figures:

Supplementary Figure 1

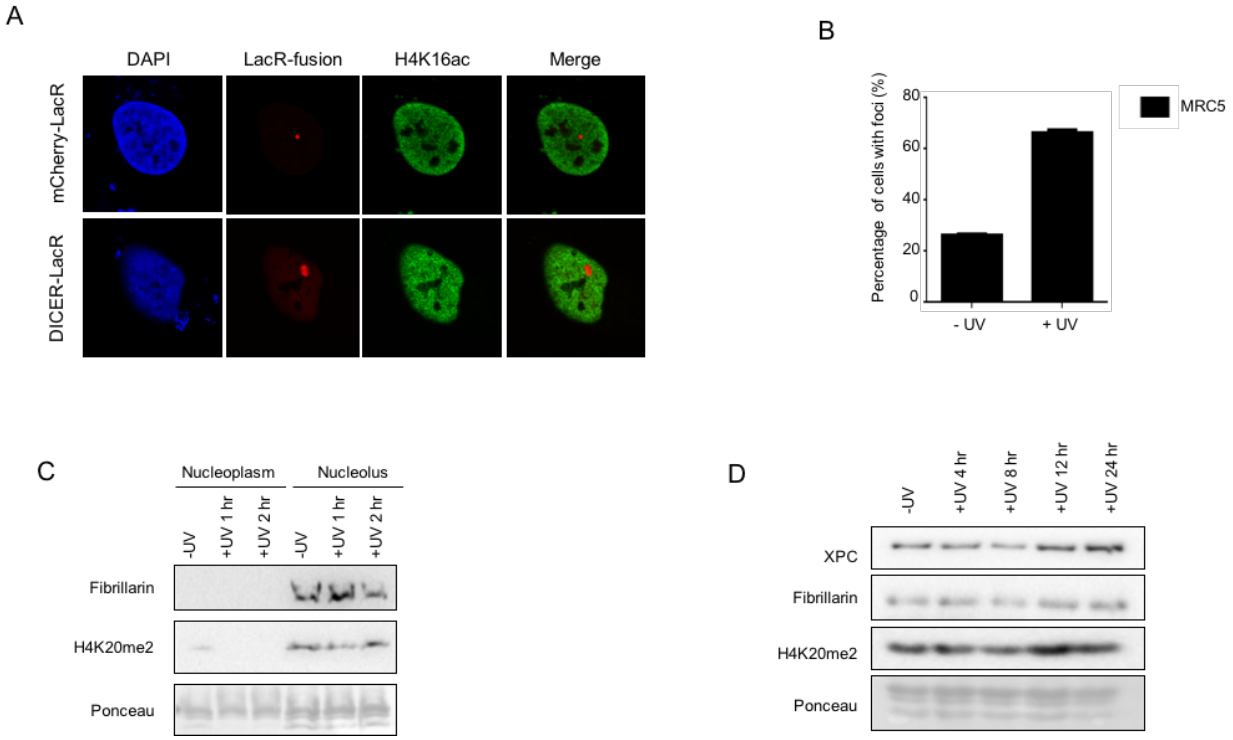


Supplementary Figure 1: UV exposure causes formation of H4K20me2 foci. (a) DICER tethering does not change the H4K16ac patter. Immunfluorescence images showing nuclear distribution of H4K16ac in control (mCherry-LacR) and DICER-LacR tethered cells. (b) Formation of H4K20me2 foci occurs in diverse select cell types. The graph shows the percentage of cells showing nucleolar foci of H4K20me2 in unexposed cells (-UV) and 2 hours after UV exposure (+UV) in MRC5 fibroblasts. (Mean ± SEM). Cells were counted from 3 independent experiments, with 200 cells counted per experiment. (c) UV exposure causes redistribution of H4K20me2. Western blot showing the distribution of H4K20me2 in the nucleoplasmic and nucleolar fraction at the indicated time points post UV exposure. Fibrillarin (a nucleolar protein) is used as a marker to show the purity of the fractions. (d)There is no global increase f H4K20me2 levels post UV damage. Western blots showing levels of the indicated proteins in whole cell extracts at various time points post UV exposure. FIbrillarin is used as a loading control.

Supplementary Figure 2

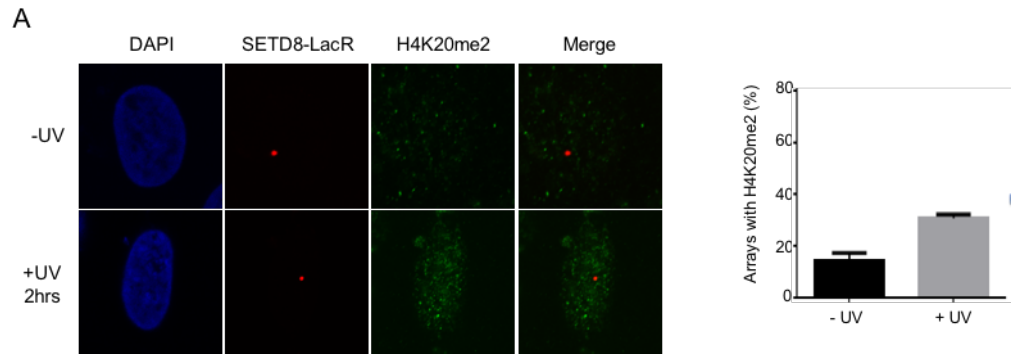


Supplementary Figure 2: SETD8 does not set a prominent H4K20me2 mark post UV exposure. (a) (Left panel) Immunofluorescence images showing H4K20me2 distribution in U2OS 2-6-3 cells, expressing mCherry-LacR-SETD8 (SETD8-LacR). The lacO array is visualized by binding of SETD8-LacR. (Right panel) The graph shows a quantification of the number of arrays showing an H4K20me2 mark in unexposed cells (-UV) and 2hours post UV exposure (+UV). Co-localization was measured from 3 independent experiments, counting 30 cells per experiment.

Supplementary Figure 3

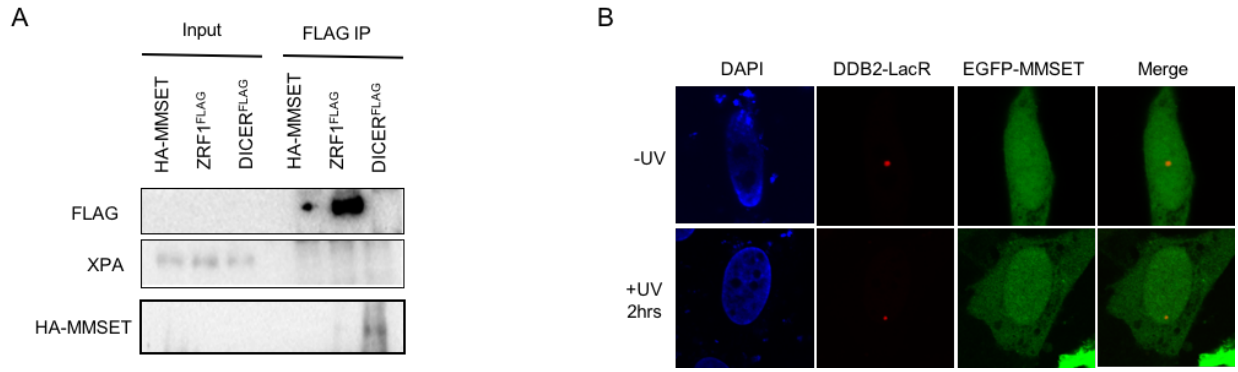


Supplementary Figure 3: MMSET interacts with DICER. (a) Western blot showing the levels of the indicated proteins in FLAG purifications performed in cells transfected with either only HA-MMSET, or HA-MMSET along with either ZRF1-FLAG or DICER-FLAG. (b) Immunofluorescence images showing distribution of MMSET-EGFP in cells with DDB2-LacR tethered arrays, in UV unexposed and exposed cells. No recruitment was seen in 20/20 cells.

Supplementary Figure 4

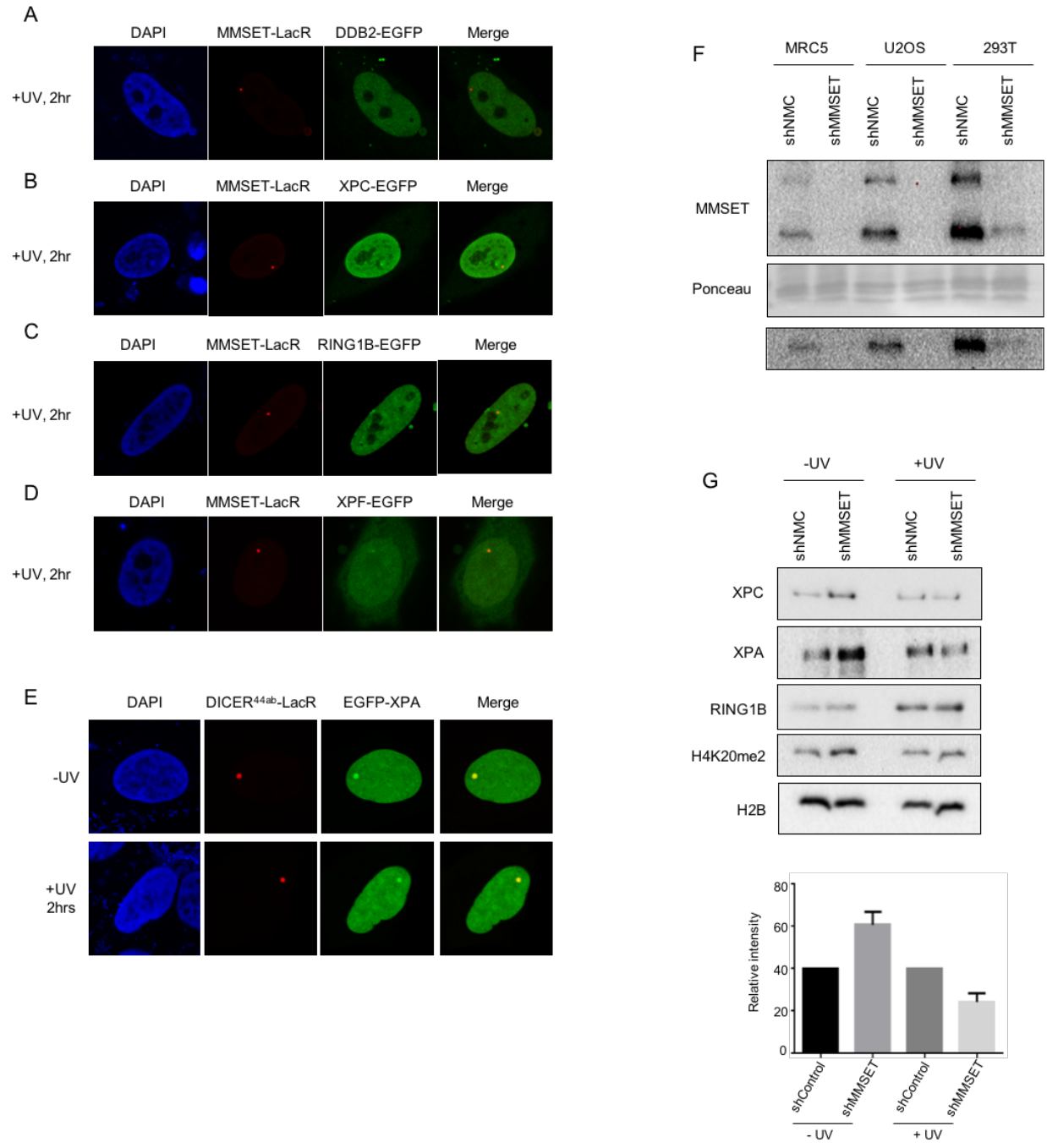


Supplementary Figure 4: MMSET-LacR recruits late NER factors to chromatin. (a) DDB2 is not recruited to MMSET-LacR tethered arrays. Immunofluorescence images showing distribution of DDB2-EGFP in cells with MMSET-LacR tethered arrays, in UV une exposed cells. No recruitment was seen in 20/20 cells. (b) XPC is not recruited to MMSET-LacR tethered arrays. Immunofluorescence images showing distribution of XPC-EGFP in cells with MMSET-LacR tethered arrays, in UV exposed cells. No recruitment was seen in 20/20 cells. (c) RING1B is not recruited to MMSET-LacR tethered arrays. Immunofluorescence images showing distribution of RING1B-EGFP in cells with MMSET-LacR tethered

arrays, in UV exposed cells. No recruitment was seen in 20/20 cells. (d) XPF is weakly recruited to MMSET-LacR tethered arrays. Immunofluorescence images showing distribution of XPF-EGFP in cells with MMSET-LacR tethered arrays, in UV exposed cells. Recruitment was seen in 15/20 cells. (e) Immunofluorescence images showing distribution of EGFP-MMSET in cells with $DICER^{44ab}$-LacR tethered arrays in UV exposed and uexposed conditions. Colocalization was seen in 20/20 cells in both conditions (f). Western blot showing the levels of MMSET in shMMSET knockdown cell lines, created in various backgrounds. (g) (LToppanel) Western blot showing chromatin association experiment in unexposed cells (-UV) and cells after 2 hours UV exposure (+UV), in the indicated knockdown cell lines. (Bottom panel) Quantification of the relative intensity of XPA in the indicated conditions. H2B was used as a loading control. (Mean± SEM, n=3)

# Discussion:

The aim of this thesis was to further elucidate mechanisms of NER regulation and recognition in the context of chromatin. I have identified novel players in the NER pathway, that regulate the chromatin accessibility of DNA to regulate NER, as well a novel mechanism for compartmentalization of NER. Based on our data, I propose a model for the various steps taking place during NER recognition.

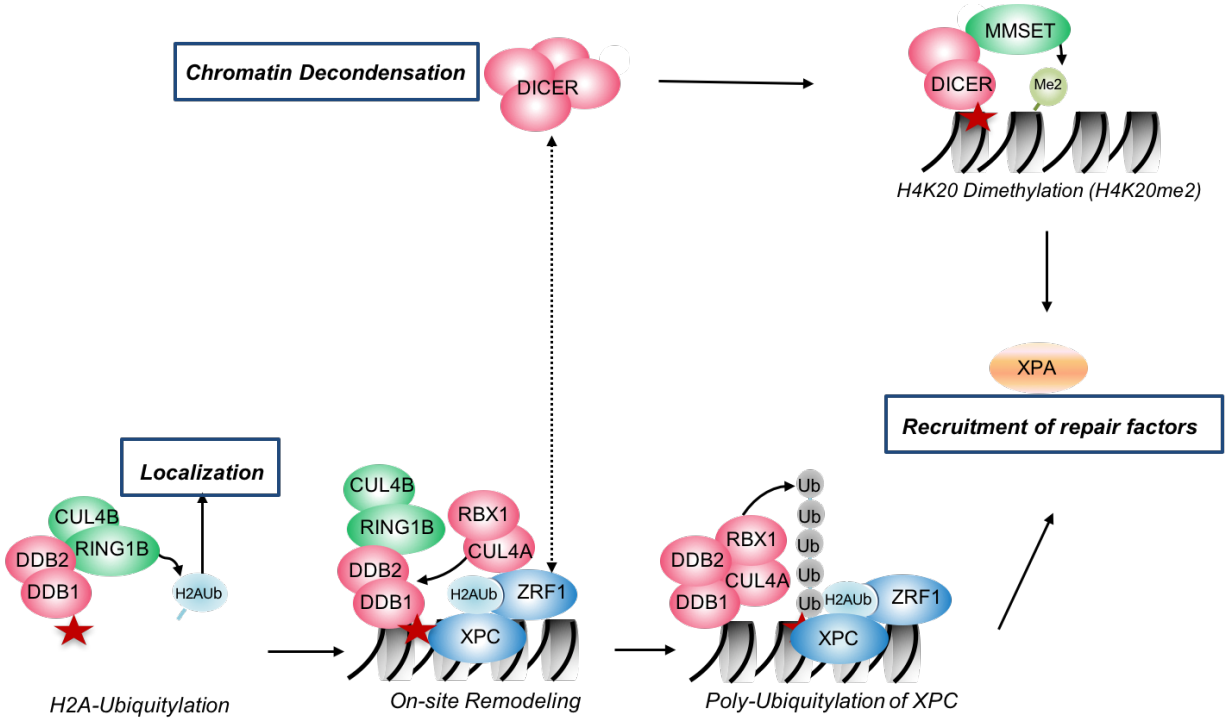


Figure 1: A model for the steps involved in lesion recognition during NER.

Lesion recognition by DDB2 is followed by formation of the UV-RING1B complex, consisting of DDB2-DDB1-CUL4B-RING1B. This complex marks the chromatin at the lesion site with the H2A-K119 ub (H2Aub) mark. This histone mark then acts as a signal for ZRF1 mediated relocation of the damaged chromatin to the nucleolus. ZRF1 is constitutively present in the nucleolus, and can bind to the H2AK119 mark in an XPC dependent manner. Thus, it acts as a nucleolar anchor for positioning of the damaged DNA. Binding of ZRF1 to the H2AK119 mark is followed by displacement of RING1B from chromatin. The UV-RING1B complex is then transformed to the UV-CUL4A (DDB2-DDB1-CUL4A-RBX1) complex, by switching of the

Cullin-E3 ligase module. The UV-CUL4A complex can then initiate further ubiquitination of DDB2, XPC and other repair proteins to facilitate repair. Translocation of the damaged DNA to the nucleolus is then followed by repair of the lesion at the nucleolus, followed by translocation of the repaired DNA out of the nucleolus. In addition to serving as a molecular chaperone to remodel the E3 ligase complexes, and serving as an anchor for positioning the damaged chromatin, ZRF1 also enables relaxation of chromatin structure. ZRF1, recruits the endoribonuclease DICER to chromatin. DICER is important for decondensation of chromatin, which enables better access of the repair machinery to the damaged DNA. DICER mediates chromatin relaxation through a PARP1 dependent mechanism, and does not require endoribonuclease activity to mediate the process. DICER in turn also recruits the histone lysine methylase MMSET to damaged chromatin. MMSET forms a complex with DICER and specifically sets the H4K20me2 mark at damaged chromatin. This mark serves as a platform for recruitment of XPA. XPA is essential for damage verification, and subsequent initiation of repair. This complex mechanism opens up several new avenues of research in the field of NER, as well as raises general questions about mechanisms of chromatin organization and regulation. The main interesting points brought up are:

1. Ubiquitin signaling as a mechanism for regulation of cellular processes, specifically DNA damage repair cascades.
2. Compartmentalization of cellular processes: how is NER compartmentalized? How universal are methods of chromatin compartmentalization used in NER?
3. Chromatin accessibility during NER: Novel players regulating chromatin accessibility and their implication in maintenance of cellular chromatin conformation
4. Signaling through histone modifications: How does crosstalk between various histone modifications occur? Can histone modification serve as signals to bridge different cellular processes.
5.

In the following sections, I will specifically discuss these questions and try to tie in our findings with what is previously known in the field, as well discuss the implications on processes other than NER.

**Ubiquitin signaling in the NER pathway.**

Cell Cycle. 2017 Jan 17, VOL. 16, NO. 2, 163–171 http://dx.doi.org/10.1080/15384101.2016.1261227

PERSPECTIVE

# Timing of DNA lesion recognition: Ubiquitin signaling in the NER pathway

Shalaka Chitale [a,b] and Holger Richly [a] [a]Laboratory of Molecular Epigenetics, Institute of Molecular Biology (IMB), Mainz, Germany; [b]Faculty of Biology, Johannes Gutenberg University, Mainz,



Germany

ABSTRACT

Damaged DNA is repaired by specialized repair factors that are recruited in a well-orchestrated manner to the damage site. The DNA damage response at UV inflicted DNA lesions is accompanied by posttranslational modifications of DNA repair factors and the chromatin environment sourrounding the lesion. In particular, mono- and poly-ubiquitylation events are an integral part of the DNA damage signaling. Whereas ubiquitin signaling at DNA doublestrand breaks has been subject to intensive studies comparatively little is known about the intricacies of ubiquitylation events occurring during nucleotide excision repair (NER), the major pathway to remove bulky helix lesions. Both, the global genomic (GG-NER) and the transcription-coupled (TC-NER) branches of NER are subject to ubiquitylation and deubiquitylation processes.Here we summarize our current knowledge of the ubiquitylation network that drives DNA repair in the NER pathway and we discuss the crosstalk of ubiquitin signaling with other prominent post-translational modfications that might be essential to time the DNA damage recognition step.

## Ubiquitin: An essential cellular signal transmitter

Ubiquitin is a small regulatory protein that is expressed in almost all tissues of eukaryotic organisms. Ubiquitylation, the attachment of ubiquitin residues to a substrate protein, can affect the fate and the function of the substrate in various ways. It triggers their degradation via the proteasome, it may alter their cellular localization, affect their enzymatic activity, and facilitate or prevent protein interactions.[1-3] Ubiquitylation is catalyzed by a set of specific enzymes, ubiquitin-activating enzymes (E1), ubiquitin-conjugating enzymes (E2), and ubiqui- tin-ligase enzymes (E3) (Fig. 1). In conjunction these enzymes generate an isopeptide bond between the c-terminus of ubiqui- tin and either a lysine or the n-terminal Methionine of the sub- strate, leading to its mono-ubiquitylation. Mono-ubiquitylation for instance occurs at a specific lysine residue, such

as Lys164 in PCNA, a key factor in DNA replication.[4] Considerable mono-ubiquitylation exists at histone H2A throughout the cell cycle. About 5 to 10 percent of histone H2A proteins are modi- fied[5] and deposition of the mono-ubiquitin mark was demon- strated to play a role in pluripotency of embryonic stem cells and during cell fate decisions,[6] during the DNA damage response at DSBs[7] and in NER.[8,9] Substrate-attached ubiquitin harbors 7 lysine residues, which may also be modified with polymeric chains. In particular homogenous ubiquitin chains where the same lysine residue is modified during chain exten- sion induce distinct outcomes in the cell.[10] Both, homogenous Lysine48- (K48) and Lysine63- (K63) linked poly-ubiquitin chains, and mono-ubiquitylation of histone H2A provide important signals in the DNA damage response in NER and other DNA repair pathways. Although many E3 ubiquitin ligases have been identified it is less clear how they functionally interact and crosstalk to each other and how the respective E3- catalyzed ubiquitin signals regulate the DNA damage response (DDR). In this review we discuss recent discoveries in ubiquitin signaling during NER and how ubiquitylation events time the transition from recognition to verification of UV-light inflicted DNA damage.

## The enzymatic machinery of nucleotide excision repair

Exposure of DNA to UV light results in the generation of pyrimidine crosslinks namely cyclobutane pyrimidine dimers (CPDs) and 6–4 photoproducts (6–4PPs). Such bulky, helix dis- torting DNA lesions are removed by nucleotide excision repair (NER), one of the major cellular DNA repair pathways.[11,12] Mammalian NER comprises of two sub-branches that differ in the way of DNA lesion recognition. Transcription-coupled NER (TC-NER) is limited to lesions located in the transcribed strand during the expression of genes. Stalled RNA Polymerase II elicits the DNA damage response by recruiting several specific DNA repair factors including the Cockayne syndrome proteins A and B (CSA and CSB).[13,14] In contrast, in global genome NER (GG- NER) DNA lesions are recognized by two lesion recognition fac- tors, XPC and DDB2 (XPE). XPC, the main damage recognition factor, scans the DNA for helix distortions[15,16] and operates as a trimeric complex with the Rad23 homologues RAD23A or RAD23B, respectively, and centrin2.[17,18] This trimeric complex



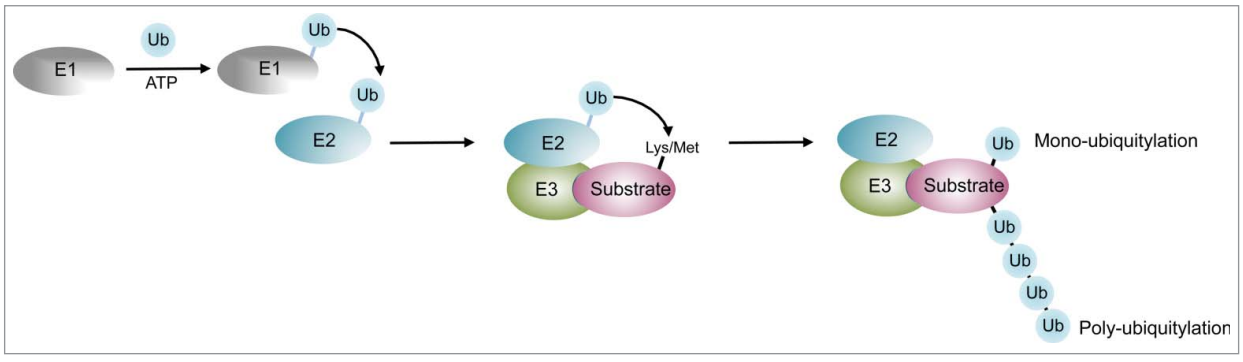

Figure 1. The cellular ubiquitylation system. Ubiquitin is activated by an ATP consuming Ubiquitin acitvating enzyme (E1), and transferred from E1 to the active site cyste- ine of the Ubiquitin-conjugating enzyme (E2). E3 enzymes are capable of interacting with both E2 and the substrate and catalyze the transfer of the ubiquitin moeity to a lysine or the n-terminal Methionine of the substrate. Repeated cycles of the ubiquitylation cascade lead to poly-ubiquitylation, where any of the lysines of ubiquitin may be utilized as attachment site.

recognizes a variety of lesions and induces NER activity.[19-21] Notably, RAD23B, which constitutes an adaptor protein that binds ubiquitylated proteins and the proteasome,[22,23] enhances the binding of XPC to the damage site but dissociates from XPC upon binding to damaged DNA.[21] The stable maintenance of XPC at damaged chromatin is probably mediated by its poly- ubiquitylation as discussed in detail below. Despite its general function as a reader of helix distortions XPC lacks specificity for CPDs, which is compensated by DDB2, an essential factor for the detection of UV light inflicted DNA lesions.[24-26] The current model for damage recognition of UV-light inflicted lesions considers DDB2 as the first reader of the damage, which hands the damage over to XPC to trigger the repair process. After damage recognition both sub-pathways converge into a common dam- age verification step. This step is performed by the repair factor XPA and by the generation of the pre-excision complex, which involves the DNA unwinding function of TFIIH via its helicase subunits XPB and XPD.[12] Finally, the DNA lesion is cut out by a dual DNA incision, which is generated by the two endonu- cleases XPF and XPG. Subsequently the gap is filled by DNA polymerases.[13,27]

The damage recognition steps of these above outlined repair mechanism are accompanied by a ubiquitylation cascade that is presumably initiated by mono-ubiquitylation of histone H2A

## Ubiquitylation events in GG-NER: Mono-ubiquitylation for starters

A distinctive histone modification at DNA damage sites is mono-ubiquitylation of histones H2A, H2AX and H1.[7,28,29] The role of mono-ubiquitylation of histone H2A has been stud- ied intensively in DSB repair. Ubiquitin-mediated signaling at DSBs commences with MDC1-dependent recruitment of the E3 ligase RNF8, which subsequently brings about the mono- ubiquitylation of histone H1.[30] Mono-ubiquitylated histone H1 in turn facilitates the recruitment of RNF168, which in con- junction with RNF8, causes the mono- and poly-ubiquitylation of histones H2A and H2AX at lysines 13–15.[28,29,31-33] These poly-ubiquitylated histones provoke the recruitment of effector proteins that promote DSB repair. Parallel to this pathway the E3 ligase RING1B causes mono-ubiquitylation of histone H2A at lysine 119,[33-36] which presumably condenses chromatin

regions sourrounding the damage site.[37] During GG-NER vari- ous E3 ligases catalyze ubiquitylation of histone H2A. In con- trast to repair at DSBs their sequence of action is less well understood. H2A-ubiquitylation during GG-NER is catalyzed by the E3 ligase

RNF8, the UV-DDB-CUL4A/B complexes and the UV-RING1B complex.[8,38-41] DDB2 forms a multiprotein complex consisting of DDB1, the E3 ligase RBX1 and either of the scaffold proteins CUL4A or CUL4B (UV-DDB-CUL4A/B), that catalyzes the mono-ubiquitylation of histones H3, H4 and H2A.[40,42-45] The UV-DDB2-CUL4A E3 ligase acts downstream of the UV-RING1B complex, which consists of the subunits DDB1, DDB2, CUL4B and the E3 ligase RING1B. The UV- RING1B complex specifically modifies lysine 119 of histone H2A, which is bound by the H2AK119-ubiquitin binding pro- tein ZRF1 (Fig. 2). ZRF1 was originally identified as a factor that promotes cellular differentiation[46-48] and only recently it was demonstrated that it facilitates the exchange of the cullin and E3 ligase proteins from E3 multiprotein complexes.[41,49] At the damage site it removes the CUL4B-RBX1 module from the DDB2-DDB1 dimer and facilitates the incorporation of CUL4A-RBX1 thus converting the UV-RING1B complex into the UV-DDB CUL4A complex (Fig. 2). In contrast, it is not known which lysine in H2A is targeted by the UV-DDB- CUL4A complex. It seems reasonable that it ubiquitylates either a specific lysine other than K119 or that it operates less specific targeting different lysine residues. In agreement with the latter, the UV-DDB-CUL4B complex, which differs from the afore- mentioned complex only in its cullin subunit, seems to have a relatively broad substrate specificity potentially promoting ubiquity-lation at multiple lysine residues.[50] Mono-ubiquityla- tion at histone H2A is additionally catalyzed by the RING-con- taining E3 ligase RNF8 at later stages of NER causing a continuous H2A-ubiquitylation.[51] However, it seems that RNF8 does not directly affect the NER process but rather links it with the DSB-induced DNA damage response. It is currently not known which lysine is targeted by RNF8, but given its importance in recruiting DSB repair factors like 53BP1 and BRCA1[51] one might speculate that RNF8-mediated H2A-ubiq-uitylation might occur at lysines 13–15. Which information does mono-ubiquitylation of histone H2A at different lysines encode? Although speculative, it seems possible that the ubiqui- tin mark at the C-terminus of histone H2A (Lys119) might

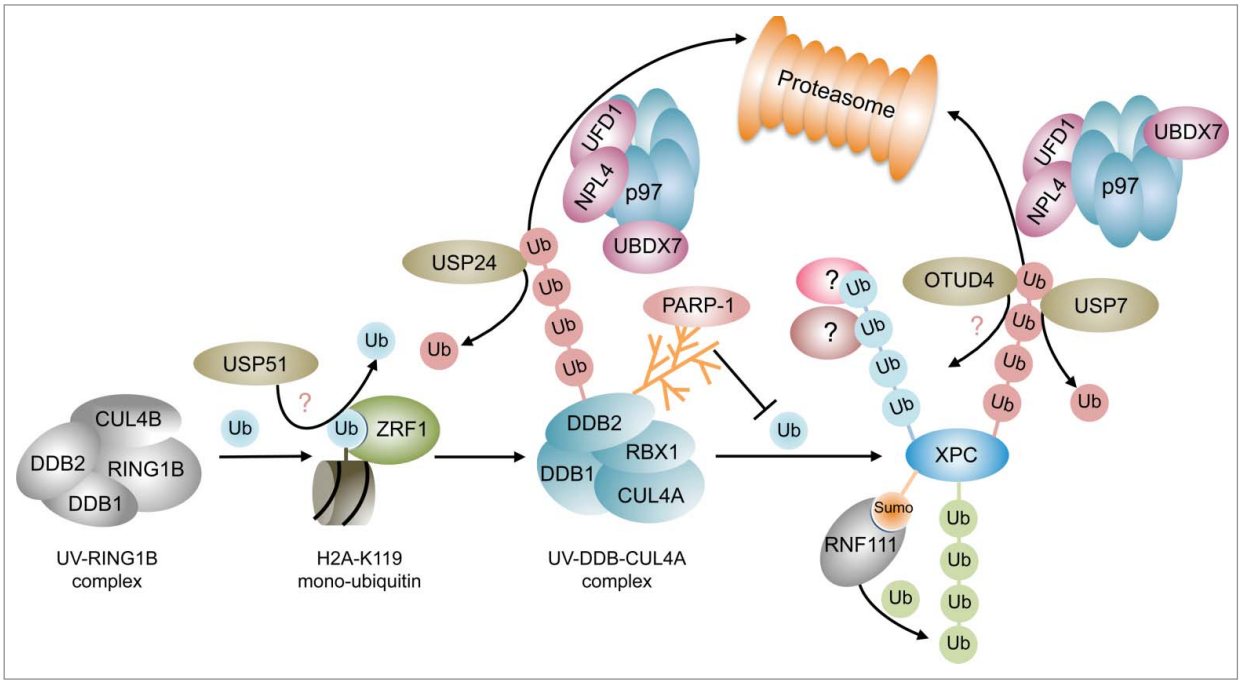


Figure 2. Ubiquitin signaling during lesion recognition in the GG-NER pathway. The ubiquitylation cascade during GG-NER is initiated the UV-RING1B E3 ligase complex that sets the H2A-ubiquitin mark specifically at lysine 119. At DSBs H2A-ubiquitin at lysines 13–15 is removed by USP51. ZRF1 reads the mono-ubiquitin mark and causes the assembly of the UV-DDB-CUL4A complex. This complex or its subunit DDB2 undergoes K48 linked self-ubiquitylation, which leads to its segregation by the p97 complex and its subsequent proteasomal degradation. Ubiquitylation of XPC by the UV-DDB-CUL4A ligase causes a poly-ubiquitylation of XPC, which is inhibited by parylation of DDB2. The linkage type and potential interactors of this ubiquitin chain are not known. XPC may be regarded a control center of damage recognition where many ubiq- uitin signals concur. XPC, like DDB2, is extracted from chromatin upon poly-ubiquitylation and also decorated by a K63-linked ubiquitin chain catalyzed by the SUMO-dependent E3 ligase RNF111. Poly-ubiquitin chains at XPC are edited by USP7 and potentially by OTUD4. Green spheres depict K63-linked ubiquitylation, red spheres depict K48-linked ubiquitylation. Blue spehres indicate mono-ubiquitylation or poly-ubiquitylation of unknown linkage.

confer a different topology than ubiquitylation at the flexible N- terminal histone tails (Lys13–15) and hence lead to the recruit- ment of different downstream acting factors. Ubiquitylation at K119 and subsequent recruitment of ZRF1 causes a remodel- ling of multiprotein complexes[41,49] whereas it has been sug- gested that mono-ubiquitylation of histones by the UV-DDB- CUL4A complex facilitates the decondensation of chromatin thereby promoting access of the NER repair machinery to dam- aged DNA.[52] Hence, ubiquitylation at different lysine residues might have different outcomes either promoting remodelling of chromatin or chromatin-associated protein complexes. Taken together these two remodelling events might contribute to the DDR by orchestrating the well-timed recruitment of DNA repair factors in a decondensed chromatin environment. Interestingly, the UV-DDB-CUL4A complex not only carries out mono-ubiquitylation events but it is well established that it cat- alyzes the poly-ubiquitylation of DNA repair factors. Hence, by remodelling the E3 ligase complexes at the damage site ZRF1 occupies a central role in the GG-NER pathway switching the signal transmission from mono- to

poly-ubiquitylation.

## Signal transmission through poly-ubiquitylation of DNA repair proteins

In analogy to DSB repair poly-ubiquitylation events are an inte- gral part of the ubiquitin signaling cascade during NER.[7] The UV-DDB-CUL4A complex poly-ubiquitylates XPC thereby increasing its binding affinity for DNA in vitro and in vivo and

it thus confers a stable binding of XPC to photolesions.[41,53,54] Hence, the linkage of this ubiquitin chain should be distinct from the K48-linkage, which is essential for proteasomal degradation (Fig. 2). Still, the UV-DDB-CUL4A complex is competent in assembling K48-linked ubiquitin chains as it gen- erates a self-ubiquitylation of its subunit DDB2 promoting its proteasomal degradation[53,55] (Fig. 2). Interestingly, this E3 ligase complex catalyzes mono-ubiquitylation of histone H2A and poly-ubiquitylation of different linkage types. This varia- tion in linkage-specificity of RING-domain E3 ligases is pre- sumably defined by employing different E2 enzymes during the ubiquitylation reactions.[10] Additionally, XPC is modified by K63-linked poly-ubiquitylation via the SUMO-targeted E3 ligase (STUbL) RNF111/Arkadia[56,57] (Fig. 2). XPC sumoylation at lysine 8 via RNF111 is a prerequisite for K63-linked ubiqui- tylation of XPC and the timely removal of DDB2 and XPC from damaged DNA.[56-58] In disagreement with these findings, an earlier study reported that upon UV-irradiation XPC was modified by SUMO-1 in a DDB2 and XPA dependent manner and that this sumoylation led to its stabilization.[59] Hence, it might be possible that sumoylation of XPC occurs at different lysines or, depending on the respective chromatin context, leads to the recruitment of different STUbLs, which either pro- mote retention or removal of XPC. Besides its sumoylation and K63-linked ubiquitylation XPC is subject to proteasomal degra- dation. Poly-ubiquitylated XPC and DDB2 are extracted from damaged chromatin by p97 in complex with its co-factors UFD1-NPL4 and UBDX7[60] (Fig. 2) indicating that XPC is also



decorated by a K48 ubiquitin chain. Depletion of p97 was shown to cause retention of XPC and DDB2, which eventually leads to genotoxicity[60] underlining the importance of the timely removal of damage recognition factors to proceed with the veri- fication and incision reactions. It is still not known which E3 ligase or which pair of E2 and E3 enzymes catalyzes K48-linked ubiquitylation to facilitate p97-mediated segregation of XPC and which lysine residues in XPC are ubiquitylated. Further, it is not resolved whether p97-mediated XPC extraction is linked to the RNF111 mediated removal of XPC[56] or whether both processes are part of independent signaling pathways.

The ubiquitin chains that are covalently linked to XPC and other DNA repair factors are additionally edited by deubiquity- lases which further increases the complexity of the

ubiquitin dependent DNA repair regulation network.

## Regulation of poly-ubiquitylation by parylation and deubiquitylation

It has been demonstrated that DDB2 and XPC are targeted by poly(ADP-ribose) polymerase-1 (PARP-1). The activity of PARP-1 is triggered by DNA damage utilizing $NAD^C$ to gener- ate ADP-ribose polymers to modify various proteins involved in recombination and DNA repair events.[61,62] PARP-1 modifies DDB2 and it stimulates recruitment of XPC by DDB2 thus ensuring the efficiency of NER[62] (Fig. 2). Parylation of DDB2 inhibits ubiquitylation and subsequent proteasomal degradation of DDB2 and hence provides a means of stabilizing DDB2 at the damage site allowing it more time to facilitate chromatin remod- eling[63] as for example by recruitment of ALC1.[64] It was further demonstrated that both XPC and RAD23B are parylated by PARP1 in response to UV irradiation.[65] Whether parylation of these factors is linked to ubiquitylation events as observed for DDB2 is currently unclear but an attractive speculation. Further, XPA shows high affinity for long PAR chains[66] suggesting that parylation might also play a role during damage verification. This non-covalent interaction with PAR chains lowers the DNA binding affinity of XPA in vitro emphasizing that parylation in general attenuates damage signaling. Taken together, parylation is an important means to regulate the timing of DNA repair fac- tors at chromatin and at least in some cases it seems to be linked to ubiquitylation events. Ubiquitylation of DNA repair factors is reversed by deubiquitylating enzymes (DUBs), which are responsible for removing covalently attached ubiquitin mole- cules from substrates or poly-ubiquitylated chains.[67] The human genome encodes for about a hundred deubiquitylases which belong to the families of Otubain domain-containing proteases (OTUs),[68,69] ubiquitin-specific proteases (USPs), ubiquitin C-terminal hydrolases (UCHs), JAMM (JAB1/MPN/Mov34) proteases and Machado-Joseph domain-containing proteins (MJDs).[10] Without any doubt, the function of the USP family in maintaining genome integrity is understood best when com- pared with the other classes of DUBs. USPs act in many genome surveillance and repair pathways probably owing to their broad substrate spectrum. Whereas many other DUBs specifically cleave K48 and K63 chains, USPs are fairly promiscous with respect to their substrates.[10] One prominent example is USP7, which acts during DNA replication, during DSB repair and dur- ing NER. DNA replication is regulated by USP7 via

deubiquitylation of sumoylated proteins at the replication fork.[70] SUMOylation was proposed to target a protein group rather than individual proteins.[71] Hence, SUMO-dependent deubiquitylation might be an effective means of generating and maintaining a Ubiquitin-poor environment at sites of DNA rep- lication as recently suggested.[70,72] Further, USP7 disassembles Rad18-dependent poly-ubiquitin chains and compromises UV- induced PCNA mono-ubiquitylation in the DNA damage toler- ance pathway.[73-75] As detailed below, USP7 operates with UVSSA during TC-NER.[76,77] In the GG-NER sub-branch USP7 was shown to physically interact with XPC and to counteract p97-mediated segregation of XPC presumably by removing the K48-linked ubiquitin chain[78] (Fig. 2).

Thus, USP7 contributes to stabilization of XPC at the DNA damage site safeguarding it from proteasomal degradation. As previously mentioned, XPC undergoes K63-linked poly-ubiquitylation via RNF111 and poly-ubiquitylation via the UV-DDB-CUL4A complex. It is cur- rently not clear which DUBs apart from USP7 might addition- ally contribute to editing XPC-ubiquitylation or whether USP7 has any specifity toward a certain chain linkage. One potential candiate for editing XPC-ubiquitylation is OTUD4[79] (Fig. 2). OTUD4 was identified as an interaction partner of XPC and it was demonstrated that it deubiquitylates preferentially K48- linked ubiquitin chains.[68] It seems therefore likely that it removes K48-linked ubiquitin chains from XPC thereby coun- teracting p97-mediated extraction and proteasomal degrada- tion. Also, the DUB USP24 is involved in the deubiquitylation events during the UV triggered DNA damage response[80,81] (Fig. 2). USP24 deubiquitylates DDB2 thereby protecting it from proteasomal degradation and stabilizing the UV-DDB- CUL4 E3 ligase at the damage site. This might in turn cause an increased poly-ubiquitylation of XPC, which likewise would sta- bilize XPC at damaged chromatin. USP45 is another DUB that operates further downstream in the NER pathway regulating the ubiquitylation of the XPF interacting protein ERCC1.[82] Although its impact on the repair of CPDs was demonstrated it not clear how it is recruited to chromatin and how it is linked to the ubiquitylation events occurring during lesion recognition.

The ubiquitylation cascade at UV damage sites is initiated by mono-ubiquitylation of histone H2A. Thus, deubiquitylation of histone H2A will also impact on the DNA damage response. Specific DUBs may exist that remove the ubiquitin moiety from the lysines of the histone. During transcriptional activa- tion for instance many DUBs have been demonstrated to deu- biquitylate H2A at lysine 119.[83] Whether these DUBs operate during DNA repair is still obscure. Very recently, USP51 was shown to deubiquitylate histone H2A at lysines 13–15 regulat- ing the DNA damage resonse at DSBs.[84] However, how H2A- ubiquitylation signals are erased during NER stays enigmatic. Hence, in the future it will be essential to identify DUBs that specifically operate at CPDs or 6–4 photoproducts.

## Ubiquitylation events in the TC-NER pathway

Whereas ubiquitylation events in GG-NER seem quite prevalent our insights into ubiquitin-dependent processes in TC-NER are relatively sparse. During lesion recognition in TC-NER stalled RNA Pol II recruits CSB. Notably, CSB is part of a multiprotein complex consisting of DDB1, the scaffold proteins CUL4A or



CUL4B, respectively, and the E3 ubiquitin ligase RBX1 (Fig. 3). This E3 ligase complex is involved in fine-tuning the progression of TC-NER presumably via ubiquitylation and subsequent pro- teasomal degradation of CSB. Ubiquitylated CSB is extracted from

chromatin by the p97/VCP segregase and its cofactors UFD1 and UBXN7,[85] which commit CSB to proteasomal degra- dation (Fig. 3). The ubiquitin chains attached to CSB may be removed by USP7, which is recruited to the damage site via its interaction partner UV-stimulated scaffold protein A (UVSSA).[76,86,87] UVSSA in turn is recruited to chromatin by either of its interaction partners RNA-Pol II or CSA.[76,86,88] Thus, UVSSA may counteract proteasomal degradation and sta- bilize CSB at chromatin through USP7-mediated deubiquityla- tion (Fig. 3). Recently it was demonstrated that the deubiquitylation activity of USP7 is suppressed by its interaction with UVSSA,[89] which suggests that the regulation of CSB ubiq- uitylation might be more complex that anticipated earlier.

Additionally, UVSSA facilitates ubiquitylation of stalled Pol II but not its proteasomal degradation.[90,91] This implies that UVSSA does not promote the generation of a K48-linked ubiq- uitin chain on Pol II but it probably facilitates K63-linked ubiq- uitylation as suggested by the authors of the underlying study.[90] In contrast, ubiquitylation and degradation of the Pol II subunit RBP1 is a two-step process that involves at least two E3 ligases.[92] The HECT domain E3 ligase NEDD4 catalyzes the mono-ubiq- uitylation of RBP1 or a K63-linked poly-ubiquitylation, which is subsequently processed by the deubiquitylase UBP2[92-95] (Fig. 3). The mono-ubiquitin moiety on RBP1 is then extended via the Elongin A ubiquitin ligase.[92,96] Removal of this poly-ubiquity- lated Pol II from sites of DNA damage is facilitated by the remodeler INO80, and the p97 segregase to enable further tran- scription of genes[97] (Fig. 3). Taken together, poly-ubiquitylation events signifcantly participate in the regulation of TC-NER. It still needs to be found out how different ubiquitin linkage types

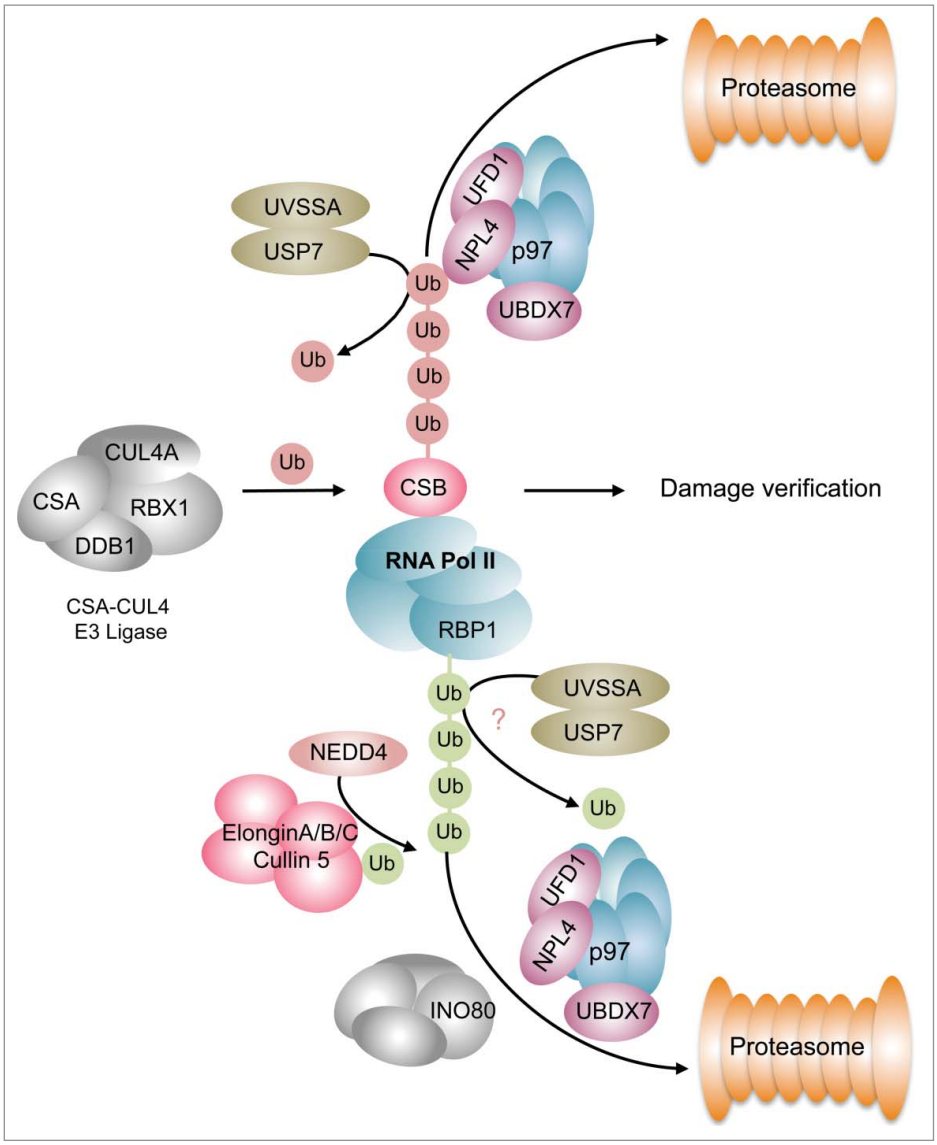


Figure 3. Ubiquitylation events during TC-NER. CSB is ubiquitylated by the CSA-CUL4 E3 ligase causing its p97-mediated segregation and proteasomal degradation. This process is counteracted by the UVSSA-USP7 complex that catalyzes the deubiquitylation of CSB. Removal of CSB is an important step handing over the damage site for damage verification. The RBP1 subunit of RNA Pol II undergoes K63-linked ubiquitylation, which is brought about by a two-step reaction involving NEDD4 and the Elongin E3 ligase complex. Ubiquitylated Polymerase is extracted from chromatin by the INO80 and p97 segregase complexes comitting it to proteasomal degradation. This is pre- sumably counteracted by the UVSSA-USP7 complex. Green spheres depict K63-linked ubiquitylation, red spheres indicate K48-linked ubiquitylation.



contribute to TC-NER and which lysine residues in the sub- strates are targeted. Very recently it was reported that site spe- cific ubiquitylation of CSB at Lys991 also participates in the repair of oxidative damage[98] foreshadowing that modulation of DNA

repair and presumably the timing of DNA damage recog- nition are subject to a complex network of ubiquitylation events.

## Timing of ubiquitylation events during DNA damage recognition in NER: An outlook

Ubiquitylation and deubiquitylation of DNA repair factors have an important impact on timing the lesion recognition. The most important player timing the damage recognition step during GG-NER is probably XPC, which seems to function as a control center that integrates different ubiquitin signals (Fig. 2). Besides K48-linked poly-ubiquitylation that is causing its proteasomal degradation, XPC is poly-ubiquitylated by the UV-DDB-CUL4A complex, which evokes its stabilization at chromatin. It is still not understood by which proteins these stabilizing ubiquitin chains are read and how this signal is linked to other XPC-ubiquitylation events. The XPC ubiquity- lation network is even more complex as RNF111 catalyzes K63-linked ubiquitylation of XPC, which seems to be impor- tant for the removal of XPC and the proper recruitment of XPG.[56] Whether these diverse ubiquitylation events describe sequentiell steps occurring during lesion recognition or if they describe perhaps independent signaling pathways that occur in different chromatin environments is still a matter of debate. Further, all ubiquitylation events occurring at XPC are edited by DUBs. Deubiquitylation in general impacts on the dwell time of factors at the damage site and fine-tunes the timing of damage recognition and its handover to damage verification and incision. As XPC modifications presumably constitute a critical control point of damage recognition it will be important to better understand the role of the ubiquitin linkage types dec- orating XPC. Whereas the fate of K48-ubiquitylated XPC is evi- dent, the role of K63-ubiquitylated XPC needs to be further investigated. Identification of K63-reading proteins or protein complexes harboring a K63-ubiquitin binding protein might give valuable new insights into the ubiquitin-mediated regula- tion of NER. Further, identification of the lysine residues that serve as ubiquitin attachment sites in XPC would facilitate to dissect the functions of the different ubiquitylation reactions. Directed mutagenesis of these lysine residues or similar muta- tions in XPC patients might help to further elucidate ubiquitin- related functions during the lesion recognition step. As to TC- NER, more ubiquitin-related processes and the respective E3 ligases and deubiquitylases need to be unveiled to better under- stand the timing of lesion recognition in this sub-branch. One major task for the future will be to identify more players of the ubiquitin signaling pathways, and more importantly, to com- prehend how they crosstalk during the DDR. In general, it would be advantagous to gain more insight into ubiquitin sig- naling in the context of the chromatin conformation at the damage site. A condensed chromatin configuration will cer- tainly rely on more elaborate remodelling activities to enable DNA repair. Could the different ubiquitin chain linkages and the use of different E3 ligases perhaps reflect DNA repair at dif- ferent chromatin configurations? It’s about time we looked

more intensively at chromatin and its localization in the nucleus to better understand DNA repair in the NER pathway.

## Abbreviations

DDR DSB NER GG-NER TC-NER UV

CDP Pol II

DNA damage response double strand breaks nucleotide excision repair global genomic nucleotide excision repair transcription coupled nucleotide excision repair ultraviolet

cyclopyrimidine dimer RNA Polymerase II

## Disclosure of potential conflicts of interest

No potential conflicts of interest were disclosed.

## Acknowledgments

We thank members of the Richly laboratory for critical reading of the manuscript. We apologize to colleagues for being unable to cite their work due to space limitations.

## Funding

H.R is supported by grants from the Boehringer Ingelheim Foundation.

## ORCID

Shalaka Chitale

Holger Richly

http://orcid.org/0000-0002-3837-269X http://orcid.org/0000-0002-7711-0350

## References

[1] Glickman MH, Ciechanover A. The ubiquitin-proteasome proteo- lytic pathway: destruction for the sake of construction. Physiol Rev 2002; 82:373-428; PMID:11917093

[2] Schnell JD, Hicke L. Non-traditional functions of ubiquitin and ubiq- uitin-binding proteins. J Biol Chem 2003; 278:35857-60; PMID:12860974

[3] Mukhopadhyay D, Riezman H. Proteasome-independent functions of ubiquitin in endocytosis and signaling. Science 2007; 315:201-5; PMID:17218518

[4] Hoege C, Pfander B, Moldovan GL, Pyrowolakis G, Jentsch S. RAD6- dependent DNA repair is linked to modification of PCNA by ubiqui- tin and SUMO. Nature 2002; 419:135-41; PMID:12226657

[5] Goldknopf IL, Taylor CW, Baum RM, Yeoman LC, Olson MO, Pre- stayko AW, Busch H. Isolation and characterization of protein A24, a “histone-like” non-histone chromosomal protein. J Biol Chem 1975; 250:7182-7; PMID:1165239

[6] Morey L, Helin K. Polycomb group protein-mediated repression of transcription. Trends Biochem Sci

2010; 35:323-32; PMID:20346678

[7] Jackson SP, Durocher D. Regulation of DNA Damage Responses by Ubiquitin and SUMO. Mol Cell 2013; 49:795-807; PMID:23416108

[8] Bergink S, Salomons FA, Hoogstraten D, Groothuis TA, de Waard H, Wu J, Yuan L, Citterio E, Houtsmuller AB, Neefjes J, et al. DNA damage triggers nucleotide excision repair-dependent monoubiqui- tylation of histone H2A. Gen Dev 2006; 20:1343-52; PMID:16702407

[9] Nouspikel T. Multiple roles of ubiquitination in the control of nucle- otide excision repair. Mech Ageing Dev 2011; 132:355-65; PMID:21466822

[10] Komander D, Rape M. The ubiquitin code. Annu Rev Biochem 2012; 81:203-29; PMID:22524316



(a) [11] de Laat WL, Jaspers NG, Hoeijmakers JH. Molecular mecha- nism of nucleotide excision repair. Gen Dev 1999; 13:768-85; PMID:10197977

(b) [12] Scharer OD. Nucleotide excision repair in eukaryotes. Cold Spring Harb Perspect Biol 2013; 5:a012609; PMID:24086042

(c) [13] Fousteri M, Mullenders LH. Transcription-coupled nucleotide exci- sion repair in mammalian cells: molecular mechanisms and biologi- cal effects. Cell Res 2008; 18:73-84; PMID:18166977

(d) [14] Marteijn JA, Lans H, Vermeulen W, Hoeijmakers JHJ. Understand- ing nucleotide excision repair and its roles in cancer and ageing. Nat Rev Mol Cell Bio 2014; 15:465-81

(e) [15] Riedl T, Hanaoka F, Egly JM. The comings and goings of nucleotide excision repair factors on damaged DNA. EMBO J 2003; 22:5293- 303; PMID:14517266

(f) [16] Sugasawa K, Ng JM, Masutani C, Iwai S, van der Spek PJ, Eker AP, Hanaoka F, Bootsma D, Hoeijmakers JH. Xeroderma pigmentosum group C protein complex is the initiator of global genome nucleotide excision repair. Mol Cell 1998; 2:223-32; PMID:9734359

(g) [17] Araki M, Masutani C, Takemura M, Uchida A, Sugasawa K, Kondoh J, Ohkuma Y, Hanaoka F. Centrosome protein centrin 2/caltractin 1 is part of the xeroderma pigmentosum group C complex that initiates global genome nucleotide excision repair. J Biol Chem 2001; 276:18665-72; PMID:11279143

(h) [18] Masutani C, Sugasawa K, Yanagisawa J, Sonoyama T, Ui M, Eno- moto T, Takio K, Tanaka K, van der Spek PJ, Bootsma D, et al. Puri- fication and cloning of a nucleotide excision repair complex involving the xeroderma pigmentosum group C protein and a human homologue of yeast RAD23. EMBO J 1994; 13:1831-43; PMID:8168482

(i) [19] Sugasawa K, Okamoto T, Shimizu Y, Masutani C, Iwai S, Hanaoka F. A multistep damage

recognition mechanism for global genomic nucle- otide excision repair. Gen Dev 2001; 15:507-21; PMID:11238373

(j) [20] Hoogstraten D, Bergink S, Ng JM, Verbiest VH, Luijsterburg MS, Geverts B, Raams A, Dinant C, Hoeijmakers JH, Vermeulen W, et al. Versatile DNA damage detection by the global genome nucleotide excision repair protein XPC. J Cell Sci 2008; 121:2850-9; PMID:18682493

(k) [21] Bergink S, Toussaint W, Luijsterburg MS, Dinant C, Alekseev S, Hoeijmakers JH, Dantuma NP, Houtsmuller AB, Vermeulen W. Rec- ognition of DNA damage by XPC coincides with disruption of the XPC-RAD23 complex. J Cell Biol 2012; 196:681-8; PMID:22431748

(l) [22] Rao H, Sastry A. Recognition of specific ubiquitin conjugates is important for the proteolytic functions of the ubiquitin-associated domain proteins Dsk2 and Rad23. J Biol Chem 2002; 277:11691-5; PMID:11805121

(m) [23] Kim I, Mi K, Rao H. Multiple interactions of rad23 suggest a mecha- nism for ubiquitylated substrate delivery important in proteolysis. Mol Biol Cell 2004; 15:3357-65; PMID:15121879

(n) [24] Tang JY, Hwang BJ, Ford JM, Hanawalt PC, Chu G. Xeroderma pig- mentosum p48 gene enhances global genomic repair and suppresses UV-induced mutagenesis. Mol Cell 2000; 5:737-44; PMID:10882109

(o) [25] Kulaksiz G, Reardon JT, Sancar A. Xeroderma pigmentosum com- plementation group E protein (XPE/DDB2): purification of various complexes of XPE and analyses of their damaged DNA binding and putative DNA repair properties. Mol Cell Biol 2005; 25:9784-92; PMID:16260596

(p) [26] Nichols AF, Itoh T, Graham JA, Liu W, Yamaizumi M, Linn S. Human damage-specific DNA-binding protein p48. Characterization of XPE mutations and regulation following UV irradiation. J Biol Chem 2000; 275:21422-8

(q) [27] Marteijn JA, Lans H, Vermeulen W, Hoeijmakers JH. Understanding nucleotide excision repair and its roles in cancer and ageing. Nat Rev Mol Cell Biol 2014; 15:465-81; PMID:24954209

(r) [28] Mailand N, Bekker-Jensen S, Faustrup H, Melander F, Bartek J, Lukas C, Lukas J. RNF8 ubiquitylates histones at DNA double-strand breaks and promotes assembly of repair proteins. Cell 2007; 131:887- 900; PMID:18001824

(s) [29] Pan MR, Peng G, Hung WC, Lin SY. Monoubiquitination of H2AX protein regulates DNA damage response signaling. J Biol Chem 2011; 286:28599-607; PMID:21676867

[30] Thorslund T, Ripplinger A, Hoffmann S, Wild T, Uckelmann M, Villumsen B, Narita T, Sixma TK, Choudhary C, Bekker-Jensen S, et al. Histone H1 couples initiation and amplification of ubiq- uitin signalling after DNA damage. Nature 2015; 527:389-93; PMID:26503038

[31] Mattiroli F, Vissers JH, van Dijk WJ, Ikpa P, Citterio E, Vermeulen W, Marteijn JA, Sixma TK. RNF168 ubiquitinates K13-15 on H2A/ H2AX to drive DNA damage signaling. Cell 2012; 150:1182-95; PMID:22980979

[32] Doil C, Mailand N, Bekker-Jensen S, Menard P, Larsen DH, Pepper- kok R, Ellenberg J, Panier S, Durocher D, Bartek J, et al. RNF168 binds and amplifies ubiquitin conjugates on damaged chromosomes to allow accumulation of repair proteins. Cell 2009; 136:435-46; PMID:19203579

[33] Pan MR, Peng G, Hung WC, Lin SY. Monoubiquitination of H2AX protein regulates DNA damage response signaling. J Biol Chem 2011; 286:28599-607; PMID:21676867

[34] Ismail IH, Andrin C, McDonald D, Hendzel MJ. BMI1-mediated his- tone ubiquitylation promotes DNA double-strand break repair. J Cell Biol 2010; 191:45-60; PMID:20921134

[35] Ginjala V, Nacerddine K, Kulkarni A, Oza J, Hill SJ, Yao M, Citterio E, van Lohuizen M, Ganesan S BMI1 is recruited to DNA breaks and contributes to DNA damage-induced H2A ubiquitination and repair. Mol Cell Biol 2011; 31:1972-82; PMID:21383063

[36] Chagraoui J, Hebert J, Girard S, Sauvageau G. An anticlastogenic function for the Polycomb Group gene Bmi1. Proc Natl Acad Sci U S A 2011; 108:5284-9; PMID:21402923

[37] Ui A, Nagaura Y, Yasui A. Transcriptional elongation factor ENL phosphorylated by ATM recruits polycomb and switches off tran- scription for DSB repair. Mol Cell 2015; 58:468-82; PMID:25921070

[38] Kapetanaki MG, Guerrero-Santoro J, Bisi DC, Hsieh CL, Rapi c-Otrin V, Levine AS. The DDB1-CUL4ADDB2 ubiquitin ligase is deficient in xeroderma pigmentosum group E and targets histone H2A at UV- damaged DNA sites. Proc Natl Acad Sci U S A 2006; 103:2588-93; PMID:16473935

[39] Marteijn JA, Bekker-Jensen S, Mailand N, Lans H, Schwertman P, Gourdin AM, Dantuma NP, Lukas J, Vermeulen W. Nucleotide exci- sion repair-induced H2A ubiquitination is dependent on MDC1 and RNF8 and reveals a universal DNA damage response. J Cell Biol 2009; 186:835-47; PMID:19797077

[40] Guerrero-Santoro J, Kapetanaki MG, Hsieh CL, Gorbachinsky I, Lev- ineAS,Rapi c-OtrinV.Thecullin4B-basedUV-damagedDNA- binding protein ligase binds to UV-damaged chromatin and ubiqui- tinates histone H2A. Cancer Res 2008; 68:5014-22; PMID:18593899

[41] Gracheva E, Chitale S, Wilhelm T, Rapp A, Byrne J, Stadler J, Medina R, Cardoso MC, Richly H. ZRF1 mediates remodeling of E3 ligases at DNA lesion sites during nucleotide excision repair. J Cell Biol 2016; 213:185-200; PMID:27091446

[42] Angers S, Li T, Yi X, MacCoss MJ, Moon RT, Zheng N. Molecular architecture and assembly of the DDB1-CUL4A ubiquitin ligase machinery. Nature 2006; 443:590-3; PMID:16964240

[43] Wang H, Zhai L, Xu J, Joo HY, Jackson S, Erdjument-Bromage H, Tempst P, Xiong Y, Zhang Y. Histone H3 and H4 ubiquitylation by the CUL4-DDB-ROC1 ubiquitin ligase facilitates cellular response to DNA damage. Mol Cell 2006; 22:383-94; PMID:16678110

[44] Shiyanov P, Nag A, Raychaudhuri P. Cullin 4A associates with the UV-damaged DNA-binding protein DDB. J Biol Chem 1999; 274:35309-12; PMID:10585395

[45] Groisman R, Polanowska J, Kuraoka I, Sawada J, Saijo M, Drapkin R, Kisselev AF, Tanaka K, Nakatani Y. The ubiquitin ligase activity in the DDB2 and CSA complexes is differentially regulated by the COP9 signalosome in response to DNA damage. Cell 2003; 113:357- 67; PMID:12732143

[46] Richly H, Rocha-Viegas L, Ribeiro JD, Demajo S, Gundem G, Lopez- Bigas N, Nakagawa T,

Rospert S, Ito T, Di Croce L. Transcriptional activation of polycomb-repressed genes by ZRF1. Nature 2010; 468:1124-8; PMID:21179169

[47] Papadopoulou T, Kaymak A, Sayols S, Richly H. Dual Role of Med12 in PRC1-dependent Gene Repression and ncRNA-mediated Tran- scriptional Activation. Cell Cycle 2016; 15:1479-1493; PMID:27096886



. [48] Kaymak A, Richly H. Zrf1 controls mesoderm lineage genes and car- diomyocyte differentiation. Cell Cycle 2016; 15(23):3306–3317; PMID:27754813

. [49] Papadopoulou T, Richly H. On-site remodeling at chromatin: How multiprotein complexes are rebuilt during DNA repair and transcriptional activation. BioEssays 2016; 38(11):1130–1140; PMID:27599465

. [50] Lan L, Nakajima S, Kapetanaki MG, Hsieh CL, Fagerburg M, Thick- man K, Rodriguez-Collazo P, Leuba SH, Levine AS, Rapi c-Otrin V. Monoubiquitinated histone H2A destabilizes photolesion-containing nucleosomes with concomitant release of UV-damaged DNA-binding protein E3 ligase. J Biol Chem 2012; 287:12036-49; PMID:22334663

. [51] Marteijn JA, Bekker-Jensen S, Mailand N, Lans H, Schwertman P, Gourdin AM, Dantuma NP, Lukas J, Vermeulen W. Nucleotide exci- sion repair-induced H2A ubiquitination is dependent on MDC1 and RNF8 and reveals a universal DNA damage response. J Cell Biol 2009; 186:835-47; PMID:19797077

. [52] Wang H, Zhai L, Xu J, Joo HY, Jackson S, Erdjument-Bromage H, Tempst P, Xiong Y, Zhang Y. Histone H3 and H4 ubiquitylation by the CUL4-DDB-ROC1 ubiquitin ligase facilitates cellular response to DNA damage. Mol Cell 2006; 22:383-94; PMID:16678110

. [53] Sugasawa K, Okuda Y, Saijo M, Nishi R, Matsuda N, Chu G, Mori T, Iwai S, Tanaka K, Tanaka K, et al. UV-induced ubiquitylation of XPC protein mediated by UV-DDB-ubiquitin ligase complex. Cell 2005; 121:387-400; PMID:15882621

. [54] Matsumoto S, Fischer ES, Yasuda T, Dohmae N, Iwai S, Mori T, Nishi R, Yoshino K, Sakai W, Hanaoka F, et al. Functional regulation of the DNA damage-recognition factor DDB2 by ubiquitination and interaction with xeroderma pigmentosum group C protein. Nucleic Acids Res 2015; 43:1700-13; PMID:25628365

. [55] El-Mahdy MA, Zhu Q, Wang QE, Wani G, Praetorius-Ibba M, Wani AA. Cullin 4A-mediated proteolysis of DDB2 protein at DNA dam- age sites regulates in vivo lesion recognition by XPC. J Biol Chem 2006; 281:13404-11; PMID:16527807

. [56] van Cuijk L, van Belle GJ, Turkyilmaz Y, Poulsen SL, Janssens RC, Theil AF, Sabatella M, Lans H, Mailand N, Houtsmuller AB, et al. SUMO and ubiquitin-dependent XPC exchange drives nucleotide exci- sion repair. Nature communications 2015; 6:7499; PMID:26151477

. [57] Poulsen SL, Hansen RK, Wagner SA, van Cuijk L, ,van Belle GJ, Streicher W, Wikstr€om M,

Choudhary C, Houtsmuller AB, Marteijn JA, et al. RNF111/Arkadia is a SUMO-targeted ubiquitin ligase that facilitates the DNA damage response. J Cell Biol 2013; 201:797-807; PMID:23751493

. [58] Akita M, Tak YS, Shimura T, Matsumoto S, Okuda-Shimizu Y, Shi- mizu Y, Nishi R, Saitoh H, Iwai S, Mori T, et al. SUMOylation of xeroderma pigmentosum group C protein regulates DNA damage recognition during nucleotide excision repair. Sci Rep 2015; 5:10984; PMID:26042670

. [59] Wang QE, Zhu Q, Wani G, El-Mahdy MA, Li J, Wani AA. DNA repair factor XPC is modified by SUMO-1 and ubiquitin following UV irradiation. Nucleic Acids Res 2005; 33:4023-34; PMID:16030353

. [60] Puumalainen MR, Lessel D, Ruthemann P, Kaczmarek N, Bachmann K, Ramadan K, Naegeli H Chromatin retention of DNA damage sen- sors DDB2 and XPC through loss of p97 segregase causes genotoxic- ity. Nat Commun 2014; 5:3695; PMID:24770583

. [61] De Vos M, Schreiber V, Dantzer F. The diverse roles and clinical rel- evance of PARPs in DNA damage repair: current state of the art. Bio- chem Pharmacol 2012; 84:137-46; PMID:22469522

. [62] Robu M, Shah RG, Petitclerc N, Brind'Amour J, Kandan-Kulangara F, Shah GM Role of poly(ADP-ribose) polymerase-1 in the removal of UV-induced DNA lesions by nucleotide excision repair. Proc Natl Acad Sci U S A 2013; 110:1658-63; PMID:23319653

. [63] Luijsterburg MS, Lindh M, Acs K, Vrouwe MG, Pines A, van Atti- kum H, Mullenders LH, Dantuma NP DDB2 promotes chromatin decondensation at UV-induced DNA damage. J Cell Biol 2012; 197:267-81; PMID:22492724

. [64] Pines A, Vrouwe MG, Marteijn JA, Typas D, Luijsterburg MS, Can- soy M, Hensbergen P, Deelder A, de Groot A, Matsumoto S, et al. PARP1 promotes nucleotide excision repair through DDB2

stabilization and recruitment of ALC1. J Cell Biol 2012; 199:235-49;

PMID:23045548 [65] Maltseva EA, Rechkunova NI, Sukhanova MV, Lavrik OI. Poly

(ADP-ribose) Polymerase 1 Modulates Interaction of the Nucleotide Excision Repair Factor XPC-RAD23B with DNA via Poly(ADP-ribo- syl)ation. J Biol Chem 2015; 290:21811-20; PMID:26170451

[66] Fischer JM, Popp O, Gebhard D, Veith S, Fischbach A, Beneke S, Lei- tenstorfer A, Bergemann J, Scheffner M, Ferrando-May E, et al. Poly (ADP-ribose)-mediated interplay of XPA and PARP1 leads to recip- rocal regulation of protein function. FEBS J 2014; 281:3625-41; PMID:24953096

[67] Komander D. Mechanism, specificity and structure of the deubiquiti- nases. Subcell Biochem 2010; 54:69-87; PMID:21222274

[68] Mevissen TE, Hospenthal MK, Geurink PP, Elliott PR, Akutsu M, Arnaudo N, Ekkebus R, Kulathu Y, Wauer T, El Oualid F, et al. OTU deu- biquitinases reveal mechanisms of linkage specificity and enable ubiquitin chain restriction analysis. Cell 2013; 154:169-84; PMID:23827681

[69] Kulathu Y, Garcia FJ, Mevissen TE, Busch M, Arnaudo N, Carroll KS, Barford D, Komander D. Regulation of A20 and other OTU deu- biquitinases by reversible oxidation. Nat Commun 2013; 4:1569; PMID:23463012

[70] Lecona E, Rodriguez-Acebes S, Specks J, Lopez-Contreras AJ, Rup- pen I, Murga M, Mun~oz J, Mendez J, Fernandez-Capetillo O. USP7 is a SUMO deubiquitinase essential for DNA replication. Nat Struct Mol Biol 2016; 23:270-7; PMID:26950370

[71] Psakhye I, Jentsch S. Protein group modification and synergy in the SUMO pathway as exemplified in DNA repair. Cell 2012; 151:807- 20; PMID:23122649

[72] Lecona E, Fernandez-Capetillo O. A SUMO and ubiquitin code coordinates protein traffic at replication factories. BioEssays 2016; 38(12):1209-1217; PMID:27667742

[73] Zlatanou A, Stewart GS. Damaged replication forks tolerate USP7 to maintain genome stability. Mol Cell Oncol 2016; 3:e1063571; PMID:27308573

[74] Zlatanou A, Sabbioneda S, Miller ES, Greenwalt A, Aggathanggelou A, Maurice MM, Lehmann AR, Stankovic T, Reverdy C, Colland F, et al. USP7 is essential for maintaining Rad18 stability and DNA damage tolerance. Oncogene 2016; 35:965-76; PMID:25961918

[75] Qian J, Pentz K, Zhu Q, Wang Q, He J, Srivastava AK, Wani AA. USP7 modulates UV-induced PCNA monoubiquitination by regulat- ing DNA polymerase eta stability. Oncogene 2015; 34:4791-6; PMID:25435364

[76] Schwertman P, Lagarou A, Dekkers DH, Raams A, van der Hoek AC, Laffeber C, Hoeijmakers JH, Demmers JA, Fousteri M, Vermeulen W, et al. UV-sensitive syndrome protein UVSSA recruits USP7 to regulate transcription-coupled repair. Nat Genet 2012; 44:598-602; PMID:22466611; http://dx.doi.org/10.1038/ng.2230

[77] Schwertman P, Vermeulen W, Marteijn JA. UVSSA and USP7, a new couple in transcription-coupled DNA repair. Chromosoma 2013; 122:275-84; PMID:23760561; http://dx.doi.org/10.1007/s00412-013- 0420-2

[78] He J, Zhu Q, Wani G, Sharma N, Han C, Qian J, Pentz K, Wang QE, Wani AA. Ubiquitin-specific protease 7 regulates nucleotide excision repair through deubiquitinating XPC protein and preventing XPC protein from undergoing ultraviolet light-induced and VCP/p97 pro- tein-regulated proteolysis. J Biol Chem 2014; 289:27278-89; PMID:25118285; http://dx.doi.org/10.1074/jbc.M114.589812

[79] Lubin A, Zhang L, Chen H, White VM, Gong F. A human XPC pro- tein interactome–a resource. Int J Mol Sci 2014; 15:141-58; ; http:// dx.doi.org/10.3390/ijms15010141

[80] Zhang L, Gong F. Involvement of USP24 in the DNA damage response. Mol Cell Oncol 2016; 3:e1011888; PMID:27308530; http:// dx.doi.org/10.1080/23723556.2015.1011888

[81] Zhang L, Nemzow L, Chen H, Lubin A, Rong X, Sun Z, Harris TK, Gong F. The deubiquitinating enzyme USP24 is a regulator of the UV damage response. Cell reports 2015; 10:140-7; PMID:25578727; http://dx.doi.org/10.1016/j.celrep.2014.12.024

[82] Perez-Oliva AB, Lachaud C, Szyniarowski P, Munoz I, Macartney T, Hickson I, Rouse J, Alessi DR. USP45 deubiquitylase controls ERCC1-

XPF endonuclease-mediated DNA damage responses. EMBO J 2015;

34:326-43; PMID:25538220; http://dx.doi.org/10.15252/embj.201489184

. [83] Vissers JH, Nicassio F, van Lohuizen M, Di Fiore PP, Citterio E. The many faces of ubiquitinated histone H2A: insights from the DUBs. Cell Div 2008; 3:8; PMID:18430235; http://dx.doi.org/10.1186/1747- 1028-3-8

. [84] Wang Z, Zhang H, Liu J, Cheruiyot A, Lee JH,Ordog T, Lou Z, You Z, Zhang Z. USP51 deubiquitylates H2AK13,15ub and regulates DNA damage response. Gen Dev 2016; 30:946-59; PMID:27083998; http://dx.doi.org/10.1101/gad.271841.115

. [85] He J, Zhu Q, Wani G, Sharma N, Wani AA. Valosin-containing Pro- tein (VCP)/p97 Segregase Mediates Proteolytic Processing of Cock- ayne Syndrome Group B (CSB) in Damaged Chromatin. J Biol Chem 2016; 291:7396-408; PMID:26826127; http://dx.doi.org/ 10.1074/jbc.M115.705350

. [86] Zhang X, Horibata K, Saijo M, Ishigami C, Ukai A, Kanno S, Tahara H, Neilan EG, Honma M, Nohmi T, et al. Mutations in UVSSA cause UV-sensitive syndrome and destabilize ERCC6 in transcription-cou- pled DNA repair. Nat Genet 2012; 44:593-7; PMID:22466612; http:// dx.doi.org/10.1038/ng.2228

. [87] Sarasin A. UVSSA and USP7: new players regulating transcription- coupled nucleotide excision repair in human cells. Genome Med 2012; 4:44; PMID:22621766; http://dx.doi.org/10.1186/gm343

. [88] Fei J, Chen J. KIAA1530 protein is recruited by Cockayne syndrome complementation group protein A (CSA) to participate in transcrip- tion-coupled repair (TCR). J Biol Chem 2012; 287:35118-26; PMID:22902626; http://dx.doi.org/10.1074/jbc.M112.398131

. [89] Higa M, Zhang X, Tanaka K, Saijo M. Stabilization of Ultraviolet (UV)-stimulated Scaffold Protein A by Interaction with Ubiquitin- specific Peptidase 7 Is Essential for Transcription-coupled Nucleotide Excision Repair. J Biol Chem 2016; 291:13771-9; PMID:27129218; http://dx.doi.org/10.1074/jbc.M116.724658

. [90] Nakazawa Y, Sasaki K, Mitsutake N, Matsuse M, Shimada M, Nardo T, Takahashi Y, Ohyama K, Ito K, Mishima H, et al. Mutations in UVSSA cause UV-sensitive syndrome and impair RNA polymerase IIo processing in transcription-coupled nucleotide-excision repair. Nat Genet 2012; 44:586-92; PMID:22466610; http://dx.doi.org/ 10.1038/ng.2229

[91] van Cuijk L, Vermeulen W, Marteijn JA. Ubiquitin at work: the ubiq- uitous regulation of the damage recognition step of NER. Exp Cell Res 2014; 329:101-9; PMID:25062985; http://dx.doi.org/10.1016/j. yexcr.2014.07.018

[92] Wilson MD, Harreman M, Svejstrup JQ. Ubiquitylation and degra- dation of elongating RNA

polymerase II: the last resort. Biochim Bio- phys Acta 2013; 1829:151-7; PMID:22960598; http://dx.doi.org/ 10.1016/j.bbagrm.2012.08.002

[93] Harreman M, Taschner M, Sigurdsson S, Anindya R, Reid J, Somesh B, Kong SE, Banks CA, Conaway RC, Conaway JW, et al. Distinct ubiquitin ligases act sequentially for RNA polymerase II polyubiqui- tylation. Proc Natl Acad Sci U S A 2009; 106:20705-10; PMID:19920177; http://dx.doi.org/10.1073/pnas.0907052106

[94] Beaudenon SL, Huacani MR, Wang G, McDonnell DP, Huibregtse JM. Rsp5 ubiquitin-protein ligase mediates DNA damage-induced degradation of the large subunit of RNA polymerase II in Saccharo- myces cerevisiae. Mol Cell Biol 1999; 19:6972-9; PMID:10490634; http://dx.doi.org/10.1128/MCB.19.10.6972

[95] Anindya R, Aygun O, Svejstrup JQ. Damage-induced ubiquitylation of human RNA polymerase II by the ubiquitin ligase Nedd4, but not Cockayne syndrome proteins or BRCA1. Mol Cell 2007; 28:386-97; PMID:17996703; http://dx.doi.org/10.1016/j.molcel.2007.10.008

[96] Yasukawa T, Kamura T, Kitajima S, Conaway RC, Conaway JW, Aso T. Mammalian Elongin A complex mediates DNA-damage-induced ubiquitylation and degradation of Rpb1. EMBO J 2008; 27:3256-66; PMID:19037258; http://dx.doi.org/10.1038/emboj.2008.249

[97] Lafon A, Taranum S, Pietrocola F, Dingli F, Loew D, Brahma S, Bartholomew B, Papamichos-Chronakis M. INO80 Chromatin Remodeler Facilitates Release of RNA Polymerase II from Chro- matin for Ubiquitin-Mediated Proteasomal Degradation. Mol Cell 2015; 60:784-96; PMID:26656161; http://dx.doi.org/10.1016/ j.molcel.2015.10.028

[98] Ranes M, Boeing S, Wang Y, Wienholz F, Menoni H, Walker J, Encheva V, Chakravarty P, Mari PO, Stewart A, et al. A ubiquityla- tion site in Cockayne syndrome B required for repair of oxidative DNA damage, but not for transcription-coupled nucleotide excision repair. Nucleic Acids Res 2016; 44:5246-55; PMID:27060134; http:// dx.doi.org/10.1093/nar/gkw216

## Compartmentalization of cellular processes: how is NER compartmentalized? How universal are methods of chromatin compartmentalization used in NER?

The nucleus is a dense structure with DNA tightly packaged into chromatin. Along with the DNA, the nucleus also contains all the proteins involved in a wide variety of cellular processes such as replication, transcription and DNA repair. Considering the highly complex and varied nuclear content, a system of organization within the nucleus seems essential. Nuclear organization is accomplished in different ways, and consists of organization of proteins, as well as organization of chromatin.

Protein organization: Nuclear proteins may be freely diffusing, or bound to a specific structure. For eg: most transcription factors are able to diffuse freely through the nucleus (Kaur et al., 2013). The nuclear lamina is present interior to the nuclear membrane and has a very specific structure. Lamin associated proteins such as lamin binding receptors are localized specifically to the periphery of the nucleus (reviewed in Meldi and Brickner 2011). In addition, the nucleus contains of different nuclear bodies, performing specialized functions. These bodies are not membrane bound, but consist of a local aggregation of specific proteins required for the particular process. Some of these are scaffolded by RNA and contain some structural proteins (reviewed in Mao et al., 2011). Some of the major nuclear compartments are listed in Table 1. Nuclear bodies serve a common purpose of bringing together proteins required for specific functions. Presumably this enables faster response times, and ease of formation of multiprotein complexes that play a role in these processes.

| **Body** | **Appearance/behaviour** | ***Postulated function(s)*** |
|---|---|---|
| Nucleolus | Large | rRNA biogenesis, RNA processing, nuclear regulation |
| Cajal body/GEM | Small, multiple, dynamic | RNP maturation |
| PML body | Small, multiple, generally static | Multiple postulated functions |
| Splicing factor compartment | Multiple "speckles" of variable size, close to active genes | Splicing factor "depots" |
| OPT domain | Small, associate with chromosomes 6 and 7 | Transcription of specific genes |
| Perinucleolar compartment | Touching the nucleolus | Transcription/RNA processing |
| Cleavage body | Small foci | RNA processing |
| GATA-1 body | Small foci | Transcription |
| PcG domain | Pericentromeric foci | Gene silencing |

Table 1: Common nuclear bodies. adapted from Newall et al.

1. Chromatin organization: The second important level of organization in the nucleus is the organization of chromatin. Depending on the state of packaging, chromatin can be roughly divided into euchromatin and heterochromatin. Euchromatin is more loosely packed and mainly consists of transcriptionally active genes. Heterochromatin on the other hand is more tightly packaged. It consists of gene rich as well as gene poor regions. Heterochromatin is mainly found at the periphery of the nucleus, in association with the lamina, and at perinucleolar regions. Euchromatin on the other hand is usually in the interior of the nucleus. This chromatin organization however varies quite a lot between different cell types. Stem cells show a distinct nuclear organization with relatively low levels of heterchromatin and a very dynamic organization, while terminally differentiated cells have a more static chromatin structure. In addition, chromosomes are positioned through the nucleus in a non-random manner, forming very well defined chromosome territories. The position of a specific genomic locus in 3D nuclear space is tightly

regulated, as are its interactions with neighbouring chromosomes and nuclear loci (reviewed in Meldi and Brickner 2011).

Considering the high level of organization found in chromatin organization, there is relatively little known on mechanisms by which this organization is set. The most well studied mechanism of chromatin compartmentalization, is the tethering of H3K9me3 marked heterochromatin to the nuclear periphery. The nuclear periphery has been implicated in gene regulation, and recruitment of chromatin to the nuclear periphery is sufficient to repress and silence the associated genes (Finlan et al., 2008; Reddy et al., 2008; Zullo et al., 2012). Large lamina-associated domains (LADS) have been mapped. LADs are enriched in repressed chromatin, however their interaction with the lamina is highly dynamic. During differentiation, LADs may gain and lose interaction with the nuclear lamina, depending on the transcriptional status of the encompassed genes (reviewed in Meldi and Brickner 2011). Lamina associated proteins such as lamin binding receptor (LBR) and PRR14 tether H3K9me3 marked chromatin to the nuclear periphery via its interaction with HP1 (reviewed in Padeken and Heun 2014). Similarly, the nucleolar periphery also is an important role in 3D organization of chromatin. Some of the known methods of chromatin tethering to the nuclear and nucleolar periphery are summarized in Figure 2.

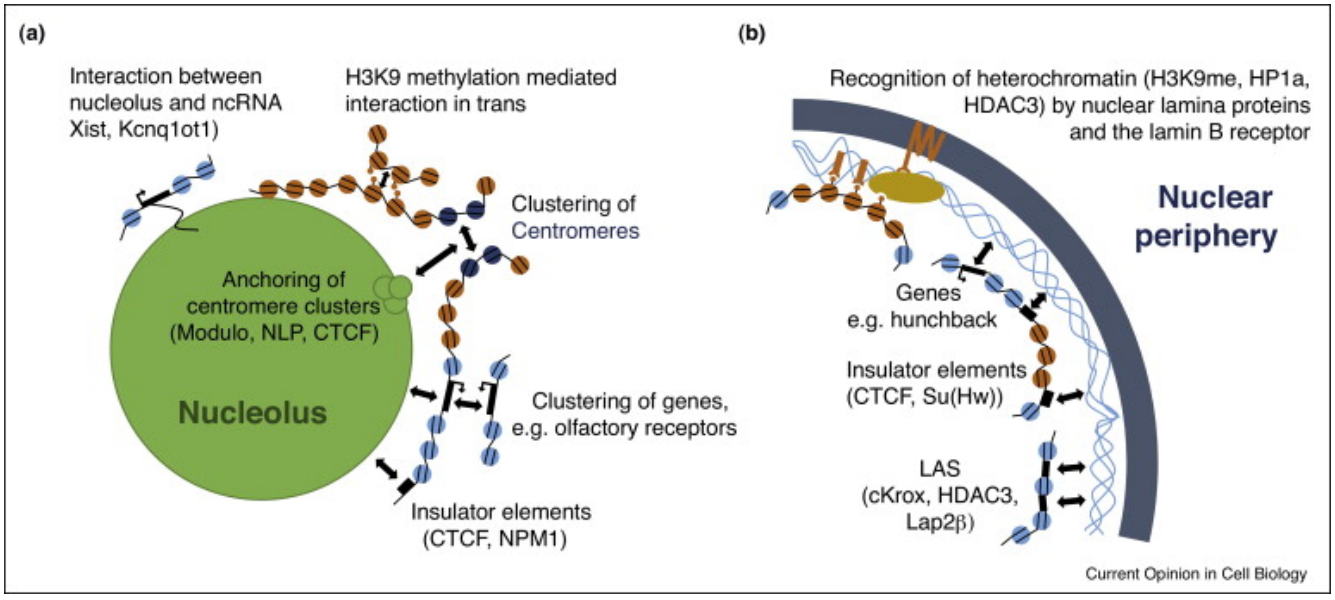


Figure 2: Schematic overview of different mechanisms that mediate attachment of heterochromatin to the nucleolus and the nuclear periphery. Interactions between genomic regions and (a) the nucleolus or (b) the lamina containing regions of the nuclear periphery are shown. Identified regulatory factors are named in

brackets. Nucleosomes in orange represent constitutive heterochromatin, in light blue facultative heterochromatin and in dark blue centromeric chromatin. Adapted from Padeken and Heun 2014.

In our research, we identify another possible mechanism of tethering chromatin. We found that marking of chromatin with H2AK119 is sufficient to target the chromatin to the nucleolus. In this case, ZRF1 tethers the H2AK119 marked chromatin to the nucleolus, by binding it directly via its ubiquitin binding domain (UBD). We verified this interaction is indeed direct, since expression of a ZRF1 mutant lacking the UBD abolished nucleolar tethering. RING1A/B are the only known proteins that set this mark. Along with its role in NER, RING1B also plays an important role in DSB repair.

The most well studied function of RING1A/B is in polycomb mediated gene repression, as part of the PRC1 complex (Vidal, 2009). PRC1 is recruited to polycomb repressed genes and sets the H2AK119 mark. ZRF1 also plays a role in activation of polycomb mediated genes by binding of the H2AK119 mark and subsequent displacement of RING1B from chromatin (Richly et al., 2010). This is very similar to its role in NER. It is conceivable that ZRF1 mediated activation of polycomb repressed genes also involves their initial translocation to the nucleolus. Indeed preliminary experiments show that tethering of components of PRC1 to chromatin is sufficient to position the chromatin in the vicinity of the nucleolus. Thus, we have identified a mechanism of nucleolar tethering of chromatin with potentially far reaching implications in a variety of nuclear processes, including gene activation.

Another interesting insight is in the specificity of the nucleolar tethering of DNA. H2AK119 ub is present at many locations throughout the genome. However, not all of these genomic loci are tethered to the nucleolus simultaneously. In the context of NER, we believe that this specificity is gained through the DDB2-XPC interaction. DDB2 is part of the UV-RING1B complex, and the H2AK119 mark is not recognized by ZRF1 in the absence of XPC. XPC and DDB2 are known to interact and XPC is recruited to chromatin in a DDB2 dependent manner. Thus the additional presence of DDB2 and XPC might regulate whether a particular histone bearing the H2AK119ub mark is tethered to the nucleolus. Similarly, this specificity may be imparted by other gene activation specific proteins during differentiation. This could provide an important insight into the specificity of chromatin tethering interactions.

We have observed NER being specifically targeted to the nucleolus, but a very interesting question is what is the role of the nucleolus in this process. The nucleolus, like the nuclear

lamina, also plays a major role in the three-dimensional organization of the genome (Lemaitre and Bickmore, 2015; Nemeth et al., 2010). Many of the identified Lamin-associated domains, also associate specifically with the nucleolus. The nucleolus is surrounded by perinucleolar heterochromatin, which like plays a part on localization of LADs to the nucleolar periphery. However the primary function of the nucleolus is in ribosome biogenesis. Ribosomal DNA is specifically targeted to the nucleolus, where it is subsequently transcribed and assembled into ribosomes (Mao et al., 2011). Thus, the nucleolus consists of multiple copies of actively transcribing rDNA genes, present in a decondensed chromatin state. A potential function of re-localizing chromatin to the nucleolus may be to aid in chromatin remodeling. Ribosome biogenesis and chromatin remodeling, both involve regulation of nucleic acid-protein interactions, and the nucleolus contains much of the machinery required for this process. Notably, Nucleophosmin functions as a histone chaperone and as a sink for histones (Keck and Pemberton, 2012). About half of the nucleolar proteome consists of proteins involved in functions other than ribosome biogenesis, viz regulation of tumor suppressor and proto-oncogene activities, cell-cycle control, DNA replication, DNA repair, and stress signaling (Anderson et al., 2002). Thus, the nucleolus is also linked to a host of cellular functions. The number and size of nucleoli in a cell is directly linked to the rate of proliferation of the cell. The nucleolus also serves as sensor for cell viability. Localization of NER to the nucleolus may also play an important role in linking repair to other DNA damage responses such as cell cycle regulation. The nucleolar-nucleoplasmic distribution of many proteins changes as a result of DNA damage, and this helps in regulation of the DNA damage response (Figure 3).

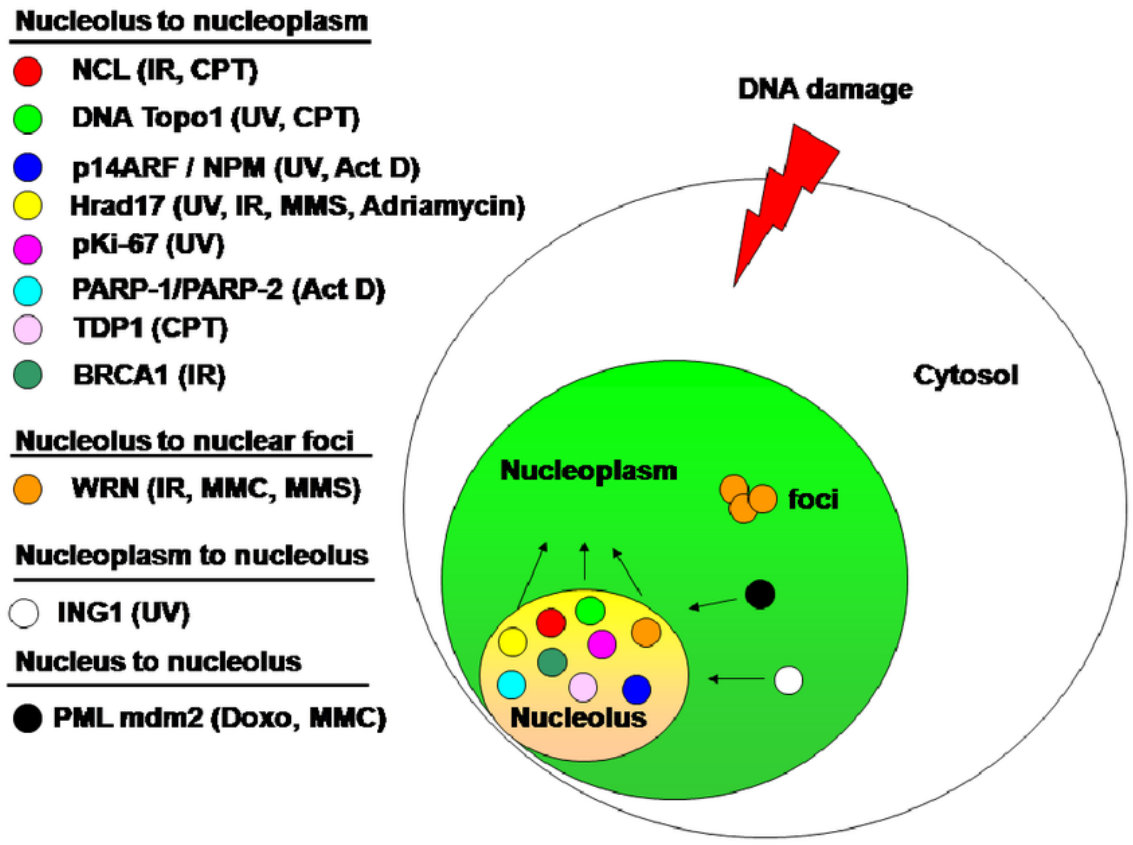


Figure 3: Nucleoli protein trafficking in response to DNA damage: The nucleolus is depopulated of its protein content in response to a variety of cellular stress. Proteins are grouped according to the direction they are moving. Arrows indicate the direction of the proteins movement. The Werner protein helicase accumulates in intranuclear repair foci in response to camptothecin (CPT). NCL: Nucleolin, IR: Ionizing Radiation, TDP1: Tyrosyl DNA phosphodiesterase 1, PML: Promyelocytic Leukemia protein, MMC: Mitomycin C, PARP: poly(ADPribose) polymerase. Adapted from Nalabothula et al., 2010

In addition to its function in chromatin structure maintenance, the nucleolus might also possibly play a role in scaffolding of protein chromatin interactions. We found that both the interaction of ZRF1 and DICER to chromatin require RNA. Upon digestion with RNAse, their association with chromatin is completely lost. This may be potentially due to a loss in nucleolar structure (Mao et al., 2011). An interesting question is whether this loss of interaction is a non-specific effect of loss of nucleolar structure, or whether there is specific transcription from the lesion surrounding DNA which then scaffolds the interaction of the protein complexes with DNA.

## Chromatin accessibility during NER: Novel players regulating chromatin accessibility and their implication in maintenance of cellular chromatin conformation

DNA is arranged in a very regular structure within the nucleus. The nucleosome consists of a central histone core, consisting of two subunits each of Histones 2A, 2B, 3 and 4, surrounded by two loops of dsDNA. Histone H1 binds to the linker DNA between two nucleosomes. Varying the spacing between nucleosomes can modulate the DNA structure from a tightly packed heterochromatin like state, to a more loosely packed euchromatin like state. Histone modifications such as acetylation and parylation add negatively charged moieties to histones. These in turn repel the negatively charged DNA and can also lead to a looser chromatin structure. Processes such as transcription, replication and DNA repair require the proteins to directly access the DNA. Thus, a pre-requisite of these processes is to make the DNA more accessible by creating a more relaxed chromatin structure.

We have further that i there is extensive chromatin rearrangement in response to UV damage, and that part of this rearrangement involves relocalization of DNA lesions to the nucleolus for repair. ZRF1, and thus nuclear translocation is required for decondensation of chromatin in response to UV damage. We found that ZRF1 mediated decondensation occurs through recruitment of DICER to chromatin, and requires PARP activation. DICER, a riboendonuclease, is most well known for its role in the miRNA pathway of post transcriptional gene regulation (Holoch and Moazed, 2015). In addition, DICER has been linked to the establishment and maintenance of H3K9me3 marked heterochromatin (Creamer and Partridge, 2011). Importantly in both these functions, the main frole of DICER is in processing dsRNAs to shorter dsRNA, which is subsequently loaded on either the RISC or RITS complex. In miRNA processing, cleaving of miRNA and pre-miRNA by DICER occurs prominently in the cytoplasm, followed by loading of the RNA onto the RISC complex and miRNA mediated gene silencing. During heterochromatin formation, dsRNA generated from a specific genomic locus is processed by DICER and then loaded onto the RITS complex. This complex specifically directs enzymes that can set the H3K9me3 mark to the genomic locus complementary to the dsRNA (Creamer and Partridge, 2011). In this case as well, DICER, presumably in the soluble nuclear fraction cleaves dsRNA. Additionally, DICER has also been shown to play a role in targeting repair machinery to site of double strand DNA breaks (Wang and Goldstein 2016; Francia et al., 2012; Wei et al., 2012). In

this case as well, DICER generated dsRNAs target the repair machinery to the site of damage via complementarity of the dsRNA to the DNA sequence around the break site. So far, all functions of DICER described have involved the main role of DICER as processing of dsRNA, which then subsequently perform diverse functions. Presumably, these are performed by soluble DICER, either in the cytoplasm of nucleus. Additionally, DICER has also been shown to bind to rDNA (Sinkkonen et al., 2010). In this case, DICER was observed to bind to both active and inactive genes, and its effect on the chromatin conformation was uncertain.

During NER, we found that DICER is directly recruited to chromatin at the damage site by ZRF1, and interacts with chromatin. This chromatin associated DICER then activates chromatin decondensation in a PARP dependent manner. Interestingly, this activity of DICER does not require its riboendonuclease activity. DICER, apart from its catalytic function, harbors multiple domains that might be involved in recruitment of factors that drive the decondensation of chromatin. One potential candidate for such a function is evidently PARP1. Moreover, though speculative, the helicase activity of DICER might be involved in the decondensation process. It is interesting to speculate if DICER plays a similar role in any other processes. One could imagine that DICER can possibly set a balance between heterochromatin and decondensed chromatin, depending on the fraction of DICER that is chromatin bound versus unbound.

## Signaling through histone modifications

Histone modifications are an important component of the epigenetic code. Cells from a single organism have identical genetic information. However, there are huge differences in gene expression and regulation between cell types. Epigenetic regulation aids in establishing these cell specific gene expression programs. In addition, the cell is constantly receiving input from external stimuli. Some of these stimuli require changes in gene expression and profile of chromatin binding proteins. Along with regulation of gene expression, other cellular processes also require association of proteins with specific chromatin loci in a co-ordinated manner. For eg: during DNA replication, replication is initiated at different genomic regions in a synchronized manner and involves co-ordinated recruitment of a variety of multi protein complexes. Similarly, during DNA repair the chromatin around the lesion site is decorated with various specific histone modifications. These aid in modifying the chromatin condensation, serving as tethering sites for DNA damage proteins and as signals for the DNA damage response. In addition, histone modifications do not function in isolation. Multiple histone modifications can be set in a co-dependent manner, and there is crosstalk between the modifications. Overall, this results in setting of a specific "histone code" on each nucleosome. We have discovered novel functions for two histone modifications in the NER pathway. Below I discuss how our findings fit into the various functions attributed to histone modifications, and how they could possibly also enable a crosstalk between the various modifications.

1. Modification of chromatin environment: The *Access-Prime –Repair* model hypothesizes that the first step required during DNA repair is relaxation of the chromatin to enable access of the repair proteins. The primary histone modification having a direct impact on chromatin structure is acetylation of H4 at lysine 16. Other histone modifications can also cause changes in chromatin structure, but in a more indirect manner, often via recruitment of chromatin modifying enzymes. A variety oof histone modifications such as acetylation, methylation and phosphorylatin have been shown to play a role in NER (reviewed in Li 2012). Ìn addition, NER requires function of the ATP dependent chromatin remodelers, SWI/SNF and INO80 (Lans et al., 2012). Lastly it has been shown that parylation plays an important role in modification of chromatin structure during NER (Marteijn et al., 2014). The exact mechanism of how parylation affects DNA structure are less well

studied. However, similar to acetylation, parylation also imparts a negative charge to histones, which repels the DNA strands and causes a more relaxed chromatin conformation. We additionally found that H2Aub also may potentially regulate chromatin conformation, however by a more indirect mechanism of change in chromatin localization. H2AK119 is required for relocating the chromatin to the nucleolus via binding of ZRF1. ZRF1 in turn recruits DICER, which leads to decondensation of chromatin in a PARP1 dependent manner. Absence of both ZRF1 or DICER results in a shift in the chromatin structure towards a more condensed state, highlighting the importance of these factors in modulating chromatin structure. Thus, H2AK119 serves as a signal for specific recruitment of chromatin remodeling proteins.

2. Tethering sites for DNA damage proteins

Many histone modifications also serve as tethering platforms for specific recruitment of proteins to a particular genomic region. In the context of DNA damage repair, one of the most studied histone modifications is H2AX phosphorylation. H2AX phosphorylation is set at sites of DNA double strand breaks, single strand breaks as well as UV damage. In DSB repair, MDC1 is the primary protein that recognizes H2AX. This interaction is the first step which leads to DNA damage signaling and repair at the site of the DSB. (reviewed in Podhorecka et al., 2010). We discovered that in the context of NER, H4K20me2 seems to provide an important tethering platform for recruitment of XPA to the sites of damage. XPA does not contain any known histone methyl binding domain, so it is possible that XPA is indirectly recruited to the damage sites. Timed recruitment of DNA repair factors is an essential determinant of damage recognition and for the transition to downstream events of repair. Thus, what is also interesting is that we observe a crosstalk between H2AK119 ub and H4K20me2, and both marks in turn lead to recruitment of different steps of the repair machinery. DICER recruits MMSET to chromatin, and enables setting of the H4K20me2 mark that subsequently leads to XPA recruitment. Thus the ZRF1-DICER-MMSET axis provides a link between a histone modification involved marking DNA damage sites (H2AK119 ub), and a histone modification that is subsequently recognized by the repair machinery (H4K20me2).

3. Signaling for DNA damage response: The DNA damage response consists of other components other than DNA damage repair. An important step of the damage response is signaling to cell cycle checkpoints. This enables assessment of damage repair before resumption of cell cycle, and in cases of persistent damage can also lead to apoptosis of the cells. The kinases ATM and ATR play an important role in signaling and cell cycle regulation. (Maréchal and Zou, 2013). They sense DNA damage through various mechanisms, and then initiate phosphorylation cascades that can lead to cell cycle regulation. 53BP1 plays a role in DSB repair as well as in enhancing phosphorylation of ATM substrates and in checkpoint activation (Maréchal and Zou, 2013). H4K20me2 also serves as a binding platform for 53BP1. It is possible that H4K20me2 also provides a link between NER and cell cycle response. It could potentially serve as an additional mechanism of damage sensing.

## References


Andersen J.S., Lyon C.E, Fox A.H, Leung A.K.L, Lam Y.W, Steen H, Mann M, Lamond A.I. (2002). Directed Proteomic Analysis of the Human Nucleolus, Current Biology. 12 (1) 1-11.

Creamer KM, Partridge JF. (2011). RITS-connecting transcription, RNA interference, and heterochromatin assembly in fission yeast. Wiley Interdiscip Rev RNA. 2(5):632-46

Finlan, L.E., D. Sproul, I. Thomson, S. Boyle, E. Kerr, P. Perry, B. Ylstra, J.R. Chubb, and W.A. Bickmore. (2008). Recruitment to the nuclear periphery can alter expression of genes in human cells. PLoS Genet. 4:e1000039

Francia, S., Michelini, F., Saxena, A., Tang, D., de Hoon, M., Anelli, V., Mione, M., Carninci, P. and d'Adda di Fagagna, F. (2012) Site-specific DICER and DROSHA RNA products control the DNA-damage response. Nature, 488, 231-235.

Holoch, D. and Moazed, D. (2015) RNA-mediated epigenetic regulation of gene expression. *Nature Reviews Genetics*, **16**, 71-84.

Kaur G., Costa M.W., Nefzger C.M., Silva J, Fierro-González J.C, Polo J.M, Bell T.D.M and Plachta N. (2013). Probing transcription factor diffusion dynamics in the living mammalian embryo with photoactivatable fluorescence correlation spectroscopy. Nature Communications 4: 1637

Keck, K. M., & Pemberton, L. F. (2012). Histone chaperones link histone nuclear import and chromatin assembly. Biochimica et Biophysica Acta, 1819(3-4), 277–289.

Lans, H., Marteijn, J. A., & Vermeulen, W. (2012). ATP-dependent chromatin remodeling in the DNA-damage response. *Epigenetics & Chromatin*, *5*, 4.

Li, S. (2012). Implication of Posttranslational Histone Modifications in Nucleotide Excision Repair. *International Journal of Molecular Sciences*, *13*(10), 12461–12486.

Mao, Y. S., Zhang, B., & Spector, D. L. (2011). Biogenesis and Function of Nuclear Bodies. *Trends in Genetics : TIG*, *27*(8), 295–306.

Maréchal, A., & Zou, L. (2013). DNA Damage Sensing by the ATM and ATR Kinases. Cold Spring Harbor Perspectives in Biology, 5(9), a012716.

Meldi, L., & Brickner, J. H. (2011). Compartmentalization of the nucleus. *Trends in Cell Biology*, *21*(12), 701–708.

Nalabothula N, Indig FE, Carrier F. (2010). The Nucleolus Takes Control of Protein Trafficking Under Cellular Stress. Mol Cell Pharmacol. 2(5):203-212.

Newall A.E.T., Wang J, Sheer D. Nuclear Compartments. Encyclopedic Reference of Genomics and Proteomics in Molecular Medicine. pp 1309-1313

Padeken J, Heun P. (2014). Nucleolus and nuclear periphery: velcro for heterochromatin. Current Opinions Cell Biology. 28:54-60

Podhorecka M, Skladanowski A, and Bozko P. (2010). H2AX Phosphorylation: Its Role in DNA Damage Response and Cancer Therapy. Journal of Nucleic Acids, vol. 2010

Reddy, K.L., J.M. Zullo, E. Bertolino, and H. Singh. (2008). Transcriptional repression mediated by repositioning of genes to the nuclear lamina. Nature. 452:243–247.

Richly H, Rocha-Viegas L, Ribeiro JD, Demajo S, Gundem G, Lopez-Bigas N, Nakagawa T, Rospert S, Ito T, Di Croce L.(2010). Transcriptional activation of polycomb-repressed genes by ZRF1. Nature. 468(7327):1124-8.

Sinkkonen, L., Hugenschmidt, T., Filipowicz, W. and Svoboda, P. (2010) Dicer is associated with ribosomal DNA chromatin in mammalian cells. PloS one, 5, e12175.

Vidal M. (2009). Role of polycomb proteins Ring1A and Ring1B in the epigenetic regulation of gene expression. The International Journal of Developmental Biology.;53(2-3):355-70

Wang, Q. and Goldstein, M. (2016) Small RNAs Recruit Chromatin-Modifying Enzymes MMSET and Tip60 to Reconfigure Damaged DNA upon Double-Strand Break and Facilitate Repair. *Cancer Res*, **76**, 1904-1915.

Wei, W., Ba, Z., Gao, M., Wu, Y., Ma, Y., Amiard, S., White, C.I., Rendtlew Danielsen, J.M., Yang, Y.G. and Qi, Y. (2012) A role for small RNAs in DNA double-strand break repair. Cell, 149, 101-112.

Zullo, J.M., I.A. Demarco, R. Piqué-Regi, D.J. Gaffney, C.B. Epstein, C.J. Spooner, T.R. Luperchio, B.E. Bernstein, J.K. Pritchard, K.L. Reddy, and H. Singh. (2012). DNA sequence-dependent compartmentalization and silencing of chromatin at the nuclear lamina. Cell. 149:1474–1487

# Acknowledgements

I would primarily like to acknowledge my supervisor, for giving me the opportunity to work on this project. Thank you for giving me the creative freedom to pursue all my scientific ideas, and the very interesting scientific discussions.

A big thank you to all the lab members for creating a fun and scientifically enriching environment to work in.

The entire scientific staff and core facilities at the IMB. Their support helped transformed many experiments from an abstract idea to a solid piece of data.